SEISMIC BEHAVIOR OF SOME VITAL HIGHWAY BRIDGES IN JORDAN

By
Amer Alkloub

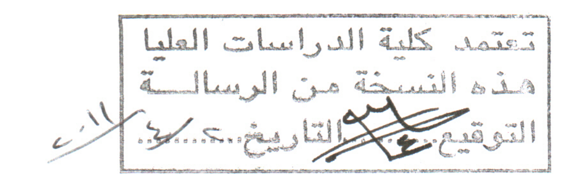
Supervisor
Dr. Nazzal Armouti

Co-Supervisor
Dr. Nasim Shatarat

This Thesis was Submitted in Partial Fulfillment of the Requirements for the Master's Degree of Science in Civil Engineering

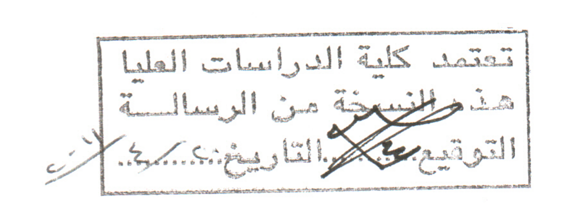
Faculty of Graduate Studies
The University of Jordan

April, 2011



This thesis (Seismic Behavior of Some Vital Highway Bridges in Jordan) was successfully defended and approved on ...7/April/2011..

Examination Committee	**Signature**
Dr. Nazzal Armouti, Chairman Associate Professor of Civil Engineering	Apr. 11, 2011 ....
Dr. Nasim Shatarat, Co-Supervisor Associate Professor of Civil Engineering – Hashemite University	....
Prof. Samih Qaqish, Member Professor of Civil Engineering	....
Prof. Abdelqader Najmi, Member Professor of Civil Engineering	....
Prof. Hassoun Hadid, Member (Private Sector)	....



The University of Jordan

Authorization Form

I, Amer Abdelkarim Alkloub, authorize the University of Jordan to supply copies of my Thesis/ Dissertation to libraries or establishments or individuals on request, according to the University of Jordan regulations.

Signature:

Date: 18, April 2011

ACKNOWLEDGMENT

I would like to express my sincere gratitude and appreciation to my supervisors, Dr. Nazzal Armouti and Dr. Nasim Shatarat, for all the support that they gave me throughout my research. Their knowledge, vision, and directions were valuable for the progress of the research presented in this dissertation. It has been a great privilege to work under their guidance. I want to thank them for their understanding, patience, and support.

I would like to express my thanks and appreciation to Eng. Ibrahim Thwieb, Design Engineer at Greater Amman Municipality, for his help in providing me with the required drawings and reports from The Greater Amman Municipality.

Many thanks to the members of the Examination Committee for their notes and comments.

DEDICATION

DEDICATED TO

MY MOM AND DAD

& MY BROTHERS FALEH, MOHAMMAD, & HAIDAR

TABLE OF CONTENTS

COMMITTEE DECISION .... **ii**
ACKNOWLEDGMENT .... **iii**
DEDICATION .... **iv**
TABLE OF CONTENTS .... **v**
LIST OF FIGURES .... **viii**
LIST OF TABLES .... **xii**
ABSTRACT .... **xiv**
CHAPTER ONE **1**
1. INTRODUCTION **1**
1.1. Background 1
1.2. Research Objectives 4
1.3. Research Methodology 5
CHAPTER TWO **10**
2. LITRETURE REVEIW **10**
2.1. Bridges Deficiencies and Corresponding Retrofit Scheme 10
2.1.1. Superstructure 10
2.1.2. Columns 14
2.1.3. Beams 18
2.1.4. Joints 20
2.1.5. Foundation 22
2.1.6. Abutments 24
CHAPTER THREE **26**
3. BRIDGE MODELING **26**
3.1. Alnasha Bridge 26
3.1.1. Bridge Description 26
3.1.2. Alnasha Bridge Mathematical Model 35
3.1.2.1. Superstructure and Piers 35
3.1.2.2. Foundation Modeling 40
3.2. Alharamain Bridge 48
3.2.1. Bridge Description 48
3.2.2. Alharamain Bridge Mathematical Model 57

3.2.2.1. Superstructure and Piers Modeling 57
3.2.2.2. Foundation Modeling 60
3.3. Almahata Bridge 62
3.3.1. Bridge Description 62
3.3.2. Almahata Bridge Mathematical Model 65
3.3.2.1. Superstructure and Pier Modeling 65
CHAPTER FOUR 68
4. CAPACITY AND DEMAND ASSESSMENT 68
4.1. Evaluation Methods 68
4.1.1. Method A1/A2 68
4.1.2. Method B 69
4.1.3. Method C 69
4.1.4. Method D1 69
4.1.5. Method D2 70
4.1.6. Method E 70
4.2. Selection of Evaluation Method 76
4.2.1. Alnasha Bridge 76
4.2.2. Alharamain Bridge 77
4.2.3. Almahata Bridge 78
4.3. Method C: Component Capacity/Demand Method 79
4.4. Demand Assesment 80
4.4.1. Determination of Design Response Spectrum 81
4.4.2. Combination of Seismic Force Effects 81
4.5. Capacity Assessment 83
4.5.1. Flexural Strength of Reinforced Concrete Columns and Beams 83
4.5.1.1. Expected Flexural Strength 84
4.5.1.2. Flexural Overstrength Capacity 86
4.5.1.3. Flexural Strength of Columns with Lap-Splices in Plastic Hinge Zones . 89
4.5.2. Shear Strength of Reinforced Concrete Columns and Beams 90
4.5.2.2. Final Shear Strength, V_f 92
4.5.3. Shear Strength of Beam-Column Joints 92
4.5.3.1. Maximum Beam-Column Joint Strength, V_{ji} 93
4.5.3.2. Cracked Beam–Column Joint Strength, V_{jf} 94

4.6. Deformation Capacity of Bridge Members 94
4.6.1. Plastic Hinge Rotation, θ_p 94
4.6.2. Characterization of Deformation-Based Limit States 95
4.6.2.1. Compression Failure of Unconfined Concrete 95
4.6.2.2. Compression Failure of Confined Concrete 96
4.6.2.3. Buckling of Longitudinal Bars 97
4.6.2.4. Fracture of the Longitudinal Reinforcement 97
4.6.2.5. Low Cycle Fatigue of Longitudinal Reinforcement 98
CHAPTER FIVE 103
5. CAPACITY / DEMAND ANALYSIS RESULTS 103
5.1. Alnasha Bridge 103
5.1.1. Response Spectrum Analysis 103
5.1.2. Method C Seismic Capacity/Demand Ratio 108
5.1.3. Method D2 116
5.2. Alharamain Bridge 126
5.2.1. Response Spectrum Analysis 126
5.2.2. Method C Seismic Capacity/Demand Ratio 131
5.2.3. Method D2 142
5.3. Almahata Bridge 154
5.3.1. Response Spectrum Analysis 154
5.3.2. Method C Seismic Capacity/Demand Ratio 157
5.3.3. Method D2 162
CHAPTER SIX 169
6. RETROFIT SCHEMES 169
6.1. Alnasha Bridge 169
6.2. Alharamain Bridge 169
6.2.1. Bearing seat upgrade at Abutment #1 169
6.2.2. Bridge Footings 171
6.3. Almahata Bridge 173
CHAPTER SEVEN 175
7. SUMMARY AND CONCLUSIONS 175
REFERENCES 177
ABSTRACT (In Arabic) 179

LIST OF FIGURES

Figure 1-1: Seismic Map of Jordan (Adapted from fetweb.ju.edu.jo/narmouti, Armouti, 2010). 2
Figure 1-2: Overview of the retrofitting process for highway bridges 7
Figure 2-1: Nishinomiya-ko Bridge approach span collapse in the 1995 Hyogo-Ken Nanbu earthquake (Adapted from Bridge engineering handbook, 2000) 11
Figure 2-2: Unseating due to bridge skew (Adapted from Priestley et al. 1996). 11
Figure 2-3: Cable restrainers for concrete superstructure movement joints. (a) Box-girder bridges; (b) I-girder bridges (Adapted from Priestley et al. 1996). 12
Figure 2-4: Cable restrainers for steel superstructure movement joints (Adapted from Priestley et al. 1996). 12
Figure 2-5: Seat extension to accommodate large longitudinal displacements (Adapted from Priestley et al. 1996) 13
Figure 2-6: Failure of columns of the Route 5/210 interchange during the 1971 San Fernando earthquake (Adapted from Bridge engineering handbook, 2000). 14
Figure 2-7: Bond failure of lap splices at column base, 1989 Loma Prieta earthquake (Adapted from Priestley et al. 1996). 15
Figure 2-8: Pullout failure, 1971 San Fernando earthquake (Adapted from www: ace-mrl.engin.umich.edu). 16
Figure 2-9: Confinement of columns by steel jacketing (Adapted from Priestley et al. 1996). 17
Figure 2-10: Cap beam positive moment cracks at inner column face, 1989 Loma Prieta earthquake (Adapted from Priestley et al. 1996). 19
Figure 2-11: Flexural and shear retrofit of free standing multi-column bents (Adapted from FHWA-SRM, 2005). 19
Figure 2-12: Joint shear failure, 1989 Loma Prieta earthquake. (a) I-880 viaduct; (b) Embarcadero viaduct (Adapted from Priestley et al. 1996). 20
Figure 2-13: Joint retrofit with external concrete jacket (Adapted from FHWA-SRM, 2005) 21
Figure 2-14: A Picture of the Clamshell Used in the Retrofit of the Beam-Joint (Adapted from McLean and Shattarat, 2005). 22
Figure 2-15: Footing retrofit measures (Adapted from Priestley et al. 1996). 23
Figure 2-16: Abutment slumping and rotation (Adapted from Priestley et al. 1996). 24
Figure 2-17: Diaphragm abutment overlay (Adapted from FHWA-SRM, 2005) 25
Figure 3-1: Aerial View of Alnasha Bridge (Adapted from Google Earth, USA) 26
Figure 3-2: A general view of Alnasha Bridge. 27
Figure 3-3: Alnasha Bridge - plan & elevation, dimensions in meter (Adapted from Greater Amman Municipality) 28
Figure 3-4: Alnasha Bridge deck typical section (Dimensions in meter). 29
Figure 3-5: Integral and Non-Integral piers details (Dimensions in meter). 30
Figure 3-6: Alnasha Bridge Pier #2 and Pier #3 spread footing details (Dimensions in meter). 31

Figure 3-7: Alnasha Bridge Pier #4 and Pier #5 pile footing details (Dimensions in meter). 32
Figure 3-8: Alnasha Bridge Pier #6 and Pier #7 pile footing details (Dimensions in meter). 32
Figure 3-9: Alnasha Bridge Abutment #1 details (Dimensions in meter). 33
Figure 3-10: Alnasha Bridge Abutment #2 details (Dimensions in meter). 34
Figure 3-11: Expansion joint details 34
Figure 3-12: Deck-crossbeam rigid connection. 35
Figure 3-13: Locations of section properties in a typical pier (L_P: Equivalent plastic hinge length) 38
Figure 3-14: Alnasha Bridge mathematical model. 39
Figure 3-15: Uncoupled elasto-plastic spring model for rigid footings, k_{sr}: spring rotational stiffness, k_{sh}: spring horizontal stiffness, and k_{sv}: spring vertical stiffness (Adapted from FHWA-SRM, 2005). 40
Figure 3-16: Recommended coefficient of variation in subgrade modulus (f) with depth of sand. (Adapted from FHWA-SRM, 2005, Figure 7-12). 44
Figure 3-17: Lateral pile-head stiffness - fixed-head condition, (Adapted from FHWA-SRM, 2005, Figure 7-8). 44
Figure 3-18: Rotational pile-head stiffness, (Adapted from FHWA-SRM, 2005). 45
Figure 3-19: Aerial View of Alharamain Bridge (Adapted from Google Earth, USA) . 48
Figure 3-20: A general view of Alharamin Bridge. 49
Figure 3-21: Alharamain bridge- plan, dimensions in meter (Adapted from Greater Amman Municipality). 50
Figure 3-22: Alharamain bridge- elevation, dimensions in meter (Adapted from Greater Amman Municipality). 51
Figure 3-23: Alharamain Bridge deck typical section (Dimensions in meter). 52
Figure 3-24: Typical pier details (Dimensions in meter). 53
Figure 3-25: Alharamain Bridge Piers #2, Pier #3, Pier #8, and Pier #9 footing details (Dimensions in meter). 54
Figure 3-26: Alharamain Bridge Pier #4 and Pier #7 footing details 55
Figure 3-27: Alharamain Bridge Pier #5 and Pier #6 footing details 55
Figure 3-28: Alharamain Bridge Abutment #1 Details (Dimensions in meter). 56
Figure 3-29: Alharamain Bridge mathematical model. 59
Figure 3-30: Locations of footing springs. 60
Figure 3-31: Aerial View of Almahata Bridge (Adapted from Google Earth, USA). 62
Figure 3-32: Almahata Bridge - plan & elevation, dimensions in meter (Adapted from Greater Amman Municipality). 63
Figure 3-33: A general view of Almahata Bridge. 64
Figure 3-34: Almahata Bridge deck typical section (Dimensions in meter). 64
Figure 3-35: Almahata Bridge mathematical model. 67
Figure 4-1: Determination of seismic retrofit category (Adapted from FHWA-SRM, 2005). 74
Figure 4-2: Construction of the seismic design response spectrum (Adapted from FHWA-SRM, 2005). 82

Figure 4-3: Confined strength ratio (K) for reinforced concrete members (Adapted from FHWA-SRM, 2005)....89
Figure 5-1: Fundamental mode shapes of Alnasha Bridge – Tension Model. 104
Figure 5-2: Fundamental mode shapes of Alnasha Bridge – Compression Model. 105
Figure 5-3: Moment-Rotation relationship for columns of Pier #2 in Alnasha Bridge. 117
Figure 5-4: Moment-Axial force interaction diagram for columns of Pier #2 in Alnasha Bridge....118
Figure 5-5: Typical bridge pier with plastic hinge location....120
Figure 5-6: Pushover curves for analysis in the transverse direction for pier #2 in Alnasha Bridge (Transverse Direction). 121
Figure 5-7: Pushover curves for analysis in the transverse direction for pier #4 & 5 in Alnasha Bridge (Transverse Direction). 121
Figure 5-8: Pushover curves for analysis in the transverse direction for pier #7 in Alnasha Bridge (Transverse Direction). 122
Figure 5-9: Pushover curves for analysis in the transverse direction for pier #2 in Alnasha Bridge (Longitudinal Direction). 122
Figure 5-10: Pushover curves for analysis in the transverse direction for pier #4 & 5 in Alnasha Bridge (Longitudinal Direction). 123
Figure 5-11: Pushover curves for analysis in the transverse direction for pier #7 in Alnasha Bridge (Longitudinal Direction). 123
Figure 5-12: Fundamental mode shapes of Alharamain Bridge – Tension Model....127
Figure 5-13: Fundamental mode shapes of Alharamain Bridge – Compression Model. 128
Figure 5-14: Moment-Rotation relationship for Pier #5 in Alharamain Bridge. 143
Figure 5-15: Moment-Axial force interaction diagram for Pier #5 in Alharamain Bridge. 143
Figure 5-16: Pushover curves for analysis in the transverse direction for pier #2 in Alharamain Bridge....146
Figure 5-17: Pushover curves for analysis in the longitudinal direction for pier #2 in Alharamain Bridge....146
Figure 5-18: Pushover curves for analysis in the transverse direction for pier #3 in Alharamain Bridge....147
Figure 5-19: Pushover curves for analysis in the longitudinal direction for pier #3 in Alharamain Bridge....147
Figure 5-20: Pushover curves for analysis in the transverse direction for pier #5 & 6 in Alharamain Bridge....148
Figure 5-21: Pushover curves for analysis in the longitudinal direction for pier #5 & 6 in Alharamain Bridge....148
Figure 5-22: Pushover curves for analysis in the transverse direction for pier #8 in Alharamain Bridge....149
Figure 5-23: Pushover curves for analysis in the longitudinal direction for pier #8 in Alharamain Bridge....149

Figure 5-24: Pushover curves for analysis in the transverse direction for pier #9 in Alharamain Bridge....150
Figure 5-25: Pushover curves for analysis in the longitudinal direction for pier #9 in Alharamain Bridge....150
Figure 5-26: Fundamental mode shapes of Almahata Bridge. 155
Figure 5-27: Moment-Rotation relationship for columns of Pier #3 in Almahata Bridge. 163
Figure 5-28: Moment-Axial force interaction diagram for columns of Pier #3 in Almahata Bridge. 163
Figure 5-29: Pushover curves for analysis in the transverse direction for pier #2 and 5 in Almahata Bridge. 165
Figure 5-30: Pushover curves for analysis in the transverse direction for pier #3 and 4 in Almahata Bridge. 165
Figure 5-31: Pushover curves for analysis in the longitudinal direction for pier #3 and 4 in Almahata Bridge. 166
Figure 6-1: Seat extension of Abutment #1 in Alharamain Bridge 170
Figure 6-2: Proposed retrofit scheme for the footings in pier #2, pier #3, pier #6, & pier #7. 171
Figure 6-3: Proposed retrofit scheme for the footings in pier #4 & pier #7. 172
Figure 6-4: Retrofit scheme for Pier #3 and Pier #4 columns in Alnasha Bridge. 174

LIST OF TABLES

Table 3-1: Alnasha Bridge Material Properties 35
Table 3-2: Component Rigidities (Adapted from FHWA SRM, 2005, Table 7-1) 37
Table 3-3: Surface stiffnesses for a rigid plate on a semi-infinite homogeneous elastic half-space (Adapted from FHWA-SRM, 2005, Table 6-1) 41
Table 3-4: Stiffness embedment factors for a rigid plate on a semi-infinite homogeneous elastic half-space (Adapted from FHWA-SRM, 2005, Table 6-2) 42
Table 3-5: Group of piles efficiency factor 46
Table 3-6: Spring values for Alnasha Bridge Footings 46
Table 3-7: Alharamain Bridge Material Properties 56
Table 3-8: Spring values for Alharamain Bridge.. 61
Table 3-9: Almahata Bridge Material Properties.. 65
Table 4-1: Service life categories (Adapted from FHWA-SRM, 2005). 71
Table 4-2: Performance levels for retrofitted bridges (Adapted from FHWA-SRM, 2005). 72
Table 4-3: Seismic hazard level (Adapted from FHWA-SRM, 2005). 73
Table 4-4: Performance-based seismic retrofit categories (Adapted from FHWA-SRM, 2005). 73
Table 4-5: Evaluation methods for existing bridges (Adapted from FHWA-SRM, 2005). 75
Table 5-1: Alnasha Bridge fundamental periods and mass participation ratios. 103
Table 5-2: Alnasha Bridge elastic displacements demand. 106
Table 5-3: Alnasha Bridge moment and shear force demand. 107
Table 5-4: Alnasha Bridge – Pier #2 C/D ratio calculations 108
Table 5-5: Alnasha Bridge – Pier #4 C/D ratio calculations 110
Table 5-6: Alnasha Bridge – Pier #7 C/D ratio calculations 112
Table 5-7: Alnasha Bridge C/D-Ratios obtained from Method C 114
Table 5-8: Moment-Rotation data-Alnasha Bridge 119
Table 5-9: Moment-Axial force interaction data-Alnasha Bridge 119
Table 5-10: Alnasha Bridge Method D2 – Pier #2. 124
Table 5-11: Alnasha Bridge Method D2 – Pier #5 & 4. 124
Table 5-12: Alnasha Bridge Method D2 – Pier #7. 125
Table 5-13: Alnasha Bridge C/D-Ratios obtained from Method D2 125
Table 5-14: Alharamain Bridge fundamental periods and mass participation ratios ... 126
Table 5-15: Alharamain Bridge displacement demand. 129
Table 5-16: Alharamain Bridge moment and shear force demand. 130
Table 5-17: Alharamain Bridge – Pier #2 C/D ratio calculations................................ 131
Table 5-18: Alharamain Bridge – Pier #3 C/D ratio calculations................................ 133
Table 5-19: Alharamain Bridge – Pier #5 & 6 C/D ratio calculations 135
Table 5-20: Alharamain Bridge – Pier #8 C/D ratio calculations................................ 137
Table 5-21: Alharamain Bridge – Pier #9 C/D ratio calculations................................ 139
Table 5-22: Alharamain Bridge C/D-Ratios obtained from Method C 141

Table 5-23: Moment-Rotation data-Alharamain Bridge 144
Table 5-24: Moment-Axial interaction data-Alharamain Bridge 145
Table 5-25: Alharamain Bridge Method D2 – Pier #2. 151
Table 5-26: Alharamain Bridge Method D2 – Pier #3. 151
Table 5-27: Alharamain Bridge Method D2 – Pier #5 & 6. 152
Table 5-28: Alharamain Bridge Method D2 – Pier #8. 152
Table 5-29: Alharamain Bridge Method D2 – Pier #9. 153
Table 5-30: Alharamain Bridge C/D-Ratios obtained from Method D2 153
Table 5-31: Almahata Bridge fundamental periods and mass participation ratios 154
Table 5-32: Almahata Bridge elastic displacement demand. 156
Table 5-33: Almahata Bridge moment and shear force demand. 156
Table 5-34: Almahata Bridge – Pier #2 and Pier #5 C/D ratio calculations 157
Table 5-35: Almahata Bridge – Pier #3 and Pier #4 C/D ratio calculations 159
Table 5-36: Almahata Bridge C/D-Ratios obtained from Method C 161
Table 5-37: Moment-Rotation data-Almahata Bridge 164
Table 5-38: Moment-Axial force interaction data-Almahata Bridge 164
Table 5-39: Almahata Bridge Method D2 – Pier #2 & Pier #4. 166
Table 5-40: Almahata Bridge Method D2 – Pier #3 & Pier #5. 167
Table 5-41: Almahata Bridge C/D-Ratios obtained from Method D2 167
Table 6-1: Materials cost estimate for seat length upgrade in Alharamain Bridge. 170
Table 6-2: Materials cost estimate for footings retrofit in Alharamain Bridge. 172
Table 6-3: Materials cost estimate for piers retrofit in Almahata Bridge. 173

SEISMIC BEHAVIOR OF SOME VITAL HIGHWAY BRIDGES IN JORDAN

By
Amer Alkloub

Supervisor
Dr. Nazzal Alarmouti

Co-Supervisor
Dr. Nasim Shatarat

ABSTRACT

The main objective of this study is to investigate the seismic behavior of three major highway bridges in Jordan and to determine the vulnerable elements in each bridge and the required retrofit scheme. The seismic force and displacement demand on the bridges were determined through elastic response spectrum analysis. The capacity of the bridges elements were determined based on the recommendations of the FHWA-Seismic Retrofit Manual and a capacity/demand ratio based on method C of the FHWA-SRM was established for each element that is susceptible to be damaged by the design earthquake. Pushover analysis based on the guidelines of method D2 of the FHWA-SRM was performed utilizing the software SAP2000 to determine the ultimate displacement capacity of the bridge in the longitudinal and the transverse directions.

The results of the seismic demand and capacity analyses showed that Alnasha Bridge would withstand the seismic demands without a need for any retrofit. However, the footings and the abutment seat length in Alharamain Bridge have a capacity/demand ratio less than one, retrofit scheme for the footings includes increasing the thickness of footings, while providing a concrete corbel was proposed to increase the seat length of Abutment #1. The results of the study showed a lack of ductility in the columns of pier #3 and pier #4 in Almahata Bridge and installation of a steel jacket was proposed to mitigate this problem.

CHAPTER ONE

1. INTRODUCTION

A highway system is typically comprised of a network of urban expressways, surface streets, bridges, intersections, computerized signals, drainage systems, utility right-of-ways, and excavations and embankments. All of these elements can be affected by seismic forces.

Transportation networks must continue to function during and after the occurrence of an earthquake, so that lifelines can continue to provide emergency services and minimize loss of life and economic distress. As evidenced in past earthquakes, highway transportation systems are often disrupted as a direct result of damage or collapse of highway system components. Of all the components of a highway system, bridges are usually considered to be the most vulnerable part to earthquake induced damage and collapse. Major earthquakes, particularly the 1989 Loma Prieta, the 1994 Northridge in California, and the 1995 Kobe earthquake in Japan, have demonstrated the seismic vulnerability of some major highway bridges, especially those bridges that were not designed or detailed to withstand the required seismic forces and displacement demands. The present study aims to study the seismic behavior and seismic capacity/demand analysis of three major bridges in Jordan and to determine the vulnerable elements of each bridge and the required retrofit scheme.

1.1. Background

A quick look at the seismic map of the Middle East shows that the Dead Sea fault is the source of the earthquakes that hit Jordan and the neighboring countries. In

fact, Jordan has experienced some major earthquakes in the past. Jarash city had encountered a high magnitude earthquake that destroyed the majority of the ancient city (Ben-Avraham et al. 2005). In 1995, a relatively strong earthquake hit the Jordan's southern port city of Aqaba which caused some material damages (Klinger et al. 2000).

Geological studies of the activities along the Dead Sea fault and the history of earthquakes that hit the area support that Jordan might encounter a major earthquake in the future (Klinger et al. 2000). Figure 1-1 shows the seismic map of Jordan based on IBC coefficients. It is clear from the figure that the capital of Jordan, where most of the population of the country is living, is located in a region of relatively moderate seismicity.

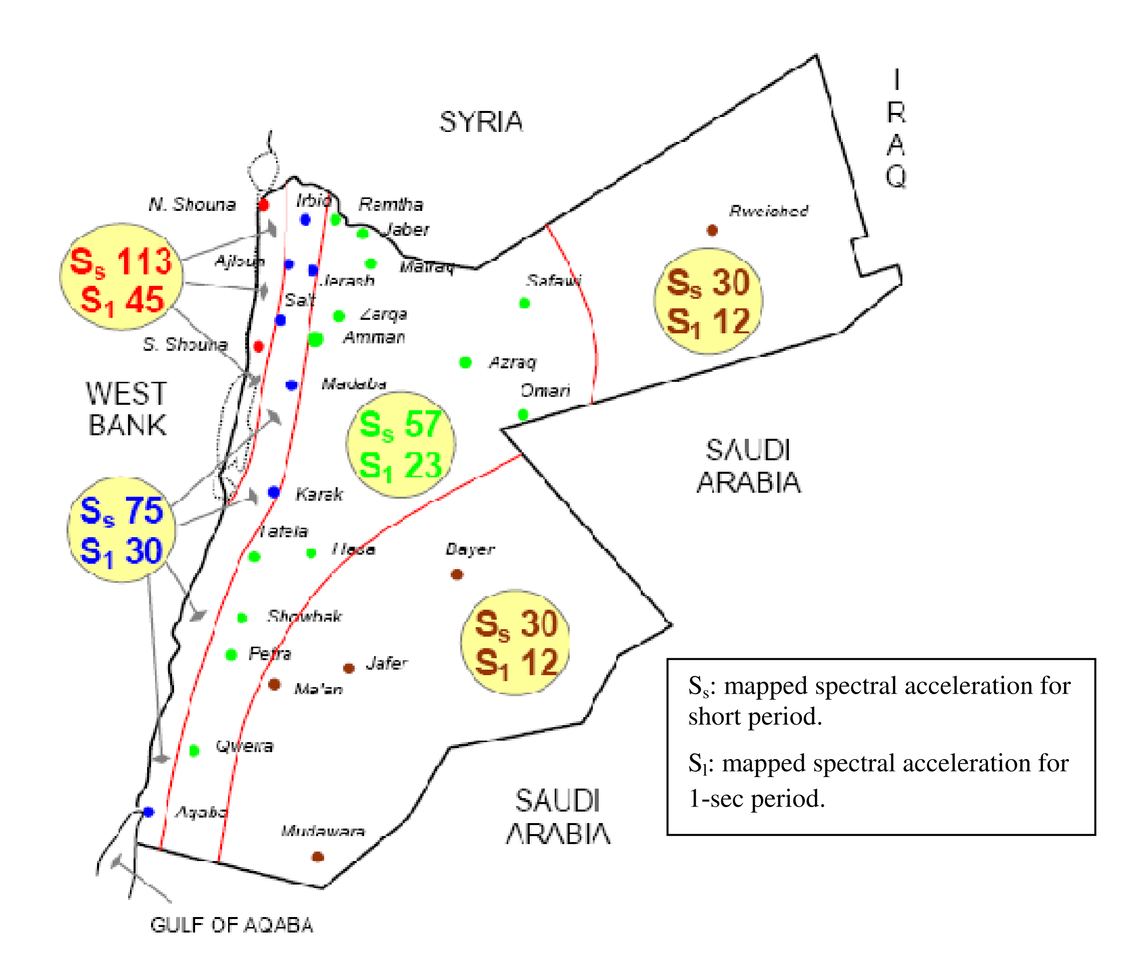


Figure 1-1: Seismic Map of Jordan (Adapted from fetweb.ju.edu.jo/narmouti, Armouti, 2010).

It is believed that the vast majority of the highway bridges in Jordan that links the major cities with the capital Amman have been designed and detailed with little to no attention to seismic design forces and displacement demands (Musmar, 2007). Therefore, it is expected that these bridges would experience some significant problems in case of a moderate to strong earthquake. Past earthquakes around the world have demonstrated the seismic vulnerability of bridges that were designed in accordance with the same design codes and guidelines that were used in designing old bridges in Jordan.

Bridge retrofitting is the most common method of mitigating risks. However, its cost may be so high that abandoning the bridge or replacing it with a new structure may be favored. Alternatively, doing nothing and accepting the consequences of damage is another possible option. The decision to retrofit, abandon, replace, or do-nothing requires that both importance and degree of vulnerability of the structure be carefully evaluated.

Seismic retrofitting attempts were firstly initiated in the United States after the 1971 San Fernando earthquake in southern California, Federal Emergency Management Agency-Seismic Retrofitting Manual for Highway Structures (FHWA-SRM, 2005). Initial retrofit measures focused on the potential for loss of support at bridge bearing seats. The principal retrofit strategy was to add restrainer cables or high strength bars within bridge superstructures in order to limit relative movements at expansion joints, and to tie individual spans to the bridge piers. After short time of this initial retrofit strategy, new earthquakes, even moderate earthquakes, caused a significant damage or failure in bridges even those had been retrofitted initially. This fact urged to initiate a higher level of evolution and retrofitting, which lead engineers to look deeply in more complicated issues like, demand ductility and deformation capacity.

1.2. Research Objectives

The purpose of this research is to study the seismic vulnerability of three vital highway bridges in Jordan according to the FHWA Seismic Retrofitting Manual for Highway Structures (FHWA-SRM, 2005). These bridges are: Alnasha Bridge, Alharamen Intersection Bridge, and Almahata Bridge. The followings are the specific objectives of the present study:

1. Establish seismic capacity/demand ratios for critical elements of the as-built structures in accordance with the recommendations of the FHWA-SRM, 2005,
2. Identify the seismic vulnerabilities of the selected highway bridges,
3. Propose proper retrofit schemes based on the identified vulnerabilities,
4. And, draw conclusions on the feasibility and effectiveness of the proposed retrofit schemes.

A linear response spectrum analysis was performed and the seismic demands were determined based on an earthquake event having a ten percent probability of exceedance in 50 years (approximate return period of 500 years). A three dimensional model representing the as-built condition of the bridges was created using the software SAP2000 (CSI, 2008). The seismic demand on the bridges was determined from the mathematical models. The capacity of the bridges elements were determined based on the FHWA-SRM (2005) recommendation and a capacity/demand ratio was established for each critical element that is sustainable to be damaged or failed by the design earthquake. For each pier in each candidate bridge, pushover analysis was also conducted utilizing the software SAP2000 to determine the displacement capacity in both longitudinal and transverse directions.

Based on the capacity/demand ratios, proper retrofit schemes that are feasible and effective were proposed to enhance the overall performance of the bridges. Since the retrofitting solutions change the structural characteristics of the bridge under consideration, its global seismic behavior could be changed. Therefore, the seismic demand on the bridge elements was checked again to make sure that the retrofitted elements do not impact inversely the other elements.

1.3. Research Methodology

The main objective of the present study is to investigate the seismic vulnerability of some vital highway bridges in Jordan. This objective was performed through investigating the seismic vulnerability of three candidate bridges. A linear response spectrum analysis was performed and the seismic demands were determined based on an earthquake event having a ten percent probability of exceedance in 50 years (approximate return period of 500 years).

The structural capacity of each bridge element was determined based on information shown in the as-built drawings. The nominal capacities of structural elements were determined using a capacity reduction factor equal to one. The force demands were established by performing a multimode elastic analysis using the software SAP2000.

As the next step, capacity/demand (C/D) ratios were used to quantify the likely performance of the candidate bridges during an earthquake. These C/D ratios can be thought of as that fraction of the design earthquake which will cause a member or component to be damaged. The consequences of this damage must then be assessed in terms of its effect on the stability and usability of the bridge following an earthquake.

The following is C/D ratios for various members and components distributed in four categories as presented in FHWA-SRM, 2005:

1. Support length and restrainer C/D ratios:

r_{ad}: displacement C/D ratio for abutment

r_{bd}: displacement C/D ratio for bearing seat or expansion joint

r_{bf}: force C/D ratio for bearing or expansion joint restrainer

2. Column C/D ratios:

r_{ca}: anchorage length C/D ratio for column longitudinal reinforcement

r_{cc}: confinement C/D ratio for column transverse reinforcement

r_{cs}: splice length C/D ratio for column longitudinal reinforcement

r_{cv}: shear force C/D ratio for column

r_{ec}: bending moment C/D ratio for column

3. Footing C/D ratios:

r_{ef}: bending moment C/D ratio for footing

r_{fr}: rotation C/D ratio for footing

4. Soil C/D ratio:

r_{sl}: acceleration C/D ratio for liquefaction potential

The relative magnitudes of these ratios were used to sequentially upgrade a deficient bridge. The preceding C/D ratios were calculated as needed for each bridge included in the study.

Seven evaluation methods are described in FHWA-SRM (2005), which are Method A1, A2, B, C, D1, D2, and E. They are listed in order of increasing sophistication and rigor. All six methods are described in detail in Chapter 4.

Method C, as described in the SRM for Highway Bridges Part 1 – Bridges published by MCEER (the Multidisciplinary and the National Center for Earthquake

Engineering Research) for the Federal Highway Administration (2005), evaluates the adequacy of bridge substructure elements susceptible to damage during a design level earthquake by calculating a force based Capacity/Demand ratio for each structural element. A Capacity/Demand ratio value less than one indicates a structural deficiency and a potential need for seismic retrofit of a structural element. Capacity/Demand ratios can also be used to evaluate the effectiveness of seismic retrofit schemes.

The flowchart below summaries the procedures mentioned in FHWA-SRM, 2005:

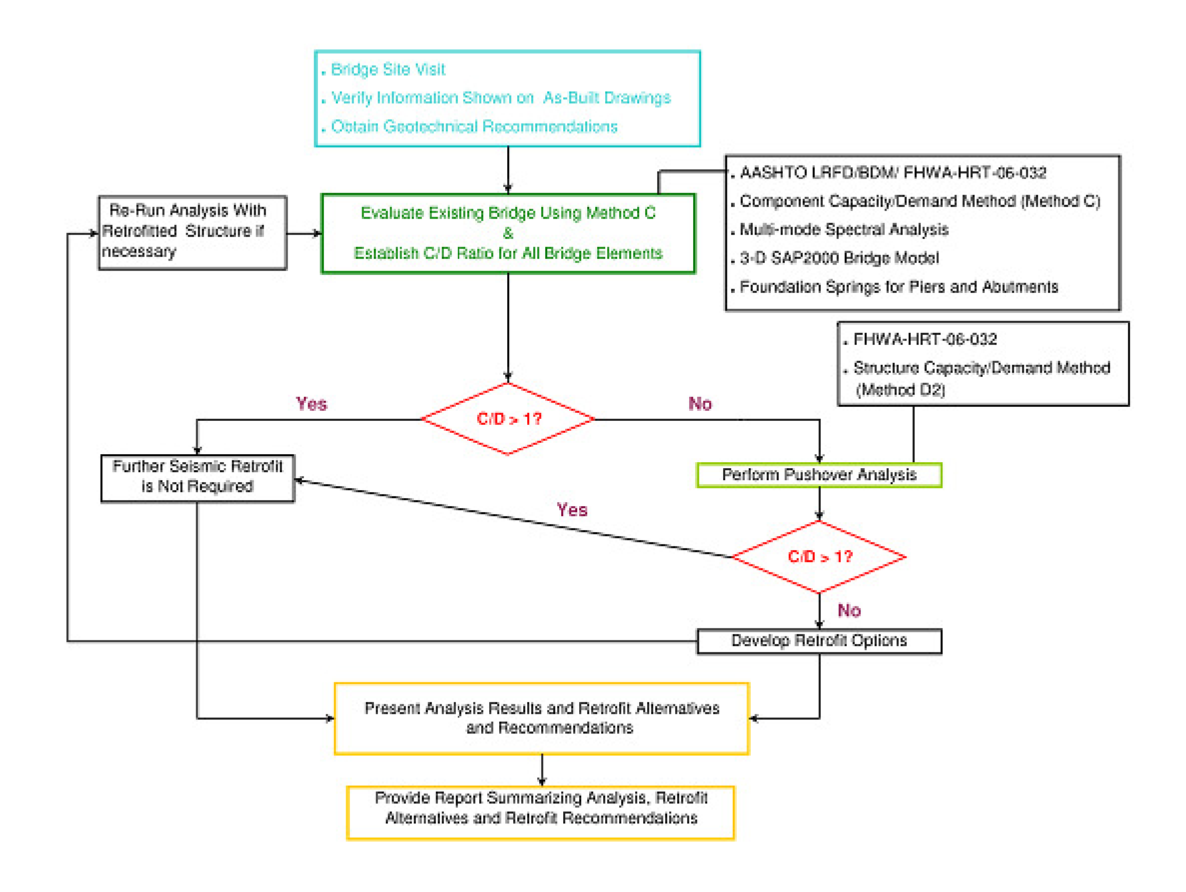


Figure 1-2: Overview of the retrofitting process for highway bridges

Once the moment Capacity/Demand ratios for the column, r_{ec}, and the footing, r_{ef}, are calculated, four cases describing the Capacity/Demand ratios that should be further investigated are identified. A column moment Capacity/Demand ratio less than

1.0 is not necessarily an indication of a need for seismic retrofit, as long as the column exhibits a ductile response under a design level seismic event. To ensure an acceptable column ductile behavior, the Capacity/Demand ratios for the anchorage and lap splice of the longitudinal reinforcement along with transverse confinement reinforcement are required to be larger than 1.0. Similarly, a footing Capacity/Demand ratio less than 1.0 may be acceptable as long as the footing does not fail in a brittle mode of failure and the footing rotation Capacity/Demand ratio is larger than 1.0. The four cases based on the relative magnitude of the column and footing Capacity/Demand ratios are identified as follows:

Method C, Case I: Both r_{ec} *and* r_{ef} *exceed 0.8*

The footing and column for this case are not expected to yield; therefore, an evaluation of their ductility is not necessary. The Capacity/Demand ratios for anchorage and lap splices of longitudinal reinforcement are the only ratios, which will need to be reported.

Method C, Case II – r_{ef} *is less than 0.8 and* r_{ec} *either exceeds 0.8 or exceeds* r_{ef} *by 25 percent*

In this case, it is assumed that the footing is more likely to yield or rotate before the column. Therefore, this case will require an evaluation of the footing’s ability to rotate and or yield. If anchorage and lap splice Capacity/Demand ratios were found to be less than 80 percent of r_{ef}, then anchorage and lap splice failure may be assumed to occur first, and an evaluation of the footing rotation and yielding is not required.

Method C, Case III – r_{ec} is less than 0.8 and r_{ef} either exceeds 0.8 or exceeds r_{ec} by 25 percent

In this case, it is assumed that the column is more likely to yield before the footing. Therefore, this case only requires an evaluation of column ductility and its ability to withstand plastic hinging. Column Capacity/Demand ratios for anchorage and lap splice of longitudinal reinforcement and transverse confinement reinforcement are required to be reported.

Method C, Case IV – r_{ec} and r_{ef} are both less than 0.8 and are within 25 percent of one another

In this case, it is assumed that the footing and column are equally likely to yield or rotate. Therefore, an evaluation of the footing's and column's ability to yield and rotate is required. If the column Capacity/Demand ratios for anchorage and lap splice of longitudinal reinforcement and transverse confinement reinforcement are found to be larger than 80 percent of r_{ef}, then the Capacity/Demand ratio for the footing rotation or yielding should be calculated.

In Method D2, seismic demands are determined by elastic methods such as the multi-mode response spectrum method. Capacity assessment is based on the displacement capacity of individual piers as determined by a pushover analysis, which includes the nonlinear behavior of the inelastic components. This method is suitable for all bridges in SRC C and D. It is also known as the Pushover Method or alternatively the Nonlinear Static Procedure.

After all required method of evaluation, Method C and/ or D2, have been conducted, retrofitting schemes were determined for each defected element, as needed.

CHAPTER TWO

2. LITRETURE REVEIW

It is believed that the majority of the highway bridges in Jordan, that were built in 1970's and 1980's, were designed and detailed with little to no attention to seismic design forces and displacement demands (Musmar, 2007). At the time, the main intention of the design was to satisfy the strength limit state and insure that the bridge elements are able to withstand the required level of forces with little to no consideration of the seismic displacement demand and the reinforcement detailing like bars cutoff location, development length, and lap splices.

In this Chapter, bridge deficiencies under the effect of seismic forces are detailed, and the corresponding retrofitting technique of bridge components are presented. A review of the up-to-date research related to the global performance of bridge retrofit and strengthening techniques is included.

2.1. Bridges Deficiencies and Corresponding Retrofit Scheme

2.1.1. Superstructure

Bridges often comprise a series of simple spans supported on bents. These spans are sustainable to being toppled from their supporting substructures either due to shaking or differential support movement associated with ground deformation. The most common superstructure failure mode due to unexpected seismic forces is unseating at movement joints due to the large anticipated displacements. Figure 2-1 shows unseating failure of a simply supported link span.



Figure 2-1: Nishinomiya-ko Bridge approach span unseating in the 1995 Hyogo-Ken Nanbu earthquake (Adapted from Bridge engineering handbook, 2000)

In skewed bridges, where the support lines are skewed to the bridge axis, it has been observed that the skewed spans usually develop larger displacement than the right spans. This behavior is believed to be caused as a consequence of the tendency for the skew span to rotate in the direction of decreasing skew, thus tending to drop off the support at the acute corner (Priestley, et al. 1996). The resulting rotation is due to a combination of longitudinal and transverse response and is illustrated schematically in Figure 2-2. The figure shows that the transverse movement in either direction will cause binding in one obtuse corner, causing a clockwise rotation.

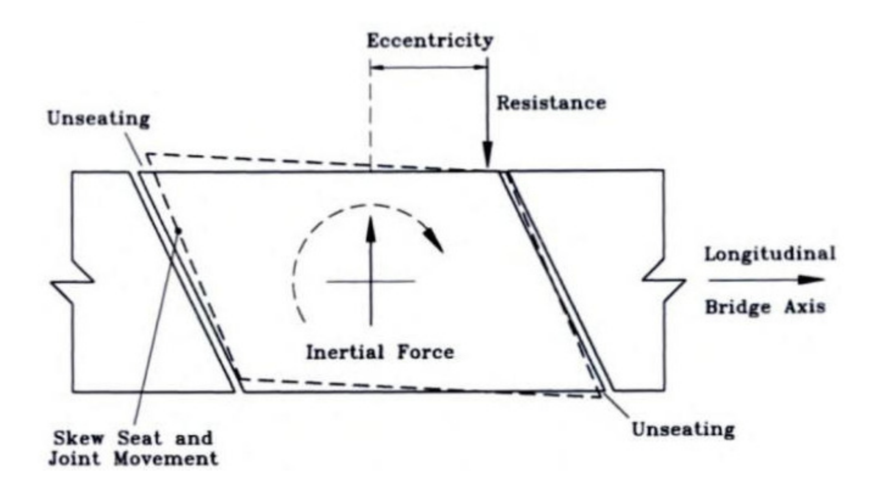
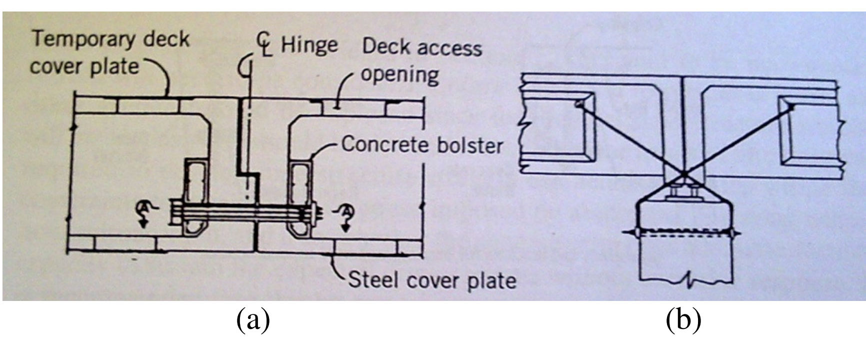


Figure 2-2: Unseating due to bridge skew (Adapted from Priestley et al. 1996).

There are two possible retrofitting schemes when displacements at movement joints are judged to be excessive. Restrainers may be placed across the joint in attempt to reduce the relative displacements between adjacent spans of the bridge, or the displacement capacity of the movement joint can be increased. Often both actions are taken. The following is a discussion on the two retrofitting schemes:

(a) **Restrainers:** As well as being used to restrain displacements, restrainers may be placed in order that longitudinal seismic force can be transferred between adjacent frames. Flexible restrainers used in California typically use high-strength steel cables anchored to the diaphragms or webs of concrete bridges, as shown in Figure 2-3, or to the bottom flange of steel girders, as shown in Figure 2-4 (Priestley, et al. 1996). Another form of restraining displacement is to use looping cables around the bent cap which anchors the spans to the bent cap as well as to the adjacent spans.



(a) (b)

Figure 2-3: Cable restrainers for concrete superstructure movement joints. (a) Box-girder bridges; (b) I-girder bridges (Adapted from Priestley et al. 1996).

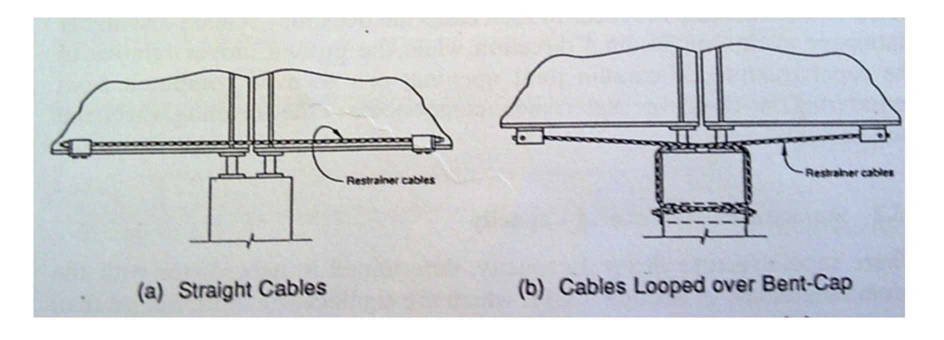
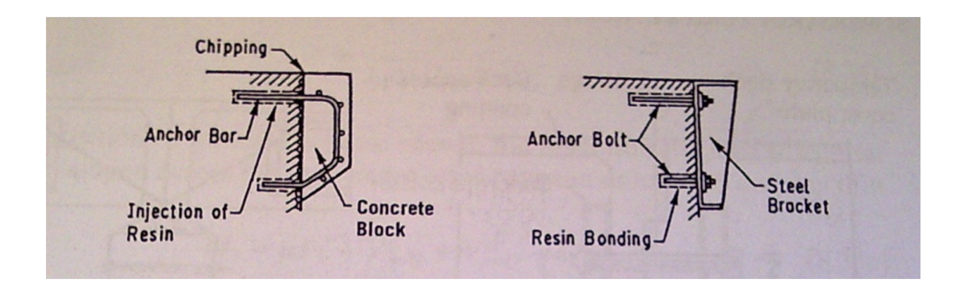
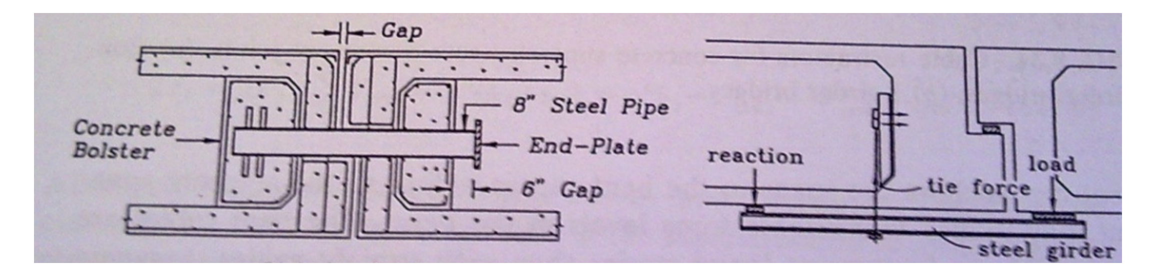


Figure 2-4: Cable restrainers for steel superstructure movement joints (Adapted from Priestley et al. 1996).

(b) Seat Extenders: Seat extenders are generally comparatively simple and inexpensive to install (Chen and Lian, 2000). Support lengths at abutments or under simply supported spans may be increased by corbels or brackets added to the sides of abutments or bents, as shown in Figure 2-5a. With internal movement joints, where the seating is provided within the depth of the superstructure section, direct seat extension is not possible. Figure 2-5b shows two alternatives that have been developed by California Department of Transportation (Caltrans) for use in California. The first alternative involves thick-walled pipe seat extenders which are connected to the diaphragm on one side of a movement joint and slide freely through the other diaphragm. The second alternative copmrises a series of underslung beams that are bolted to the diaphragm of the supporting half of the movement joint and designed to carry the span by cantilever action if unseating occurs.



(a) extended corbels and brackets for bearing supported superstructures



(a) devices for support following unseating at internal movement joints

Figure 2-5: Seat extension to accommodate large longitudinal displacements (Adapted from Priestley et al. 1996).

2.1.2. Columns

Many older bridges were designed primarily for gravity loads with little or no consideration of lateral forces from seismic loading (Endeshaw, 2008). As a result, older columns lack sufficient transverse reinforcement to provide satisfactory performance in a major seismic event. Typically, 10 mm or 12 mm diameter hoops distributed transversely at 300 mm on center were used in columns regardless of the column cross-sectional dimensions. The hoops were anchored by 90-degree hooks with short extensions which become ineffective once the cover concrete spalls. Furthermore, intermediate ties were rarely used. These details result in many older columns being susceptible to shear failure, and the hoops provide insufficient confinement to develop the full flexural capacity of the column. The limited level of confinement is also unable to prevent buckling of the longitudinal reinforcement once spalling of the cover concrete occurs. Figure 2-6 shows failure of columns due to lack of confinement.



Figure 2-6: Failure of columns of the Route 5/210 interchange during the 1971 San Fernando earthquake (Adapted from Bridge engineering handbook, 2000).

Lap splices of longitudinal reinforcement in older reinforced-concrete bridges may be vulnerable because, typically, the splices are short (on the order of 20 to 30 bar diameters), poorly confined and are located in regions of high flexural demand. In particular, for construction convenience splices are often located directly above the footing. With these details, the splices may be unable to develop the flexural capacity of the column, and thus the columns may be more vulnerable to shear failure. Figure 2-7 shows failure of columns due to short length of the lap splice.

Concrete columns also can fail if the anchorage of the longitudinal reinforcement is inadequate. Such failures can occur both at the top of a column at the connection with the bent cap and at the bottom of a column at the connection with the foundation. Figure 2-8 shows pullout failure of column longitudinal reinforcement.



Figure 2-7: Bond failure of lap splices at column base, 1989 Loma Prieta earthquake (Adapted from Priestley et al. 1996).



Figure 2-8: Pullout failure, 1971 San Fernando earthquake (Adapted from www: ace-mrl.engin.umich.edu).

Previous studies have shown that steel jacketing is an effective retrofit technique for seismically-deficient concrete columns. Based on satisfactory laboratory results, steel jackets have been employed to retrofit both circular and rectangular columns around the world (Itani and Liao, 2003). For circular columns, two half circle steel shells, which have been rolled to a radius equal to the column radius plus ½ in. (13 mm) to 1 in. (25 mm) for clearance, are positioned over the portion of the column to be retrofitted, and the vertical seams are then welded (FHWA, 2006). The space between the jacket and the column is flushed with water and then filled with a pure cement grout. To avoid any significant increase in the column flexural strength, a gap of approximately 2 in. (50 mm) is typically provided between the end of the jacket and any supporting member (e.g., footing, cap beam, or girders). This gap will insure that at large drift angles, the jacket will not act as a compression member as it bears against the supporting members (Itani and Liao, 2003).

When the column cross section is rectangular, a rectangular steel jacket will be effective for enhancing the shear resisting capacity. However, for rectangular columns lacking proper confinement and with lap splices at the base of the columns, the rectangular cross section is often modified into oval/elliptical shape before a steel jacket is applied using similar procedures as for circular columns (Chai et al. 1991; FHWA-SRM, 2005; Priestley et al. 1996). Figure 2-9 shows steel jacketing general practicing approach for both circular and rectangular column sections.

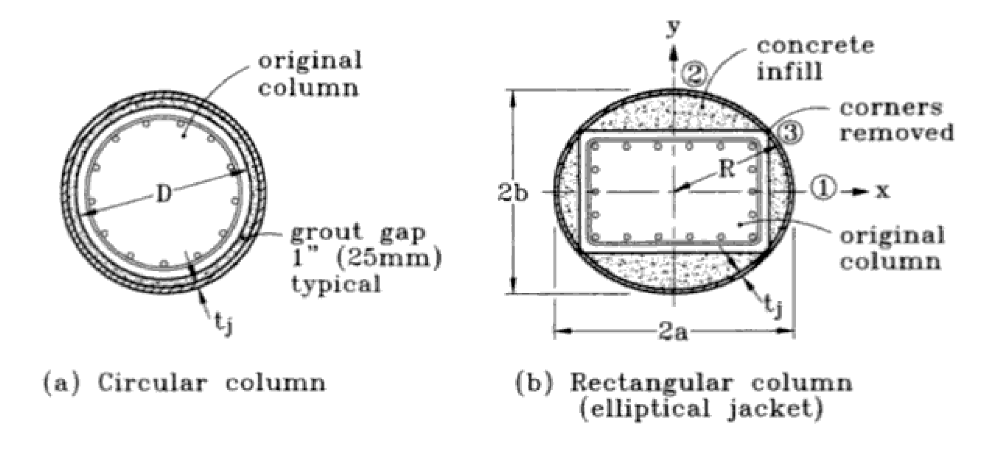


Figure 2-9: Confinement of columns by steel jacketing (Adapted from Priestley et al. 1996).

Yeou-Fong Li et al, (2005) presented theoretical and experimental results of two as-built circular reinforced concrete bridge columns and two columns retrofitted with steel jackets. A constitutive model for concrete confined by a steel jacket was also proposed. The proposed model was implemented into a sectional analysis to predict the lateral load-deformation relationship of the retrofitted columns. Two-fifth scaled reinforced concrete bridge columns were designed based on the standard details of the existing bridge columns mostly built in late 1980s and early 1990s, in Taiwan. Displacement-controlled cyclic loading tests were conducted to obtain the seismic performance of the columns. The experimental results showed that the bridge column

retrofitted with steel jacketing could greatly improve seismic performance measured based by the strength and ductility.

2.1.3. Beams

In the weak column strong beam philosophy, beams are always required to remain elastic under the effect of seismic forces. In addition, beams are generally built integrally with the superstructure deck so they are strong enough to withstand seismic forces. Typically, beams are built perpendicular to the center line of the bridge so it will not receive any significant seismic forces from the longitudinal seismic excitation which is usually govern the first mode in typical highway bridges.

Beams, specially cap beams, can be susceptible to significant deficiencies in three areas: (1) shear capacity, particularly where seismic and gravity shears are additive; (2) premature termination of cap beam negative moment, top reinforcement; and (3) insufficient anchor of cap beam reinforcement into the end regions. Figure 2-10 shows an uncollapsed portion of the Cyperess viaduct, where a wide flexural crack has formed at the inner face of a column as a result of the inadequate anchorage length of the beam reinforcement.

The cost of cap beams retrofit is usually high besides the fact that the construction can be complicated. One method to reduce the cap beam seismic forces is to launch a link beam at proper height to redistribute the load demand. If flexural strength of cap beam is to be enhanced, reinforced concrete bolsters can be added to the sides of existing cap beams after roughening the interface. The new and old concrete members should be connected by dowels, preferably passing through the existing cap beam. Thus, the section of the integral cap beam is enlarged, and shear strength can be

increased. Figure 2-11 shows a schematic view of a cap beam strengthened by reinforced concrete bolsters.

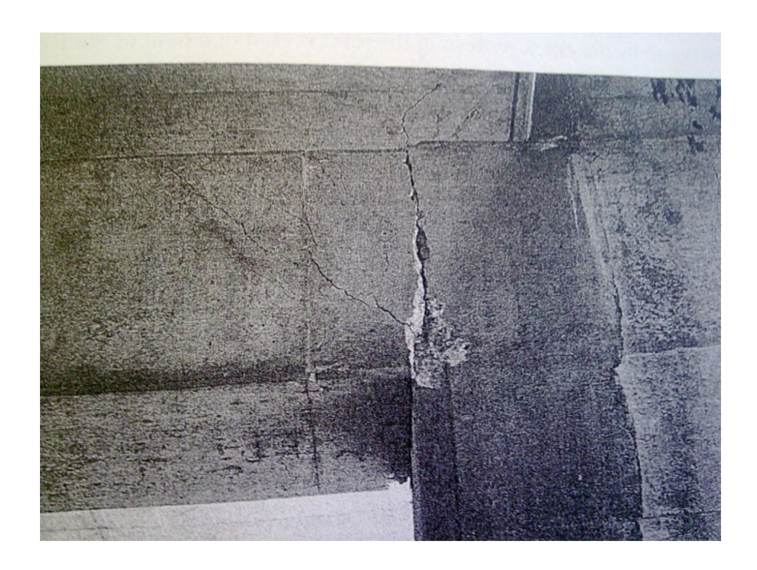


Figure 2-10: Cap beam positive moment cracks at inner column face, 1989 Loma Prieta earthquake (Adapted from Priestley et al. 1996).

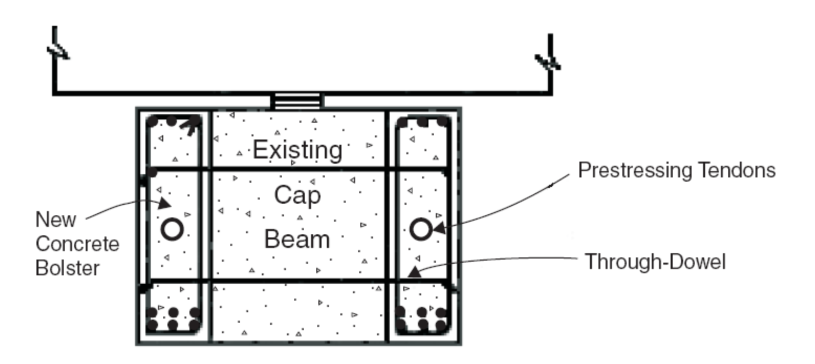


Figure 2-11: Flexural and shear retrofit of free standing multi-column bents (Adapted from FHWA-SRM, 2005).

An alternative, or supplemental means of flexural strength enhancement is to prestress the cap beam using strong-backs at the cap beam ends. The prestress may be inside bolsters, as shown in Figure 2-11, or using external prestress without bolsters. In this case the prestress essentially acts as an additional axial compression force on the cap beam, hence enhancing its flexural strength.

2.1.4. Joints

Through connections between cap beams and columns, member forces transfer results in horizontal and vertical joint shear forces that may be many times higher than the shear forces in the connected members. It has been uncommon for these shear forces to be considered in bridge design, and until recently, properly designed joint shear reinforcement was almost never provided (Priestley, et al. 1996). Without this reinforcement, joint shear failure may occur. Figure 2-12 shows a joint shear failure in the I-880 viaduct in California after the 1989 Loma Prieta earthquake.

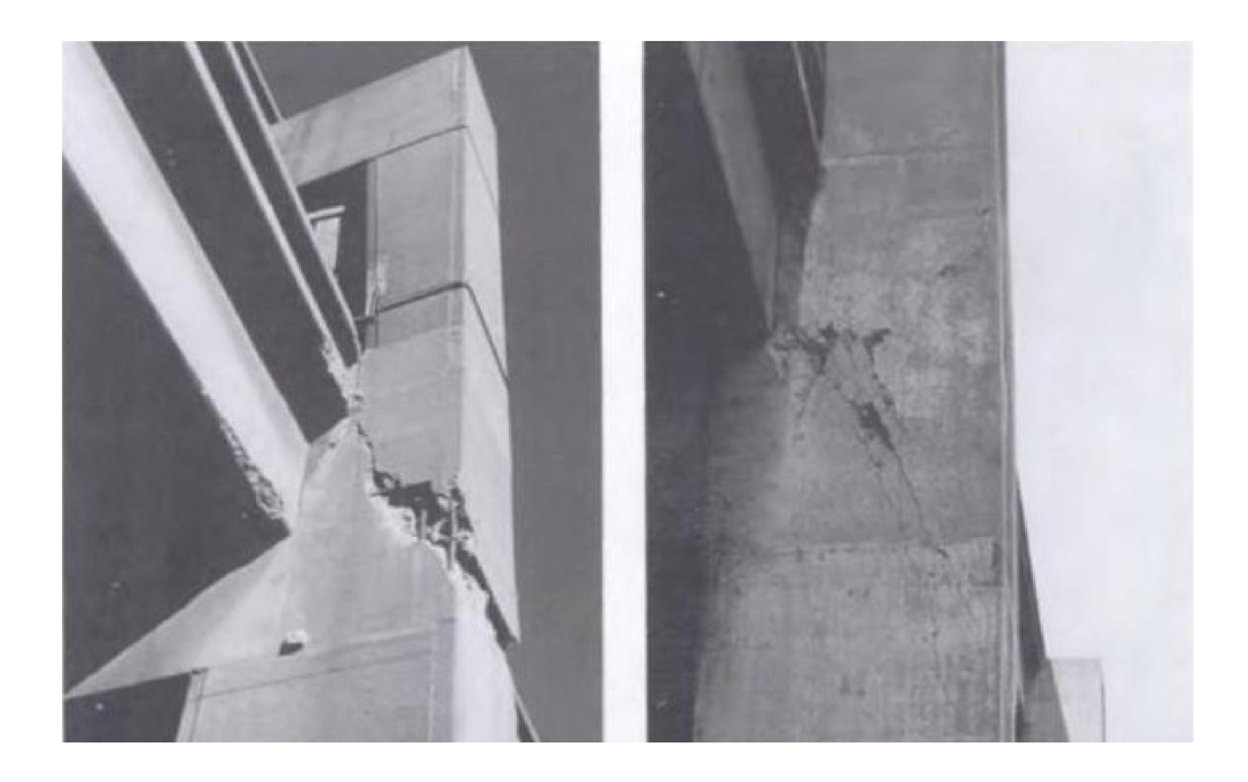


Figure 2-12: Joint shear failure, 1989 Loma Prieta earthquake. (a) I-880 viaduct; (b) Embarcadero viaduct (Adapted from Priestley et al. 1996).

Priestly et al, (1996) discussed different methods to retrofit bridge joints. The first alternative includes joint force reduction by adding link-beam to the bridge piers which will result in reducing of joint forces and cap beam forces as well. The second alternative is to accept the probability of damage in a major earthquake with subsequent

joint repair or replacement. The third alternative includes addition of prestressing which will reduce the tendency for joint cracking because of the increase in horizontal stress. And the fourth alternative comprises concrete jacketing which extend beyond the original joint dimensions into the cap beam and column, utilizing a haunch, and increasing of the joint thickness, thus reducing joint stress level, as shown schematically in Figure 2-13.

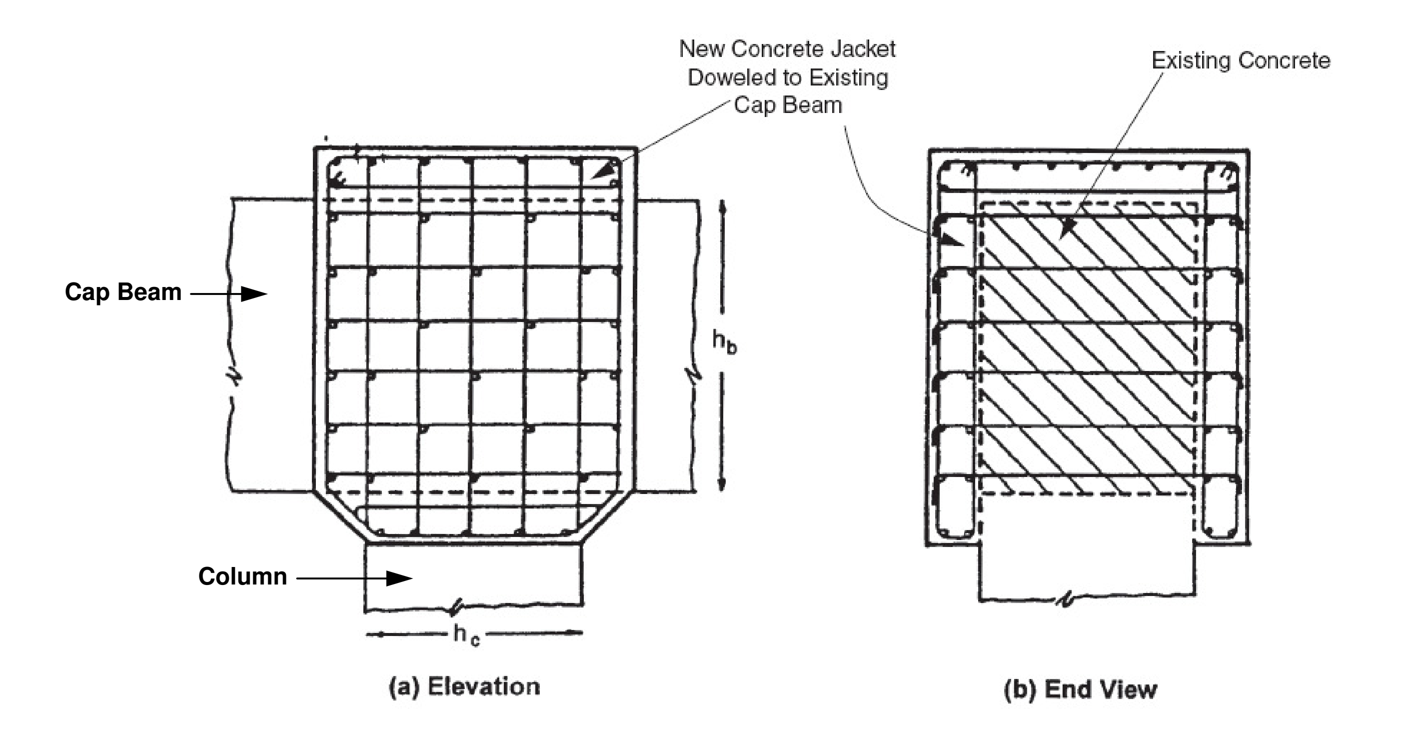


Figure 2-13: Joint retrofit with external concrete jacket (Adapted from FHWA-SRM, 2005)

McLean and Shattarat, (2005) conducted an experimental test on seven 1/3-scale specimens to define the vulnerabilities of existing outrigger knee joints under in-plane and out-of-plane seismic loading and to develop appropriate retrofit measures that address the identified vulnerabilities. The specimens represented bents with short and long outrigger beams in the SR-99 Spokane Street Overcrossing in western Washington State. The retrofit measures developed in this study consisted of an elbow-shaped steel jacket around the beam and the joint region. The retrofitted specimens formed a plastic

hinge in a gap introduced at the top of the column with improved ductility, torsional strength, and energy dissipation capacities when compared to the behavior of the similar as-built specimens. Figure 2-14 shows the elbow-shaped steel jacket that was used to retrofit the outrigger knee system.



Figure 2-14: A Picture of the Clamshell Used in the Retrofit of the Beam-Joint (Adapted from McLean and Shattarat, 2005).

2.1.5. Foundation

Very limited literature discussed the failure of foundation due to seismic forces as it is hard to investigate such failure below the ground surface level. Older bridges foundation were typically designed based on gravity loads only without consideration of seismic forces. This design may lead to failure in the footings due to overturning, sliding, or even flexural failure due to lack of top of reinforcement.

Priestley et al. (1996) and despite the lack of reported damage analyzed typical details common in earlier footing designs and revealed the following deficiencies: The first deficiency is footing flexural strength deficiency particularly due to the common omission of a top reinforcement mat. The second one is footing shear deficiency, since footing shear reinforcement was rarely provided. The third deficiency is joint shear strength deficiency in the region immediately below the column, which is subjected to

high shear forces, as with the cap beam-column connections. The fourth deficiency is anchorage and development of column reinforcement deficiency; and the last deficiency is due to inadequate connection between tension piles and footing.

Retrofitting of foundations, either is it shallow or deep, is an expensive process and complicated at the same time, because it needs high-tech construction methods (Itani and Liao, 2003). Increasing the foundation size and adding additional piles, if necessary, is one of the most common foundation retrofitting techniques. Figure 2-15 shows an existing bridge foundation to be enlarged with additional piles.

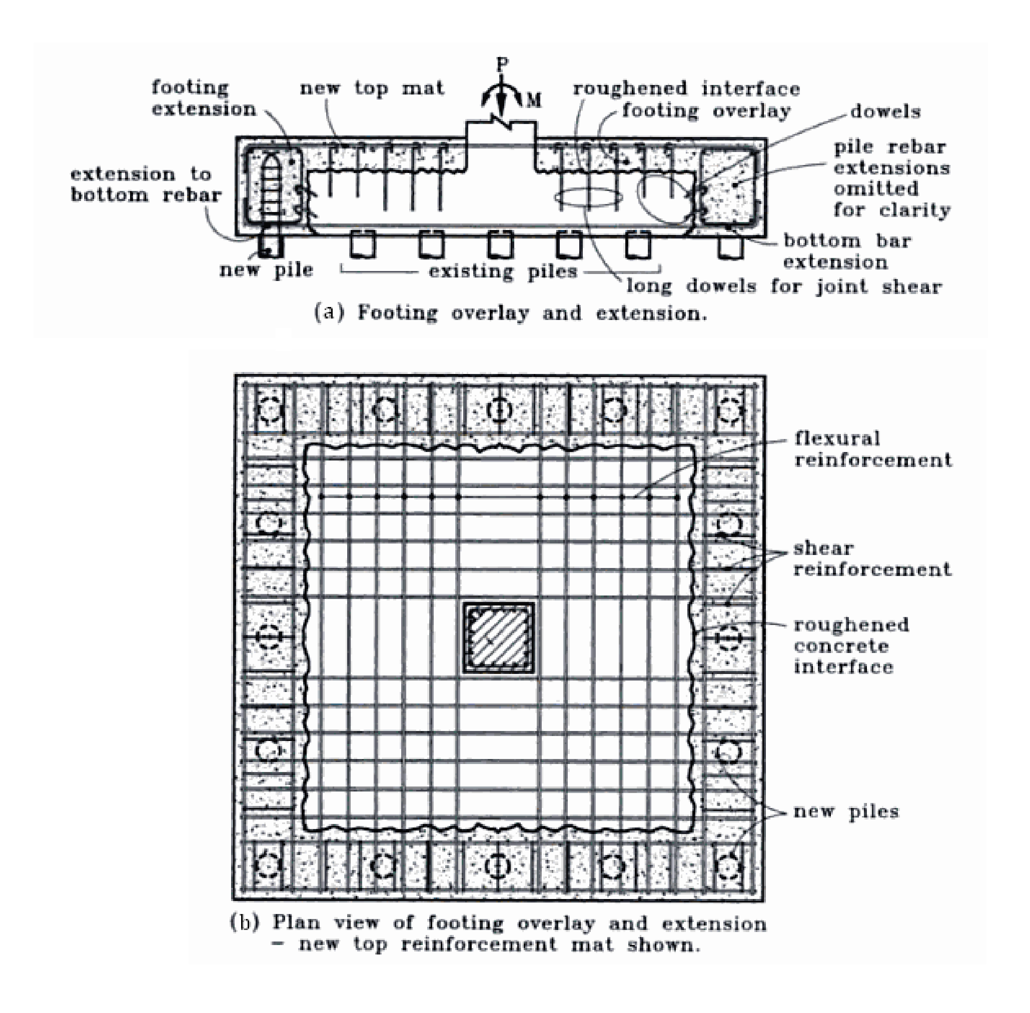


Figure 2-15: Footing retrofit measures (Adapted from Priestley et al. 1996).

2.1.6. Abutments

Under bridge longitudinal response, earth pressure on the abutment increases due to seismic acceleration. Impact of the bridge acceleration and the abutment acceleration may generate high passive pressure, which will induce an increase in lateral pressure at levels below the point of deck or superstructure impact. Inadequately compacted natural or fill soils tend to slump toward the bridge, pushing the lower part of the abutment inward with the moving soil. Contact between the top of the abutment and the superstructure limits the inward displacement at the top, resulting in a rotation of the abutment. Figure 2-16 shows typical consequences and damage to the top of the abutment backwall from the superstructure impact, and damage to the pile support system if abutment rotations are large.

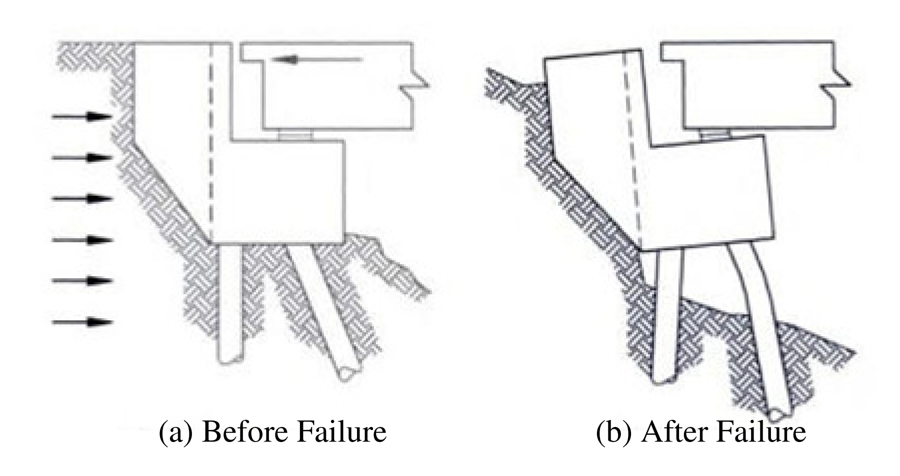


Figure 2-16: Abutment slumping and rotation (Adapted from Priestley et al. 1996).

In case of integral abutment, when an abutment is driven into an approach fill during an earthquake, large passive pressures on the back of the abutment wall are generated (FHWA-SRM, 2005). This can result in structural failure of the wall that will, in turn, reduce the passive resistance at the back of the wall. If displacements are sufficiently large, support can be lost at the abutment, severely damaging the bridge and rendering it

unusable. To avoid this type of failure, it may be necessary to strengthen the wall. This can be done by constructing a reinforced concrete overlay on the face of the abutment wall, as shown in Figure 2-17. If the old and new concrete can be made to act as a composite member, then the entire section may be considered effective in resisting the forces generated by the passive soil pressure. To achieve composite action, the existing concrete surface should be roughened and the overlay must be connected to the existing backwall with a sufficient number of dowels to provide for shear transfer through friction at the interface between the existing and new concrete. In addition, flexural reinforcement in the overlay must be continuous or, as a minimum, adequately spliced.

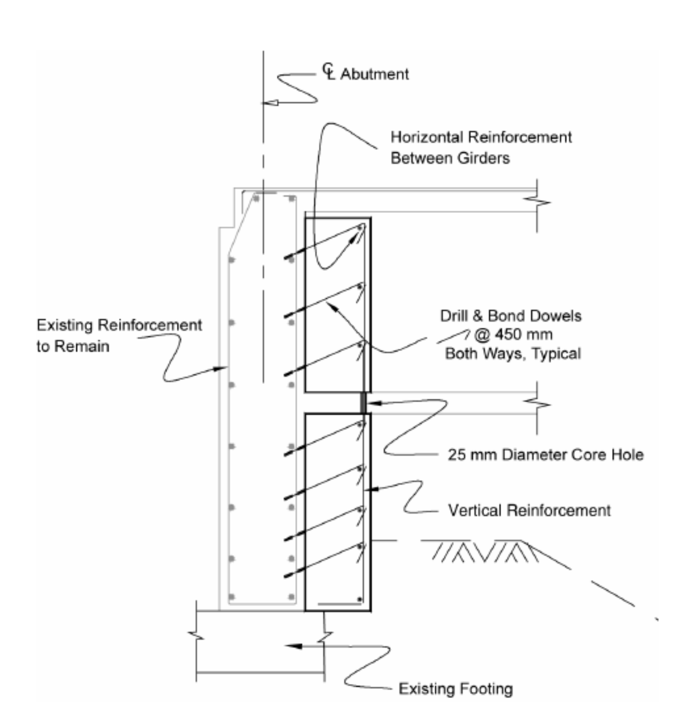


Figure 2-17: Diaphragm abutment overlay (Adapted from FHWA-SRM, 2005)

CHAPTER THREE

3. BRIDGE MODELING

Three bridges were selected for the purpose of the present study. They are: Alnasha Bridge, Alharamain Bridge, and Almahata Bridge. These bridges are considered vital links in the local highway transportation system of the country. This chapter includes a description of each bridge and the associated mathematical model.

3.1. Alnasha Bridge

3.1.1. Bridge Description

Figure 3-1 shows an Aerial view of Alnasha Bridge. The bridge is on Alyarmouk Street crossing King Abdullah I Street. This bridge carries 68,624 AVDT as reported in a traffic study conducted by Amman Greater Municipality, 2008.

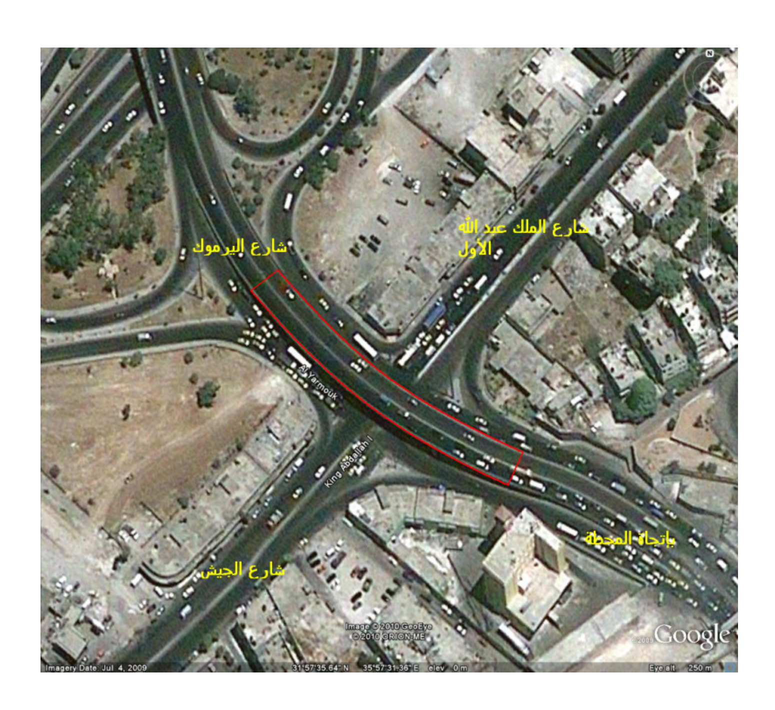


Figure 3-1: Aerial View of Alnasha Bridge (Adapted from Google Earth, USA)

Alnasha Bridge is a seven-span bridge with a total length of 141.22 m. Figure 3-2 shows a general view of the bridge. The outer spans are 18.82 m long, while the interior spans are 18.83 m long, except the middle span, which is 28.27 m long. The abutment walls simply support the superstructure at the ends of the bridge. Expansion joints were installed across pier #3 and pier #6. The bridge elevation and plan views are shown in Figures 3-3.



Figure 3-2: A general view of Alnasha Bridge.

The deck is cast-in-place, reinforced concrete voided slab section with an overall average width of 14.7 m and a 13.7 m roadway width. The depth of the deck is 1.6 m. The bridge deck cross-section is shown in Figure 3-4.

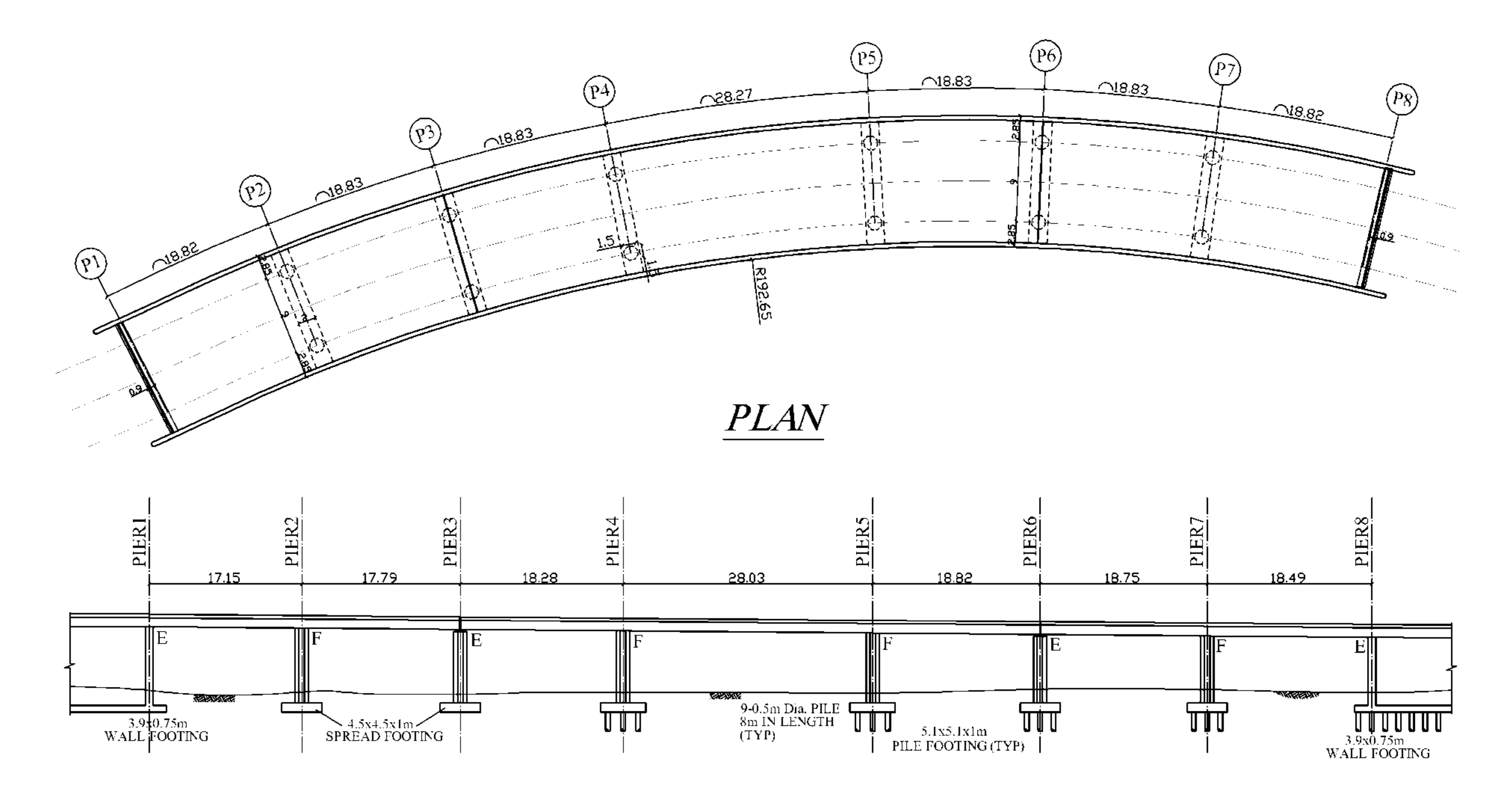


Figure 3-3: Alnasha Bridge - plan & elevation, dimensions in meter (Adapted from Greater Amman Municipality).

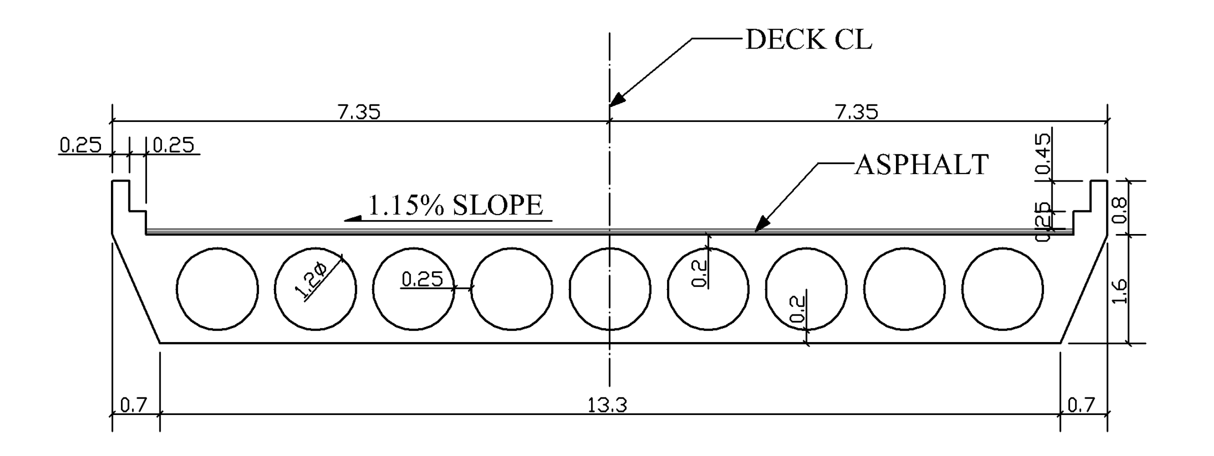
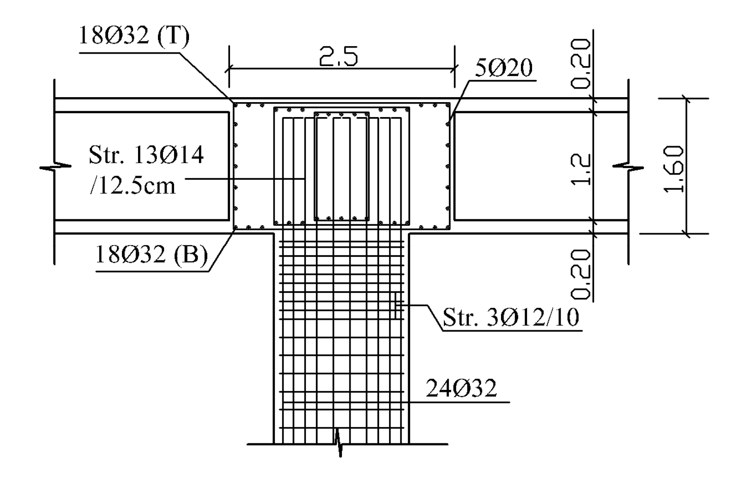


Figure 3-4: Alnasha Bridge deck typical section (Dimensions in meter).

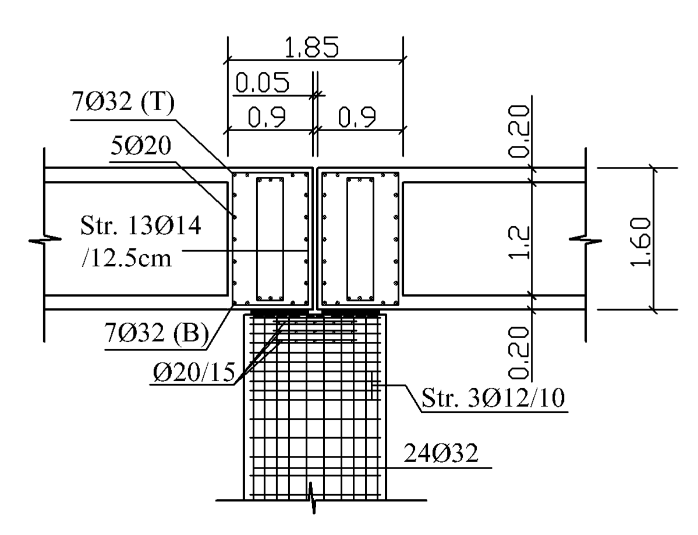
At each interior integral pier, a 2.0 m wide by 1.6 m deep transverse crossbeam distributes the bridge loads to a couple of columns. At pier #3 and pier #6, where expansion joints were installed, a couple of 0.90 m wide by 1.6 m deep transverse diaphragms separated by 50 mm gap distributes the bridge loads to a couple of columns.

The columns at pier #2 and pier #3 are 1.7 m and 3.13 m long, respectively. The longest columns are located at pier #4 and pier #5 which are 6.22 m and 6.46 m long, respectively. The shortest columns have a length of 1.7 m and are located at pier #7. Pier #6 columns are 3.13 m long.

The columns have an octagonal shape which is 1.5 m in diameter with a clear cover of 40 mm, reinforced by three 12 mm diameter stirrups spaced at 200 mm on center. Column transverse reinforcement spacing is changed to 100 mm at a distance 0.95 m below the soffit of the cross beam. Longitudinal reinforcement of the column is comprised of 24 equally spaced 32 mm diameter bars. The column lap splice length is 2.0 m which starts at 1.5 m above the base level. Integral and non-integral piers details are shown in Figure 3-5.



(a) Integral Pier details.



(b) Non-Integral Pier details.

Figure 3-5: Integral and Non-Integral piers details (Dimensions in meter).

All spread footings and pile caps are located 1.5 m below the existing ground level. Pier #2 and pier #3 are supported by square spread footings that are 1.0 m deep and 4.5 m long. The reinforcement in the spread footings consist of a top mesh of 20 mm diameter bars spaced at 300 mm and a bottom mesh of 20 mm diameter bars spaced at 150 mm. Spread footing details are shown in Figure 3-6.

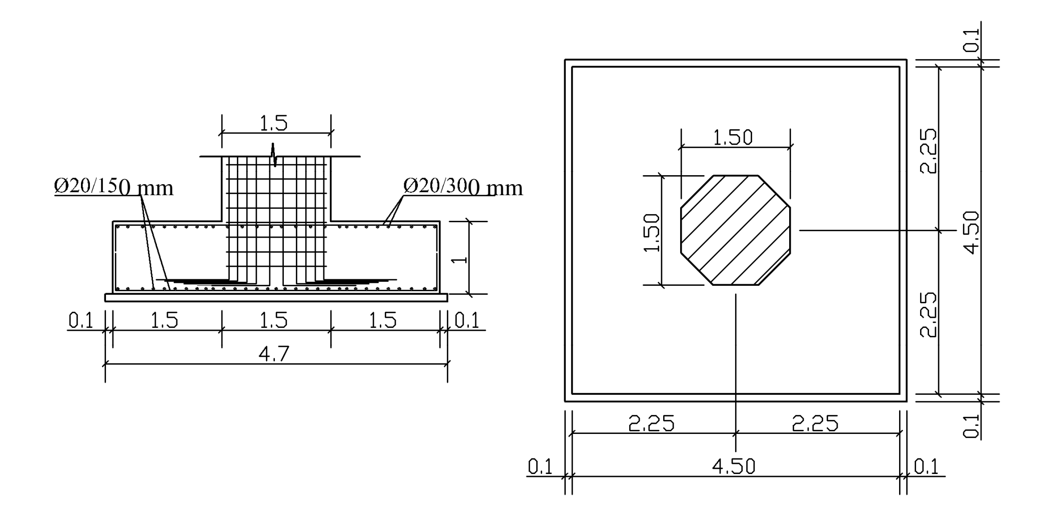


Figure 3-6: Alnasha Bridge Pier #2 and Pier #3 spread footing details (Dimensions in meter).

Piers #4 to pier #7 are supported by pile caps. Pier #4 and pier #5 are supported by square pile caps that have a side length of 5.1 m and a depth of 1.0 m. The pile caps at pier #6 and pier #7 have a side length of 4.5 m and a depth of 1.0 m. The reinforcement in the pile caps consist of a top mesh of 20 mm diameter bars spaced at 300 mm and a bottom mesh of 20 mm diameter bars spaced at 150 mm. Each pile cap is supported by three rows of three reinforced concrete piles that are embedded 700 mm into the pile cap. The piles are 8 m long and are reinforced longitudinally by eight 14 mm diameter bars and transversely with 10 mm diameter spiral at 150 mm pitch. Piles and pile cap details are shown in Figures 3-7 and 3-8.

The bridge ends at Abutment #1 and Abutment #2 are supported simply by abutment walls that are 0.9 m thick and reinforced vertically by 20 mm diameter bars spaced at 200 mm and reinforced horizontally by 14 mm diameter bars spaced at 200 mm, at each face of the wall. There is a 50 mm gap between the end diaphragm and the wall. The abutment wall at Abutment #1 is supported on a 3.9 m wide wall footing and a depth of 0.75 m. The wall footing is reinforced in the short direction by 20 mm

diameter bars spaced at 200 mm, top and the bottom reinforcement. Longitudinal reinforcement consist of 14 mm diameter bars spaced at 200 mm were at the top and the bottom of the footing in the longitudinal direction. Abutment wall details at Abutment #1 are shown in Figure 3-9.

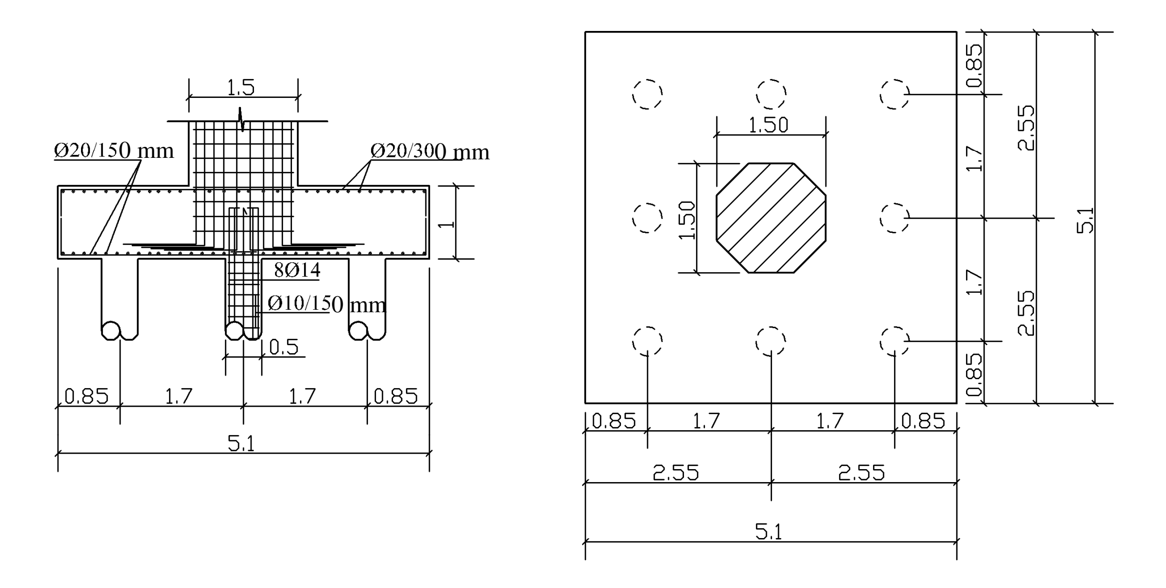


Figure 3-7: Alnasha Bridge Pier #4 and Pier #5 pile footing details (Dimensions in meter).

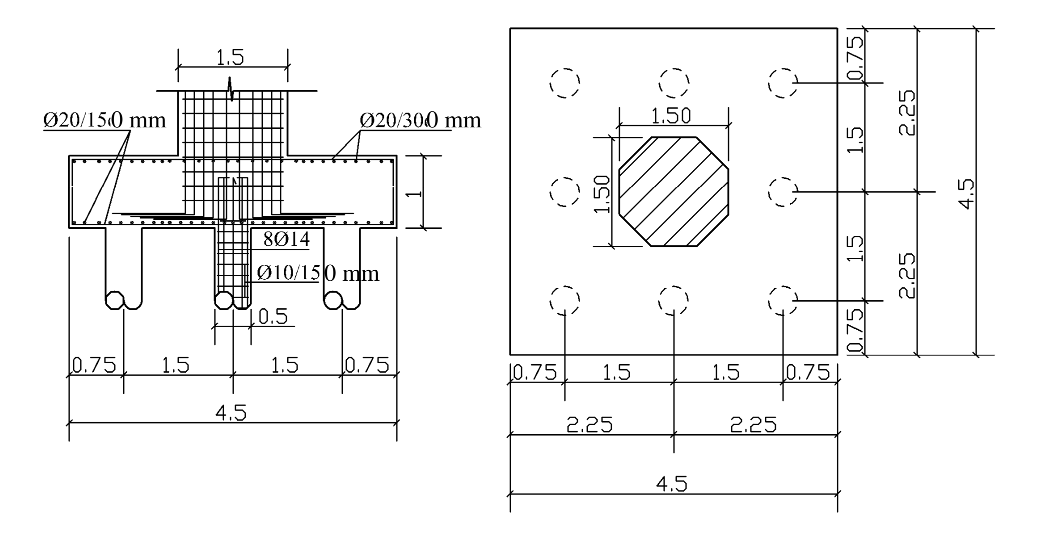


Figure 3-8: Alnasha Bridge Pier #6 and Pier #7 pile footing details (Dimensions in meter).

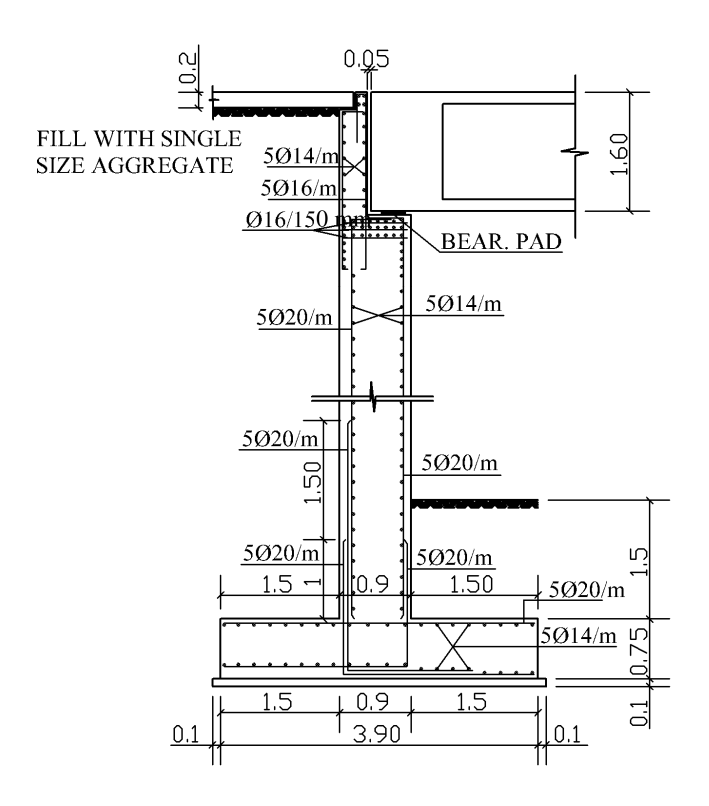


Figure 3-9: Alnasha Bridge Abutment #1 details (Dimensions in meter).

The abutment wall at Abutment #2 is supported on a 3.9 m wide pile cap. The pile cap has a depth equal to 0.75 m. The pile cap is reinforced in the short direction by 20 mm diameter bars spaced at 200 mm at the top and the bottom of the footing and by 14 mm diameter bars spaced at 200 mm in the long direction at the top and the bottom of the footing. The pile cap is supported by 10 rows of three reinforced concrete piles that are embedded 500 mm into the pile cap. The piles are 8 m long in length reinforced longitudinally by eight 14 mm diameter bars and transversely by 10 mm diameter spirals at 150 mm pitch. Abutment wall details at Abutment #2 are shown in Figure 3-10.

Figure 3-3 shows the location of the expansion joints which are provided at the ends of the bridge and at pier #3 and pier #5 along the width of the bridge. Expansion joint details are shown in Figure 3-11.

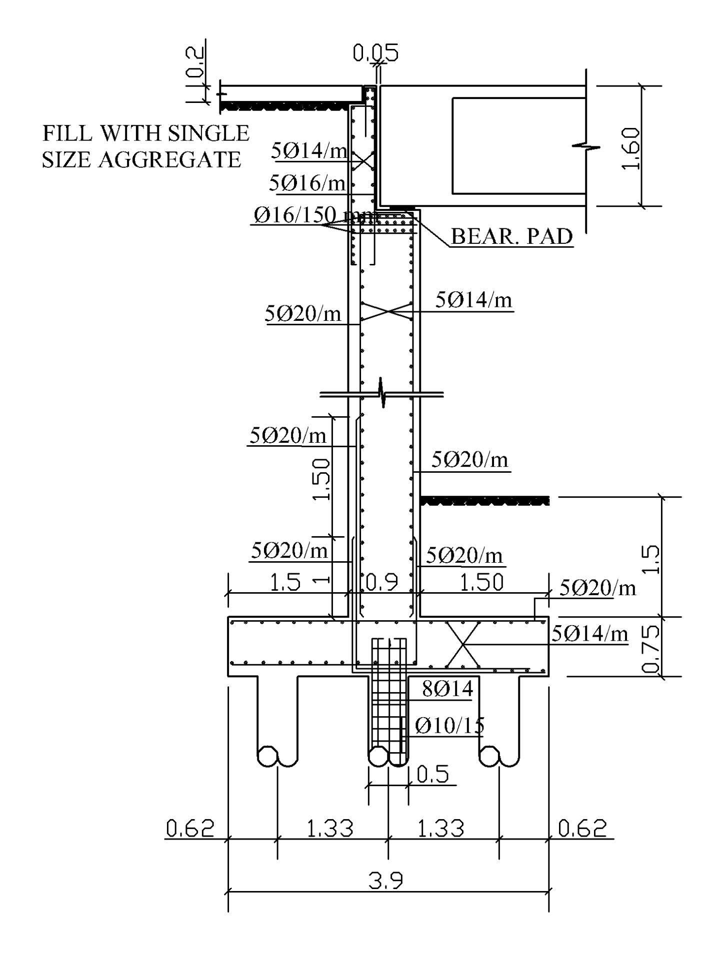


Figure 3-10: Alnasha Bridge Abutment #2 details (Dimensions in meter).

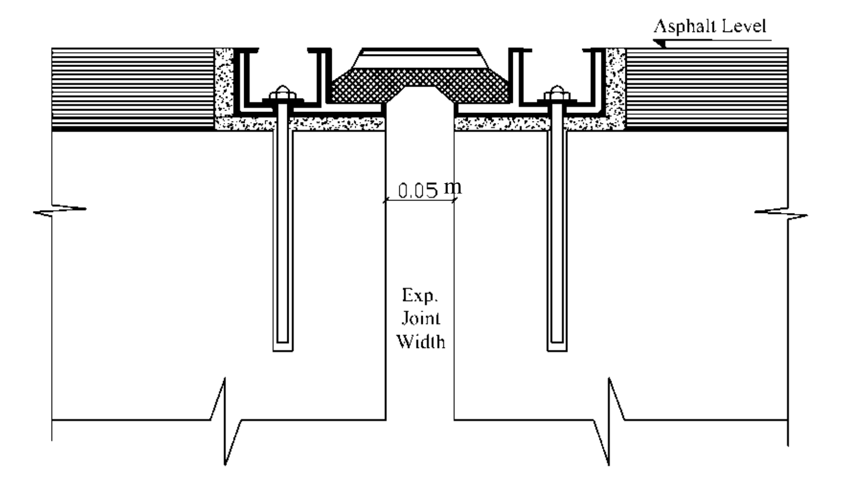


Figure 3-11: Expansion joint details

Table 3-1 shows the specified material properties of the bridge.

Table 3-1: Alnasha Bridge Material Properties

Material Properties	
Bars yield strength	414 MPa
28 days – Concrete strength (Cube) (For piers and deck)	40 MPa
28 days – Concrete strength (Cube) (For walls and foundation)	40 MPa

3.1.2. Alnasha Bridge Mathematical Model

3.1.2.1. Superstructure and Piers

Based on the FHWA-SRM (2005) recommendations, a spine-type model was used to represent the bridge superstructure utilizing the software SAP2000. Superstructure was represented by a single line of multiple three-dimensional frame elements, which passes through the centroid of the superstructure. As most of the mass of the bridge is in the superstructure, four to five members per span were used to represent the superstructure (FHWA-SRM, 2005). Rigid elements were provided between the centroid of the superstructure and the centroid of the crossbeams (FHWA-SRM, 2005). This connection element is shown schematically in Figure 3-12.

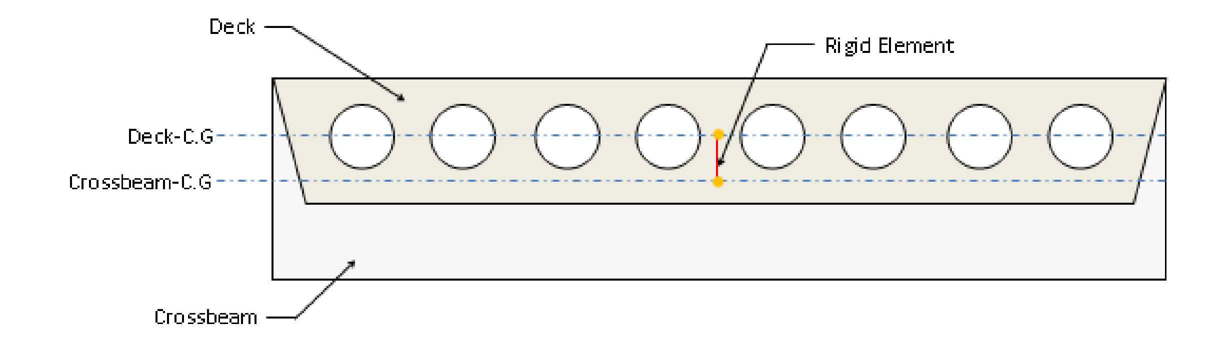


Figure 3-12: Deck-crossbeam rigid connection.

The mass of the structure was specified per unit length of the members with half the member mass being subsequently assigned to each node. Superstructure cross-

sectional properties were obtained using the "Section Designer" in SAP2000. A body constraint was assigned at the nodes of the members representing the crossbeam to ensure that, as would expected for the actual bridge, the columns attract approximately equal forces.

Effective stiffness properties were assigned to the moment of inertia of the entire cross section of the superstructure. The derivation of effective moment of inertia is based on the cracked section properties. Since the superstructure is a reinforced concrete voided slab, it was sufficient to use fifty percent of the gross moment of inertia as effective (Priestley et al. 1996).

Since the bridge columns are expected to respond inelastically under the input ground motions, effective column properties were used to reflect concrete cracking and reinforcement yielding. FHWA-SRM, 2005 (Table 7-1) was used to determine the effective rigidities for different components, which is shown in Table 3-2.

For the torsional stiffness, FHWA-SRM (2005) recommends to use an effective stiffness equal to 20% of the uncracked stiffness value. Figure 3-13 shows a typical bridge pier and the associated stiffness properties of the frame elements.

At locations of expansion joints, releases of Moment in both directions, torsion, and shear in transverse direction (direction perpendicular to the bridge main axis) were released at the ends of frame elements that are located at the expansion joints to represent the boundary conditions at these ends.

The parameter L_p shown in Figure 3-13 is the equivalent plastic hinge length. The equivalent plastic hinge length is given by the following semi-empirical equation (FHWA-SRM, 2005):

$$L_p = 0.08L + 4400\varepsilon_y d_b \qquad (3\text{-}1)$$

Where d_b is the diameter of the longitudinal tension reinforcement, and L is the shear span or effective height (i.e., L = M/V).

Table 3-2: Component Rigidities (Adapted from FHWA SRM, 2005, Table 7-1)

Component	Flexural Rigidity	Shear Rigidity	Axial Rigidity
Reinforced concrete columns, beams and caps where cracking (but not hinging) is expected	$0.5\ E_c\ I_g$	$0.4\ E_c\ A_w$	$E_c\ A_g$
Prestressed concrete beams, caps and piles where cracking is not expected	$E_c\ I_g$	$0.4\ E_c\ A_w$	$E_c\ A_g$
Concrete columns, piles and walls where plastic hinging is expected	$\frac{M_n D'}{2\varepsilon_y}$	$0.2\ E_c\ A_g$	$0.5\ E_c\ A_g$

Note:

E_c = elastic modulus of concrete,
I_g = moment of inertia using gross dimensions,
A_w = shear area of column or beam,
A_g = cross-sectional area of column or beam using gross dimensions,
M_n = nominal moment capacity of column or beam,
D' = distance between outer layers of longitudinal reinforcement, and
ε_y = yield strain of steel reinforcement.

Detailed calculations of the flexural stiffness reduction factors are shown in Appendix D. Alnasha bridge mathematical model is shown in Figure 3-14.

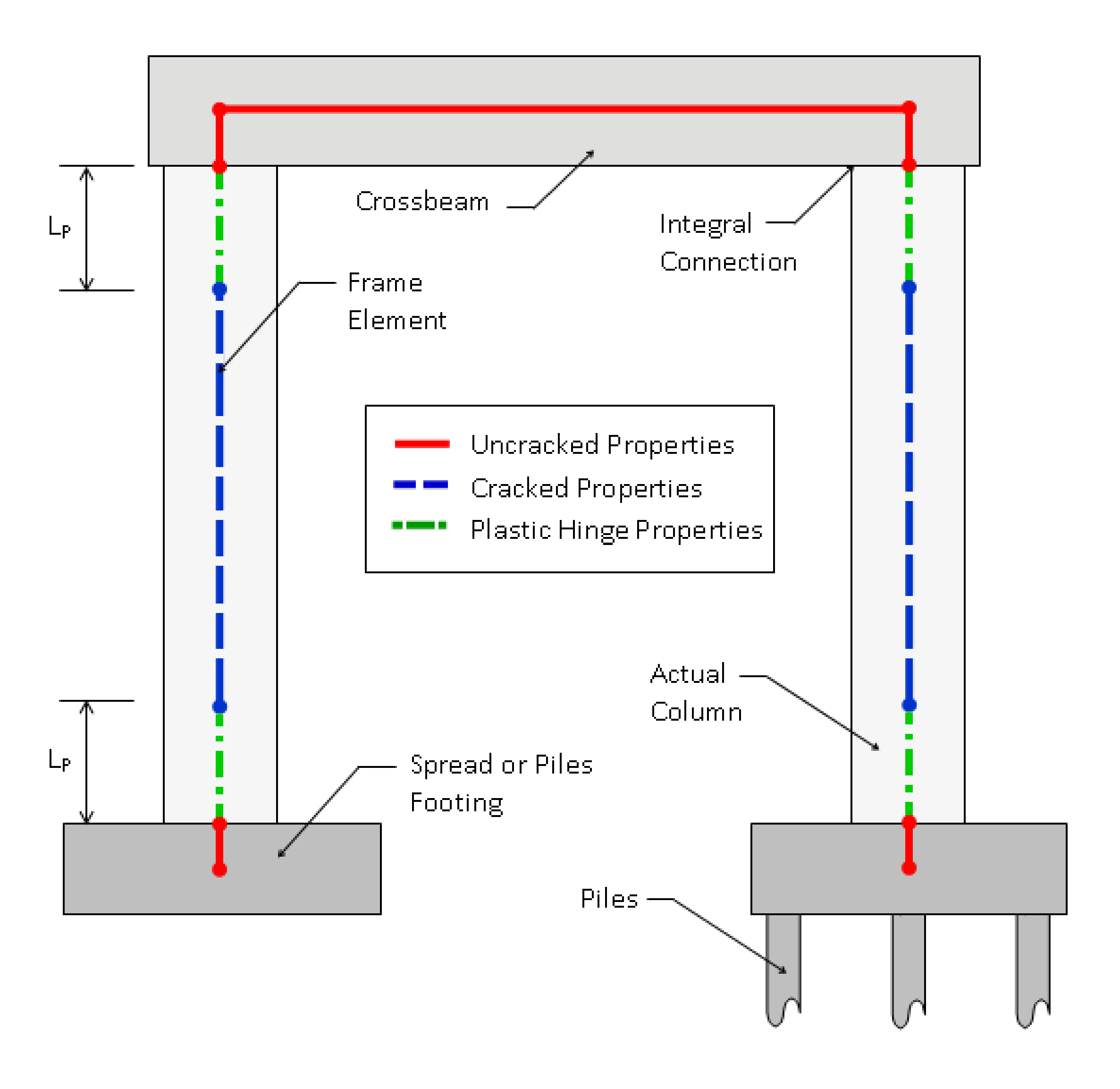


Figure 3-13: Locations of section properties in a typical pier (L_P: Equivalent plastic hinge length)

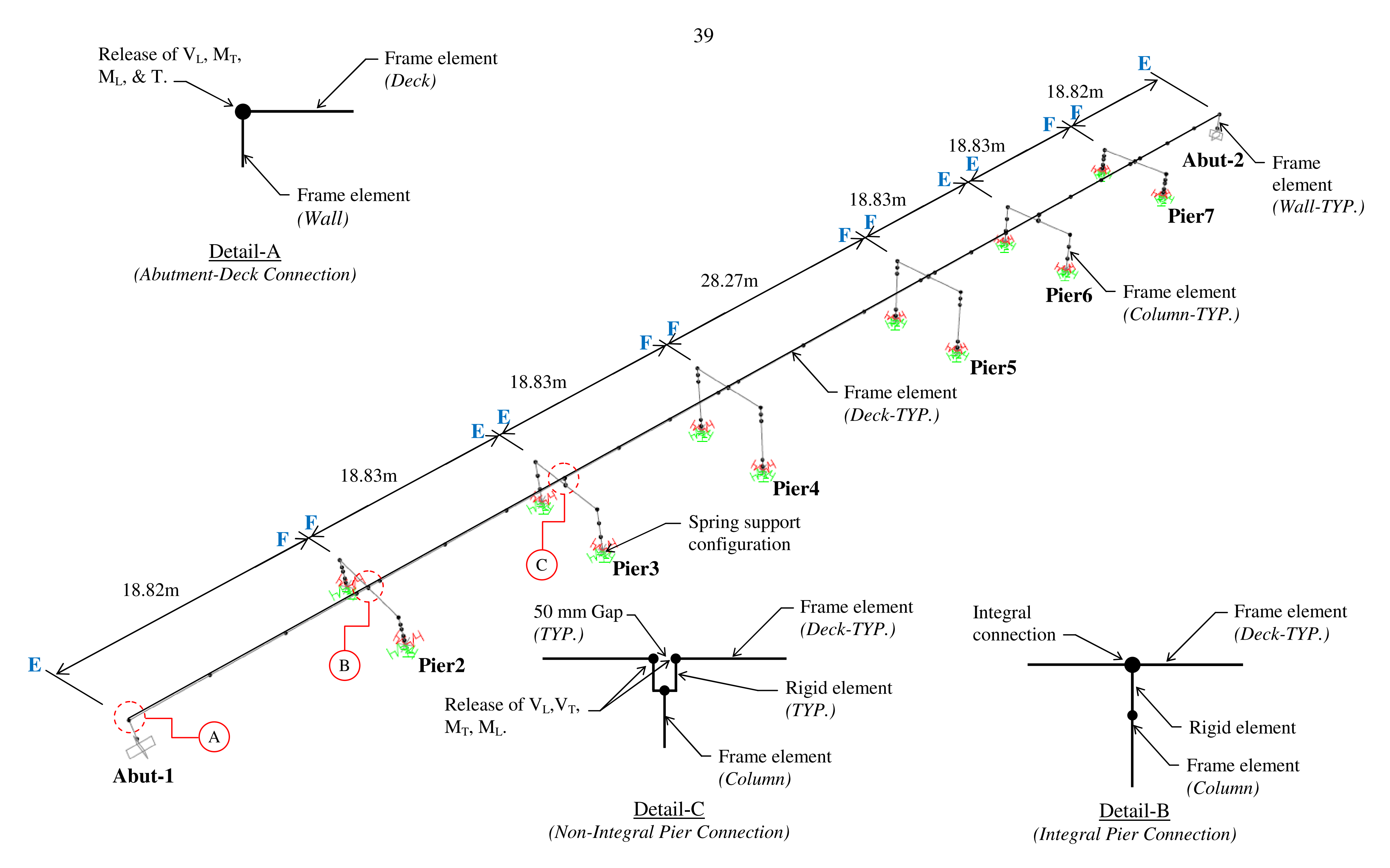


Figure 3-14: Alnasha Bridge mathematical model.
(E: Expansion, F: Fixed, V_L and V_T: Shear in longitudinal and transverse direction, M_L and M_T: Moment about longitudinal and transverse direction)

3.1.2.2. Foundation Modeling

Each spread footing was modeled using the spring element in SAP2000. Three translational springs and three rotational springs where used to model each spread footing. These springs were connected to the column at the mid depth of the footing. According to the FHWA-SRM (2005), most shallow spread footings are stiff relative to the soil on which they rest, and for analytical purposes, an uncoupled spring model as shown in Figure 3-15 could be employed. Parameters related to spring stiffness include the soil modulus of elasticity, E, soil Poisson's ratio, υ, dimensions of the foundation and the embedment depth. Elastic solutions for the spring constants are provided in the FHWA-SRM (2005) which are shown in Table 3-3. The following steps are used to determine the spring constants:

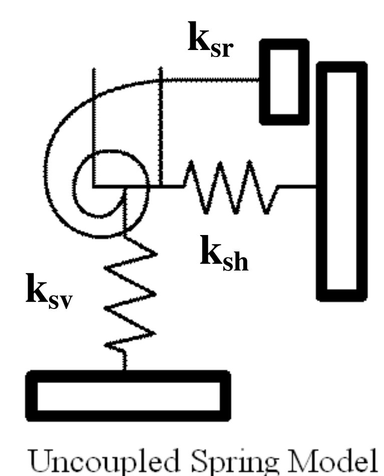


Figure 3-15: Uncoupled elasto-plastic spring model for rigid footings, k_{sr}: spring rotational stiffness, k_{sh}: spring horizontal stiffness, and k_{sv}: spring vertical stiffness (Adapted from FHWA-SRM, 2005).

Step 1: Determine the uncoupled total surface stiffnesses, K_i', of the foundation element by assuming it to be a rigid plate bearing at the surface of a semi-infinite elastic half-space, as shown in Table 3-3.

Step 2: Adjust the uncoupled total surface stiffnesses, K_i', for the effect of the depth of bearing by multiplying by embedment factors shown in Table 3-4. The uncoupled total embedded stiffnesses is then equal to $e_i . K_i$

Detailed calculations for spring constants are shown in Appendix A for all piers in each bridge.

Table 3-3: Surface stiffnesses for a rigid plate on a semi-infinite homogeneous elastic half-space (Adapted from FHWA-SRM, 2005, Table 6-1)

Stiffness Parameter	Rigid Plate Stiffness at Surface, K_i'
Vertical Translation, K_Z'	$\frac{GL}{(1-\nu)}\left[0.73+1.54\left(\frac{B}{L}\right)^{0.75}\right]$
Horizontal Translation, K_y' (toward long side)	$\frac{GL}{(2-\nu)}\left[2+2.5\left(\frac{B}{L}\right)^{0.85}\right]$
Horizontal Translation, K_x' (toward short side)	$\frac{GL}{(2-\nu)}\left[2+2.5\left(\frac{B}{L}\right)^{0.85}\right]-\frac{GL}{(0.75-\nu)}\left[0.1\left(1-\frac{B}{L}\right)\right]$
Rotation, $K_{\theta x}'$ (about x axis)	$\frac{G}{(1-\nu)}I_x^{0.75}\left(\frac{L}{B}\right)^{0.25}(2.4+0.5\frac{B}{L})$
Rotation, $K_{\theta y}'$ (about y axis)	$\frac{G}{(1-\nu)}I_y^{0.75}\left[3\left(\frac{L}{B}\right)^{0.15}\right]$

Note:

G = shear modulus of soil,
υ = poisson's ratio of the soil,
L = footing dimension,
B = footing dimension,
I_x, I_y = moments of inertia of the footing about the x- and y-axes, respectively,
D = footing depth, and,
d = footing thickness.

Table 3-4: Stiffness embedment factors for a rigid plate on a semi-infinite homogeneous elastic half-space (Adapted from FHWA-SRM, 2005, Table 6-2)

Stiffness Parameter	Embedment Factors, e_i
Vertical Translation, e_Z	$\left[1+0.095\frac{D}{B}\left(1+13\frac{B}{L}\right)\right]\left[1+0.2\left(\frac{(2L+2B)}{LB}d\right)^{0.67}\right]$
Horizontal Translation, e_y (toward long side)	$\left[1+0.15\left(\frac{2D}{B}\right)^{0.5}\right]\left[1+0.52\left[\frac{\left(D-\frac{d}{2}\right)16(L+B)d}{BL^2}\right]^{0.4}\right]$
Horizontal Translation, e_x (toward short side)	$\left[1+0.15\left(\frac{2D}{B}\right)^{0.5}\right]\left[1+0.52\left[\frac{\left(D-\frac{d}{2}\right)16(L+B)d}{LB^2}\right]^{0.4}\right]$
Rotation, $e_{\theta x}$ (about x axis)	$1+2.52\frac{d}{B}\left[1+\frac{2d}{B}\left(\frac{d}{D}\right)^{-0.2}\left(\frac{B}{L}\right)^{0.5}\right]$
Rotation, $e_{\theta y}$ (about y axis)	$1+0.92\left(\frac{2d}{L}\right)^{0.6}\left[1.5+\left(\frac{2d}{L}\right)^{1.9}\left(\frac{d}{D}\right)^{-0.6}\right]$

Pile foundations generally comprise pile groups connected to a footing or a pile cap, with pile diameters (normally driven piles) usually less than 0.6 m in diameter. These types of foundations are the most typical in bridges construction and are found on a variety of bridge types. For the purpose of calculating the stiffness of a pile footing, the FHWA-SRM (2005) suggests that the footing or the pile cap is normally uncoupled from the piles. The contributions from the two components are then evaluated separately. Lateral stiffness in both directions of the pile cap is generally much higher than that of the group of piles due to the soil passive pressure applied on the pile cap. Therefore, it is recommended to compute the pile cap stiffness in the lateral direction typical to the way used in the case of spread footings.

The following is a detailed discussion of the procedure used to calculate piles stiffness constants:

To compute pile stiffness in the vertical direction, the elastic procedure was employed (Priestly, et al, 1996):

$$K_{Axial} = \frac{EA}{L} \qquad (3\text{-}2)$$

Where, A is the pile cross sectional area, E is the concrete modulus of elasticity, and L is the pile length. Soil friction along the pile and at the end bearing was not included in axial stiffness calculations.

For the pile stiffness in the lateral direction, the FHWA-SRM (2005) presents single-layer linear design charts. These charts use a discrete Winkler spring soil model in which the stiffness increases linearly with depth, from zero at grade level where the location of the pile-head is assumed to be located. The charts that were used in the study are shown in Figure 3-17 and Figure 3-18. Two parameters should be used to define this soil-pile system: the pile bending stiffness, EI, and the coefficient of variation of the inelastic subgrade modulus, f, which can be determined based on Figure 3-16.

The lateral stiffness for a pile with a fixed head condition can be determined from the following equation, (FHWA-SRM, 2005):

$$K_{Lateral} = \frac{1.0765 EI_p}{T^3} \qquad (3\text{-}3)$$

Where, EI_p is the flexural stiffness of the pile, f is the coefficient of variation of the inelastic subgrade modulus, and T is given in the following equation:

$$T = \left(\frac{EI_p}{f}\right)^{1/5} \qquad (3\text{-}4)$$

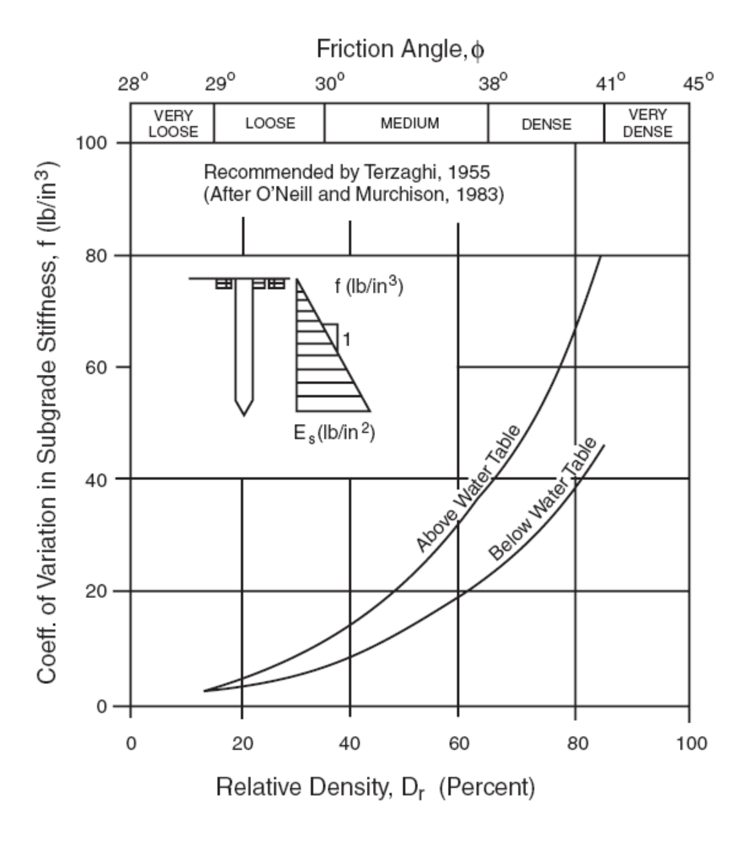


Figure 3-16: Recommended coefficient of variation in subgrade modulus (f) with depth of sand. (Adapted from FHWA-SRM, 2005, Figure 7-12).

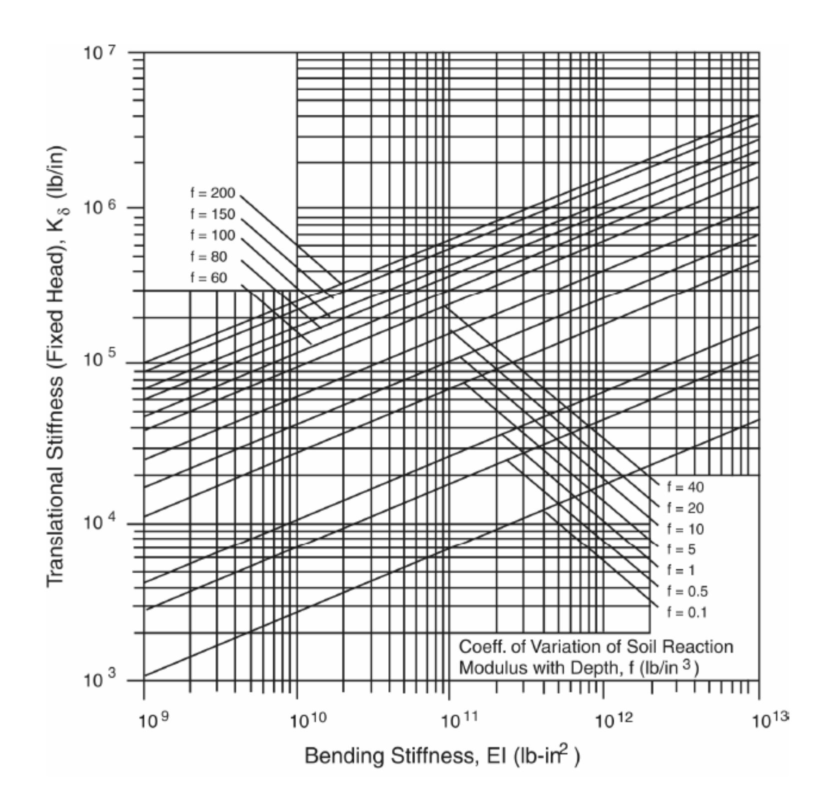


Figure 3-17: Lateral pile-head stiffness - fixed-head condition, (Adapted from FHWA-SRM, 2005, Figure 7-8).

The rotational stiffness for a pile is presented by the following equation (FHWA-SRM, 2005):

$$K_{Rotational} = \frac{1.499EI_p}{T^3} \qquad (3\text{-}5)$$

Figure 3-18 shows rotational stiffness relation with different pile bending stiffness.

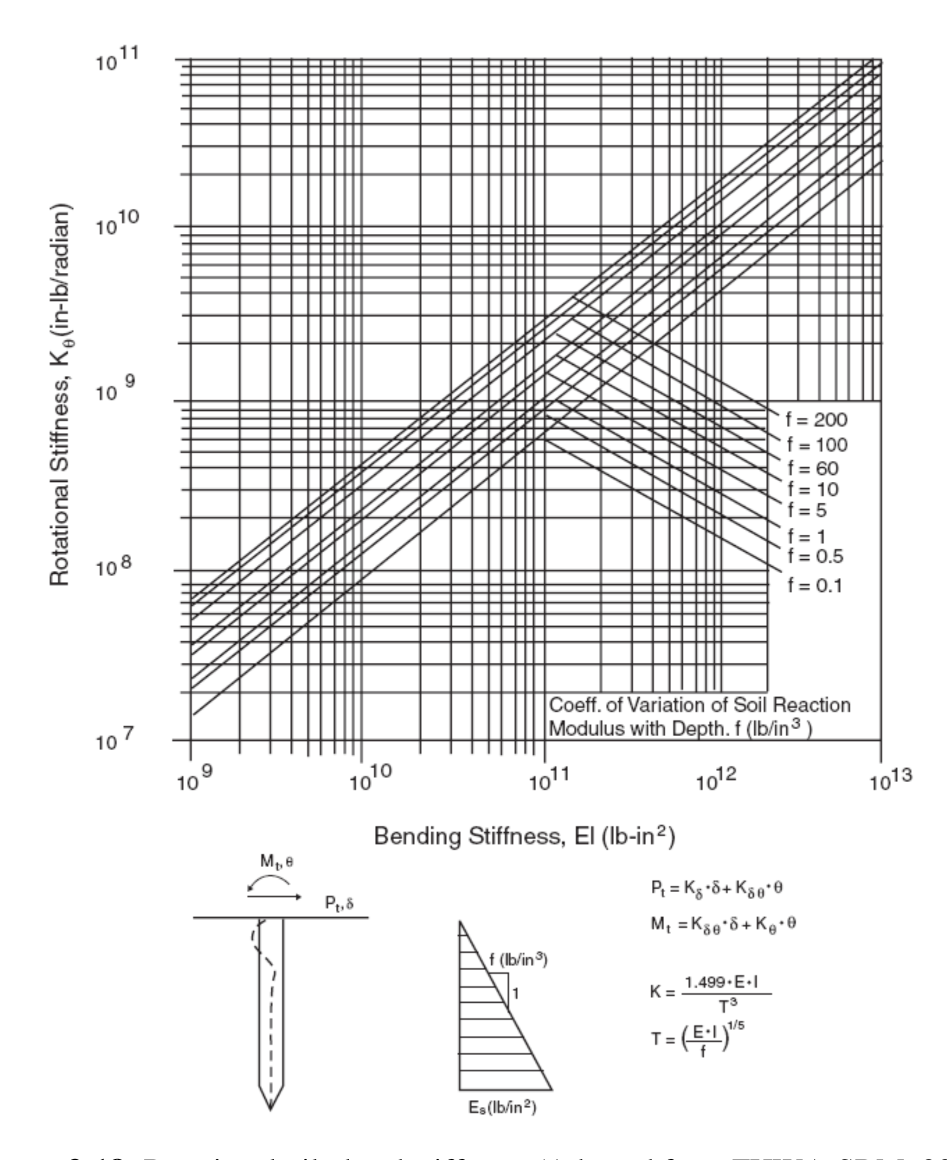


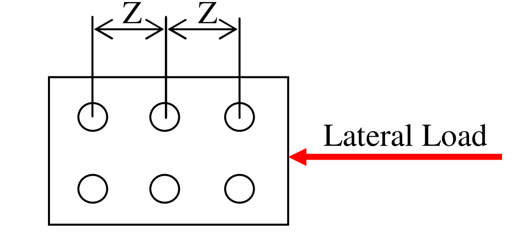
Figure 3-18: Rotational pile-head stiffness, (Adapted from FHWA-SRM, 2005).

To account for pile group effect, Washington State Department of Transportation Bridge Design Manual (WSDOT-BDM) recommends multiplying the individual pile stiffness by an efficiency factor, as shown in Table 3-5.

Table 3-5: Group of piles efficiency factor

Z	Efficiency (Reduction) Factor
8D	*1.0*
6D	*0.8*
4D	*0.5*
3D	*0.4*

Adapted from WSDOT-BDM, Table 4.4.3-1, D = Pile diameter.



Group Pile Plan

Table 3-6 summarizes spring coefficients that were used in modeling of Alnasha Bridge.

Table 3-6: Spring values for Alnasha Bridge Footings

Pier No.	Footing Type	K_X	K_Y	K_Z	R_X	R_Y
2		*686x*10^4	*686x*10^4	*842x*10^4	*118x*10^4	*103x*10^4
3		*686x*10^4	*686x*10^4	*842x*10^4	*118x*10^4	*103x*10^4
4		*121x*10^5	*121x*10^5	*656x*10^4	*514x*10^5	*514x*10^5
5		*121x*10^5	*121x*10^5	*656x*10^4	*514x*10^5	*514x*10^5
6		*107x*10^5	*107x*10^5	*656x*10^4	*446x*10^5	*446x*10^5
7		*107x*10^5	*107x*10^5	*656x*10^4	*446x*10^5	*446x*10^5

Notes:

K_X, K_Y, and K_Z = Translation stiffness in global X, Y, and Z, respectively. (kN/m)
R_X and R_y = Rotational stiffness in global X and Y, respectively. (kN.m/rad)
X-Axis = Axis parallel to the bridge main longitudinal axis.
Y-Axis = Axis parallel to the bridge main transverse axis.
Z-Axis = Axis perpendicular to the X-Y plane.

= Indicates spread footing foundation.

= Indicates piles footing foundation.

Response Spectrum analysis of Alnasha Bridge model, as will be shown in Chapter Five, showed that the gap between the frames will be closed under the seismic forces in the longitudinal direction. To account for this case, two models were created. The tension model where the gaps between the frames remain open. This tension model represents an upper bound on displacement demands. The other model is a compression model where the gaps width set equal to zero. This model represents an upper bound on demand.

3.2. Alharamain Bridge

3.2.1. Bridge Description

Figure 3-19 shows an Aerial view of Alharamain Bridge. The bridge is on Almadina Almonwara Street crossing Makka Street. This bridge carries 77,424 AVDT as reported in a traffic study conducted by Amman Greater Municipality, 2008.



Figure 3-19: Aerial View of Alharamain Bridge (Adapted from Google Earth, USA)

Alharamain Bridge is a nine-span bridge with a total length of 270 m. Figure 3-20 shows a general view of the bridge. The exterior and interior spans are 29 m long, except the middle span and the first interior spans, which are 32 m long. The abutment walls simply support the superstructure at the ends of the bridge. Expansion joints were introduced at pier #4 and pier #7. The bridge elevation and plan views are shown in Figures 3-21 and Figures 3-22, respectively.



Figure 3-20: A general view of Alharamin Bridge.

The deck is cast-in-place, reinforced concrete voided slab with an overall average width of 15.6 m and a 14.5 m roadway width. The depth of the deck is 1.5 m. The bridge deck cross-section is shown in Figure 3-23. The depth of the deck in the vicinity of the piers is increased linearly from 1.5 m to 2.1 m. This variation happens at a distance 4.9 m from the center line of the piers, as shown in Figure 3-22.

At each interior integral pier, a 2.6 m wide by 2.1 m deep transverse crossbeam distributes the bridge loads to a couple of columns. At pier #4 and pier #7, where expansion joints are installed, a couple of 1.3 m wide by 2.1 m deep transverse diaphragms separated by a 60 mm gap distributes the bridge loads to a couple of columns. All piers consist of two inclined columns forming a Y-shape with constant length of 3.44 m, carrying the deck load from the superstructure and intersect with each other at the bottom where they rest on top of a single square column.

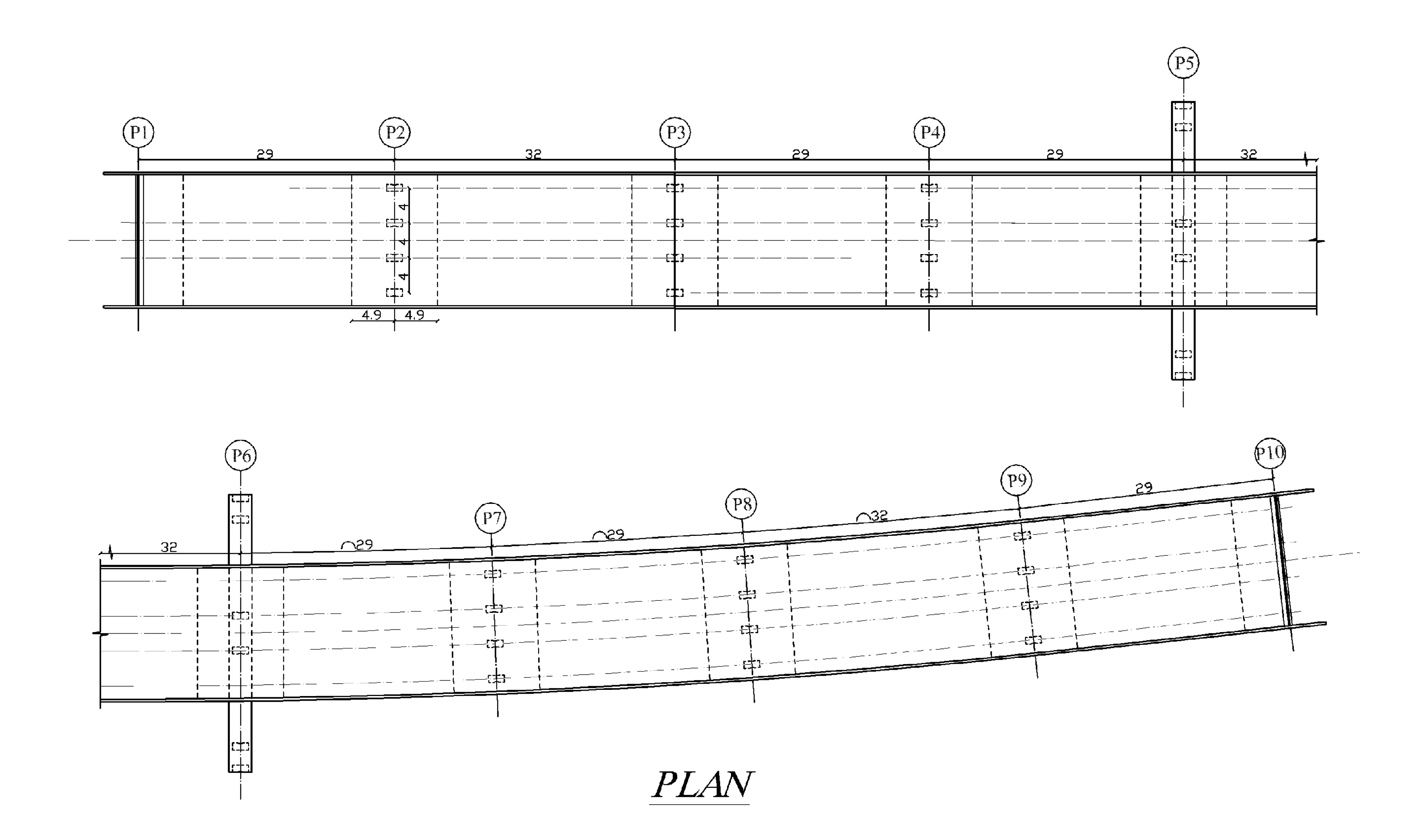


Figure 3-21: Alharamain bridge- plan, dimensions in meter (Adapted from Greater Amman Municipality).



PIER1 PIER2 PIER3 PIER4 PIER5

29 32 29 29 32

E F F E F

5.1x0.80m WALL FOOTING

15x6m COMBINED FOOTING

15x6m COMBINED FOOTING

8x4m COMBINED FOOTING

32.8x5m COMBINED FOOTING

PIER6 PIER7 PIER8 PIER9 PIER10

32 29 29 32 29

F E F F E

32.8x5m COMBINED FOOTING

8x4m COMBINED FOOTING

15x6m COMBINED FOOTING

15x6m COMBINED FOOTING

5.1x0.80m WALL FOOTING

ELEVATION

F : FIXED JOINT

E : EXPANSION JOINT

Figure 3-22: Alharamain bridge- elevation, dimensions in meter (Adapted from Greater Amman Municipality).

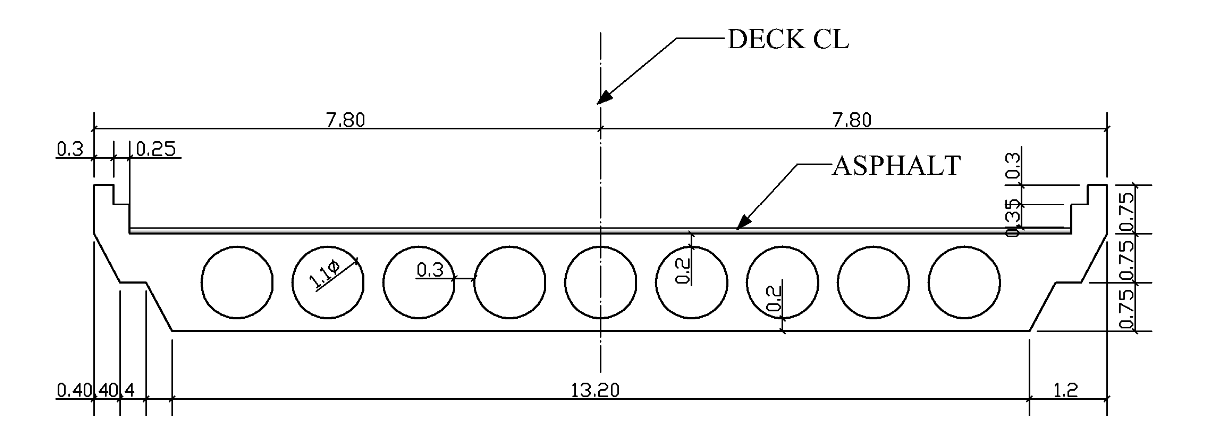


Figure 3-23: Alharamain Bridge deck typical section (Dimensions in meter).

The columns of pier #2 are 6.98 m long, while the columns of pier #3 are 7.29 m long. The columns of pier #4 and pier #7, where expansion joints exist, are 7.77 m and 7.74 m long, respectively. The columns of pier #8 are 6.72 m long. The longest columns are the columns at pier #5 and pier #6 with a length equal to 8.38 m. The shortest columns have a length equal to 5.51 m at pier #9. The columns have square cross section with a side length of 1.8 m. The columns are reinforced with five pieces of 14 mm stirrups spaced transversely at 200 mm on center. Longitudinal reinforcement is comprised of 40 equally spaced 32 mm bars. Typical pier details are shown in Figure 3-24.

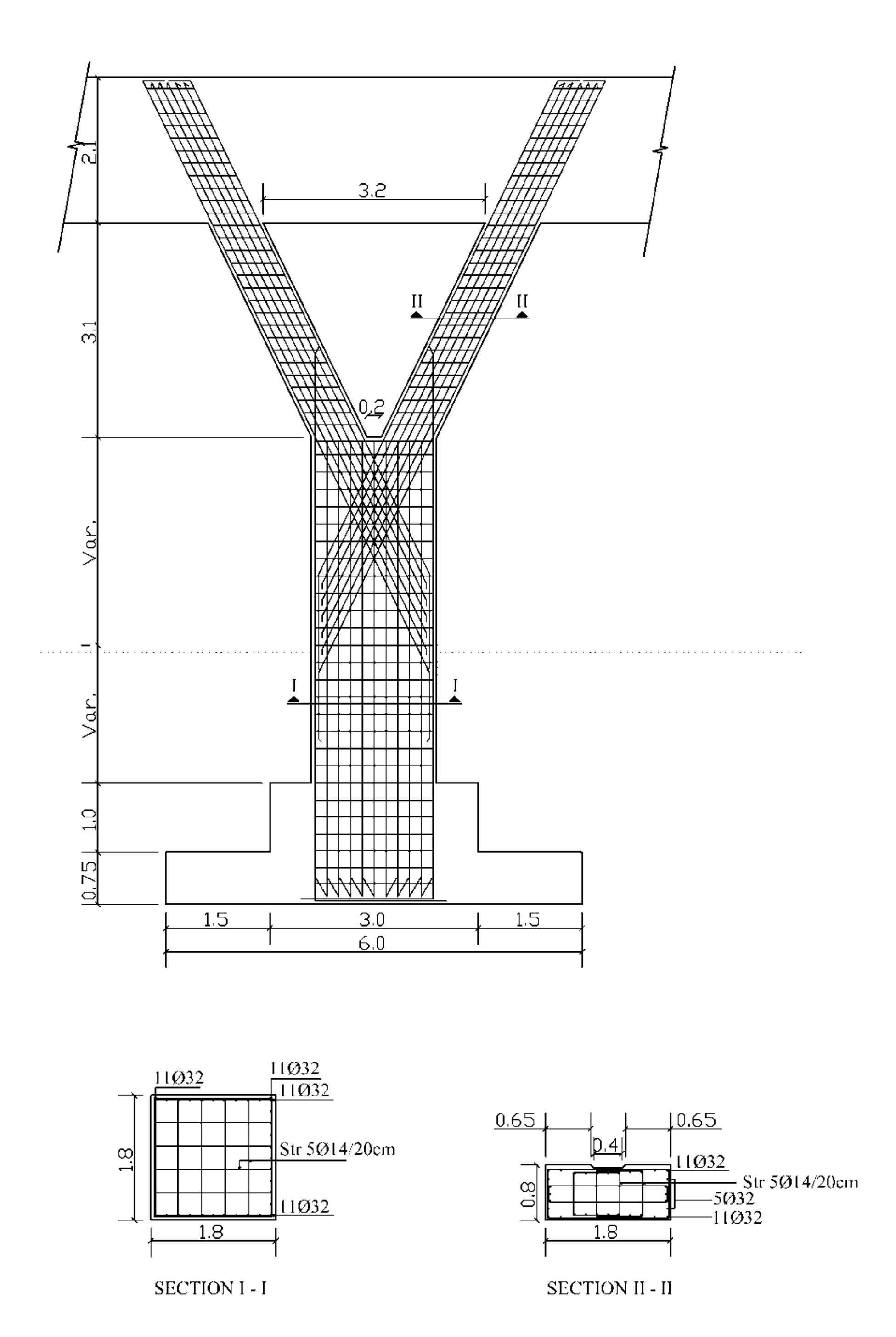


Figure 3-24: Typical pier details (Dimensions in meter).

The inclined columns have a rectangular cross section, 800 mm by 1800 mm, reinforced by four 14 mm stirrups spaced at 150 mm on center. Longitudinal reinforcement is comprised of 32 equally spaced 32 mm bars. Pier #5 and pier #6

consist of three columns, sized and reinforced identical to the columns of the other piers.

All columns are supported by rectangular combined footings. The footings are located at distance 3.5 m to 4.0 m below the ground level. Piers #2, pier #3, pier #8, and pier #9 are supported by rectangular combined footings which are 15 m long and 6 m wide. The footing is reinforced by 30 equally spaced 32 mm bottom bars and 30 equally spaced 20 mm top bars. The shear reinforcement in the footing consists of three pieces of 16 mm stirrups spaced at 200 mm on center. The geometry of the combined footing is shown in Figure 3-25.

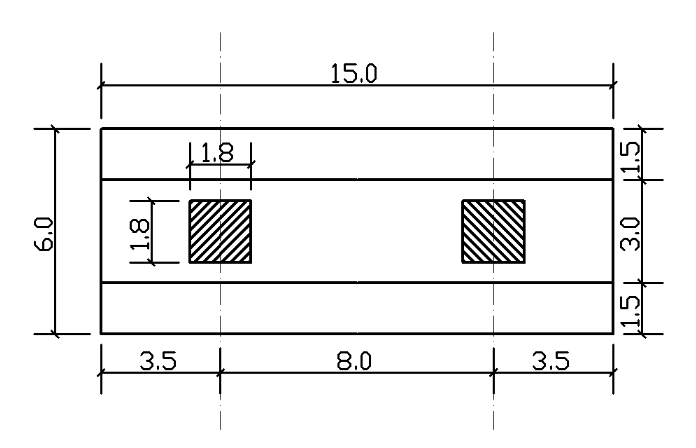


Figure 3-25: Alharamain Bridge Piers #2, Pier #3, Pier #8, and Pier #9 footing details (Dimensions in meter).

Piers #4 and pier #7 are supported by rectangular combined footing which is 8 m long and 4 m wide. The footing is reinforced by 30 equally spaced 32 mm bottom bars and 30 equally spaced 20 mm top bars. Two 16 mm stirrups spaced 200 mm on center form the shear reinforcement in the footing. The geometry of the combined footing is shown in Figure 3-26. Piers #5 and pier #6 are supported by rectangular combined footing which is 32.8 m long and 5 m wide. The footing is reinforced by 30 equally spaced 32 mm bottom bars and 15 equally spaced 20 mm top bars. Three 16

mm stirrups spaced at 200 mm on center are introduced as shear reinforcement. Figure 3-27 shows the geometry of the footing.

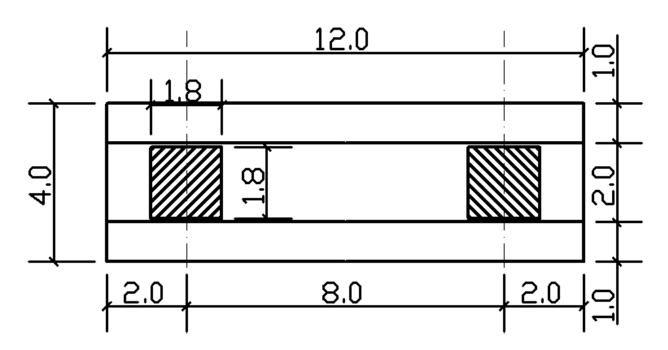


Figure 3-26: Alharamain Bridge Pier #4 and Pier #7 footing details (Dimensions in meter).

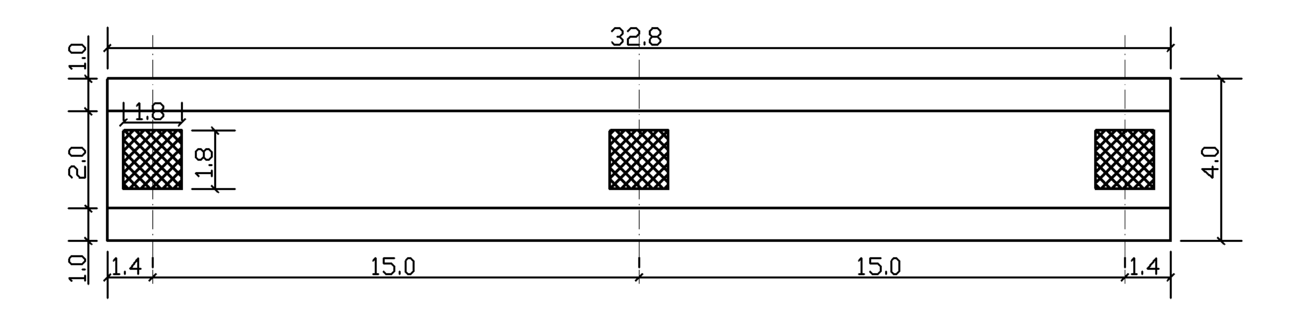


Figure 3-27: Alharamain Bridge Pier #5 and Pier #6 footing details (Dimensions in meter).

The bridge ends at Abutment #1 and Abutment #2 are simply supported by abutment walls that are 1.1 m thick. The walls are reinforced vertically with 25 mm bars spaced at 200 mm, and horizontally with 16 mm bars spaced at 200 mm at each face of the wall. There is a 60 mm gap between the end diaphragm of the deck and the wall. The abutment walls are supported by a 5.1 m wide footing. The wall footing is reinforced in the short direction by 25 mm bars spaced at 200 mm at the bottom face and 25 mm bars spaced at 100 mm at the top face of the footing. The longitudinal

reinforcement consists of 12 mm bars spaced at 200 mm. Figure 3-28 shows the abutment wall details at Abutment #1.

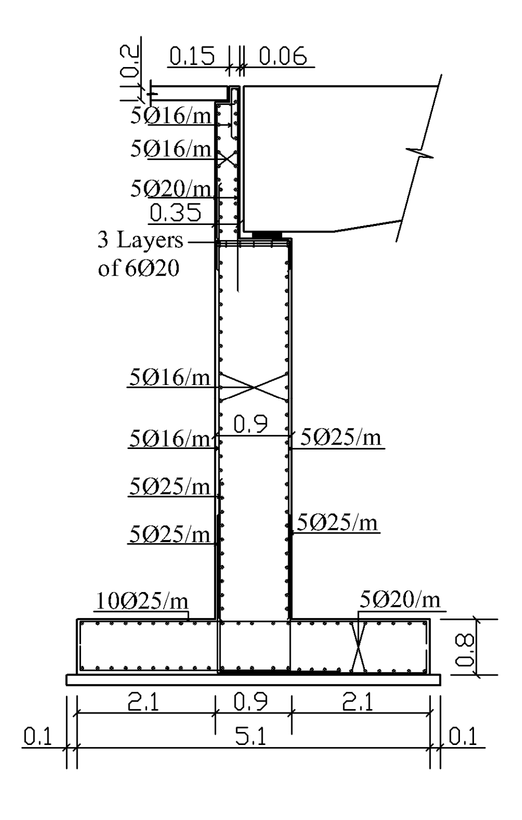


Figure 3-28: Alharamain Bridge Abutment #1 Details (Dimensions in meter).

Table 3-7 shows the specified material properties of the bridge.

Table 3-7: Alharamain Bridge Material Properties

Material Properties	
Bars yield strength (Bars -32 mm,25 mm, and 20 mm)	520 MPa
Bars yield strength (Other sizes)	414 MPa
28 days – Concrete strength (Cube) (For piers and deck)	45 MPa
28 days – Concrete strength (Cube) (For walls and foundation)	40 MPa

3.2.2. Alharamain Bridge Mathematical Model

3.2.2.1. Superstructure and Piers Modeling

Based on the FHWA-SRM (2005) recommendations, the superstructure was modeled as a three dimensional spine model utilizing the software SAP2000. The superstructure was represented by a single line of multiple three-dimensional frame elements, which passes through the centroid of the superstructure as shown in Figure 3-29. Rigid elements were introduced to connect the centroid of the superstructure to the centroid of the crossbeams (FHWA-SRM, 2005), This connection is shown schematically in Figure 3-12.

Effective stiffness properties were assigned to the moment of inertia of the entire cross section of the superstructure. The derivation of effective moment of inertia is based on the cracked section properties. Since the superstructure is a reinforced concrete voided slab, it was sufficient to use fifty percent of the gross moment of inertia as effective, (Priestley et al, 1996).

Following the recommendations of the FHWA-SRM (2005) and as most of the mass of the bridge is in the superstructure, four to five frame element per span were used to represent the superstructure. The mass was specified per unit length of the members with half the member mass being subsequently assigned to each node. Superstructure cross-sectional properties were obtained from the “Section Designer” in SAP2000. A body constraint was assigned at the nodes of the members representing the crossbeam to ensure that, as would be expected for the actual bridge, the columns attract approximately equal forces.

Since the bridge columns are expected to respond inelastically under the input ground motions, effective column properties were used to reflect concrete cracking and

reinforcement yielding. Table 7-1 in FHWA-SRM (2005) was used to determine the effective rigidities for the different components of the bridge, which is presented in Table 3-2.

For the torsional stiffness FHWA-SRM (2005) recommends to use 20% of the uncracked torsional stiffness to represent the effects of cracking. Figure 3-13 shows a typical bridge pier with the location of the effective section properties.

Detailed calculations of the flexural stiffness reduction factors for all piers in all bridges are shown in Appendix D. Alharamain bridge mathematical model is shown in Figure 3-29.

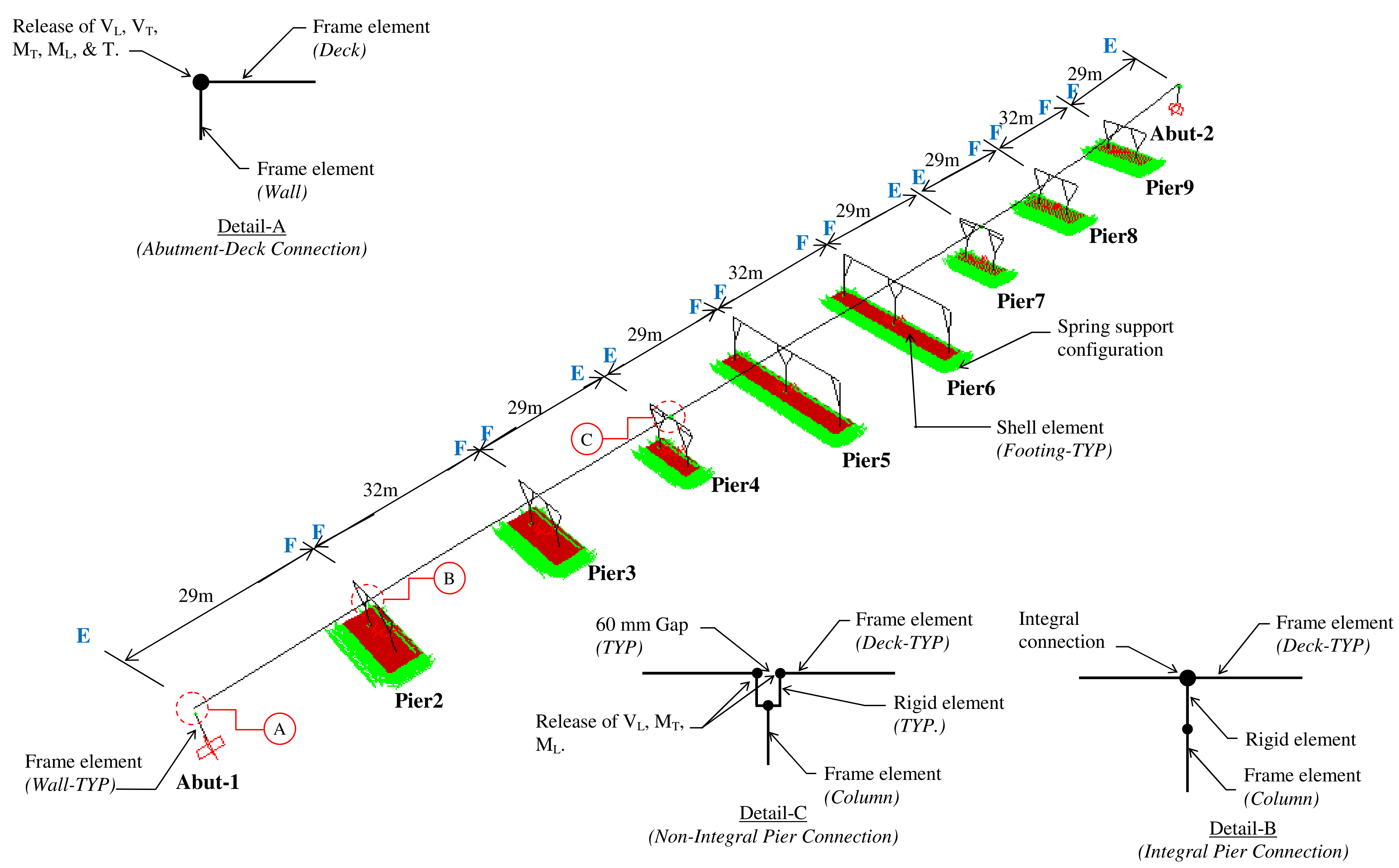


Figure 3-29: Alharamain Bridge mathematical model.

Response Spectrum analysis of Alharamain Bridge model, as will be shown in Chapter Five, showed that the gap between the frames will be close under the seismic forces in the longitudinal direction. To account for this case, two models were created. The tension model where the gaps between the frames remain open. This tension model represents an upper bound on displacement demands. The other model is a compression model where the gaps width set equal to zero. This model represents an upper bound on demand.

3.2.2.2. Foundation Modeling

Combined footings were modeled using shell elements with a maximum size of 500x500 mm. Spring elements were used to support the shell elements at four nodes. Spring constants, both rotational and translational constants, were calculated based on the FHWA-SRM (2005) recommendations discussed in details in section 3.1.2. Spring vertical stiffness was assigned based on the respective tributary area of each node. Horizontal translational stiffness of the footing was assigned to the perimeter nodes perpendicular to the direction under consideration. Footing rotational stiffness was assigned at the middle node of the footing, as shown in Figure 3-30. Detailed calculations for spring constants are shown in Appendix A for all piers in each bridge.

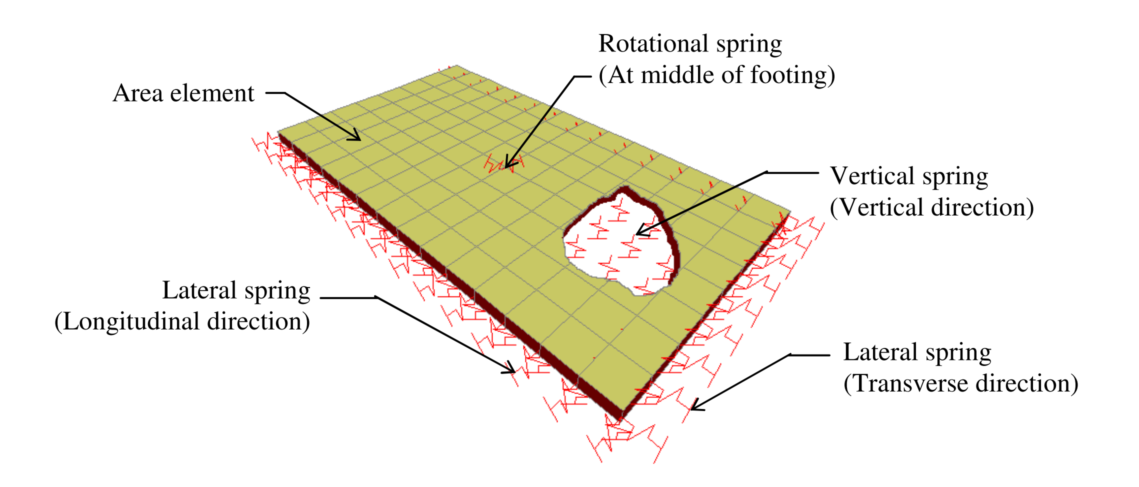


Figure 3-30: Locations of footing springs.

Table 3-8 summarizes spring stiffness coefficients that were used in modeling of Alharamain Bridge.

Table 3-8: Spring values for Alharamain Bridge

Pier No.	K_X	K_Y	K_Z	R_X	R_Y
2 & 3	$141x10^5$	$161x10^5$	$146x10^5$	$781x10^4$	$340x10^4$
4	$120x10^5$	$143x10^5$	$120x10^5$	$565x10^4$	$186x10^4$
5 & 6	$241x10^5$	$309x10^5$	$214x10^5$	$546x10^5$	$739x10^4$
7	$120x10^5$	$143x10^5$	$120x10^5$	$565x10^4$	$186x10^4$
8 & 9	$141x10^5$	$161x10^5$	$146x10^5$	$781x10^4$	$340x10^4$

Notes:

K_X, K_Y, *and* K_Z = Translation stiffness in global X, Y, and Z, respectively. (kN/m)
R_X *and* R_y = Rotational stiffness in global X and Y, respectively. (kN.m/rad)
X-Axis = Axis parallel to the bridge main longitudinal axis.
Y-Axis = Axis parallel to the bridge main transverse axis.
Z-Axis = Axis perpendicular to the X-Y plane.

3.3. Almahata Bridge

3.3.1. Bridge Description

Figure 3-31 shows an Aerial view of Almahata Bridge. This bridge carries 66,754 AVDT as reported in a traffic study conducted by Amman Greater Municipality, 2008.

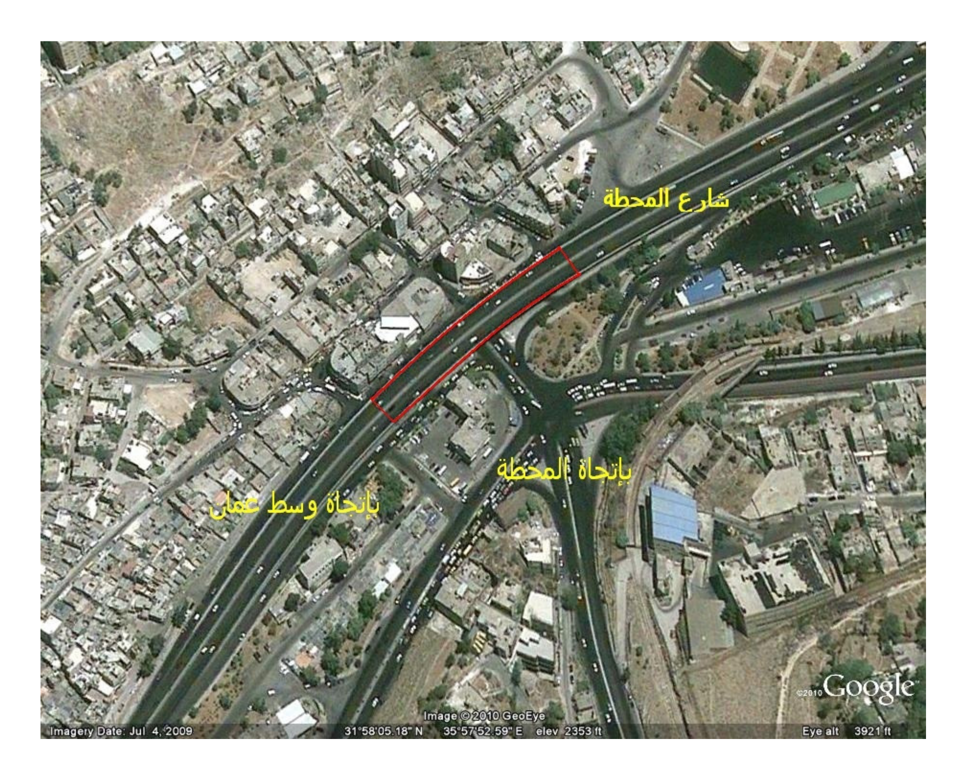


Figure 3-31: Aerial View of Almahata Bridge (Adapted from Google Earth, USA)

Almahata Bridge is a five-span bridge with a total length of 120 m. The exterior spans are 21 m long, while the interior spans are 26 m long. The abutment walls simply support the superstructure at the ends of the bridge. The bridge elevation and plan views are shown in Figures 3-32. Figure 3-33 shows a general view of the bridge.

The deck is cast-in-place, reinforced concrete multi cells box girders section with an overall average width of 20 m and a 19 m roadway width, the depth of the deck is 1.0 m. The bridge deck cross-section is shown in Figure 3-34.

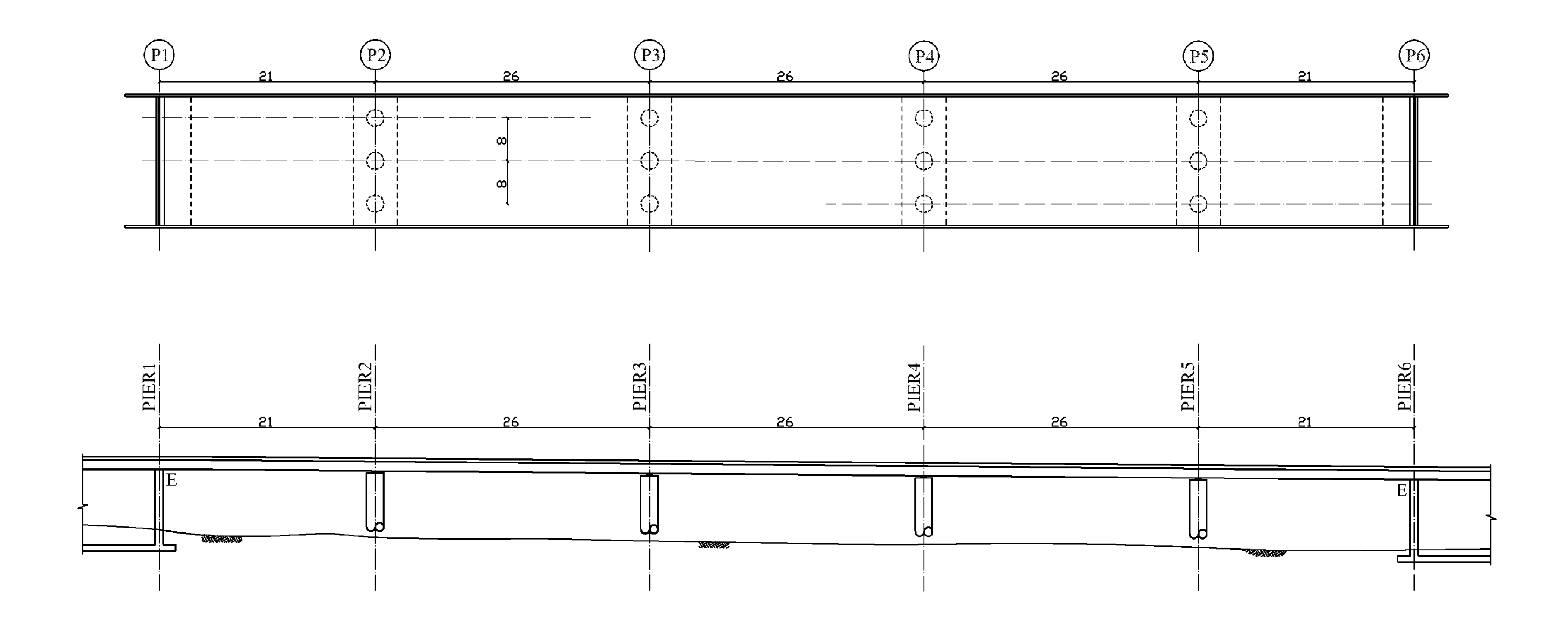


Figure 3-32: Almahata Bridge - plan & elevation, dimensions in meter (Adapted from Greater Amman Municipality).



Figure 3-33: A general view of Almahata Bridge.

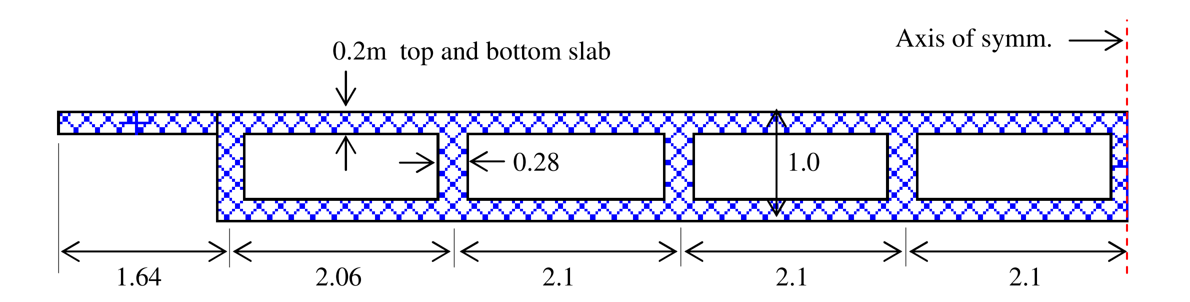


Figure 3-34: Almahata Bridge deck typical section (Dimensions in meter).

At each interior pier, a 3.2 m wide by 1.0 m deep transverse crossbeam distributes the bridge loads to three columns. The columns at pier #2 are 5.65 m long, while columns at pier #3 and pier #4 are 5.87 m and 5.81 m long, respectively. The longest columns have a length of 6.06 m and are located at pier #5. The columns have a circular shape with a diameter equal to 1.0 m and a clear cover of 40 mm, reinforced by 14 mm hoops spaced at 300 mm on center. Longitudinal reinforcement of the column is comprised of 26 equally spaced 32 mm bars.

The bridge ends at Abutment #1 and Abutment #6 are supported simply by abutment walls that are 1.1 m thick. There is a 60 mm gap between the end diaphragm and the wall. Table 3-9 shows the specified material properties of the bridge.

Table 3-9: Almahata Bridge Material Properties

Material Properties	
Bars yield strength	414 MPa
28days – Concrete strength (Cube) (For deck)	45 MPa
28days – Concrete strength (Cube) (For walls and piers)	35 MPa

3.3.2. Almahata Bridge Mathematical Model

3.3.2.1. Superstructure and Pier Modeling

Based on the FHWA-SRM (2005) recommendations, a spine-type model was used to represent the bridge superstructure utilizing the software SAP2000. Superstructure was represented by a single line of multiple three-dimensional frame elements, which passes through the centroid of the superstructure. As most of the mass of a bridge is in the superstructure, four to five members per span were used to represent the superstructure (FHWA-SRM, 2005). Rigid elements were provided between the centroid of the superstructure and the centroid of the crossbeams (FHWA-SRM, 2005). This connection element is shown schematically in Figure 3-12.

The mass of the structure was specified per unit length of the members with half the member mass being subsequently assigned to each node. Superstructure cross-sectional properties were obtained using the "Section Designer" in SAP2000. A body constraint was assigned at the nodes of the members representing the crossbeam to ensure that, as would be expected for the actual bridge, the columns attract approximately equal forces.

Gross stiffness properties were assigned to the moment of inertia of the entire cross section of the superstructure. Since the superstructure is a post-tensioned concrete box girder, it is recommended to use one hundred percent of the gross moment of inertia as effective, (Priestley et al, 1996).

Since the bridge columns are expected to respond inelastically under the input ground motions, effective column properties were used to reflect concrete cracking and reinforcement yielding. Table 7-1 in FHWA-SRM (2005) was used to determine the effective stiffness for the different components of the bridge, which is presented in Table 3-2.

For the torsional stiffness FHWA-SRM (2005) recommends to use 20% of the uncracked torsional stiffness to represent the effects of cracking. Figure 3-13 shows a typical bridge pier with the location of the effective section properties.

Detailed calculations for the flexural stiffness reduction factors for all piers in all Bridges are shown in Appendix D. Almahata bridge mathematical model is shown in Figure 3-34.

The superstructure is supported on bearing pads at Abutment #1, pier #2, pier #5 and Abutment #2. The bearing pads at Abutment #1 and Abutment #2 allow for translation movement in the transverse and longitudinal directions of the bridge. The bearing pads at pier #2 and pier #5 allow for translation movement in the longitudinal direction of the bridge. These support conditions were represented in the model by releasing the associated degree of freedom at the top of the column at the intersection with the superstructure. The bottom ends of the columns are connected to a rigid box culvert underneath. Fixed supports were assumed at these ends to represent the existing boundary conditions.

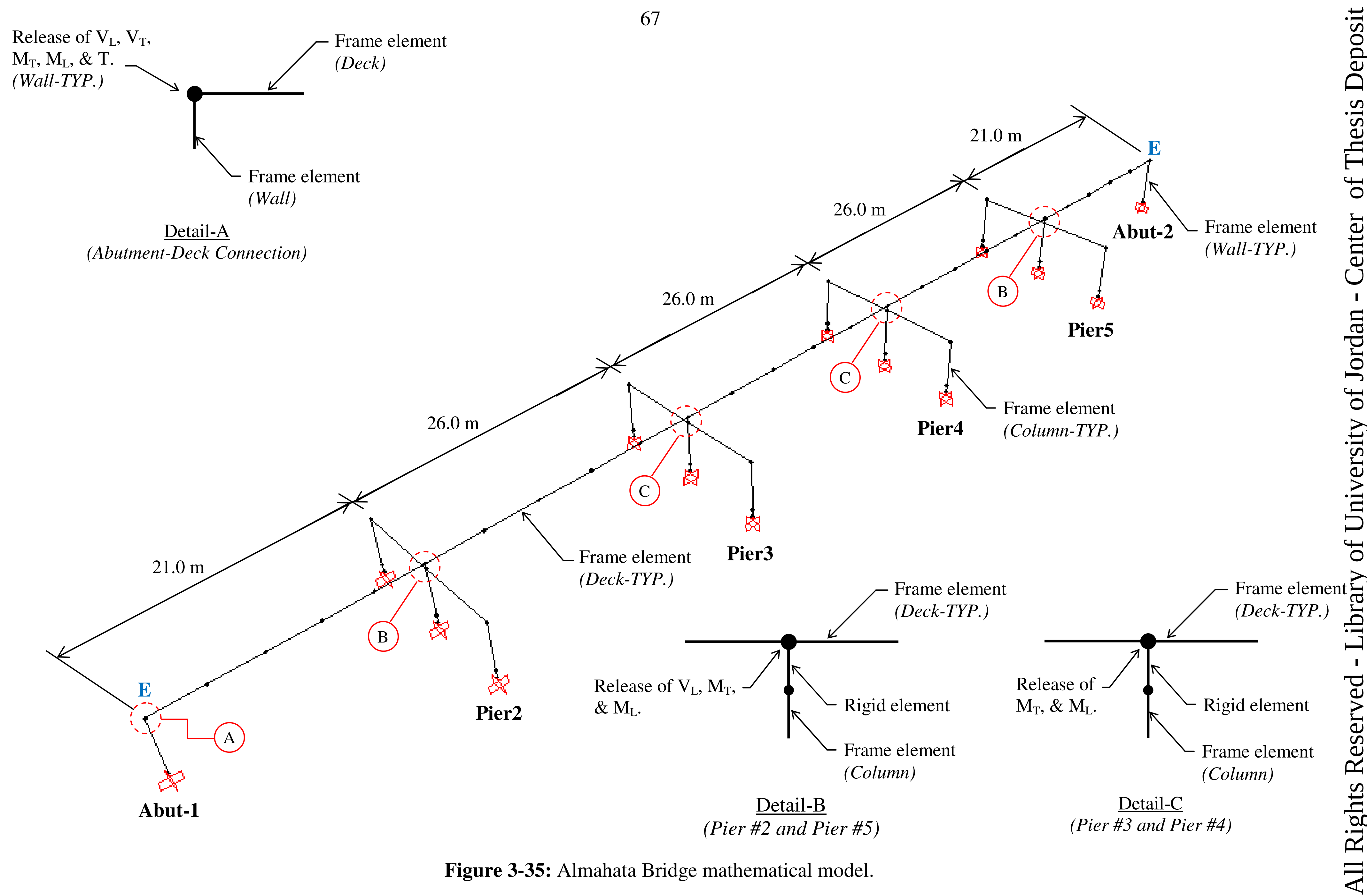


Figure 3-35: Almahata Bridge mathematical model.

CHAPTER FOUR

4. CAPACITY AND DEMAND ASSESSMENT

Bridge evaluation is essentially a two-part process. A demand analysis is first required to determine the forces and displacements imposed on a bridge by an earthquake. This is followed by an assessment of the capacity to withstand the demand. If the bridge has the capacity to withstand the required demand, retrofitting is not required, but if the capacity is less than the demand, a decision needs to be made as to the extent of retrofitting that will be undertaken. Many evaluation methods express the assessment results as capacity/demand ratios where a ratio less than one indicates a need for retrofitting.

4.1. Evaluation Methods

Six evaluation methods are described in the FHWA-SRM (2005) and are listed below in an increasing order of sophistication and rigor.

4.1.1. Method A1/A2

Connection forces and seat width checks. Seismic demand analysis is not required in this method, but the capacity of connections details and seat width adequacy is checked against minimum values. The method is suitable for all single-span bridges and others in low hazard zones. The method is divided into two categories, A1 and A2.

Method A1: Seismic demand analysis is not required in this method, but the capacity of the connections must exceed 10 percent of the vertical reactions at each connection. Seat width requirements are checked against minimum requirements.

Method A2: Seismic demand analysis is not required in this method, but the capacity of the connections must exceed 25 percent of the vertical reactions at each connection, and seat width requirements are checked against minimum requirements. Pile reinforcement must also meet minimum requirements.

4.1.2. Method B

Component capacity checks. Seismic demand analysis is not required, but the relative strength of the members and the adequacy of certain key details (including connection forces and seat widths) are checked against specified requirements. This method is suitable for regular bridges in Seismic Retrofit Category C, subject to restrictions on F_VS_1.

4.1.3. Method C

Component capacity/demand method. Seismic demands are determined by an elastic analysis such as the uniform load method, multi-mode response spectrum method, or an elastic time history method. The uniform load method is adequate for bridges with regular configurations. Otherwise, the multi-mode method is used as a minimum. Capacity/demand ratios are calculated for all relevant components. This method is suitable for all bridges in Seismic Retrofit Categories C and D, but gives best results for bridges that behave elastically or nearly so.

4.1.4. Method D1

Capacity spectrum method. Seismic demands are determined by simple models such as the uniform load method, and capacity assessment is based on a simplified bilinear lateral strength curve for the complete bridge. A capacity spectrum is used to calculate the capacity/demand ratio for the bridge, for each limit state. This method is suitable for regular bridges in Seismic Retrofit Category C and D.

4.1.5. Method D2

Structure capacity/demand method. Seismic demands are determined by elastic methods, such as the multi-mode response spectrum method, or an elastic time history method. Capacity assessment is based on the displacement capacity of individual piers as determined by a 'pushover' analysis which includes the nonlinear behavior of the inelastic components. A capacity spectrum is used to calculate the capacity/demand ratio for each pier, bearing and foundation of the bridge for each limit state. This method is suitable for all bridges in Seismic Retrofit Category C and D. This Method is also known as the pushover method or alternatively the Nonlinear Static Procedure.

4.1.6. Method E

Nonlinear dynamic procedure (time history analysis). Seismic demands are determined by a nonlinear dynamic analysis using earthquake ground motion records to evaluate the displacement and force demands. Capacities of individual components are explicitly modeled in the demand analysis. This method is suitable for irregular complex bridges, or when site specific ground motions are to be used, as in the case of a bridge of major importance.

FHWA-SRM (2005) provides guidelines on how to determine the most appropriate evaluation method for a specific bridge. The selection of the appropriate evaluation method depends on different factors. They are bridge importance, anticipated service life (ASL), spectral accelerations (S_s and S_l), and soil factors (F_a and F_v). The following is a detailed discussion on each factor.

Bridge Importance: Classification of bridge importance based on traffic counts and detour lengths has been proposed in the past and importance indices developed. A broad classification based on engineering judgment is preferred, FHWA-SRM (2005)

recommends two such classes: essential and standard. Essential Bridges are those that are expected to function well during and after an earthquake or which cross routes that are expected to remain open immediately following an earthquake. All other bridges are classified as Standard. The determination of importance is therefore subjective and consideration should be given to societal/survival and security/defense requirements when making this judgment (FHWA-SRM, 2005).

Anticipated Service Life (ASL): An important factor in determining which evaluation method should be used is the anticipated service life (ASL). Retrofitting a bridge with a short service life is difficult to justify in view of the very low likelihood that the design earthquake will occur during the remaining life of the structure. On the other hand, a bridge that is almost new or being rehabilitated to extend its service life, should be retrofitted for the longer remaining service life (FHWA-SRM, 2005).

Bridges in category ASL 1 are considered to be near the end of their service life and retrofitting may not be economically justified. Thus, these bridges need not be retrofitted and are assigned to the lowest seismic retrofit category, i.e., category A. Bridges in category ASL 3 are almost new, and retrofitting to the standard of a new design may be justified. Table 4-1 shows service life category according to the anticipated service life.

Table 4-1: Service life categories (Adapted from FHWA-SRM, 2005).

Service Life Category	Anticipated Service Life	Age
ASL 1	0 - 15 yrs	60 - 75 yrs
ASL 2	16 - 50 yrs	25 - 60 yrs
ASL 3	> 50 yrs	< 25 yrs

After determination of bridge importance and service life category, performance levels can be determined based on Table 4-2 according to the bridge importance and service life category.

Table 4-2: Performance levels for retrofitted bridges (Adapted from FHWA-SRM, 2005).

Bridge Importance and Service Life Category					
Standard			Essential		
ASL 1	ASL 2	ASL 3	ASL 1	ASL 2	ASL 3
PL0	PL1	PL1	PL0	PL1	PL2

Spectral Accelerations (S_s and S_l): To determine the seismic demand on a bridge due to a particular earthquake ground motion, FHWA-SRM (2005) recommend the use of a two-point method to define the design response spectrum from which earthquake forces are calculated. The S_l and S_s ordinates (S_1 = Spectral acceleration at 1.0 sec period, S_s = Spectral acceleration at 0.2 sec period) are first scaled by the soil factors F_a and F_v (F_a = Site factor in short-period range of design spectrum, and F_v = Site factor in long-period range of design spectrum) and the resulting products S_{DS} and S_{D1} are used to plot the spectrum. Detailed discussion is introduced in the following section.

Soil Factors (F_a and F_v): The behavior of a bridge during an earthquake is strongly connected to the soil conditions. Soils can amplify ground motions in the underlying rock, sometimes by factors of two or more. The extent of this amplification is dependent on the profile of soil types at the site and the intensity of shaking in the rock below. Sites are classified by type and profile for the purpose of defining the overall seismic hazard, which is quantified as the product of the soil amplification and the intensity of shaking in the underlying rock (FHWA-SRM, 2005).

After determination of spectral acceleration coefficients and soil factors, seismic hazard level (SHL) can be determined, based on Table 4-3.

Table 4-3: Seismic hazard level (Adapted from FHWA-SRM, 2005).

Hazard Level	Using $S_{D1} = F_v S_1$	Using $S_{DS} = F_a S_s$
I	$S_{D1} \leq 0.15$	$S_{DS} \leq 0.15$
II	$0.15 < S_{D1} \leq 0.25$	$0.15 < S_{DS} \leq 0.35$
III	$0.25 < S_{D1} \leq 0.40$	$0.35 < S_{DS} \leq 0.60$
IV	$0.40 < S_{D1}$	$0.60 < S_{DS}$

After determination of the seismic hazard level and the required performance level, seismic retrofit category can be determined by Table 4-4.

Table 4-4: Performance-based seismic retrofit categories (Adapted from FHWA-SRM, 2005).

Hazard Level	Performance Level		
	PL0	PL1	PL2
I	A	A	B
II	A	B	B
III	A	B	C
IV	A	C	D

Figure 4-1 shows a flow chart of the main steps that are needed to determine the seismic retrofit category for a bridge. Section 4.2 discusses in details the determination of seismic retrofit category for the candidate bridges. Table 4-5 describes the requirements of each evaluation method.

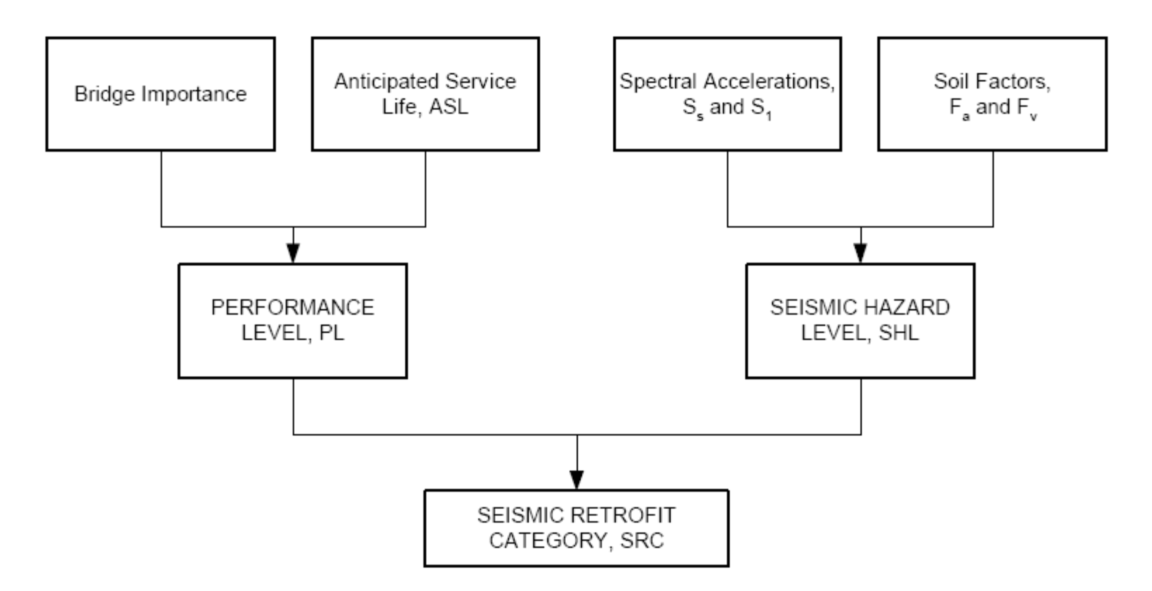


Figure 4-1: Determination of seismic retrofit category (Adapted from FHWA-SRM, 2005).

Table 4-5: Evaluation methods for existing bridges (Adapted from FHWA-SRM, 2005).

METHOD		CAPACITY ASSESSMENT	DEMAND ANALYSIS	APPLICABILITY		COMMENTS
				SRC[1]	Bridge Type	
A1/ A2	**Connection and Seat Width Checks**	Uses default capacity due to non-seismic loads for connections and seat widths.	Not required	A – D	All single-span bridges.	Hand method, spreadsheet useful.
				B	Bridges in low hazard zones.	
B	**Component Capacity Checks**	Uses default capacity due to non-seismic loads for connections, seats, columns and foundations.	Not required	C	Regular bridges, but subject to limitations on F_vS_1.	Hand method, spreadsheet useful.
C	**Component Capacity/Demand Method**	Uses component capacities for connections, seat widths, column details, footings, and liquefaction susceptibility (11 items).	Elastic Methods[2]: • ULM • MM • TH	C & D	Regular and irregular bridges that respond almost elastically, such as those in low-to-moderate seismic zones and those with stringent performance criteria.	Calculates C/D ratios for individual components. This is the C:D Method of previous FHWA Highway Bridge Retrofitting Manuals. Software required for demand analysis.
D1	**Capacity Spectrum Method**	Uses bilinear representation of structure capacity for lateral load, subject to restrictions on bridge regularity.	Elastic Methods[2]: • ULM	C & D	Regular bridges that behave as single-degree-of-freedom systems and have 'rigid' in-plane superstructures.	Calculates C/D ratios for complete bridge, for specified limit states. Spreadsheet useful.
D2	**Structure Capacity/Demand Method**	Uses pushover curve from detailed analysis of superstructure, individual piers and foundation limit states.	Elastic Methods[2]: • ULM • MM • TH	C & D	Regular and irregular bridges.	Calculates C/D ratios for bridge superstructure, individual piers, and foundations. Also known as *Nonlinear Static Procedure, Pushover Method* or *Displacement Capacity Evaluation Method*. Software required for demand and capacity analysis.
E	**Nonlinear Dynamic Method**	Uses component capacities for connections, seat widths, columns and footings.	Inelastic Methods[2] • TH	D	Irregular complex bridges, or when site specific ground motions are to be used such as for bridges of major importance.	Most rigorous method, expert skill required. Software essential.

Notes: 1. SRC = Seismic Retrofit Category
2. ULM = Uniform Load Method; MM = Multi-Mode Spectral Method; TH = Time History Method

4.2. Selection of Evaluation Method

The following section provides a discussion on selecting the appropriate evaluation method for each candidate bridge.

4.2.1. Alnasha Bridge

Step 1: Importance, Anticipated Service Life, and Site Class

A. Bridge is stated to be essential: Essential bridges are those that are expected to function after an earthquake or which cross routes that are expected to remain open immediately following an earthquake.

B. For an anticipated service life of 64 years, the service life category is ASL 3 (FHWA-SRM, 2005, Table 1-1).

C. For the given soil description and shear wave velocity, the site class is D (FHWA-SRM, 2005, Table 1-3).

Step 2: Performance Criteria

From FHWA-SRM, 2005, Table 1-2, the performance level is PL2.

Step 3: Seismic Retrofit Category for upper level ground motion

A. According to Jordan Seismic Map (fetweb.ju.edu.jo/narmouti, 2010 Armouti), the mapped spectral accelerations are $S_S = 0.57$ and $S_1 = 0.23$

B. For site class D and the values obtained for S_S and S_1, the site coefficients are: $F_a = 1.344$ and $F_v = 1.94$ (FHAW-SRM, 2005, Table 1-4).

C. Calculate $F_aS_S = 0.7661$ and $F_vS_1 = 0.4462$, and obtain seismic hazard level (SHL) = IV (FHAW-SRM, 2005, Table 1-5).

D. Seismic retrofit category for PL2 and SHL = IV, is D (FHWA-SRM, 2005, Table 1-6).

Based on a seismic retrofit category equal to D, and the type of the bridge which is claimed to be regular, evaluation method C can be used to evaluate the bridge.

4.2.2. Alharamain Bridge

Step 1: Importance, Anticipated Service Life, and Site Class

A. Bridge is stated to be essential.

B. For an anticipated service life of 66 years, the service life category is ASL 3 (FHWA-SRM, 2005, Table 1-1).

C. For the given soil description and shear wave velocity, the site class is D (FHWA-SRM, 2005, Table 1-3).

Step 2: Performance Criteria

From FHWA-SRM, 2005, Table 1-2, the performance level is PL2.

Step 3: Seismic Retrofit Category for upper level ground motion

A. According to Jordan Seismic Map (fetweb.ju.edu.jo/narmouti, 2010 Armouti), the mapped spectral accelerations are $S_S = 0.57$ and $S_1 = 0.23$

B. For site class D and the values obtained for S_S and S_1, the site coefficients are: $F_a = 1.344$ and $F_v = 1.94$ (FHAW-SRM, 2005, Table 1-4)

C. Calculate $F_aS_S = 0.7661$ and $F_vS_1 = 0.4462$, and obtain seismic hazard level (SHL) = IV (FHAW-SRM, 2005, Table 1-5)

D. Seismic retrofit category for PL2 and SHL = IV, is D (FHWA-SRM, Table 1-6).

Based on a seismic retrofit category equal to D, and the type of the bridge which is claimed to be regular, evaluation method C can be used to evaluate the bridge.

4.2.3. Almahata Bridge

Step 1: Importance, Anticipated Service Life, and Site Class

A. Bridge is stated to be essential.

B. For an anticipated service life of 39 years, the service life category is ASL 2 (FHWA-SRM, 2005, Table 1-1).

C. For the given soil description and shear wave velocity, the site class is D (FHWA-SRM, 2005, Table 1-3).

Step 2: Performance Criteria

From FHWA-SRM, 2005, Table 1-2, the performance level is PL1.

Step 3: Seismic Retrofit Category for upper level ground motion

A. According to Jordan Seismic Map (fetweb.ju.edu.jo/narmouti, 2010 Armouti), the mapped spectral accelerations are $S_S = 0.57$ and $S_1 = 0.23$

B. For site class D and the values obtained for S_S and S_1, the site coefficients are: $F_a = 1.344$ and $F_v = 1.94$ (FHAW-SRM, 2005, Table 1-4)

C. Calculate $F_aS_S = 0.7661$ and $F_vS_1 = 0.4462$, and obtain seismic hazard level (SHL) = IV (FHAW-SRM, 2005, Table 1-5)

D. Seismic retrofit category for PL2 and SHL = IV, is C (FHWA-SRM, 2005, Table 1-6).

Based on a seismic retrofit category equal to C, and the type of the bridge which is claimed to be regular, evaluation method C can be used to evaluate the bridge.

4.3. Method C: Component Capacity/Demand Method

Method C calculates capacity/demand ratios for bridge components that may be damaged during an earthquake. Ratios greater than one indicate sufficient capacity to withstand the required earthquake forces, while ratios less than one indicate components that need of evaluation and possible retrofitting (FHWA-SRM, 2005). Capacity/demand ratios are therefore used to indicate the need for retrofitting.

One feature that distinguishes this method from Method D1, is that the demand is based on the elastic response of the structure calculated by either the uniform load method or a spectral modal analysis. Another difference is that this method focuses on individual component behavior rather than the response of a bridge as a complete structure. In this way, it gives a detailed view of the potential deficiencies of a bridge, but may overestimate the overall vulnerability of a bridge and imply a greater need for retrofitting than is actually necessary. This is because the method ignores 'system' response and the ability of a bridge, acting as a system, to redistribute loads from one member to another. The error here is small if the bridge responds elastically or nearly so. Method C gives conservative results and the degree of conservatism generally increases with the extent of plastic hinging in the bridge. If the indicated retrofit needs are high, it may be wise to use one of the more refined methods (D or E) to re-evaluate the situation (FHWA-SRM, 2005).

In addition to calculating elastic demands by spectral methods, some minimum requirements can be treated as demands. For example, minimum bearing connection forces and minimum support length requirements are useful indicators of demand when calculating C/D ratios for bearing forces and superstructure displacements.

Seismic capacities are calculated at their nominal ultimate values without the use of capacity reduction factors, ϕ, to account for possible understrength and/or undersize members. This is done because the objective of a C/D ratio is to determine the most likely level of failure. The basic equation for determining the C/D ratio, r, for a particular component is:

$$r = \frac{R_C - \sum Q_{NSi}}{Q_{EQ}} \qquad (4\text{-}1)$$

Where:

R_C = nominal ultimate displacement or force capacity of the structural component being evaluated,

ΣQ_{NSi} = sum of the displacement or force demands on a component from nonseismic loads, and

Q_{EQ} = displacement or force demand for the earthquake loading under consideration.

4.4. Demand Assesment

A linear response spectrum analysis was performed and the seismic demands were determined based on an earthquake event having a ten percent probability of exceedance in 50 years (approximate return period of 500 years). For each candidate

bridge, the elastic demand was determined by creating a three-dimensional model, utilizing SAP2000 finite element structural analysis program.

4.4.1. Determination of Design Response Spectrum

Based on FHWA-SRM (2005) recommendations, a two-point method is used to define the design response spectrum from which earthquake forces are calculated to determine seismic demand on a bridge due to a particular earthquake ground motion. Figure 4-2 shows how this spectrum is drawn from the two given points. The S_s and S_1 ordinates are first scaled by the soil factors F_a and F_v, respectively, and the resulting products S_{DS} and S_{D1} are used to plot the spectrum where:

$$S_{DS} = F_a . S_s \qquad and \qquad S_{D1} = F_v . S_1 \qquad (4\text{-}2)$$

Where:

S_1 = Spectral acceleration at 1.0 sec period,

S_s = Spectral acceleration at 0.2 sec period,

F_a = Site factor in short-period range of design spectrum, and

F_v = Site factor in long-period range of design spectrum.

4.4.2. Combination of Seismic Force Effects

When combining the responses of two orthogonal directions, direction along the main bridge axis and perpendicular axis, the design value of any quantity of interest (displacement, bending moment, shear or axial force) was obtained by the 100-40 percent combination rule. According to this rule, the design value is obtained from the largest value given by the following two load cases:

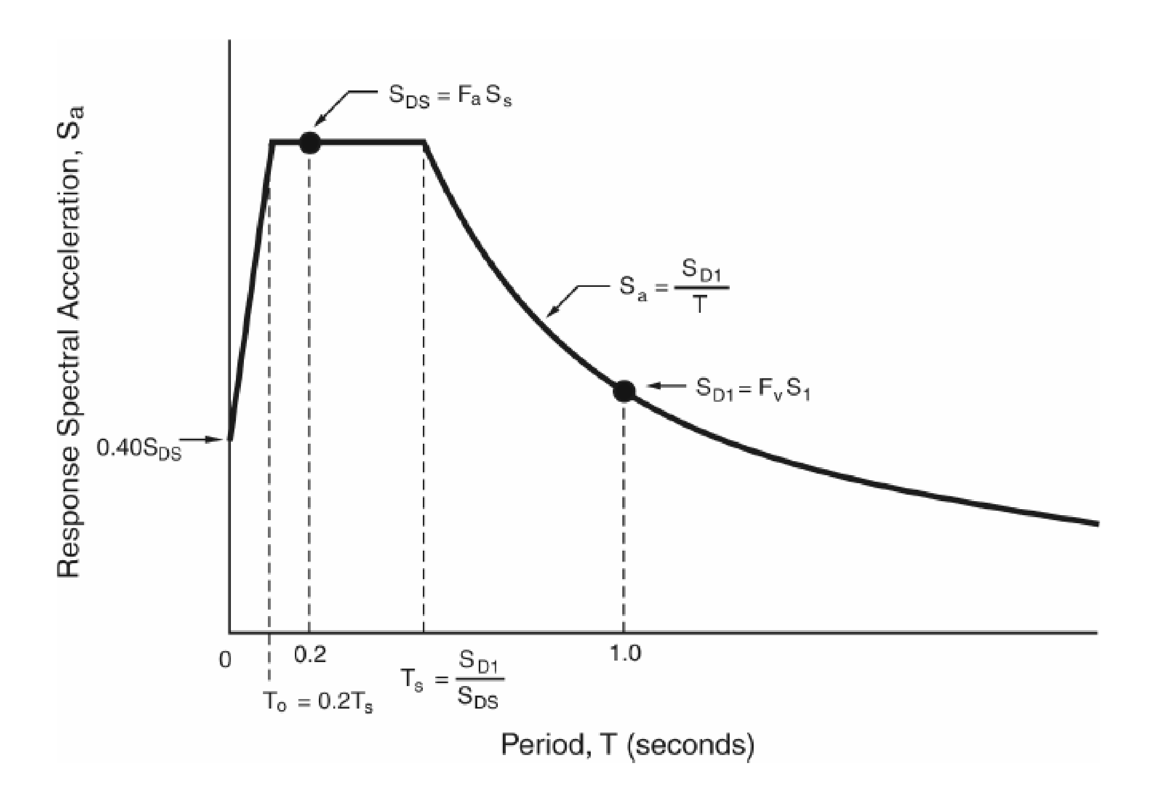


Figure 4-2: Construction of the seismic design response spectrum (Adapted from FHWA-SRM, 2005).

Load Case 1 (LC1) – 100 percent of the absolute value of the response resulting from the analysis in one orthogonal direction (transverse) is added to 40 percent of the response resulting from analyses in the orthogonal longitudinal direction:

$$M_x^{LC1} = 1.0M_x^T + 0.4M_x^L \quad (4\text{-}3)$$

Where M_x^T, and M_x^L are the x-components of moment calculated from a transverse, and longitudinal analysis, respectively.

Load Case 2 (LC2) – 100 percent of the absolute value of the response resulting from an analysis in one of the other orthogonal directions (longitudinal) added to 40 percent of the responses resulting from analysis in the orthogonal transverse direction:

$$M_x^{LC2} = 0.4M_x^T + 1.0M_x^L \quad (4\text{-}4)$$

4.5. Capacity Assessment

Guidelines for determining the strength capacity of bridge members are given in FHWA-SRM (2005) for use when assessing the strength capacity of complete bridges or bridge substructures. In particular, procedures are given for calculating the following:

A. Flexural strength of reinforced concrete columns and beams:
   1. Expected flexural strength,
   2. Flexural overstrength capacity, and
   3. Flexural strength of columns with lap-splices in plastic hinge zones.
B. Shear strength of reinforced concrete columns and beams:
   1. Initial shear strength, and
   2. Final shear strength.
C. Shear strength of reinforced concrete beam-column joints:
   1. Maximum beam-column joint strength, and
   2. Cracked beam-column joint strength.

The following sections discuss the details of the procedure followed for determining the required strength values:

4.5.1. Flexural Strength of Reinforced Concrete Columns and Beams

Several types of member flexural strength are required for a detailed capacity assessment of a bridge. These include the followings:

A. Expected flexural strength based on material expected strength factors and equation.
B. Flexural overstrength based on member overstrength factors and equation.

C. Expected flexural strength of columns with lap-splices located in potential plastic hinge zones, based on expected strength factors.

4.5.1.1. Expected Flexural Strength

The flexural strength of members (either with or without axial loads) is determined based on monotonic behavior, where strains are assumed to vary linearly across the section, and the stresses are related to strains through material property laws (FHWA-SRM, 2005).

The expected flexural strength (at theoretical yield) is based on a modified form of the nominal strength calculations required in the AASHTO-LRFD Specification. A rectangular stress block for unconfined concrete and elasto-plastic behavior for steel is assumed. The following assumptions are made:

A. Maximum concrete strain at the outermost concrete fiber is 0.003. Average concrete stress in the effective compression zone is $0.85f'_{ce}$, where f'_{ce} is the expected concrete strength.
B. Expected yield stress of the longitudinal reinforcement (f_{ye}) is 300 MPa and 450 MPa for Grade 40 and Grade 60 steel, respectively.
C. Effective depth of the concrete stress block is $a = \beta_1 c$, where c is the neutral axis depth, and $\beta_1 = 0.85$ for $f'_{ce} \leq 30$ MPa and $\beta_1 = 0.65$ for $f'_{ce} \geq 60$ MPa. Linear interpolation is used for β_1 if 30 MPa $< f'_{ce} <$ 60 MPa.

The expected flexural strength (M_e) is calculated using a plastic analysis approach as given below (Mander et al, 1998b):

$$\frac{M_e}{f'_{ce}A_g D} = \frac{M_b}{f'_{ce}A_g D}\left[1 - \left(\frac{\frac{P_e}{f'_{ce}A_g} - \frac{P_b}{f'_{ce}A_g}}{\frac{P_t}{f'_{ce}A_g} - \frac{P_b}{f'_{ce}A_g}}\right)^2\right] \qquad (4\text{-}5)$$

Where:

A_g = Gross area of the column section,

P_e = Axial load on the bridge column including both gravity and seismic effects,

f_{ye} = Expected yield strength of the longitudinal reinforcement in the lap-splice zone,

f'_{ce} = Expected concrete strength,

ρ_t = Volumetric ratio of the longitudinal reinforcement,

$\frac{P_e}{f'_{ce}A_g}$ = axial stress ratio based on gravity load and seismic actions,

$\frac{P_t}{f'_{ce}A_g} = -\rho_t \frac{f_{ye}}{f'_{ce}}$ = axial tensile capacity ratio of the column based on the expected material properties,

$\frac{P_b}{f'_{ce}A_g} = 0.425\beta_1$ = axial load capacity ratio at the maximum nominal (balanced) moment on the section,

$$\frac{M_b}{f'_{ce}A_g D} = \left(K_{shape}\rho_t \frac{f_{ye}}{f'_{ce}}\frac{D'}{D} + \frac{P_b}{f'_{ce}A_g}\frac{1-k_o}{2}\right) \quad (4\text{-}6)$$

β_1 = stress block factor (≤ 0.85),

D' = pitch circle diameter of the reinforcement in a circular section, or the out-to-out dimension of the reinforcement in a rectangular section, generally assumed to be equal to 80 percent of overall diameter of column, D,

K_{shape} = shape factor:

= 0.32 for circular sections,

= 0.375 for square sections with 25% of the reinforcement placed in each face,

= 0.25 for walls with strong axis bending, and

= 0.50 for walls with weak axis bending.

κ_o = factor related to the centroid of the stress block:

= 0.6 for circular sections, and

= 0.5 for rectangular sections.

4.5.1.2. Flexural Overstrength Capacity

In any method of capacity assessment that is based on a collapse mechanism, it is necessary to know the upper bound on flexural capacity, i.e., the flexural moment overstrength capacity, M_{po}, of the columns, piers, and piles that form the primary load resisting mechanism (FHWA-SRM, 2005).

The flexural overstrength capacity, M_{po}, is estimated from a sectional plastic analysis using the properties of confined concrete and the ultimate tensile strength for the stress in the longitudinal reinforcement. (Mander et al, 1998a). In this method, M_{po} is given by:

$$\frac{M_{po}}{f'_c A_g D} = \frac{M_b}{f'_c A_g D}\left[1 - \left(\frac{\frac{P_e}{f'_c A_g} - \frac{P_{bcc}}{f'_c A_g}}{\frac{P_{to}}{f'_c A_g} - \frac{P_{bcc}}{f'_c A_g}}\right)^2\right] \quad (4\text{-}7)$$

Where:

$\frac{P_e}{f'_c A_g}$ = column axial stress ratio based on gravity loads and seismic actions,

$\frac{P_{to}}{f'_c A_g} = -\rho \frac{f_{su}}{f'_c}$ = axial tensile capacity ratio of the column,

$\frac{P_{bcc}}{f'_c A_g} = 0.5\alpha\beta \frac{A_{cc}}{A_g}$ = axial load capacity ratio at the maximum confined (balanced) moment on the section,

$$\frac{M_{bo}}{f'_c A_g D} = \left(K_{shape}\rho_t \frac{f_{su}}{f'_c}\frac{D'}{D} + \frac{P_{bcc}}{f'_c A_g}\frac{1-k_o}{2}\right) \quad (4\text{-}8)$$

f_{su} = ultimate tensile strength of the longitudinal reinforcement = 1.5 f_{ye} unless determined otherwise by coupon tests,

A_{cc} = area of confined concrete core, and

A_g = gross section area.

Stress block factors α, β are as follows:

α = ratio of average concrete stress in compression zone to confined concrete strength

= $0.85+0.12(K-1)^{0.4}$

K = strength enhancement factor due to the confining action of the transverse reinforcement, and is given below for circular and rectangular sections = f'_{cc}/f'_{ce},

f'_{cc} = confined concrete strength, and

β = depth of stress block

= $0.85+0.13(K-1)^{0.6}$.

For circular sections, the confined strength parameter (K) is given by Mander et al. (1988):

$$K = 2.254\sqrt{1 + 7.94\frac{f'_l}{f'_{ce}}} - 2\frac{f'_l}{f'_{ce}} - 1.254 \qquad (4\text{-}9)$$

Where:

$f'_l = \frac{1}{2}k_e\rho_s f_{yh}$ = lateral stress supplied by the transverse reinforcement at yield,

$\rho_s = \frac{4A_{bh}}{sD''}$ = volumetric ratio of spirals or circular hoops to the core concrete,

$k_e = \frac{(1-\chi s/D'')}{(1-\rho_{cc})}$ = confinement effectiveness coefficient for spirals and hoop steel,

χ = coefficient with values of 0.5 and 1.0 for spirals and hoops, respectively,

s = spacing of spirals or hoops, and

D'' = diameter of transverse hoop or spiral (measured to the centerline of the hoop). For rectangular sections, the confined strength parameter (K) is obtained from Figure 4-3 which uses the x- and y- confining stresses (f'_{lx} and f'_{ly} respectively) to give K (Mander et al., 1988; Paulay and Priestley, 1991). Stresses f'_{lx} and f'_{ly} are defined as follows:

$f'_{lx} = k_e \rho_x f_{yh}$ is the lateral confining stress in the x-direction,

$f'_{ly} = k_e \rho_y f_{yh}$ is the lateral confining stress in the y-direction,

$\rho_x = \frac{A_{sx}}{sD''}$ is the volume ratio of transverse hoops or ties to the core concrete in x direction,

$\rho_y = \frac{A_{sy}}{sb''}$ is the volume ratio of transverse hoops or ties to the core concrete in y direction,

k_e = confinement effectiveness coefficient for rectangular sections with hoops or ties:

= 0.75 for rectangular columns, and

= 0.6 for rectangular wall sections.

f_{yh} = yield stress of the transverse hoops,

D'' = width of column normal to x-direction (measured to the centerline of hoops or ties), and

b'' = width of column normal to y-direction (measured to the centerline of hoops or ties).

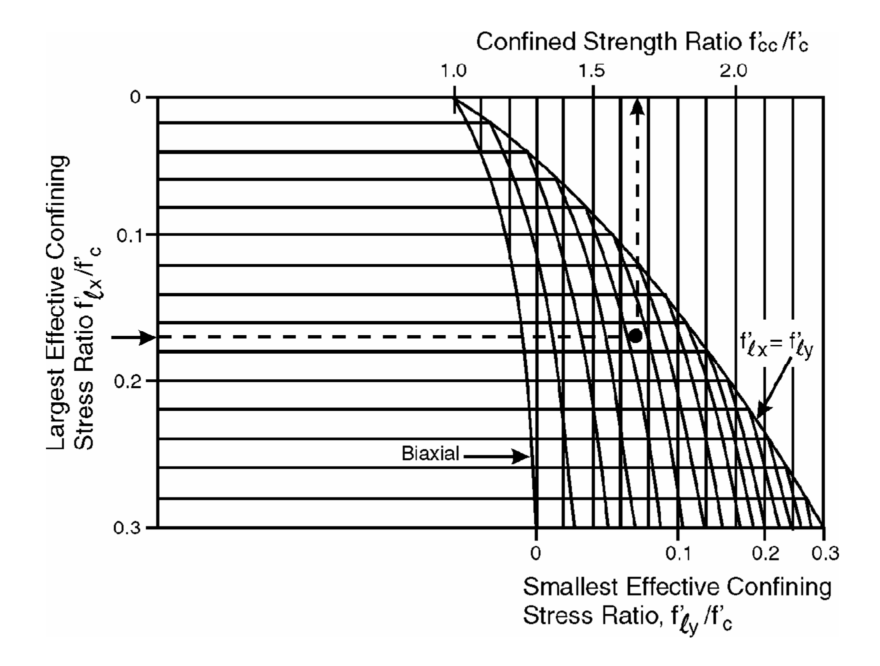


Figure 4-3: Confined strength ratio (K) for reinforced concrete members (Adapted from FHWA-SRM, 2005)

4.5.1.3. Flexural Strength of Columns with Lap-Splices in Plastic Hinge Zones

The flexural strength of a column is reduced when the longitudinal steel is lapped in the plastic hinge zone, which is a common occurrence near the base of columns in older bridges. FHWA-SRM, 2005 as a first approximation, assumes the reduction in strength is depends solely on the length of the splice, l_{lap}, compared to the minimum required value. The reduced moment (M_s) is then given by:

$$M_s = M_e\ (l_{lap}/l_s) \quad \text{but not greater than } M_e \qquad (4\text{-}10)$$

Where:

M_e = expected flexural strength,

l_s = theoretical lap-splice length and is determined from:

$$l_s = 0.4 \frac{f_{ye}}{\sqrt{f'_{ce}}} d_b \qquad (4\text{-}11)$$

d_b = diameter of the longitudinal reinforcing bar in the lap,

f_{ye} = expected yield strength (MPa) of the longitudinal reinforcement in the lap-splice zone, and

f'_{ce} = expected strength (MPa) of concrete surrounding the lap-splice zone.

4.5.2. Shear Strength of Reinforced Concrete Columns and Beams

The shear resistance of cracked structural concrete members is reduced by load reversals and increasing plastic hinge rotations. As a consequence, two shear strength states are defined:

1. The initial shear strength, V_i, and
2. The final shear strength, V_f.

The difference between the two states is due to deterioration in the concrete as the cyclic loading progresses with a corresponding reduction in the concrete contribution, V_c, to the shear capacity. This contribution diminishes due to the presence of widely-spaced tensile cracks and yielding of the longitudinal bars. Expressions for the initial and final shear strengths are given in the following sections.

4.5.2.1. Initial Shear Strength, V_i

Initial shear strength, V_i, is given by:

$$V_i = V_s + V_p + V_{ci} \tag{4-12}$$

Where:

V_s = contribution to the shear strength provided by rebar truss action,

V_p = contribution provided arch (strut) action, and

V_{ci} = contribution provided by diagonal tension field in the concrete.

Each of these contributions is described below.

The shear resistance provided by truss action in the reinforcing steel is given by:

$$V_s = A_v f_{yh} \frac{D''}{s} \cot\theta \tag{4-13}$$

Where:

A_v = shear area provided by the transverse hoops:

= 2 A_{bh} for rectangular columns, and

= π A_{bh} / 2 for circular columns.

A_{bh} = area of one spiral or hoop bar,

f_{yh} = yield stress of the transverse hoops or spirals,

D'' = diameter of transverse hoop or spiral (measured to the centerline of the hoop),

s = center-to-center longitudinal spacing of the transverse hoop steel,

θ = angle of the principal crack plane (Kim and Mander, 1999) and given by

$$\tan\theta = \left(\frac{1.6\sigma_v A_e}{\Lambda\sigma_t A_g}\right)^{0.25} \geq \tan\alpha \qquad (4\text{-}14)$$

Λ = fixity factor:

= 2 for fixed-fixed column conditions, and

= 1 for fixed-pinned conditions.

A_e = effective shear area (assumed as 80 percent of the gross area, A_g, for rectangular and circular sections),

ρ_t = ratio of the total area of longitudinal reinforcement to the gross section area

= A_{st} / A_g,

ρ_v = volumetric ratio of transverse steel:

= A_v / $b_w s$ for rectangular columns, and

= $\rho_s/2$ = 2 A_{bh}/sD'' for circular columns.

A_v = area of transverse shear steel,

b_w = center-to-center spacing of transverse shear steel across width of rectangular column,

tan α = corner-to-corner strut angle:

= jd/L,

jd = internal lever arm of the concrete compression member, and

L = length of the column.

The shear resistance provided by the arch (strut) action is given by:

$$V_p = \frac{\Lambda}{2} P \tan\alpha \quad (4\text{-}15)$$

Where Λ is the fixity factor defined above, P is the axial load on member (compression only), and tan α is the corner-to-corner strut angle defined above.

The shear resistance provided by the diagonal tension field in the concrete is:

$$V_{ci} = 0.3\sqrt{f'_{ce}}A_e \quad (4\text{-}16)$$

Where A_e is the effective shear area equal to $0.8A_g$.

4.5.2.2. Final Shear Strength, V_f

The final shear strength is given by:

$$V_f = V_s + V_p + V_{cf} \quad (4\text{-}17)$$

In this equation, V_s and V_p are as defined above, while V_{cf} is the final shear strength carried by the concrete, which is reduced to allow for plastification, cracking, and cyclic loading effects. This is given by:

$$V_{cf} = 0.05\sqrt{f'_{ce}}A_e \quad (4\text{-}18)$$

4.5.3. Shear Strength of Beam-Column Joints

The shear strength of beam–column joints can be assessed in a manner similar to column elements. A principal stress approach is usually adopted, as this is a major determinant in joint performance. A beam–column joint will remain essentially elastic and uncracked, providing that the principal tensile stress in the joint is less than $0.29\sqrt{f'_{ce}}$ MPa. When the principal tensile stress exceeds this level, diagonal cracking of the joint can be expected. The joint strength will be limited to a maximum principal stress of $0.42\sqrt{f'_{ce}}$ MPa, at which point, full diagonal cracking of the joint will have developed. If the joint shear demand arising from the flexural overstrength capacity exceeds this limit, then the joint is said to be shear-critical and the structural

performance will be governed by the reduced joint strength. The shear strength of the beam-column joint is therefore given by:

$$V_j = v_j A_{jh} \quad (4\text{-}19)$$

In which A_{jh} is the area of the beam-column joint in a horizontal plane, and v_j is the average joint shear stress acting on the joint. The latter can be found from a Mohr's circle analysis for principal stresses in a joint subject to the combined actions of f_v, f_h and v_j as follows:

$$v_j = \sqrt{p_t^2 - p_t(f_v + f_h) + 2f_v f_h} \quad (4\text{-}20)$$

where:

f_v = average axial stress on the joint (compression is negative),

f_h = average horizontal axial stress on the joint (has a zero value unless the joint has horizontal prestress, or similar, applied), and

p_t = major principal tension stress (tension is positive). This term dominates performance of the joint.

4.5.3.1. Maximum Beam-Column Joint Strength, V_{ji}

The maximum joint shear capacity is achieved when full diagonal cracking develops. This occurs when the principal tensile stress in the joint is given by:

$$p_t = 0.42\sqrt{f'_{ce}}\ \text{MPa} \quad (4\text{-}21)$$

Where f'_{ce} is the expected concrete strength in MPa. This principal stress is used to calculate V_{ji}.

4.5.3.2. Cracked Beam–Column Joint Strength, V_{jf}

The residual joint shear capacity is maintained after the strength has deteriorated. This occurs when the principal tensile stress in the joint is given by:

$$p_t = 0.29\sqrt{f'_{ce}}\ \text{MPa} \qquad (4\text{-}22)$$

Where f'_{ce} is the expected concrete strength in MPa. This principal stress is used to calculate V_{jf}.

4.6. Deformation Capacity of Bridge Members

A displacement capacity evaluation of a bridge, or pushover analysis (Method D2), should be able to track the nonlinear relationship between load and deformation for the columns and beams as the lateral load is monotonically increased from an initial elastic condition to failure. This requires the estimation of the capacity of each of the critical structural members, from first yield until collapse, and at intermediate limit states. Therefore, member performance is expressed in terms of force versus deformation, moment versus rotation, or shear force versus distortion.

The FHWA-SRM, 2005 provides procedures for calculating the plastic curvatures of the structural members based on the critical deformation limit state.

4.6.1. Plastic Hinge Rotation, θ_p

It is often more convenient to express deformation behavior in relative terms, i.e., drift which is the ratio of lateral displacement to column height, and is the same as the angular rotation of the member chord. Thus, in terms of drifts (or rotations), the ultimate drift (θ_u) is given by:

$$\theta_u = \theta_y + \theta_p \qquad (4\text{-}23)$$

Where the elastic drift at yield for a cantilever column is given by:

$$\theta_y = \frac{\Delta_y}{L} = \frac{1}{3}\phi_y L = \frac{2}{3}\varepsilon_y \frac{L}{D'} \tag{4-24}$$

and the plastic drift is given by:

$$\theta_p = \phi_p L_p \tag{4-25}$$

The elastic component of the total drift is related to the member slenderness (L/D’) and the plastic drift is given by the plastic hinge rotation, which in turn is related to the plastic curvature within the hinge zone.

4.6.2. Characterization of Deformation-Based Limit States

The plastic rotational capacity of a member is based on the governing limit state for that member. The governing limit state is the state that has the least plastic rotational (or plastic curvature) capacity. Plastic curvatures (and therefore plastic rotations) for the following limit states are discussed in this section:

1. Compression failure of unconfined concrete.
2. Compression failure of confined concrete.
3. Compression failure due to buckling of the longitudinal reinforcement.
4. Longitudinal tensile reinforcing bar fracture.
5. Low cycle fatigue of the longitudinal reinforcement.
6. Failure in the lap-splice zone.
7. Shear failure of the member that limits ductile behavior.

4.6.2.1. Compression Failure of Unconfined Concrete

The plastic curvature corresponding to compression failure in unconfined concrete is given by:

$$\phi_p = \frac{\varepsilon_{cu}}{c} - \phi_y \quad (4\text{-}26)$$

Where ε_{cu} is the ultimate concrete compression strain for concrete, which should be limited to 0.005 for unconfined concrete, and c is the depth from the extreme compression fiber to the neutral axis.

4.6.2.2. Compression Failure of Confined Concrete

For concrete confined by transverse hoops, cross-ties, or spirals, the compression strain is limited by first fracture within the confining steel. While this type of failure depends on the cyclic load history, a conservative estimate of the plastic curvature can be obtained from:

$$\phi_p = \frac{\varepsilon_{cu}}{(c-d'')} - \phi_y \quad (4\text{-}27)$$

Where:

c = depth from the extreme compression fiber of the cover concrete (which is expected to spall) to the neutral axis,

d" = distance from the extreme compression fiber of the cover concrete to the centerline of the perimeter hoop (thus, c – d" is the depth of confined concrete under compression), and

ε_{cu} = ultimate compression strain of the confined core concrete, as given by:

$$\varepsilon_{cu} = 0.005 + \frac{1.4\rho_s f_{yh}\,\varepsilon_{su}}{f'_{cc}} \quad (4\text{-}28)$$

ε_{su} = strain at the maximum stress of the transverse reinforcement,

f_{yh} = yield stress of the transverse steel,

ρ_s = volumetric ratio of transverse steel, and

f'_{cc} = confined concrete strength.

For bridge columns that have confined concrete details, it is unlikely that this failure mode will govern, as low cycle fatigue is a more likely controlling mechanism. This is because the axial load in bridge columns is relatively low, and the transverse reinforcement is primarily required to provide restraint against buckling of the longitudinal reinforcement, FHWA-SRM (2005).

4.6.2.3. Buckling of Longitudinal Bars

If a compression member has inadequate transverse reinforcement and the spacing of the spirals, hoops, or cross-ties, s, in potential plastic hinge zones exceeds six longitudinal bar diameters (i.e., s > 6db), then local buckling at high compressive strains in the longitudinal reinforcement is likely to happen. The plastic curvature of this failure mode can be determined from:

$$\phi_p = \frac{\varepsilon_b}{(c - d')} - \phi_y \tag{4-29}$$

Where d' is the distance from the extreme compression fiber to the center of the nearest compression reinforcing bars, and ε_b is the buckling strain in the longitudinal reinforcing steel. If $6d_b < s < 30d_b$, the buckling strain may be taken as twice the yield strain of the longitudinal steel, i.e.,

$$\varepsilon_b = \frac{2f_y}{E_s} \tag{4-30}$$

4.6.2.4. Fracture of the Longitudinal Reinforcement

Tensile fracture occurs when the tensile strain reaches a critical level, as given by ε_{smax}. This failure mode is only likely under near-field impulse-type ground motions

where there is essentially a monotonic (pushover) response. The plastic curvature in this case is given by:

$$\phi_p = \frac{\varepsilon_{smax}}{(d-c)} - \phi_y$$

Where d is the depth to the outer layer of tension steel from the extreme compression fiber, and c is the depth to the neutral axis. The tensile strain ε_{smax} should be limited to a value less than or equal to 0.10.

4.6.2.5. Low Cycle Fatigue of Longitudinal Reinforcement

Since earthquakes induce cyclic loads in bridges, low cycle fatigue failure of the longitudinal reinforcement is possible. This is especially so if the column is well confined and other types of failure, as described above, are prevented. The plastic curvature that leads to a low cycle fatigue failure is given by:

$$\phi_p = \frac{2\varepsilon_{ap}}{(d-d')} = \frac{2\varepsilon_{ap}}{D'} \qquad (4\text{-}32)$$

Where:

D' = distance between the outer layers of longitudinal steel in a rectangular section (d – d'), or the pitch circle diameter of the longitudinal reinforcement in a circular section,

ε_{ap} = plastic strain amplitude, as given by:

$$\varepsilon_{ap} = 0.08(2N_f)^{-0.5} \qquad (4\text{-}33)$$

N_f = effective number of equal-amplitude cycles of loading that lead to fracture, which can be approximated by:

$$N_f = 3.5(T_n)^{-1/3} \tag{4-34}$$

Provided that: $2 \leq N_f \leq 10$, and

T_n = natural period of vibration of the bridge.

4.6.2.6. Failure in the Lap-splice Zone

It is common to have a lap-splice zone at the base of a column where the starter bars from the footing or pile cap are lapped with the flexural reinforcement of the column. This is generally also the location of the plastic hinge zone. The presence of the lap-splice within the plastic hinge may lead to two different behavior modes, which depend on the length of the lap-splice that is provided, l_{lap}, compared to the required length, given by:

$$l_s = 0.4 \frac{f_{ye}}{\sqrt{f'_{ce}}} d_b \tag{4-35}$$

Where d_b is the diameter of the longitudinal reinforcing bar in the l_{ap}, f_{ye} is the expected yield strength of the longitudinal reinforcement in the lap-splice zone, and f'_{ce} is the expected strength of concrete surrounding the lap-splice zone (MPa).

4.6.2.6.1. *Long or Confined Lap-splice, $l_{lap} > l_s$*

Some lap-splice zones in existing bridge columns were designed as tension splices and generous lap lengths were provided by some 40 bar diameters or more. It is possible that if the bond between the reinforcing steel and column concrete is satisfactory, the effective plastic hinge is reduced in length and behavior is then governed by low cycle fatigue of the longitudinal bars. Equation 4-36 determines the length of plastic hinge:

$$L_p = the\ minimum\ of \left[\left(8800\varepsilon_y d_b\right)\ or\ \left(0.08L + 4400\varepsilon_y d_b\right)\right] \tag{4-36}$$

4.5.2.6.2 *Short and Unconfined Lap-splice,* $l_{lap} \leq l_s$

Many lap-splices in bridge columns were designed as compression splices with a lap of 20 bar diameters or less. Initially, such a lap-splice may function quite well and be capable of sustaining the flexural strength capacity of the column. However, under the effect of earthquake induced cyclic loading, the bond in the lap-splice zone deteriorates and the moment capacity of the hinge is reduced.

For a short and unconfined lap-splice zone where $l_{lap} \leq l_s$, the component has a reduced ductility that depends on the curvature ductility of the member. The effective plastic hinge length can be taken as:

$$L_p = L_{lap} \tag{4-37}$$

The lap-splice-limited plastic curvature capacity is given by:

$$\phi_p = (\mu_{lap\phi} + 7)\phi_y \tag{4-38}$$

Where:

ϕ_y = yield curvature, and

$\mu_{lap\phi}$ = curvature ductility at the initial breakdown of bond in the lap-splice zone:

= 0 when $M_s < M_e$, where M_s is given by equation 4-10; i.e., when the lap-splice strength (M_s) is less than the expected flexural strength (M_e), the deterioration in strength commences as soon as the moment reaches M_s (FHWA-SRM, 2005),and

= curvature ductility in the member when it reaches an ultimate strain of 0.002, when $M_e < M_s < M_{po}$, i.e., when the strength of the lap-splice (M_s) exceeds the expected flexural strength (M_e), but is less than the

flexural overstrength (M_{po}), strength deterioration can still be expected but will be delayed (FHWA-SRM, 2005).

4.6.2.7. Shear Failure

If the shear strength of the member is less than the shear demand (based on its flexural strength), the plastic rotation will be limited. Two limiting cases are: (a) brittle shear, and (b) semi-ductile shear. These cases are based on the shear strength relative to the flexural strength. The shear demand (V_m), based on flexure, is given by:

$$V_m = M_p / L \tag{4-39}$$

Where M_p is the expected plastic moment capacity, and L is the distance to the inflection point from the point of maximum moment in the member.

4.6.2.7.1 *Brittle Shear, $V_i \leq V_m$*

When the initial shear strength (V_i) is less than or equal to the shear demand (V_m), the member is considered to be 'shear-critical' and will fail in shear in a brittle manner. Since the member has no ductility capacity,

$$\phi_p = 0 \tag{4-40}$$

4.6.2.7.2 *Semi-ductile Shear, $V_f < V_m < V_i$*

If the shear demand, based on flexure, lies between the initial (V_i) and final shear strength (V_f) of the member, the member has limited ductility capacity given by:

$$\phi_p = \left(5\left(\frac{V_m - V_f}{V_i - V_f}\right) + 2\right)\phi_y \tag{4-41}$$

Where ϕ_y is the yield curvature, V_i is the initial shear strength (as defined previously) which is maintained until a curvature ductility of three is reached after

which deterioration commences, and V_f is the final (residual) shear strength that is maintained when the curvature ductility exceeds eight. However, if $V_m < V_f$, the shear demand is less than the final shear strength of the member and the rotational capacity is limited by flexure and not shear.

CHAPTER FIVE

5. CAPACITY / DEMAND ANALYSIS RESULTS

Elastic and inelastic analyses were carried out to determine the seismic force and displacement demands on each candidate bridge. Capacity/demand (C/D) ratios were determined in accordance to FHWA-SRM (2005) to quantify the likely performance of each bridge during an earthquake. This Chapter presents the analysis results for the three candidate bridges.

5.1. Alnasha Bridge

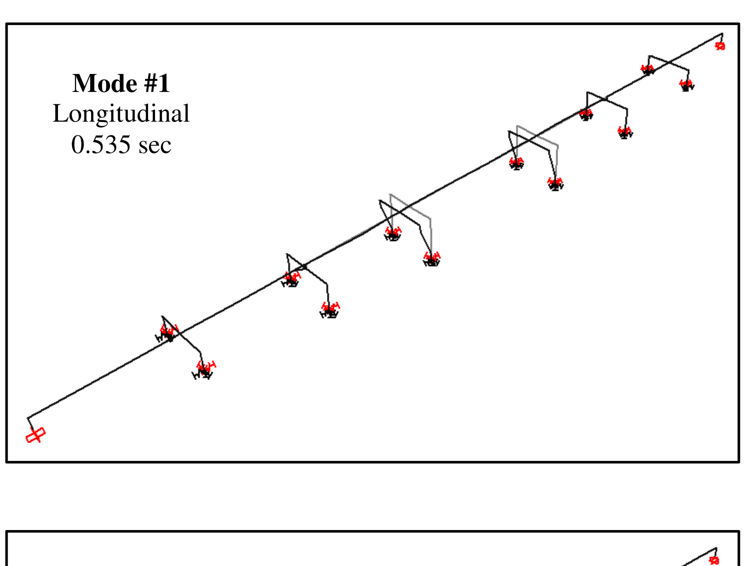
5.1.1. Response Spectrum Analysis

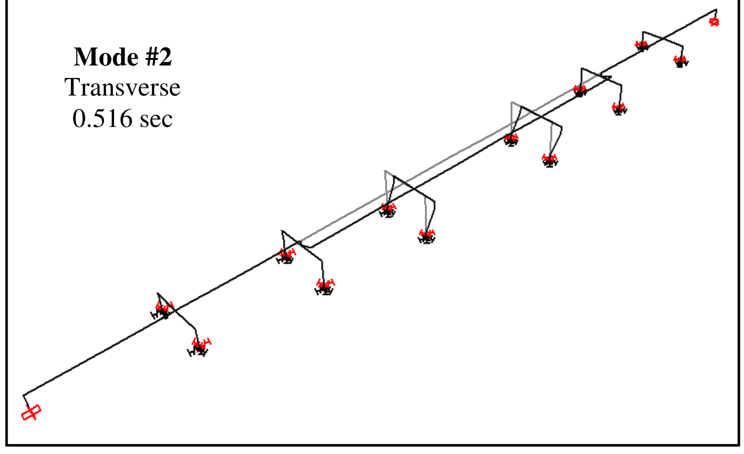
The response spectrum analysis begins with determining the natural frequencies and mode shapes via an eigenvalue analysis. The longitudinal and transverse natural periods and the associated modal participating mass ratios (i.e., effective modal mass to total mass ratios) are shown for the compression model and the tension model in Table 5-1. The longitudinal and the transverse mode shapes for the compression and tension models are shown in Figure 5-1 and Figure 5-2, respectively.

Table 5-1: Alnasha Bridge fundamental periods and mass participation ratios.

Model type	Mode No.	Natural period (sec)	Modal participating mass ratio (%)
Tension model	1 (Longitudinal Mode)	0.535	45.3
	2 (Transverse Mode)	0.516	45.5
	3 (Longitudinal Mode)	0.264	22.8
Compression model	1 (Transverse Mode)	0.516	45.5
	2 (Transverse Mode)	0.256	18.0
	3 (Longitudinal Mode)	0.247	94.0

Table 5-1 shows that the bridge has almost the same natural period in the transverse and longitudinal directions. This result is mainly due to the presence of the intermediate expansion joints in the bridge.





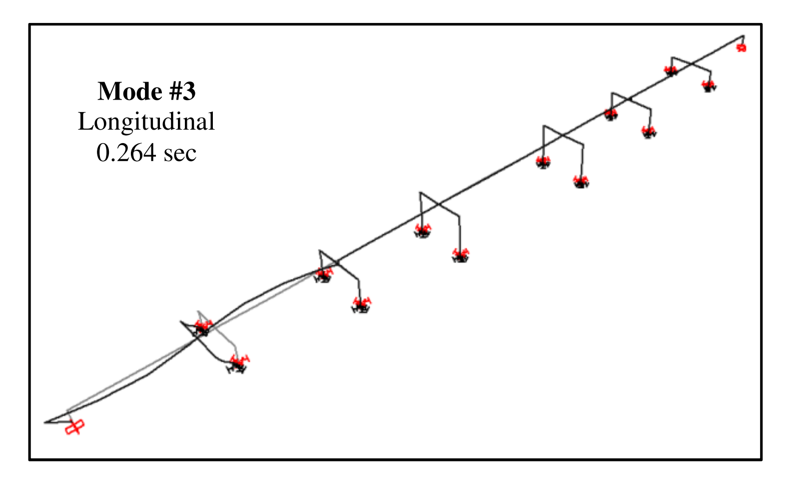
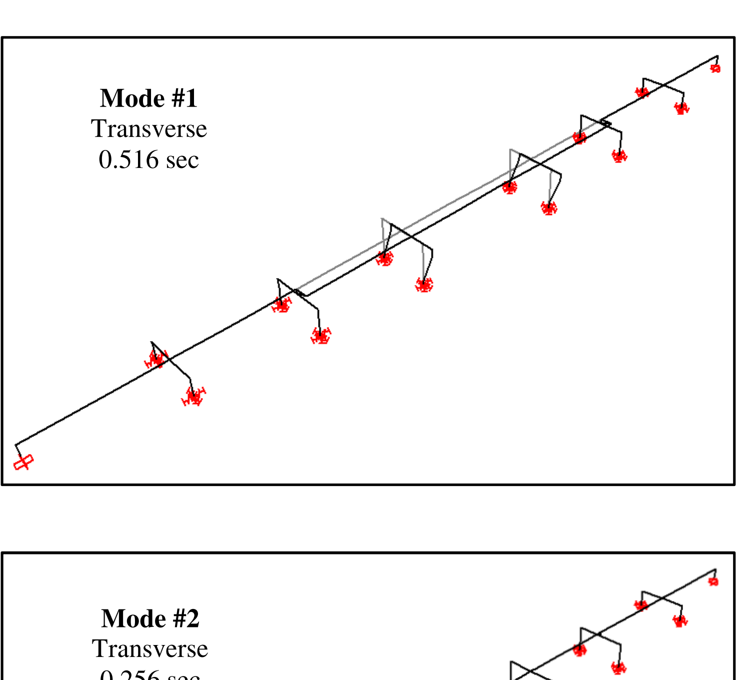
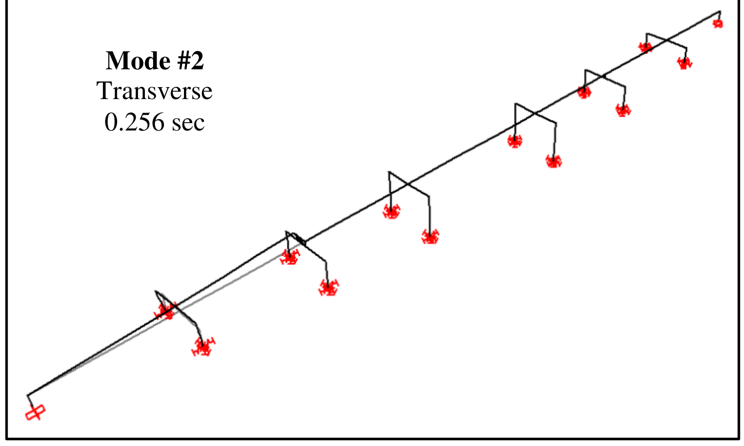


Figure 5-1: Fundamental mode shapes of Alnasha Bridge – Tension Model.





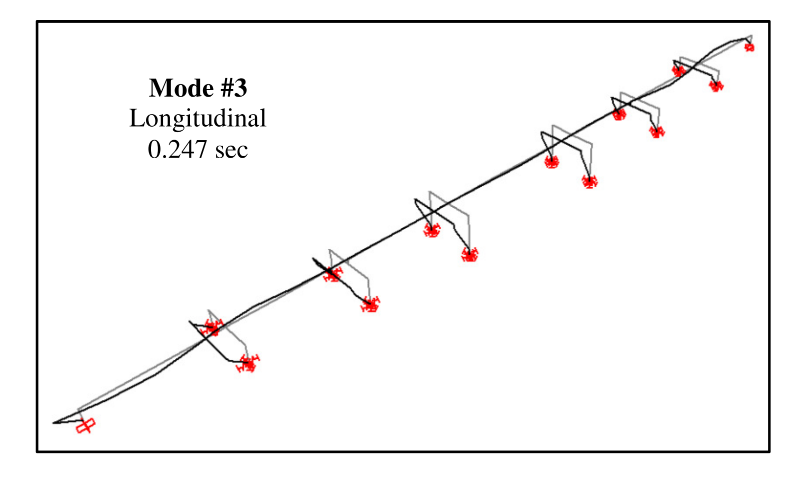


Figure 5-2: Fundamental mode shapes of Alnasha Bridge – Compression Model.

The response spectrum analysis determines the bridge response under the effect of the expected seismic forces. The response includes displacements, moment, and shear forces in the longitudinal and transverse directions of the bridge. The 100-40

percent load combination rule as recommended by FHWA-SRM (2005) was used to determine the seismic demand on the bridge. Table 5-2 shows the displacements demand on the bridge as obtained from the elastic response spectrum analysis.

Table 5-2: Alnasha Bridge elastic displacements demand.

Model	**Pier No.**	**Longitudinal displacement Δ_x** (mm)	**Transverse displacement Δ_y** (mm)
Tension model	Abut-1	11.86	0.03
	2	11.73	8.39
	3	11.84(L)* 54.74(R)*	19.40(L)* 52.29(R)*
	4	54.62	50.30
	5	54.62	50.62
	6	54.74(L)* 5.31(R)*	53.07(L)* 11.33(R)*
	7	5.21	4.38
	Abut-2	5.32	0.03
Compression model	Abut-1	11.63	0.03
	2	11.40	8.39
	3	11.58	19.40(L)* 52.24(R)*
	4	11.62	50.28
	5	11.28	50.60
	6	10.80	53.03(L)* 11.33(R)*
	7	10.27	4.38
	Abut-2	10.40	0.03

*L: to the left of the expansion joints.
*R: to the right of the expansion joints.

It is clear from Table 5-2 that the longitudinal displacement demands on the bridge at pier #3 and pier #6 are greater than the width of the expansion joint gap which is 50 mm. Therefore, it is expected that this gap between the frames will close during an earthquake and the compression model would be representable of the seismic behavior and demand.

Table 5-2 shows that the displacement demand in the transverse direction is almost identical for the tension and the compression models. This result is due to the fact that the expansion joints at pier #3 and pier #6 only affects the longitudinal behavior of the bridge.

Moment and shear demand on the top and bottom of the pier columns for the compression and tension models are shown in Table 5-3. M_{22} indicates moment about the longitudinal axis of the bridge, while M_{33} indicates moment about an axis perpendicular to the longitudinal bridge axis. V_{22} indicates shear force in the direction parallel to the main bridge axis, while V_{33} indicates shear force perpendicular to that axis.

Table 5-3: Alnasha Bridge moment and shear force demand.

Model type	Pier No.	Location	M_{22} (kN.m)	M_{33} (kN.m)	V_{22} (kN)	V_{33} (kN)
Tension model ($1.0M_x+0.4M_y$)	2	Bottom	387	1530	4870	1750
		Top	2580	6754	4846	1742
	4 & 5	Bottom	5500	14255	4340	1734
		Top	5347	12630	4250	1700
	7	Bottom	5533	14250	4337	1745
		Top	5280	12615	4250	1710
Tension model ($0.4M_x+1.0M_y$)	2	Bottom	966	773	2944	4372
		Top	6450	6230	2930	4355
	4 & 5	Bottom	13720	5757	1753	4328
		Top	13901	5107	1718	4238
	7	Bottom	3838	2874	2800	4226
		Top	3337	1970	2790	4213
Compression model ($1.0M_x+0.4M_y$)	2	Bottom	387	1402	5102	1750
		Top	2585	7260	5077	1744
	4 & 5	Bottom	5486	3128	975	1730
		Top	5235	2832	886	1695
	7	Bottom	1535	9043	8548	1694
		Top	1340	5490	8530	1688
Compression model ($0.4M_x+1.0M_y$)	2	Bottom	967	721	3036	4373
		Top	6454	4433	3022	4355
	4 & 5	Bottom	13715	1307	408	4326
		Top	13089	1186	371	4237
	7	Bottom	3838	4595	4520	4227
		Top	3340	3088	4510	4215

Table 5-3 shows that the demand on the columns of the bridge in the transverse direction M_{22} and V_{33}, is almost identical for the tension and compression models. However, Table 5-3 shows a reasonable difference of the demand on the columns in the

longitudinal direction for the tension and compression models, especially on pier #4, pier #5, and pier #7.

5.1.2. Method C Seismic Capacity/Demand Ratio

Tables 5-4 through 5-6 show the input and output quantities that were used in calculation of Alnasha Bridge C/D ratios. Detailed calculations for the quantities shown in Tables 5-4 through Table 5-6 are shown in Appendix C.

Table 5-4: Alnasha Bridge – Pier #2 C/D ratio calculations

Pier Geometry:		
Clear Height of Column:	2.2	m
Column Length:	2.2	m (For bending about X)
	2.2	m (For bending about Y)
Crossbeam Depth:	1.6	m
Material Properties:		
Specified Compressive Strength of Concrete:	32	MPa
Specified Yield Strength of Reinforcement:	414	MPa
Column Cross-Section:		
Column Cross-sectional Area:	1.863	m^2
Column Dimensions:	1.5	m (Dim. parallel to X)
	1.5	m (Dim. parallel to Y)
Longitudinal Reinforcement:		
Number of Long. Bars Reinf.:	24	
Longitudinal Bar Dia.:	32	
Longitudinal Bar Area:	804.25	mm^2
Clear Cover:	40	mm (To transverse rebars)
Clear Spacing:	180	mm
Transverse Reinforcement:		
Transverse Bar Dia.:	12	mm
Spacing of Transverse Reinf.:	200	mm
No of Legs:	4	
No of Legs:	4	
Diameter of transverse hoop or spiral:	1.408	m
Effective Depth of Section:	1.432	m
Area of confined concrete core:	1.982	m^2
Volumetric Ration of Long. Reinforcement:	0.01	

Table 5-4 (Continue): Alnasha Bridge – Pier #2 C/D ratio calculations

Demand Forces:			
Axial Force due to DL:	5192	kN (1.25DL)	
Axial Force due to EQ:	2290	kN (100-40Comb.)	
Max. Plastic Force:	7500	kN	
Min. Plastic Force:	920	kN	
Moment due to DL about X:	35	kN.m	
Moment due to DL about Y:	9.2	kN.m	
Moment due to EQ about X:	M22: 6454	M33: 6230	kN.m
Moment due to EQ about Y:	M22: 2585	M33: 7260	kN.m
Nominal Col. Capacity:	5830	(About X, At P_{min_p})	
Nominal Col. Capacity:	7980	(About Y, At P_{DL})	
Overstrength Factor:	1.4		
Plastic Moment Capacity:	8162	kN.m (About X)	
Plastic Moment Capacity:	11172	kN.m (About Y)	
Column CD ratio, r_{ec-x}:	0.898	(About X)	
Column CD ratio, r_{ec-y}:	1.098	(About Y)	
Column CD ratio, r_{ec}:	0.898		
Shear-X-Axis:			
Maximum calculated elastic shear force, V_e:	5280	kN	
The maximum column shear force resulting from plastic hinging, V_u:	9481	kN	
Initial shear strength, V_i:	6409	kN	
Final shear strength, V_f:	4006	kN	
Case A, r_{cv-x}:	1.025	(Eq. D-16)	
Case B, r_{cv-x}:	0.608	(Eq. D-17)	
Case C, r_{cv-x}:	3.177	(Eq. D-18)	
Controlling Case - X-Direction:	1.025		
Shear-Y-Axis:			
Maximum calculated elastic shear force, V_e:	4373	kN	
The maximum column shear force resulting from plastic hinging, V_u:	7000	kN	
Initial shear strength, V_i:	6409	kN	
Final shear strength, V_f:	4006	kN	
Case A, r_{cv-y}:	0.847	(Eq. D-16)	
Case B, r_{cv-y}:	1.465	(Eq. D-17)	
Case C, r_{cv-y}:	2.625	(Eq. D-18)	
Controlling Case - Y-Direction:	0.847		
Transverse Confinement Reinforcement:			
Volumetric ratio of existing transverse reinforcement, ρ_c:	0.004		
Required volumetric ratio of transverse reinforcement, ρ_d:	0.009		
k_1:	0.564		
k_2:	0.96		
μ:	2.44		
C/D ratio for transverse confinement, r_{cc}:	2.066	(Eq. D-20)	

Table 5-4 (Continue): Alnasha Bridge – Pier #2 C/D ratio calculations

Splices in Longitudinal Reinforcement:		
Since splices aren't occur at region of plastic hinge, C/D isn't available in this case, r_{cs}:	N/A	
Anchorage of longitudinal reinforcement:		
Anchorage with 90° standard hooks, the effective anchorage length, in mm, is;		
The required effective anchorage length of longitudinal reinforcement, L_{ad}:	480	mm (Eq. D-7a)
K_m:	0.7	
The effective anchorage length of longitudinal reinforcement, L_{ac}:	1285	mm
Detail 5: When the top of the footing contains adequately anchored flexural reinforcement, as for the above detail, and the column bars have been provided with 90° standard hooks, the C/D ratio for anchorage should be taken as 1.0.		
Anchorage length C/D ratio for column longitudinal reinforcement, r_{ca}:	1.0	

Table 5-5: Alnasha Bridge – Pier #4 C/D ratio calculations

Pier Geometry:		
Clear Height of Column:	6.22	m
Column Length:	6.22	m (For bending about X)
	6.22	m (For bending about Y)
Crossbeam Depth:	1.6	m
Material Properties:		
Specified Compressive Strength of Concrete:	32	MPa
Specified Yield Strength of Reinforcement:	414	MPa
Column Cross-Section:		
Column Cross-sectional Area:	1.863	m^2
Column Dimensions:	1.5	m (Dim. parallel to X)
	1.5	m (Dim. parallel to Y)
Longitudinal Reinforcement:		
Number of Long. Bars Reinf.:	24	
Longitudinal Bar Dia.:	32	
Longitudinal Bar Area:	804.25	mm^2
Clear Cover:	40	mm (To transverse rebars)
Clear Spacing:	180	mm
Transverse Reinforcement:		
Transverse Bar Dia.:	12	mm
Spacing of Transverse Reinf.:	200	mm
No of Legs:	6	
No of Legs:	6	
Diameter of transverse hoop or spiral:	1.408	m
Effective Depth of Section:	1.432	m
Area of confined concrete core:	1.982	m^2
Volumetric Ration of Long. Reinforcement:	0.01	

Table 5-5 (Continue): Alnasha Bridge – Pier #4 C/D ratio calculations

Demand Forces:			
Axial Force due to DL:	6007	kN (1.25DL)	
Axial Force due to EQ:	3870	kN (100-40Comb.)	
Max. Plastic Force:	8140	kN	
Min. Plastic Force:	2100	kN	
Moment due to DL about X:	25	kN.m	
Moment due to DL about Y:	372	kN.m	
Moment due to EQ about X:	M22: 13091	M33: 5107	kN.m
Moment due to EQ about Y:	M22: 12630	M33: 5347	kN.m
Nominal Col. Capacity:	6580	(About X, At P_{min_p})	
Nominal Col. Capacity:	8390	(About Y, At P_{DL})	
Overstrength Factor:	1.4		
Plastic Moment Capacity:	9212	kN.m (About X)	
Plastic Moment Capacity:	11746	kN.m (About Y)	
Column CD ratio, r_{ec-x}:	0.501	(About X)	
Column CD ratio, r_{ec-y}:	0.635	(About Y)	
Column CD ratio, r_{ec}:	0.501		
Shear-X-Axis:			
Maximum calculated elastic shear force, V_e:	4504	kN	
The maximum column shear force resulting from plastic hinging, V_u:	4141	kN	
Initial shear strength, V_i:	6858	kN	
Final shear strength, V_f:	4455	kN	
Case A, r_{cv-x}:	0.619	(Eq. D-16)	
Case B, r_{cv-x}:	3.339	(Eq. D-17)	
Case C, r_{cv-x}:	3.096	(Eq. D-18)	
Controlling Case - X-Direction:	3.096		
Shear-Y-Axis:			
Maximum calculated elastic shear force, V_e:	4325	kN	
The maximum column shear force resulting from plastic hinging, V_u:	3691	kN	
Initial shear strength, V_i:	6858	kN	
Final shear strength, V_f:	4455	kN	
Case A, r_{cv-y}:	0.592	(Eq. D-16)	
Case B, r_{cv-y}:	3.527	(Eq. D-17)	
Case C, r_{cv-y}:	2.962	(Eq. D-18)	
Controlling Case - Y-Direction:	2.962		
Transverse Confinement Reinforcement:			
Volumetric ratio of existing transverse reinforcement, ρ_c:	0.004		
Required volumetric ratio of transverse reinforcement, ρ_d:	0.009		
k_1:	0.823		
k_2:	0.96		
μ:	2.971		
C/D ratio for transverse confinement, r_{cc}:	1.76	(Eq. D-20)	
Splices in Longitudinal Reinforcement:			
Since splices aren't occur at region of plastic hinge, C/D isn't available in this case, r_{cs}:	N/A		

Table 5-5 (Continue): Alnasha Bridge – Pier #4 C/D ratio calculations

Anchorage of longitudinal reinforcement:		
Anchorage with 90° standard hooks, the effective anchorage length, in mm, is;		
The required effective anchorage length of longitudinal reinforcement, L_{ad}:	480	mm (Eq. D-7a)
K_m:	0.7	
The effective anchorage length of longitudinal reinforcement, L_{ac}:	890	mm
Detail 5: When the top of the footing contains adequately anchored flexural reinforcement, as for the above detail, and the column bars have been provided with 90° standard hooks, the C/D ratio for anchorage should be taken as 1.0.		
Anchorage length C/D ratio for column longitudinal reinforcement, r_{ca}:	1.0	

Table 5-6: Alnasha Bridge – Pier #7 C/D ratio calculations

Pier Geometry:		
Clear Height of Column:	2.2	m
Column Length:	2.2	m (For bending about X)
	2.2	m (For bending about Y)
Crossbeam Depth:	1.6	m
Material Properties:		
Specified Compressive Strength of Concrete:	32	MPa
Specified Yield Strength of Reinforcement:	414	MPa
Column Cross-Section:		
Column Cross-sectional Area:	1.863	m^2
Column Dimensions:	1.5	m (Dim. parallel to X)
	1.5	m (Dim. parallel to Y)
Longitudinal Reinforcement:		
Number of Long. Bars Reinf.:	24	
Longitudinal Bar Dia.:	32	
Longitudinal Bar Area:	804.25	mm^2
Clear Cover:	40	mm (To transverse rebars)
Clear Spacing:	180	mm
Transverse Reinforcement:		
Transverse Bar Dia.:	12	mm
Spacing of Transverse Reinf.:	200	mm
No of Legs:	4	
No of Legs:	4	
Diameter of transverse hoop or spiral:	1.408	m
Effective Depth of Section:	1.432	m
Area of confined concrete core:	1.982	m^2
Volumetric Ration of Long. Reinforcement:	0.01	

Table 5-6 (Continue): Alnasha Bridge – Pier #7 C/D ratio calculations

Demand Forces:			
Axial Force due to DL:	5232	kN (1.25DL)	
Axial Force due to EQ:	1573	kN (100-40Comb.)	
Max. Plastic Force:	6070	kN	
Min. Plastic Force:	2490	kN	
Moment due to DL about X:	35	kN.m	
Moment due to DL about Y:	13	kN.m	
Moment due to EQ about X:	M22: 3340	M33: 3088	kN.m
Moment due to EQ about Y:	M22: 12615	M33: 5280	kN.m
Nominal Col. Capacity:	6400	(About X, At P_{min_p})	
Nominal Col. Capacity:	7450	(About Y, At P_{DL})	
Overstrength Factor:	1.4		
Plastic Moment Capacity:	8960	kN.m (About X)	
Plastic Moment Capacity:	10430	kN.m (About Y)	
Column CD ratio, $r_{ec\text{-}x}$:	1.906	(About X)	
Column CD ratio, $r_{ec\text{-}y}$:	1.355	(About Y)	
Column CD ratio, r_{ec}:	1.355		
Shear-X-Axis:			
Maximum calculated elastic shear force, V_e:	8743	kN	
The maximum column shear force resulting from plastic hinging, V_u:	9481	kN	
Initial shear strength, V_i:	5950	kN	
Final shear strength, V_f:	3547	kN	
Case A, $r_{cv\text{-}x}$:	0.681	(Eq. D-16)	
Case B, $r_{cv\text{-}x}$:	0.52	(Eq. D-17)	
Case C, $r_{cv\text{-}x}$:	4.199	(Eq. D-18)	
Controlling Case - X-Direction:	0.681		
Shear-Y-Axis:			
Maximum calculated elastic shear force, V_e:	4237	kN	
The maximum column shear force resulting from plastic hinging, V_u:	8145	kN	
Initial shear strength, V_i:	5950	kN	
Final shear strength, V_f:	3547	kN	
Case A, $r_{cv\text{-}y}$:	1.404	(Eq. D-16)	
Case B, $r_{cv\text{-}y}$:	1.897	(Eq. D-17)	
Case C, $r_{cv\text{-}y}$:	5.908	(Eq. D-18)	
Controlling Case - Y-Direction:	1.404		
Transverse Confinement Reinforcement:			
Volumetric ratio of existing transverse reinforcement, ρ_c:	0.004		
Required volumetric ratio of transverse reinforcement, ρ_d:	0.009		
k_1:	0.564		
k_2:	0.96		
μ:	2.44		
C/D ratio for transverse confinement, r_{cc}:	3.305	(Eq. D-20)	
Splices in Longitudinal Reinforcement:			
Since splices aren't occur at region of plastic hinge, C/D isn't available in this case, r_{cs}:	N/A		

Table 5-6 (Continue): Alnasha Bridge – Pier #7 C/D ratio calculations

Anchorage of longitudinal reinforcement:		
Anchorage with 90° standard hooks, the effective anchorage length, in mm, is;		
The required effective anchorage length of longitudinal reinforcement, L_{ad}:	480	mm (Eq. D-7a)
K_m:	0.7	
The effective anchorage length of longitudinal reinforcement, L_{ac}:	1285	mm
Detail 5: When the top of the footing contains adequately anchored flexural reinforcement, as for the above detail, and the column bars have been provided with 90° standard hooks, the C/D ratio for anchorage should be taken as 1.0.		
Anchorage length C/D ratio for column longitudinal reinforcement, r_{ca}:	1.0	

Table 5-7 presents a summary of the C/D ratios for Alnasha Bridge according to FHWA-SRM (2005) method C.

Table 5-7: Alnasha Bridge C/D-Ratios obtained from Method C

C/D-Ratios	**Pier2**		**Pier4&5**		**Pier7**	
	Top	**Bot**	**Top**	**Bot**	**Top**	**Bot**
r_{bd} displacement C/D ratio for bearing seat or expansion joint	1.557	N/A	1.160	N/A	1.557	N/A
r_{ec} bending moment C/D ratio for column	0.898	6.674	0.501	0.644	0.632	0.728
r_{cv} shear force C/D ratio for column shear capacity	0.898	1.404	2.504	3.221	0.632	0.728
r_{cc} confinement C/D ratio for column transverse reinf.	2.192	19.866	1.217	1.914	1.541	2.169
r_{cs} splice length C/D ratio for column longitudinal reinf.	N/A	N/A	N/A	N/A	N/A	N/A
r_{ca} anchorage length C/D ratio for column longitudinal reinf.	1	1	1	1	1	1
r_{ef} bending moment C/D ratio for footing	N/A	1.106	N/A	N/A	N/A	N/A
r_{fr} rotation C/D ratio for footing	N/A	1.106	N/A	N/A	N/A	N/A
r_{bd} displacement C/D ratio for bearing seat – Pier1 (Abutment)	1.074					
r_{bd} displacement C/D ratio for bearing seat – Pier8 (Abutment)	1.074					

The Capacity/Demand ratios of the columns and footing for pier #2 were found to correspond to Case I as described in the Method C analysis approach in FHWA-SRM (2005). Under Case I, the footing and columns are not expected to yield and an

evaluation of their ductility is not necessary. Splice length C/D ratio was not reported for pier #2 because the splices occur outside the plastic hinge region.

The Capacity/Demand ratios of the columns and footing for pier #4 and pier #5 were found to correspond to Case III as described in the Method C analysis approach in FHWA-SRM (2005). Under Case III, it is assumed that the column is more likely to yield before the footing. Therefore, this requires an evaluation of columns ductility and their ability to withstand plastic hinging. Splice length C/D ratios were not reported for pier #4 and pier #5 because the splices occur outside the plastic hinge region.

Summary of Method C and Analysis Results

Method C analysis results showed bending moment C/D ratios less than 1 for the columns in pier #2, pier #4 and pier #5. It also showed shear force C/D ratio less than 1 for columns in pier #2 and pier #7.

According to the FHWA-SRM (2005), C/D ratios for pier #4 and pier #5 were found to correspond to case III. Therefore, an evaluation of columns ductility and their ability to withstand the seismic demand is required. This evaluation will be done in accordance with Method D2 in the FHWA-SRM (2005) which requires a nonlinear static analysis of the bridge in the transverse and longitudinal directions.

The Capacity/Demand ratios of the columns and footing for pier #7 were found to correspond to Case III as described in the Method C analysis approach in FHWA-SRM (2005). Under Case III, it is assumed that the column is more likely to yield before the footing. Therefore, this requires an evaluation of columns ductility and their ability to withstand plastic hinging. Pushover analysis was performed to ensure that at the maximum elastic displacement will be withstandable. Pier #7 has enough shear

capacity to withstand the induced forces, which is shown in Method D2 in section 5.1.3. Splice length C/D ratio was not reported because the splices occur outside the plastic hinge region.

5.1.3. Method D2

Method D2 requires a pushover analysis of the bridge piers under consideration. For pushover analysis, nonlinear behavior is assumed to occur within frame elements at concentrated plastic hinges with default or user-defined hinge properties being assigned to each hinge. The user-defined hinge types include an uncoupled moment hinge, an uncoupled axial hinge, an uncoupled shear hinge, and a coupled axial force and biaxial bending moment hinge. The latter is a hinge which yields based on the interaction of axial force and bending moments at the hinge location, Symans et al, 2003.

In this study, the coupled axial force and bending moment hinge ($P\text{-}M_{33}$ hinge) was assigned to the ends of the columns of the bridge model in conducting pushover analysis in the longitudinal direction, while ($P\text{-}M_{22}$ hinge) was assigned to the ends of the columns of the bridge model in conducting pushover analysis in the transverse direction.

The hinge properties are defined through the definition of the moment-rotation relation, and the interaction surface. The moment-rotation relation, which can either be user-defined or determined by SAP2000 based on section properties, characterizes the hinge deformation curve in the moment-rotation plane where the moment and rotation are normalized by the yield moment and yield rotation, respectively. Both moment-rotation curves and interaction curves were obtained following the guidelines mentioned in FHWA-SRM (2005). MathCAD (PTC, 2007) sheets were developed to obtain these curves.

Figure 5-3 shows the moment-rotation curve for the columns of pier #2 at their different axial load levels. Curve A present moment-rotation curve at axial force level equal to the load capacity at the maximum confined moment on the section. Curve B presents the moment-rotation curve at axial force level equal to the axial load due to seismic force. Curve C presents the moment-rotation curve at axial load level equal to zero. Figure 5-4 shows the interaction diagrams for columns of pier #2. Detailed calculations of the moment-interaction curves for each pier columns are shown in Appendix B. Table 5-8 and Table 5-9 summarize the coordinates of the moment-interaction curves and the moment-rotation curves for the pier columns of Alnasha Bridge.

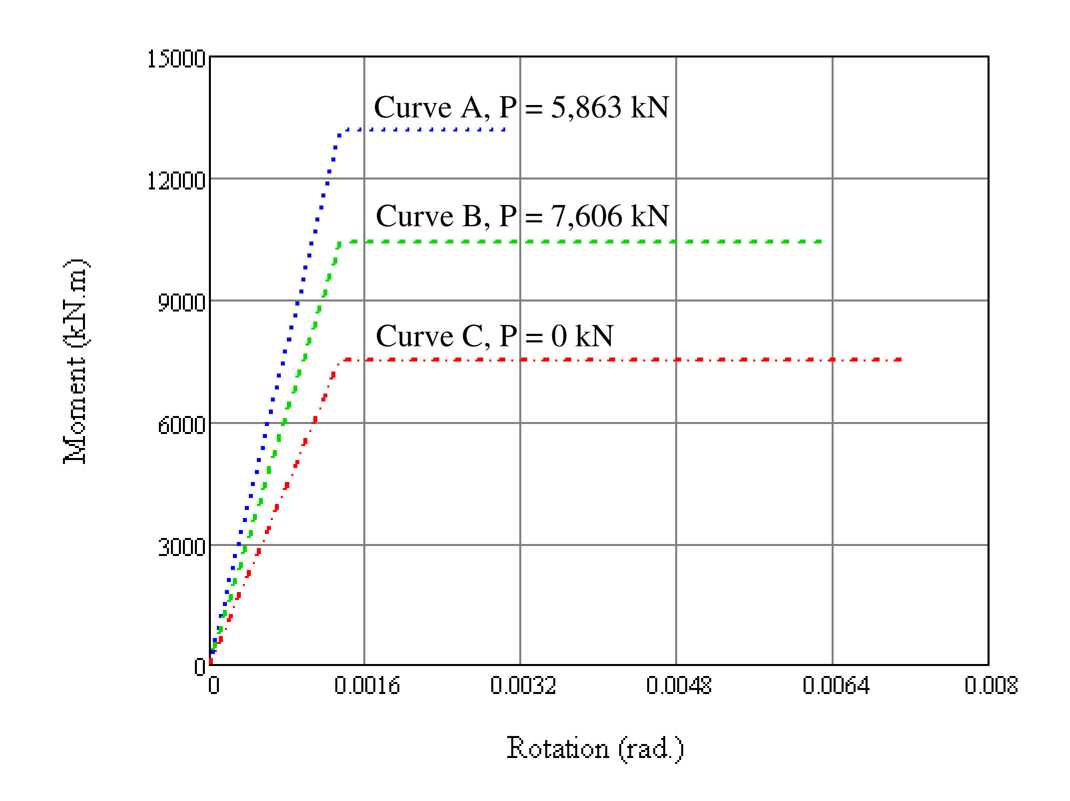


Figure 5-3: Moment-Rotation relationship for columns of Pier #2 in Alnasha Bridge.

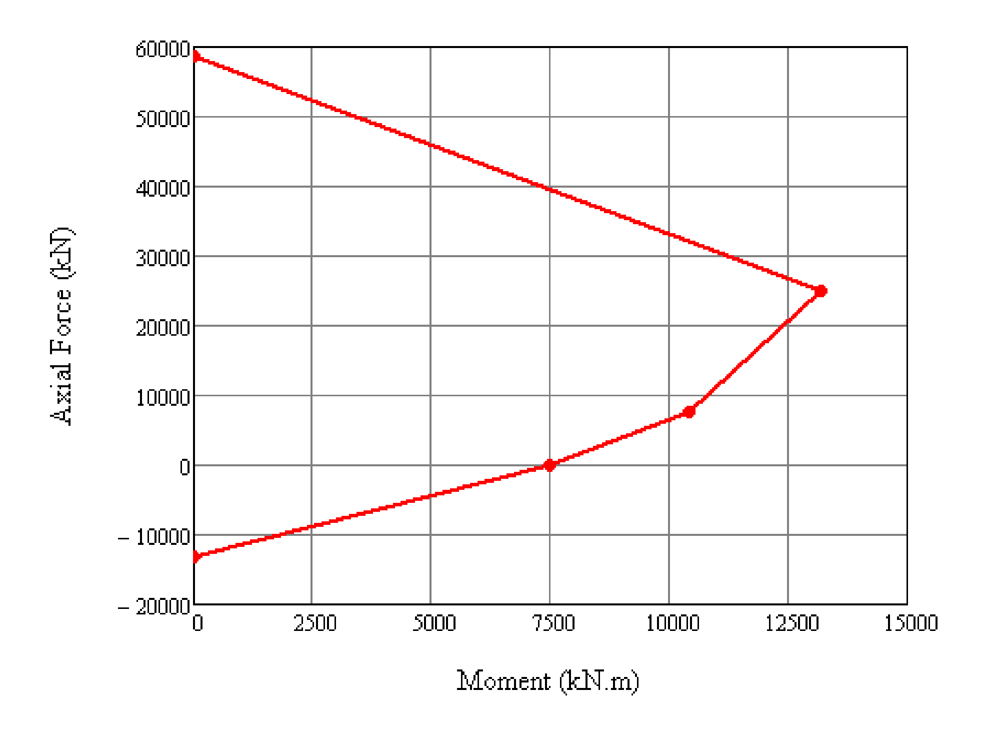


Figure 5-4: Moment-Axial force interaction diagram for columns of Pier #2 in Alnasha Bridge.

Table 5-8: Moment-Rotation data-Alnasha Bridge

Pier No.	Direction	Curve A				Curve B			
		Point1		Point2		Point1		Point2	
		Rotation (rad.)	Moment (kN.m)	Rotation (rad.)	Moment (kN.m)	Rotation (rad.)	Moment (kN.m)	Rotation (rad.)	Moment (kN.m)
Pier #2	Long	0.001342	13180	0.001711	13180	0.001342	9194	0.003019	9194
	Trans	0.001342	13180	0.001711	13180	0.001342	10430	0.005024	10430
Pier #4 & Pier #5	Long	0.001652	13180	0.001867	13180	0.001652	9458	0.007966	9458
	Trans	0.001652	13180	0.001867	13180	0.001652	11120	0.005208	11120
Pier #7	Long	0.001342	13180	0.001307	13180	0.001342	9220	0.005989	9220
	Trans	0.001342	13180	0.001259	13180	0.001342	10190	0.003596	10190

Pier No.	Direction	Curve C			
		Point1		Point2	
		Rotation (rad.)	Moment (kN.m)	Rotation (rad.)	Moment (kN.m)
Pier #2	Long	0.001342	7487	0.005796	7487
	Trans	0.001342	7487	0.005796	7487
Pier #4 & Pier #5	Long	0.001652	7487	0.015	7487
	Trans	0.001652	7487	0.015	7487
Pier #7	Long	0.001342	7487	0.008826	7487
	Trans	0.001342	7487	0.008826	7487

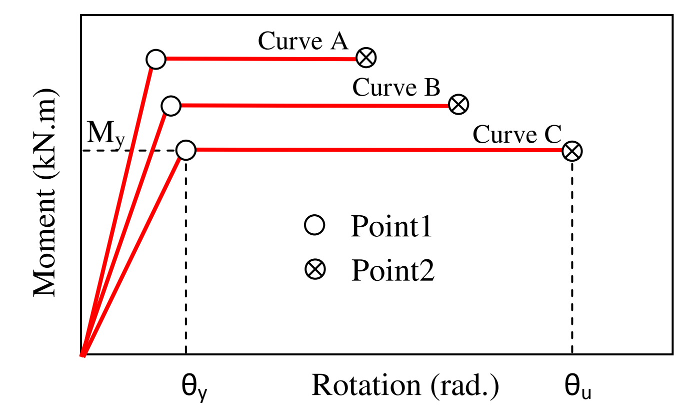


Table 5-9: Moment-Axial force interaction data-Alnasha Bridge

Pier No.	Point1		Point2		Point3		Point4		Point5	
	Force (kN)	Moment (kN.m)	Force (kN)	Moment (kN.m)	Force (kN)	Moment (kN.m)	Force (kN)	Moment (kN.m)	Force (kN)	Moment (kN.m)
Pier #2	58630	0	24970	13180	7606	10430	0	7487	-13030	0
Pier #4 &5	58630	0	24970	13180	9960	11120	0	7487	-13030	0
Pier #7	58630	0	24970	13180	6875	10190	0	7487	-13030	0

Once the plastic hinge properties have been defined, the next step was to define the static pushover cases and the type of pushover analysis to be performed. In general, a pushover analysis consists of more than one pushover case. Typically, the analysis consists of two load cases. The first load case applies gravity load to the bridge and the second load case applies a specific lateral load pattern to the bridge.

SAP2000 (CSI, 2008) can perform force-controlled analysis where the pushover proceeds to the full load value defined by the load pattern or displacement-controlled analysis where the pushover proceeds to the specified displacement in the specified direction at the specified node. In this study, the pushover curve was obtained using SAP2000 by first analyzing the bridge under the effect of dead load and then pushing the pier under consideration longitudinally or transversely until either the predetermined maximum displacement 100 mm (displacement-controlled analysis) was achieved at the control node (located at the centroid of the superstructure; shown in Figure 5-5) or the pier failed. Note that SAP2000 (CSI, 2008) automatically stops the analysis when a plastic hinge reaches its ultimate rotation capacity.

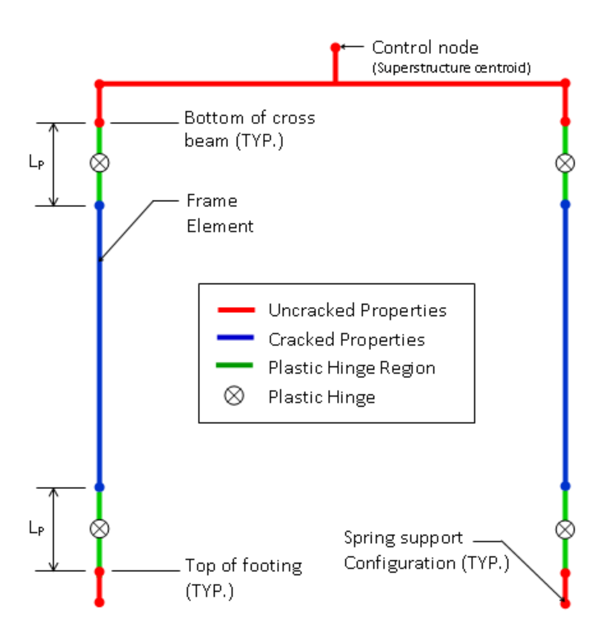


Figure 5-5: Typical bridge pier with plastic hinge location.

The pushover curve in the transverse and longitudinal direction obtained from the pushover analysis using SAP2000 is shown in Figure 5-6 through Figure 5-11 for pier #2, pier #4, pier #5 and pier #7 in Alnasha Bridge.

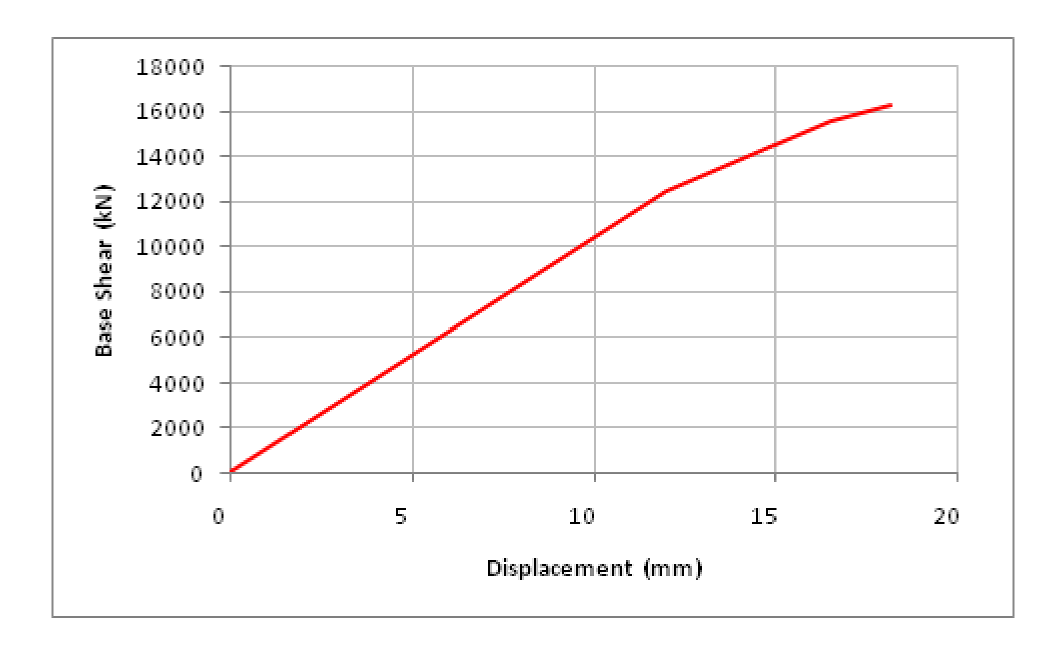


Figure 5-6: Pushover curves for analysis in the transverse direction for pier #2 in Alnasha Bridge.

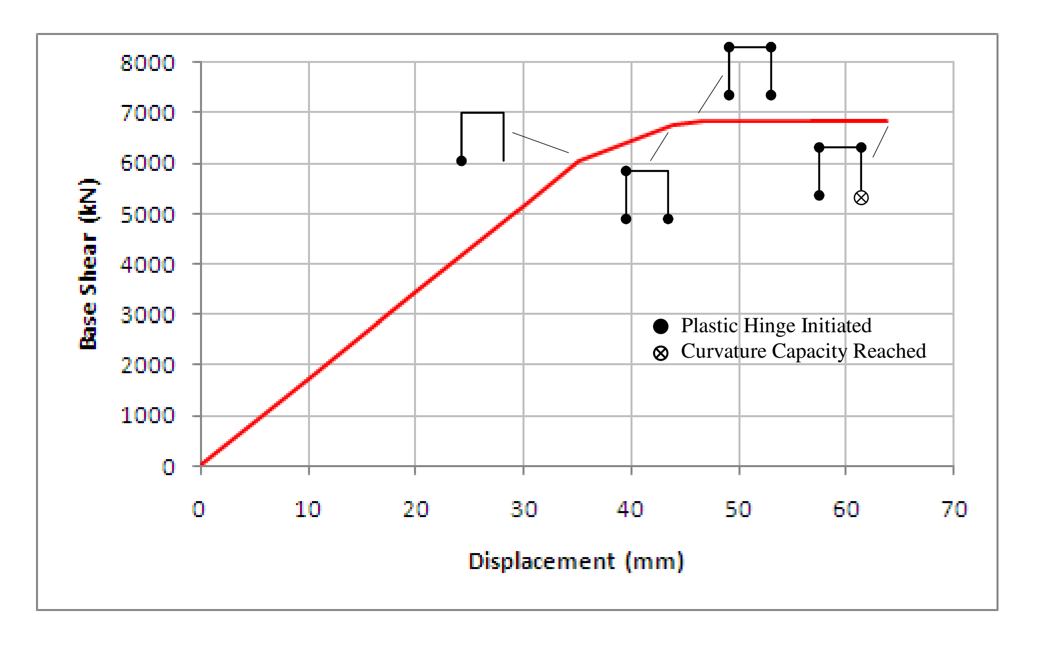


Figure 5-7: Pushover curves for analysis in the transverse direction for pier #4 & 5 in Alnasha Bridge.

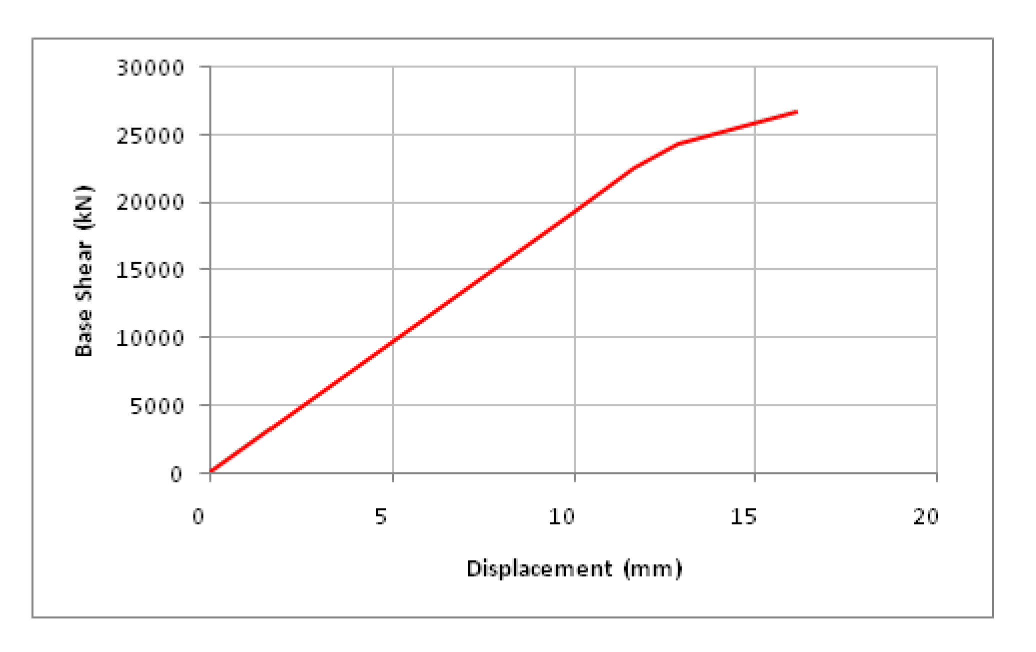


Figure 5-8: Pushover curves for analysis in the transverse direction for pier #7 in Alnasha Bridge.

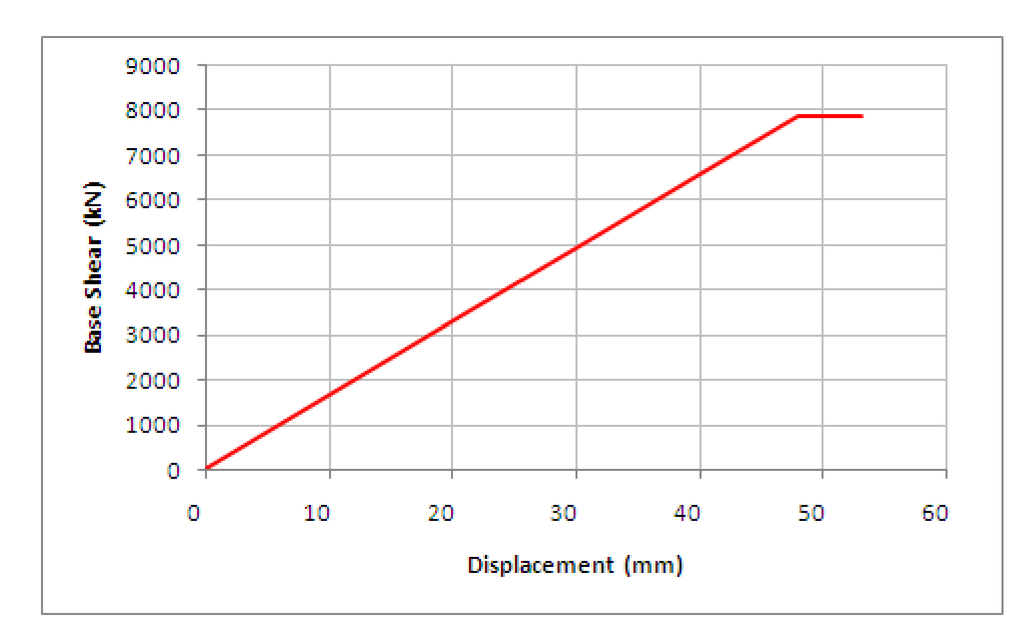


Figure 5-9: Pushover curves for analysis in the longitudinal direction for pier #2 in Alnasha Bridge.

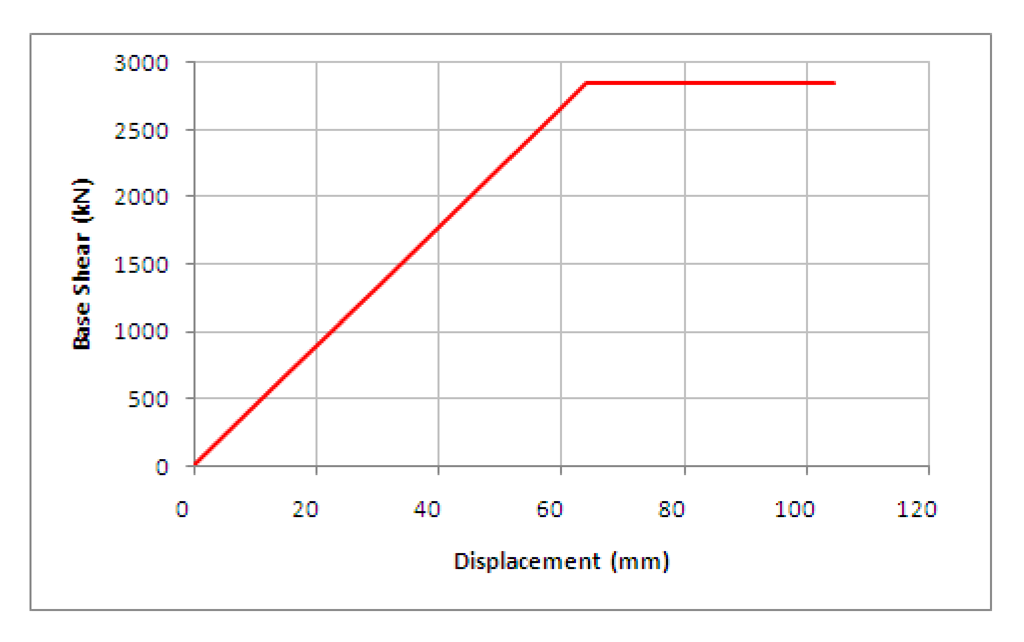


Figure 5-10: Pushover curves for analysis in the longitudinal direction for pier #4 & 5 in Alnasha Bridge.

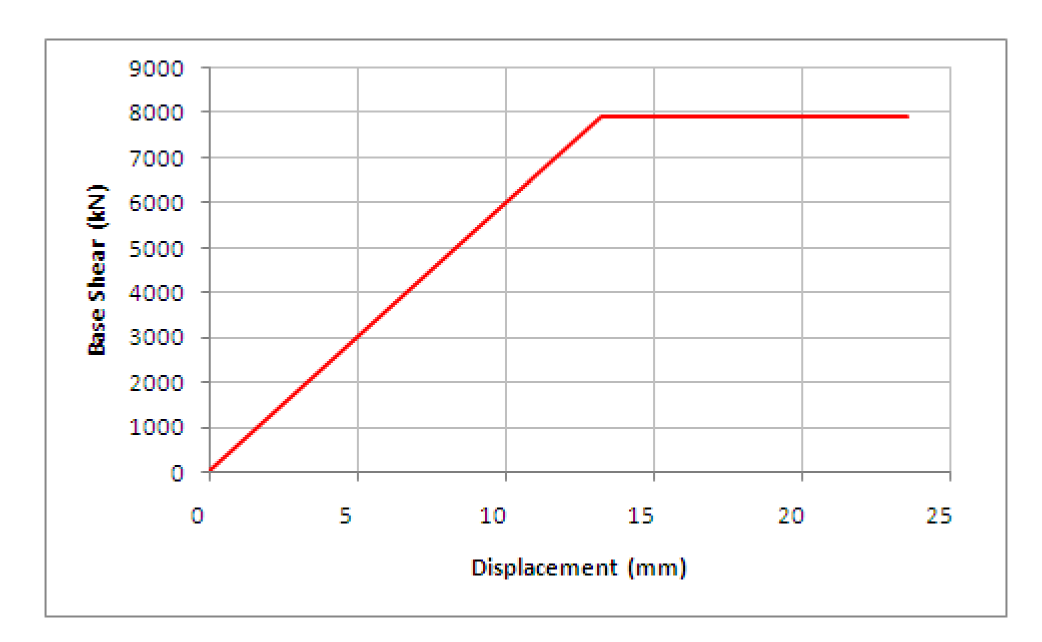


Figure 5-11: Pushover curves for analysis in the longitudinal direction for pier #7 in Alnasha Bridge.

Table 5-10 through Table 5-12 show the displacement C/D ratios for pier #2, pier #4, pier #5 and pier #7. The displacement capacity is obtained from pushover analysis while displacement demand is obtained from elastic response spectra analysis.

Table 5-10: Alnasha Bridge Method D2 – Pier #2.

Non-seismic Displacement Demand:		
Nonseismic displacement demand in global x-axis:	0	mm
Nonseismic displacement demand in global y-axis:	0	mm
Seismic Displacement Demand:		
Compression Model		
($1.0EQ_x + 0.4EQ_y$)		
Seismic displacement demand in global x-axis:	11.74	mm
Seismic displacement demand in global y-axis:	3.36	mm
($0.4EQ_x + 1.0EQ_y$)		
Seismic displacement demand in global x-axis:	4.7	mm
Seismic displacement demand in global y-axis:	8.4	mm
Tension Model		
($1.0EQ_x + 0.4EQ_y$)		
Seismic displacement demand in global x-axis:	11.5	mm
Seismic displacement demand in global y-axis:	3.36	mm
($0.4EQ_x + 1.0EQ_y$)		
Seismic displacement demand in global x-axis:	4.6	mm
Seismic displacement demand in global y-axis:	8.4	mm
Structural Displacement Capacity:		
Displacement Capacity - Transverse Direction:	18.19	mm
Displacement Capacity - Longitudinal Direction:	54.64	mm
C/D Ratios:		
Displacement CD ratio in the transverse direction:	1.90	
Displacement CD ratio in the longitudinal direction:	4.50	
Displacement CD ratio:	1.90	

Table 5-11: Alnasha Bridge Method D2 – Pier #5 & 4.

Non-seismic Displacement Demand:		
Nonseismic displacement demand in global x-axis:	0	mm
Nonseismic displacement demand in global y-axis:	0	mm
Seismic Displacement Demand:		
Compression Model		
($1.0EQ_x + 0.4EQ_y$)		
Seismic displacement demand in global x-axis:	54.62	mm
Seismic displacement demand in global y-axis:	20.29	mm
($0.4EQ_x + 1.0EQ_y$)		
Seismic displacement demand in global x-axis:	21.85	mm
Seismic displacement demand in global y-axis:	50.30	mm
Tension Model		
($1.0EQ_x + 0.4EQ_y$)		
Seismic displacement demand in global x-axis:	11.62	mm
Seismic displacement demand in global y-axis:	20.10	mm
($0.4EQ_x + 1.0EQ_y$)		
Seismic displacement demand in global x-axis:	4.65	mm
Seismic displacement demand in global y-axis:	50.29	mm
Structural Displacement Capacity:		
Displacement Capacity - Transverse Direction:	63.13	mm
Displacement Capacity - Longitudinal Direction:	105.17	mm
C/D Ratios:		
Displacement CD ratio in the transverse direction:	1.17	
Displacement CD ratio in the longitudinal direction:	1.82	
Displacement CD ratio:	1.17	

Table 5-12: Alnasha Bridge Method D2 – Pier #7.

Non-seismic Displacement Demand:		
Nonseismic displacement demand in global x-axis:	0	mm
Nonseismic displacement demand in global y-axis:	0	mm
Seismic Displacement Demand:		
Compression Model		
(1.0EQ$_x$ + 0.4EQ$_y$)		
Seismic displacement demand in global x-axis:	5.22	mm
Seismic displacement demand in global y-axis:	1.75	mm
(0.4EQ$_x$ + 1.0EQ$_y$)		
Seismic displacement demand in global x-axis:	2.09	mm
Seismic displacement demand in global y-axis:	4.39	mm
Tension Model		
(1.0EQ$_x$ + 0.4EQ$_y$)		
Seismic displacement demand in global x-axis:	10.27	mm
Seismic displacement demand in global y-axis:	1.76	mm
(0.4EQ$_x$ + 1.0EQ$_y$)		
Seismic displacement demand in global x-axis:	4.11	mm
Seismic displacement demand in global y-axis:	4.39	mm
Structural Displacement Capacity:		
Displacement Capacity - Transverse Direction:	16.18	mm
Displacement Capacity - Longitudinal Direction:	24.42	mm
C/D Ratios:		
Displacement CD ratio in the transverse direction:	3.28	
Displacement CD ratio in the longitudinal direction:	2.34	
Displacement CD ratio:	2.34	

According to method C of the FHWA-SRM (2005) discusses in Chapter one, pushover analysis should be performed in case C/D ratio for any element is less than one. Accordingly, pushover analysis was conducted for all piers. Table 5-13 shows C/D ratios adapted by applying Method D2.

Table 5-13: Alnasha Bridge C/D-Ratios obtained from Method D2

C/D-Ratios	**Pier2**		**Pier4&5**		**Pier7**	
	Top	**Bot**	**Top**	**Bot**	**Top**	**Bot**
r_{ec} bending moment C/D ratio for column	1.636	4.603	1.084	1.076	2.239	1.934
r_{cv} shear force C/D ratio for column shear capacity	1.636	2.388	5.133	5.379	1.239	1.567
r_{cc} confinement C/D ratio for column transverse reinf.	3.992	13.702	2.634	3.197	5.464	5.767
r_{ef} bending moment C/D ratio for footing	N/A	1.106	N/A	N/A	N/A	N/A
r_{fr} rotation C/D ratio for footing	N/A	1.106	N/A	N/A	N/A	N/A
Displacement – Method D2						
Longitudinal Direction	4.499		1.829		2.345	
Transverse Direction	1.905		1.179		3.289	

Table 5-13 shows that all C/D ratios are greater than one which means that the ultimate capacity of the columns is higher than the required demand. Therefore, there is no need for any retrofitting scheme for this bridge. As it would be able to withstand seismic forces and displacement demands.

5.2. Alharamain Bridge

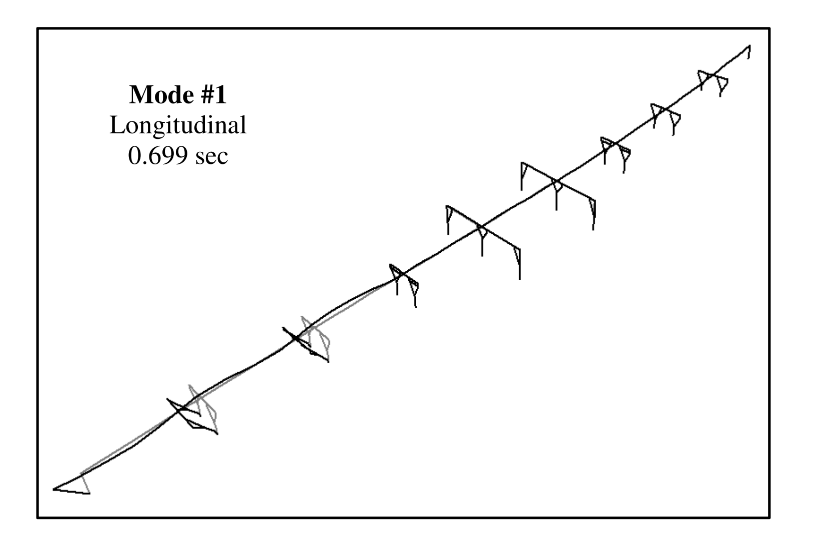
5.2.1. Response Spectrum Analysis

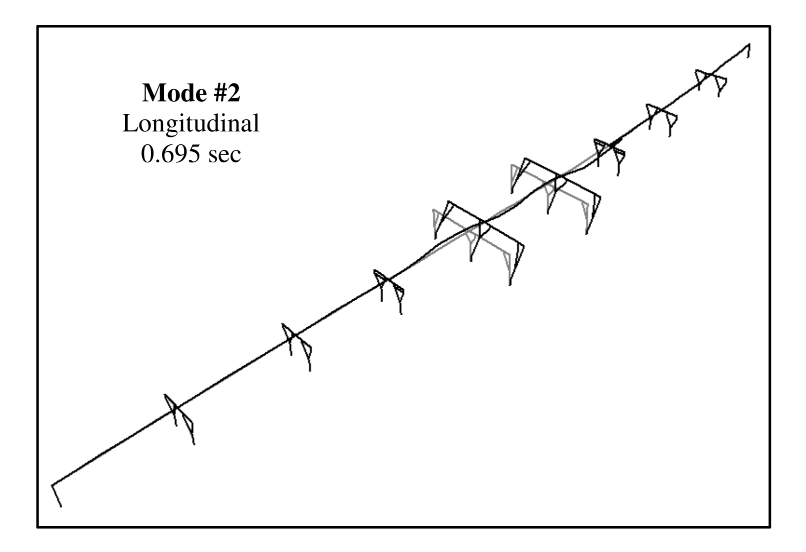
The response spectrum analysis begins with determining the natural frequencies and mode shapes via an eigenvalue analysis. The longitudinal and transverse natural periods and the associated modal participating mass ratios (i.e., effective modal mass to total mass ratios) are shown for the compression model and the tension model in Table 5-14. The longitudinal and the transverse mode shapes for the bridge tension and compression models are shown in Figure 5-12 and Figure 5-13, respectively.

Table 5-14: Alharamain Bridge fundamental periods and mass participation ratios

Model type	Mode No.	Natural period (sec)	Modal participating mass ratio (%)
Tension model	1 (Longitudinal Mode)	0.699	24.5
	2 (Longitudinal Mode)	0.695	25.3
	3 (Transverse Mode)	0.599	24.0
Compression model	1 (Longitudinal Mode)	0.613	74.8
	2 (Torsional Mode)	0.522	1.7
	3 (Transverse Mode)	0.445	53.2

Table 5-14 shows that the bridge is stiffer in the transverse direction than in the longitudinal direction. This noticeable difference between the longitudinal and the transverse stiffness is mainly due to the expansion joints in span #3 and span #6. The expansion joints results in a discontinuity of the bridge deck to behave as a diaphragm over all the bents in the out of plane direction.





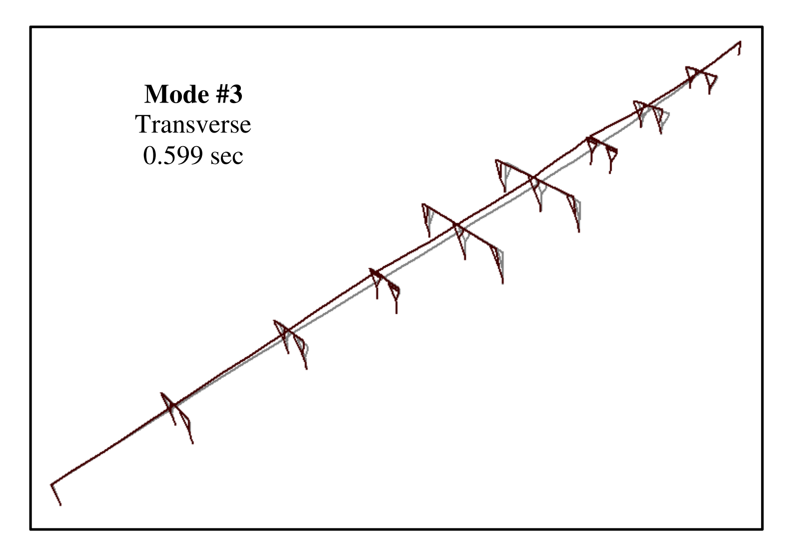
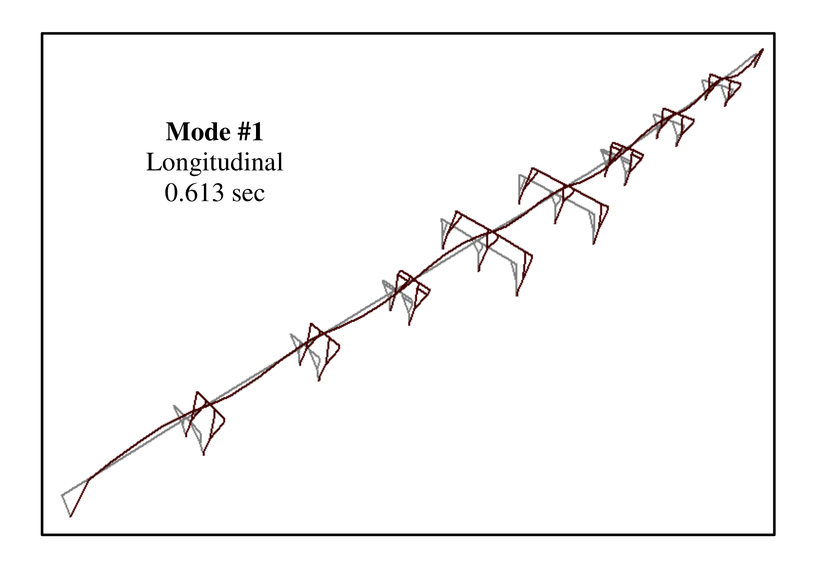
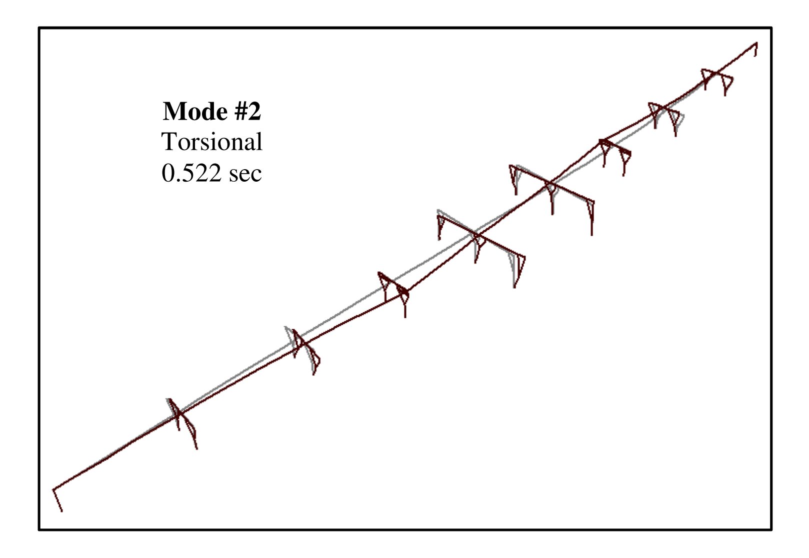


Figure 5-5-12: Fundamental mode shapes of Alharamain Bridge – Tension Model.





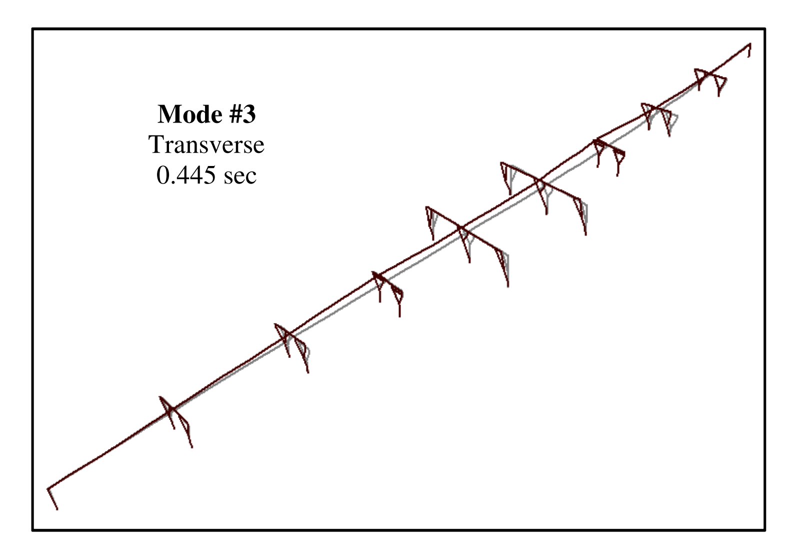


Figure 5-5-13: Fundamental mode shapes of Alharamain Bridge – Compression Model.

The response spectrum analysis determines the bridge response under the effect of the expected seismic forces. The response includes displacements, moment, and shear forces in the longitudinal and transverse directions of the bridge. The 100-40 percent load combination rule as recommended by FHWA-SRM (2005) was used to determine the seismic demand on the bridge. Table 5-15 shows the displacements demand on the bridge as obtained from the elastic response spectrum analysis.

Table 5-15: Alharamain Bridge displacement demand.

Model	**Pier No.**	**Longitudinal displacement Δ_x** (mm)	**Transverse displacement Δ_y** (mm)
Tension model	Abut-1	78.29	0.24
	2	77.93	10.55
	3	78.01	26.67
	4	77.27(L)* 77.68(R)*	50.01(L)* 50.01(R)*
	5	77.38	36.01
	6	77.43	39.85
	7	77.85(L)* 66.31(R)*	60.93(L)* 60.93 (R)*
	8	65.48	28.96
	9	65.08	10.24
	Abut-10	65.72	0.23
Compression model	Abut-1	68.56	0.24
	2	68.41	10.85
	3	68.47	26.84
	4	68.48	49.51(L)* 49.51(R)*
	5	67.92	40.05
	6	67.62	40.05
	7	67.53	62.01(L)* 62.01 (R)*
	8	66.48	29.42
	9	66.33	10.49
	Abut-10	66.94	0.23

*L: to the left of the expansion joints.
*R: to the right of the expansion joints.

It is clear from Table 5-15 that the longitudinal displacement demands on the bridge at pier #4 and pier #7 are greater than the width of the expansion joint gap which is 60 mm. Therefore, it is expected that this gap between the frames will close during an earthquake and the compression model would be representable of the seismic behavior and demand

Table 5-15 shows that the displacement demand in the transverse direction is almost identical for the tension and the compression models. This result is due to the fact that the expansion joints at pier #4 and pier #7 only affects the longitudinal behavior of the bridge.

Moment and shear demand on the top and bottom of the pier columns for the compression and tension models are shown in Table 5-16. M_{22} indicates moment about the longitudinal axis of the bridge, while M_{33} indicates moment about an axis perpendicular to the longitudinal bridge axis. V_{22} indicates shear force in the direction parallel to the main bridge axis, while V_{33} indicates shear force perpendicular to that axis.

Table 5-16: Alharamain Bridge moment and shear force demand.

Model type	Pier No.	M_{22} (kN.m)	M_{33} (kN.m)	V_{22} (kN)	V_{33} (kN)
Tension model ($1.0M_x+0.4M_y$)	2	2955	29757	7601	1270
	3	7503	29366	6920	2733
	5&6	7865 (O)* 10083 (C)*	21903 (O)* 24745 (C)*	5012 (O)* 4744 (C)*	2780 (O)* 2577 (C)*
	8	8640	26860	7340	3812
	9	4087	29640	9424	2047
Tension model ($0.4M_x+1.0M_y$)	2	6878	12531	3217	2955
	3	17550	12793	3038	6393
	5&6	18793 (O)* 24150 (C)*	10400 (O)* 9934 (C)*	2435 (O)* 1905 (C)*	6613 (O)* 6173 (C)*
	8	18430	13640	3923	8537
	9	5386	13888	4561	3910
Compression model ($1.0M_x+0.4M_y$)	2	2961	25778	6553	1273
	3	7325	25778	6086	2671
	5&6	7602 (O)* 9780 (C)*	19101 (O)* 21611 (C)*	4353 (O)* 4128 (C)*	2683 (O)* 2500 (C)*
	8	8240	27276	7453	3636
	9	4078	30000	9600	1985
Compression model ($0.4M_x+1.0M_y$)	2	2961	25778	6553	2962
	3	7325	25778	6086	2671
	5&6	7602 (O)* 9780 (C)*	19101 (O)* 21611 (C)*	4353 (O)* 4128 (C)*	2683 (O)* 2500 (C)*
	8	8240	27276	7452	3635
	9	4078	30000	9600	4078

*C: centered column in the pier.
*O: outer column in the pier.

Table 5-16 shows that the demand on the columns of the bridge in the transverse direction M_{22} and V_{33}, is almost identical for the tension and compression models. However, Table 5-16 shows a reasonable difference of the demand on the columns in the longitudinal direction for the tension and compression models, especially on pier #2 and pier #3.

5.2.2. Method C Seismic Capacity/Demand Ratio

Tables 5-17 through 5-21 show the input and output quantities that were used in calculation of Alharamain Bridge C/D ratios. Detailed calculations for the quantities shown in Tables 5-17 through Table 5-21 are shown in Appendix C.

Table 5-17: Alharamain Bridge – Pier #2 C/D ratio calculations

Pier Geometry:		
Clear Height of Column:	6.98	m
Column Length:	6.98	m (For bending about X)
	2.85	m (For bending about Y)
Crossbeam Depth:	2.1	m
Material Properties:		
Specified Compressive Strength of Concrete:	36	MPa
Specified Yield Strength of Reinforcement:	520	MPa
Column Cross-Section:		
Column Cross-sectional Area:	3.24	m^2
Column Dimensions:	1.8	m (Dim. parallel to X)
	1.8	m (Dim. parallel to Y)
Longitudinal Reinforcement:		
Number of Long. Bars Reinf.:	40	
Longitudinal Bar Dia.:	32	
Longitudinal Bar Area:	804.25	mm^2
Clear Cover:	40	mm (To transverse rebars)
Clear Spacing:	180	mm
Transverse Reinforcement:		
Transverse Bar Dia.:	14	mm
Spacing of Transverse Reinf.:	200	mm
No of Legs:	6	
No of Legs:	6	
Diameter of transverse hoop or spiral:	1.706	m

Table 5-17 (Continue): Alharamain Bridge – Pier #2 C/D ratio calculations

Effective Depth of Section:	1.73	m	
Area of confined concrete core:	2.91	m^2	
Volumetric Ration of Long. Reinforcement:	0.01		
Demand Forces:			
Axial Force due to DL:	10625	kN (1.25DL)	
Axial Force due to EQ:	5000	kN (100-40Comb.)	
Max. Plastic Force:	20900	kN	
Min. Plastic Force:	-2860	kN	
Moment due to DL about X:	224	kN.m	
Moment due to DL about Y:	830	kN.m	
Moment due to EQ about X:	M22: 6878	M33: 12531	kN.m
Moment due to EQ about Y:	M22: 29760	M33: 2955	kN.m
Nominal Col. Capacity:	12866	(About X, At P_{min_p})	
Nominal Col. Capacity:	21400	(About Y, At P_{DL})	
Overstrength Factor:	1.4		
Plastic Moment Capacity:	18012.4	kN.m (About X)	
Plastic Moment Capacity:	29960	kN.m (About Y)	
Column CD ratio, r_{ec-x}:	1.838	(About X)	
Column CD ratio, r_{ec-y}:	0.691	(About Y)	
Column CD ratio, r_{ec}:	0.691		
Shear-X-Axis:			
Maximum calculated elastic shear force, V_e:	8060	kN	
The maximum column shear force resulting from plastic hinging, V_u:	8263	kN	
Initial shear strength, V_i:	12760	kN	
Final shear strength, V_f:	8327	kN	
Case A, r_{cv-x}:	0.664	(Eq. D-16)	
Case B, r_{cv-x}:	3.288	(Eq. D-17)	
Case C, r_{cv-x}:	3.261	(Eq. D-18)	
Controlling Case - X-Direction:	3.261		
Shear-Y-Axis:			
Maximum calculated elastic shear force, V_e:	3080	kN	
The maximum column shear force resulting from plastic hinging, V_u:	11691	kN	
Initial shear strength, V_i:	12760	kN	
Final shear strength, V_f:	8327	kN	
Case A, r_{cv-y}:	1.67	(Eq. D-16)	
Case B, r_{cv-y}:	4.512	(Eq. D-17)	
Case C, r_{cv-y}:	8.199	(Eq. D-18)	
Controlling Case - Y-Direction:	4.512		
Transverse Confinement Reinforcement:			
Volumetric ratio of existing transverse reinforcement, ρ_c:	0.005		
Required volumetric ratio of transverse reinforcement, ρ_d:	0.008		
k_1:	1		
k_2:	0.96		
μ:	2.99		
C/D ratio for transverse confinement, r_{cc}:	1.992	(Eq. D-20)	

Table 5-17 (Continue): Alharamain Bridge – Pier #2 C/D ratio calculations

Splices in Longitudinal Reinforcement:		
Since splices aren't occur at region of plastic hinge, C/D isn't available in this case, r_{cs}:	N/A	
Anchorage of longitudinal reinforcement:		
Anchorage with 90° standard hooks, the effective anchorage length, in mm, is;		
The required effective anchorage length of longitudinal reinforcement, L_{ad}:	480	mm (Eq. D-7a)
K_m:	0.7	
The effective anchorage length of longitudinal reinforcement, L_{ac}:	1670	mm
Detail 5: When the top of the footing contains adequately anchored flexural reinforcement, as for the above detail, and the column bars have been provided with 90° standard hooks, the C/D ratio for anchorage should be taken as 1.0.		
Anchorage length C/D ratio for column longitudinal reinforcement, r_{ca}:	1.0	

Table 5-18: Alharamain Bridge – Pier #3 C/D ratio calculations

Pier Geometry:		
Clear Height of Column:	7.01	m
Column Length:	7.01	m (For bending about X)
	2.85	m (For bending about Y)
Crossbeam Depth:	2.1	m
Material Properties:		
Specified Compressive Strength of Concrete:	36	MPa
Specified Yield Strength of Reinforcement:	520	MPa
Column Cross-Section:		
Column Cross-sectional Area:	3.24	m^2
Column Dimensions:	1.8	m (Dim. parallel to X)
	1.8	m (Dim. parallel to Y)
Longitudinal Reinforcement:		
Number of Long. Bars Reinf.:	40	
Longitudinal Bar Dia.:	32	
Longitudinal Bar Area:	804.25	mm^2
Clear Cover:	40	mm (To transverse rebars)
Clear Spacing:	180	mm
Transverse Reinforcement:		
Transverse Bar Dia.:	14	mm
Spacing of Transverse Reinf.:	200	mm
No of Legs:	6	
No of Legs:	6	
Diameter of transverse hoop or spiral:	1.706	m
Effective Depth of Section:	1.73	m
Area of confined concrete core:	2.91	m^2
Volumetric Ration of Long. Reinforcement:	0.01	

Table 5-18 (Continue): Alharamain Bridge – Pier #3 C/D ratio calculations

Demand Forces:			
Axial Force due to DL:	10625	kN (1.25DL)	
Axial Force due to EQ:	10316	kN (100-40Comb.)	
Max. Plastic Force:	20400	kN	
Min. Plastic Force:	-1980	kN	
Moment due to DL about X:	422	kN.m	
Moment due to DL about Y:	1005	kN.m	
Moment due to EQ about X:	M22: 17550	M33: 12793	kN.m
Moment due to EQ about Y:	M22: 29370	M33: 7503	kN.m
Nominal Col. Capacity:	13460	(About X, At P_{min_p})	
Nominal Col. Capacity:	21240	(About Y, At P_{DL})	
Overstrength Factor:	1.4		
Plastic Moment Capacity:	18844	kN.m (About X)	
Plastic Moment Capacity:	29736	kN.m (About Y)	
Column CD ratio, r_{ec-x}:	0.743	(About X)	
Column CD ratio, r_{ec-y}:	0.689	(About Y)	
Column CD ratio, r_{ec}:	0.689		

Shear-X-Axis:		
Maximum calculated elastic shear force, V_e:	7380	kN
The maximum column shear force resulting from plastic hinging, V_u:	8228	kN
Initial shear strength, V_i:	13921	kN
Final shear strength, V_f:	9488	kN
Case A, r_{cv-x}:	0.667	(Eq. D-16)
Case B, r_{cv-x}:	3.837	(Eq. D-17)
Case C, r_{cv-x}:	3.283	(Eq. D-18)
Controlling Case - X-Direction:	3.283	
Shear-Y-Axis:		
Maximum calculated elastic shear force, V_e:	6630	kN
The maximum column shear force resulting from plastic hinging, V_u:	11887	kN
Initial shear strength, V_i:	13921	kN
Final shear strength, V_f:	9488	kN
Case A, r_{cv-y}:	0.659	(Eq. D-16)
Case B, r_{cv-y}:	2.2	(Eq. D-17)
Case C, r_{cv-y}:	3.241	(Eq. D-18)
Controlling Case - Y-Direction:	2.2	
Transverse Confinement Reinforcement:		
Volumetric ratio of existing transverse reinforcement, ρ_c:	0.005	
Required volumetric ratio of transverse reinforcement, ρ_d:	0.008	
k_1:	1	
k_2:	0.96	
μ:	2.99	
C/D ratio for transverse confinement, r_{cc}:	1.975	(Eq. D-20)
Splices in Longitudinal Reinforcement:		
Since splices aren't occur at region of plastic hinge, C/D isn't available in this case, r_{cs}:	N/A	

Table 5-18 (Continue): Alharamain Bridge – Pier #3 C/D ratio calculations

Anchorage of longitudinal reinforcement:		
Anchorage with 90° standard hooks, the effective anchorage length, in mm, is;		
The required effective anchorage length of longitudinal reinforcement, L_{ad}:	480	mm (Eq. D-7a)
K_m:	0.7	
The effective anchorage length of longitudinal reinforcement, L_{ac}:	1670	mm
Detail 5: When the top of the footing contains adequately anchored flexural reinforcement, as for the above detail, and the column bars have been provided with 90° standard hooks, the C/D ratio for anchorage should be taken as 1.0.		
Anchorage length C/D ratio for column longitudinal reinforcement, r_{ca}:	1.0	

Table 5-19: Alharamain Bridge – Pier #5 & 6 C/D ratio calculations

Pier Geometry:		
Clear Height of Column:	8.35	m
Column Length:	8.35	m (For bending about X)
	5.28	m (For bending about Y)
Crossbeam Depth:	2.1	m
Material Properties:		
Specified Compressive Strength of Concrete:	36	MPa
Specified Yield Strength of Reinforcement:	520	MPa
Column Cross-Section:		
Column Cross-sectional Area:	3.24	m^2
Column Dimensions:	1.8	m (Dim. parallel to X)
	1.8	m (Dim. parallel to Y)
Longitudinal Reinforcement:		
Number of Long. Bars Reinf.:	40	
Longitudinal Bar Dia.:	32	
Longitudinal Bar Area:	804.25	mm^2
Clear Cover:	40	mm (To transverse rebars)
Clear Spacing:	180	mm
Transverse Reinforcement:		
Transverse Bar Dia.:	14	mm
Spacing of Transverse Reinf.:	200	mm
No of Legs:	6	
No of Legs:	6	
Diameter of transverse hoop or spiral:	1.706	m
Effective Depth of Section:	1.73	m
Area of confined concrete core:	2.91	m^2
Volumetric Ration of Long. Reinforcement:	0.01	

Table 5-19 (Continue): Alharamain Bridge – Pier #5 & 6 C/D ratio calculations

Demand Forces:			
Axial Force due to DL:	12107	kN (1.25DL)	
Axial Force due to EQ:	800	kN (100-40Comb.)	
Max. Plastic Force:	9700	kN	
Min. Plastic Force:	9700	kN	
Moment due to DL about X:	6.3	kN.m	
Moment due to DL about Y:	684	kN.m	
Moment due to EQ about X:	M22: 24150	M33: 9934	kN.m
Moment due to EQ about Y:	M22: 24745	M33: 10083	kN.m
Nominal Col. Capacity:	13720	(About X, At P_{min_p})	
Nominal Col. Capacity:	21750	(About Y, At P_{DL})	
Overstrength Factor:	1.4		
Plastic Moment Capacity:	19208	kN.m (About X)	
Plastic Moment Capacity:	30450	kN.m (About Y)	
Column CD ratio, r_{ec-x}:	0.568	(About X)	
Column CD ratio, r_{ec-y}:	0.851	(About Y)	
Column CD ratio, r_{ec}:	0.568		

Shear-X-Axis:		
Maximum calculated elastic shear force, V_e:	5020	kN
The maximum column shear force resulting from plastic hinging, V_u:	6907	kN
Initial shear strength, V_i:	11805	kN
Final shear strength, V_f:	7372	kN
Case A, r_{cv-x}:	0.805	(Eq. D-16)
Case B, r_{cv-x}:	4.278	(Eq. D-17)
Case C, r_{cv-x}:	4.025	(Eq. D-18)
Controlling Case - X-Direction:	4.025	
Shear-Y-Axis:		
Maximum calculated elastic shear force, V_e:	6115	kN
The maximum column shear force resulting from plastic hinging, V_u:	10924	kN
Initial shear strength, V_i:	11805	kN
Final shear strength, V_f:	7372	kN
Case A, r_{cv-y}:	0.853	(Eq. D-16)
Case B, r_{cv-y}:	2.214	(Eq. D-17)
Case C, r_{cv-y}:	4.264	(Eq. D-18)
Controlling Case - Y-Direction:	2.214	
Transverse Confinement Reinforcement:		
Volumetric ratio of existing transverse reinforcement, ρ_c:	0.005	
Required volumetric ratio of transverse reinforcement, ρ_d:	0.008	
k_1:	1	
k_2:	0.96	
μ:	2.99	
C/D ratio for transverse confinement, r_{cc}:	2.414	(Eq. D-20)
Splices in Longitudinal Reinforcement:		
Since splices aren't occur at region of plastic hinge, C/D isn't available in this case, r_{cs}:	N/A	

Table 5-19 (Continue): Alharamain Bridge – Pier #5 & 6 C/D ratio calculations

Anchorage of longitudinal reinforcement:		
Anchorage with 90° standard hooks, the effective anchorage length, in mm, is;		
The required effective anchorage length of longitudinal reinforcement, L_{ad}:	480	mm (Eq. D-7a)
K_m:	0.7	
The effective anchorage length of longitudinal reinforcement, L_{ac}:	1670	mm
Detail 5: When the top of the footing contains adequately anchored flexural reinforcement, as for the above detail, and the column bars have been provided with 90° standard hooks, the C/D ratio for anchorage should be taken as 1.0.		
Anchorage length C/D ratio for column longitudinal reinforcement, r_{ca}:	1.0	

Table 5-20: Alharamain Bridge – Pier #8 C/D ratio calculations

Pier Geometry:		
Clear Height of Column:	6.72	m
Column Length:	6.72	m (For bending about X)
	2.6	m (For bending about Y)
Crossbeam Depth:	2.1	m
Material Properties:		
Specified Compressive Strength of Concrete:	36	MPa
Specified Yield Strength of Reinforcement:	520	MPa
Column Cross-Section:		
Column Cross-sectional Area:	3.24	m^2
Column Dimensions:	1.8	m (Dim. parallel to X)
	1.8	m (Dim. parallel to Y)
Longitudinal Reinforcement:		
Number of Long. Bars Reinf.:	40	
Longitudinal Bar Dia.:	32	
Longitudinal Bar Area:	804.25	mm^2
Clear Cover:	40	mm (To transverse rebars)
Clear Spacing:	180	mm
Transverse Reinforcement:		
Transverse Bar Dia.:	14	mm
Spacing of Transverse Reinf.:	200	mm
No of Legs:	6	
No of Legs:	6	
Diameter of transverse hoop or spiral:	1.706	m
Effective Depth of Section:	1.73	m
Area of confined concrete core:	2.91	m^2
Volumetric Ration of Long. Reinforcement:	0.01	

Table 5-20 (Continue): Alharamain Bridge – Pier #8 C/D ratio calculations

Demand Forces:			
Axial Force due to DL:	10500	kN (1.25DL)	
Axial Force due to EQ:	12995	kN (100-40Comb.)	
Max. Plastic Force:	21500	kN	
Min. Plastic Force:	-3300	kN	
Moment due to DL about X:	65	kN.m	
Moment due to DL about Y:	1000	kN.m	
Moment due to EQ about X:	M22: 18430	M33: 13640	kN.m
Moment due to EQ about Y:	M22: 27276	M33: 8240	kN.m
Nominal Col. Capacity:	12260	(About X, At P_{min_p})	
Nominal Col. Capacity:	20800	(About Y, At P_{DL})	
Overstrength Factor:	1.4		
Plastic Moment Capacity:	17164	kN.m (About X)	
Plastic Moment Capacity:	29120	kN.m (About Y)	
Column CD ratio, r_{ec-x}:	0.662	(About X)	
Column CD ratio, r_{ec-y}:	0.726	(About Y)	
Column CD ratio, r_{ec}:	0.662		

Shear-X-Axis:		
Maximum calculated elastic shear force, V_e:	8183	kN
The maximum column shear force resulting from plastic hinging, V_u:	8583	kN
Initial shear strength, V_i:	14636	kN
Final shear strength, V_f:	10203	kN
Case A, r_{cv-x}:	0.719	(Eq. D-16)
Case B, r_{cv-x}:	4.184	(Eq. D-17)
Case C, r_{cv-x}:	3.449	(Eq. D-18)
Controlling Case - X-Direction:	3.449	
Shear-Y-Axis:		
Maximum calculated elastic shear force, V_e:	8688	kN
The maximum column shear force resulting from plastic hinging, V_u:	11630	kN
Initial shear strength, V_i:	14636	kN
Final shear strength, V_f:	10203	kN
Case A, r_{cv-y}:	0.575	(Eq. D-16)
Case B, r_{cv-y}:	2.241	(Eq. D-17)
Case C, r_{cv-y}:	2.76	(Eq. D-18)
Controlling Case - Y-Direction:	2.241	
Transverse Confinement Reinforcement:		
Volumetric ratio of existing transverse reinforcement, ρ_c:	0.005	
Required volumetric ratio of transverse reinforcement, ρ_d:	0.008	
k_1:	1	
k_2:	0.96	
μ:	2.99	
C/D ratio for transverse confinement, r_{cc}:	1.724	(Eq. D-20)
Splices in Longitudinal Reinforcement:		
Since splices aren't occur at region of plastic hinge, C/D isn't available in this case, r_{cs}:	N/A	

Table 5-20 (Continue): Alharamain Bridge – Pier #8 C/D ratio calculations

Anchorage of longitudinal reinforcement:		
Anchorage with 90° standard hooks, the effective anchorage length, in mm, is;		
The required effective anchorage length of longitudinal reinforcement, L_{ad}:	480	mm (Eq. D-7a)
K_m:	0.7	
The effective anchorage length of longitudinal reinforcement, L_{ac}:	1670	mm
Detail 5: When the top of the footing contains adequately anchored flexural reinforcement, as for the above detail, and the column bars have been provided with 90° standard hooks, the C/D ratio for anchorage should be taken as 1.0.		
Anchorage length C/D ratio for column longitudinal reinforcement, r_{ca}:	1.0	

Table 5-21: Alharamain Bridge – Pier #9 C/D ratio calculations

Pier Geometry:		
Clear Height of Column:	5.51	m
Column Length:	5.51	m (For bending about X)
	1.38	m (For bending about Y)
Crossbeam Depth:	2.1	m
Material Properties:		
Specified Compressive Strength of Concrete:	36	MPa
Specified Yield Strength of Reinforcement:	520	MPa
Column Cross-Section:		
Column Cross-sectional Area:	3.24	m^2
Column Dimensions:	1.8	m (Dim. parallel to X)
	1.8	m (Dim. parallel to Y)
Longitudinal Reinforcement:		
Number of Long. Bars Reinf.:	40	
Longitudinal Bar Dia.:	32	
Longitudinal Bar Area:	804.25	mm^2
Clear Cover:	40	mm (To transverse rebars)
Clear Spacing:	180	mm
Transverse Reinforcement:		
Transverse Bar Dia.:	14	mm
Spacing of Transverse Reinf.:	200	mm
No of Legs:	6	
No of Legs:	6	
Diameter of transverse hoop or spiral:	1.706	m
Effective Depth of Section:	1.73	m
Area of confined concrete core:	2.91	m^2
Volumetric Ration of Long. Reinforcement:	0.01	

Table 5-21 (Continue): Alharamain Bridge – Pier #9 C/D ratio calculations

Demand Forces:			
Axial Force due to DL:	10500	kN (1.25DL)	
Axial Force due to EQ:	6250	kN (100-40Comb.)	
Max. Plastic Force:	15250	kN	
Min. Plastic Force:	-2790	kN	
Moment due to DL about X:	162	kN.m	
Moment due to DL about Y:	722	kN.m	
Moment due to EQ about X:	M22: 5386	M33: 13888	kN.m
Moment due to EQ about Y:	M22: 4078	M33: 30000	kN.m
Nominal Col. Capacity:	12000	(About X, At P_{min_p})	
Nominal Col. Capacity:	20650	(About Y, At P_{DL})	
Overstrength Factor:	1.4		
Plastic Moment Capacity:	16800	kN.m (About X)	
Plastic Moment Capacity:	28910	kN.m (About Y)	
Column CD ratio, $r_{ec\text{-}x}$:	2.198	(About X)	
Column CD ratio, $r_{ec\text{-}y}$:	0.664	(About Y)	
Column CD ratio, r_{ec}:	0.664		
Shear-X-Axis:			
Maximum calculated elastic shear force, V_e:	9990	kN	
The maximum column shear force resulting from plastic hinging, V_u:	10468	kN	
Initial shear strength, V_i:	13420	kN	
Final shear strength, V_f:	8987	kN	
Case A, $r_{cv\text{-}x}$:	0.654	(Eq. D-16)	
Case B, $r_{cv\text{-}x}$:	2.309	(Eq. D-17)	
Case C, $r_{cv\text{-}x}$:	2.811	(Eq. D-18)	
Controlling Case - X-Direction:	2.309		
Shear-Y-Axis:			
Maximum calculated elastic shear force, V_e:	9990	kN	
The maximum column shear force resulting from plastic hinging, V_u:	23739	kN	
Initial shear strength, V_i:	13420	kN	
Final shear strength, V_f:	8987	kN	
Case A, $r_{cv\text{-}y}$:	1.343	(Eq. D-16)	
Case B, $r_{cv\text{-}y}$:	6.952	(Eq. D-17)	
Case C, $r_{cv\text{-}y}$:	8.931	(Eq. D-18)	
Controlling Case - Y-Direction:	1.963		
Transverse Confinement Reinforcement:			
Volumetric ratio of existing transverse reinforcement, ρ_c:	0.005		
Required volumetric ratio of transverse reinforcement, ρ_d:	0.008		
k_1:	1		
k_2:	0.96		
μ:	2.99		
C/D ratio for transverse confinement, r_{cc}:	1.963	(Eq. D-20)	
Splices in Longitudinal Reinforcement:			
Since splices aren't occur at region of plastic hinge, C/D isn't available in this case, r_{cs}:	N/A		

Table 5-21 (Continue): Alharamain Bridge – Pier #9 C/D ratio calculations

Anchorage of longitudinal reinforcement:		
Anchorage with 90° standard hooks, the effective anchorage length, in mm, is;		
The required effective anchorage length of longitudinal reinforcement, L_{ad}:	480	mm (Eq. D-7a)
K_m:	0.7	
The effective anchorage length of longitudinal reinforcement, L_{ac}:	1670	mm
Detail 5: When the top of the footing contains adequately anchored flexural reinforcement, as for the above detail, and the column bars have been provided with 90° standard hooks, the C/D ratio for anchorage should be taken as 1.0.		
Anchorage length C/D ratio for column longitudinal reinforcement, r_{ca}:	1.0	

Table 5-22 presents a summary of the C/D ratios for Alharamain Bridge according to FHWA-SRM (2005) method C.

Table 5-22: Alharamain Bridge C/D-Ratios obtained from Method C

C/D-Ratios	Pier2	Pier3	Pier5&6 (Outer col)	Pier5&6 (Center col)	Pier8	Pier9
r_{bd} displacement C/D ratio for bearing seat or expansion joint	1.265	1.263	1.203	1.203	1.277	1.343
r_{ec} bending moment C/D ratio for column	0.691	0.689	0.774	0.568	0.662	0.664
r_{cv} shear force C/D ratio for column shear capacity	3.276	1.827	3.869	2.839	1.922	1.343
r_{cc} confinement C/D ratio for column transverse reinforcement	2.073	2.066	2.321	1.703	1.984	1.992
r_{cs} splice length C/D ratio for column longitudinal reinforcement	N/A	N/A	N/A	N/A	N/A	N/A
r_{ca} anchorage length C/D ratio for column longitudinal reinforcement	1	1	1	1	1	1
r_{ef} bending moment C/D ratio for footing	0.402	0.402	0.280	0.280	0.357	0.322
r_{fr} rotation C/D ratio for footing	0.402	0.402	1.118	1.118	0.357	0.322
r_{bd} displacement C/D ratio for bearing seat – Pier1 (Abutment)	0.983					
r_{bd} displacement C/D ratio for bearing seat – Pier10 (Abutment)	1.013					

Summary of Method C and Analysis Results

Method C analysis results showed bending moment C/D ratios less than 1 for the columns in all piers. It also showed bending moment for footing C/D ratio less than 1 for all piers.

The Capacity/Demand ratios of the columns and footings for Piers # 2, 3, 5, 6, 8, and 9 were found to correspond to Case IV as described in the Method C analysis approach in the FHWA-SRM (2005). Under Case IV, the footing and column are equally likely to yield or rotate. Therefore, an evaluation of the footings and columns ductility and their ability to withstand the seismic demand is required. This evaluation will be done in accordance with Method D2 in the FHWA-SRM (2005) which requires a nonlinear static analysis of the bridge in the transverse and longitudinal directions. Splice length C/D ratio was not reported because the splices occur outside the plastic hinge region.

5.2.3. Method D2

Method D2 requires a pushover analysis of the bridge piers under consideration. For pushover analysis, nonlinear behavior is assumed to occur within frame elements at concentrated plastic hinges with default or user-defined hinge properties being assigned to each hinge.

Figure 5-14 shows the moment-rotation curve for the columns of pier #5 at their different axial load levels. Curve A present moment-rotation curve at axial force level equal to the load capacity at the maximum confined moment on the section. Curve B presents the moment-rotation curve at axial force level equal to the axial load due to seismic force. Curve C presents the moment-rotation curve at axial load level equal to zero. Figure 5-15 shows the interaction diagrams for columns of pier #5. Detailed

calculations of the moment-interaction curves for each pier columns are shown in Appendix C. Table 5-23 and Table 5-24 summarize the coordinates of the moment-interaction curves and the moment-rotation curves for the pier columns of Alharamain Bridge.

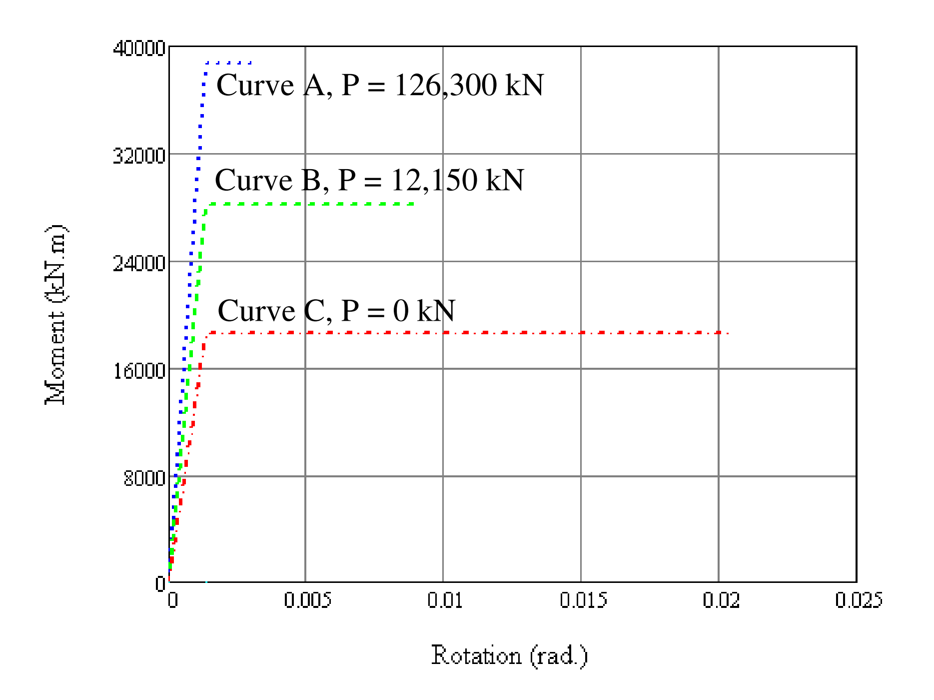


Figure 5-14: Moment-Rotation relationship for Pier #5 in Alharamain Bridge.

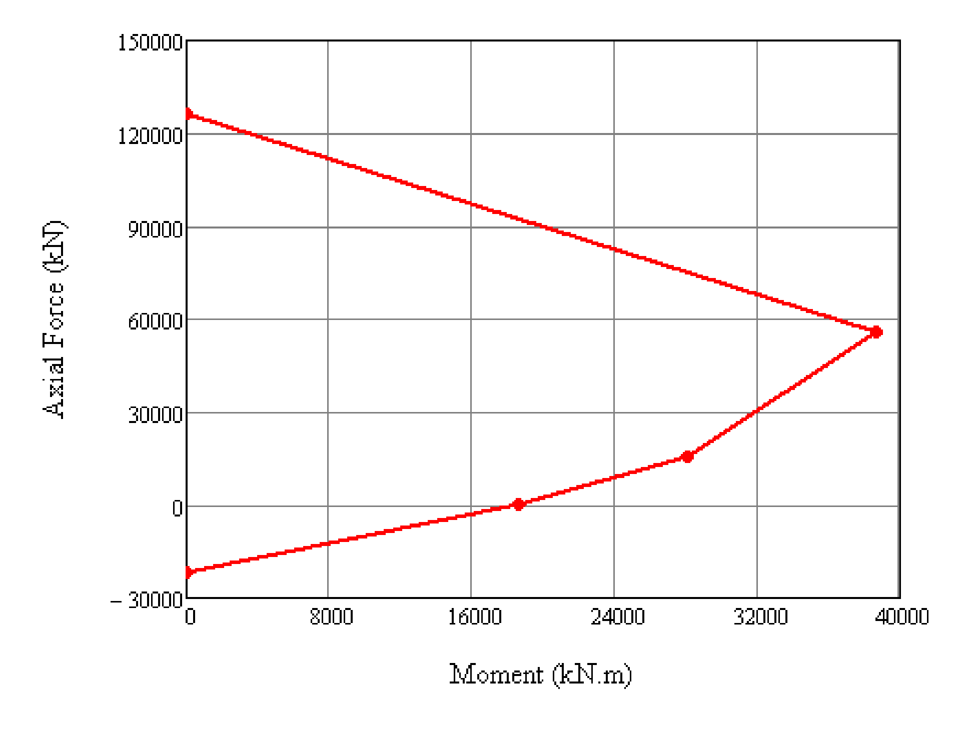


Figure 5-15: Moment-Axial force interaction diagram for Pier #5 in Alharamain Bridge.

Table 5-23: Moment-Rotation data-Alharamain Bridge

Pier No.	Direction	Curve A				Curve B			
		Point1		Point2		Point1		Point2	
		Rotation (rad.)	Moment (kN.m)	Rotation (rad.)	Moment (kN.m)	Rotation (rad.)	Moment (kN.m)	Rotation (rad.)	Moment (kN.m)
Pier #2	Long	0.001357	38690	0.001646	38690	0.001357	24190	0.011	24190
	Trans	0.001357	38690	0.001646	38690	0.001357	28090	0.007802	28090
Pier #3	Long	0.001357	38690	0.001646	38690	0.001357	24280	0.011	24280
	Trans	0.001357	38690	0.001646	38690	0.001357	30950	0.005866	30950
Pier #5 & Pier #6	Long	0.001357	38690	0.001646	38690	0.001357	21530	0.015	21530
	Trans	0.001357	38690	0.001646	38690	0.001357	25120	0.011	25120
Pier #8	Long	0.001357	38690	0.001646	38690	0.001357	24250	0.011	24250
	Trans	0.001357	38690	0.001646	38690	0.001357	32060	0.005178	32060
Pier #9	Long	0.001357	38690	0.001646	38690	0.001357	24250	0.011	24250
	Trans	0.001357	38690	0.001646	38690	0.001357	27930	0.00792	27930

Pier No.	Direction	Curve C			
		Point1		Point2	
		Rotation (rad.)	Moment (kN.m)	Rotation (rad.)	Moment (kN.m)
Pier #2	Long	0.001357	18610	0.019	18610
	Trans	0.001357	18610	0.019	18610
Pier #3	Long	0.001357	18610	0.019	18610
	Trans	0.001357	18610	0.019	18610
Pier #5 & Pier #6	Long	0.001357	18610	0.019	18610
	Trans	0.001357	18610	0.019	18610
Pier #8	Long	0.001357	18610	0.019	18610
	Trans	0.001357	18610	0.019	18610
Pier #9	Long	0.001357	18610	0.019	18610
	Trans	0.001357	18610	0.019	18610

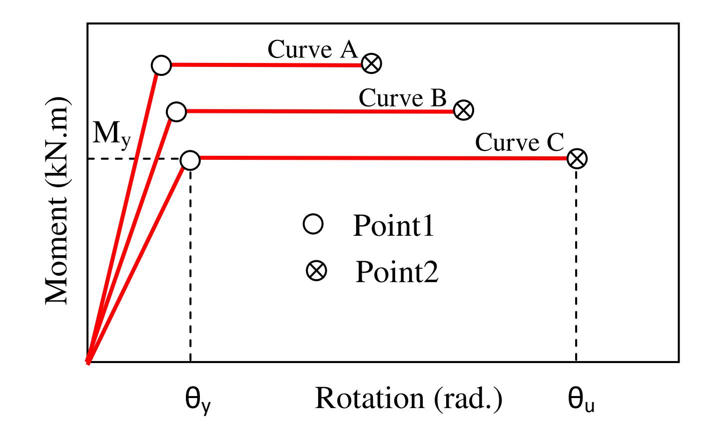


Table 5-24: Moment-Axial interaction data-Alharamain Bridge

Pier No.	Point1		Point2		Point3		Point4		Point5	
	Force (kN)	Moment (kN.m)	Force (kN)	Moment (kN.m)	Force (kN)	Moment (kN.m)	Force (kN)	Moment (kN.m)	Force (kN)	Moment (kN.m)
Pier #2	126300	0	55930	38690	15300	28090	0	18610	-21710	0
Pier #3	126300	0	55930	38690	21200	30950	0	18610	-21710	0
Pier #5	126300	0	55930	38690	9950	25120	0	18610	-21710	0
Pier #6	126300	0	55930	38690	9950	25120	0	18610	-21710	0
Pier #8	126300	0	55930	38690	23800	32060	0	18610	-21710	0
Pier #9	126300	0	55930	38690	14990	27930	0	18610	-21710	0

The pushover curve in the transverse and longitudinal direction obtained from the pushover analysis using SAP2000 is shown in Figure 5-16 through Figure 5-25 for pier #2, pier #3, pier #5 & 6, pier #8 and pier #9 in Alharamain Bridge.

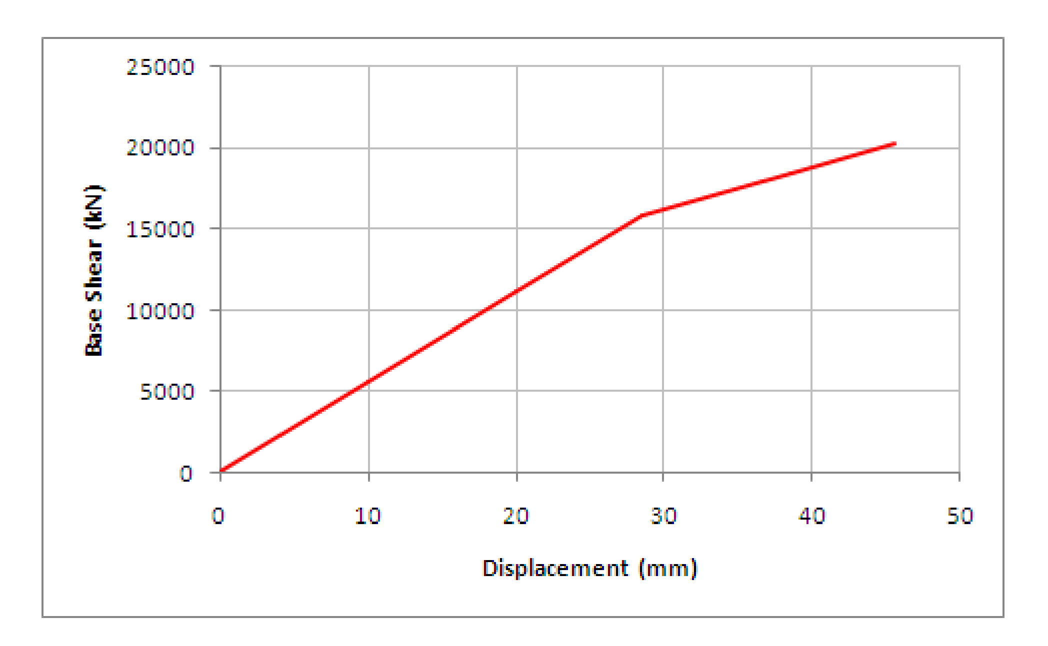


Figure 5-16: Pushover curves for analysis in the transverse direction for pier #2 in Alharamain Bridge.

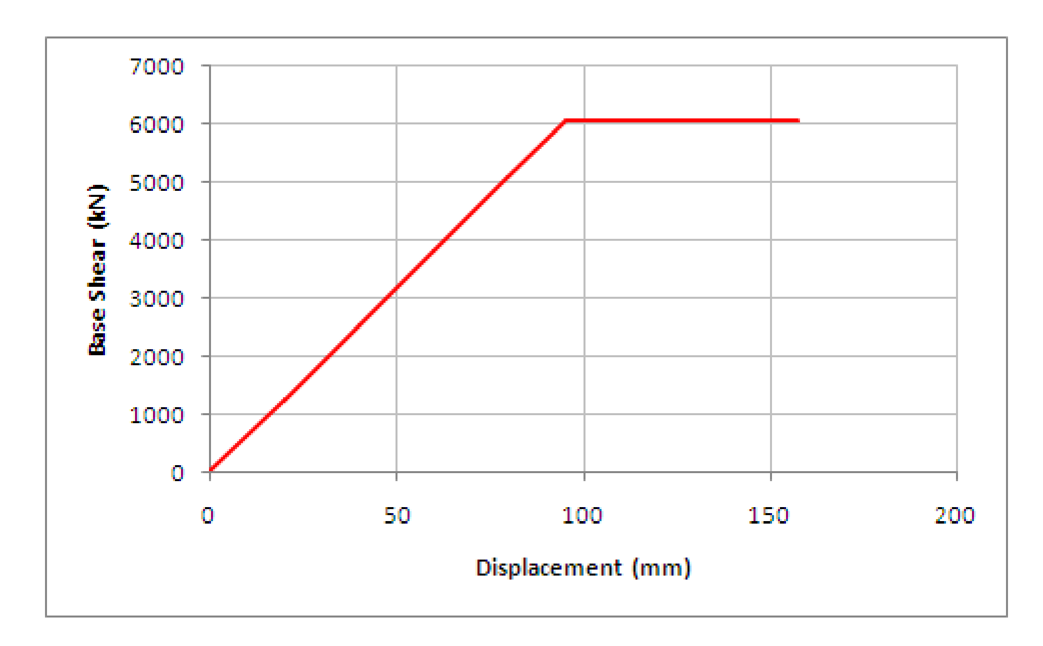


Figure 5-17: Pushover curves for analysis in the longitudinal direction for pier #2 in Alharamain Bridge.

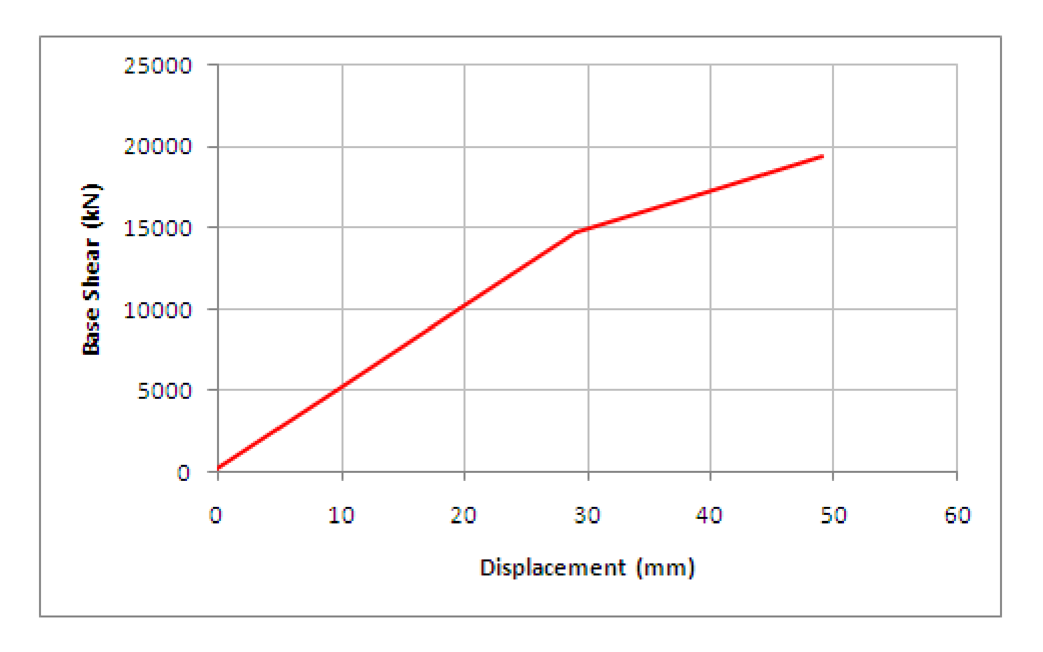


Figure 5-18: Pushover curves for analysis in the transverse direction for pier #3 in Alharamain Bridge.

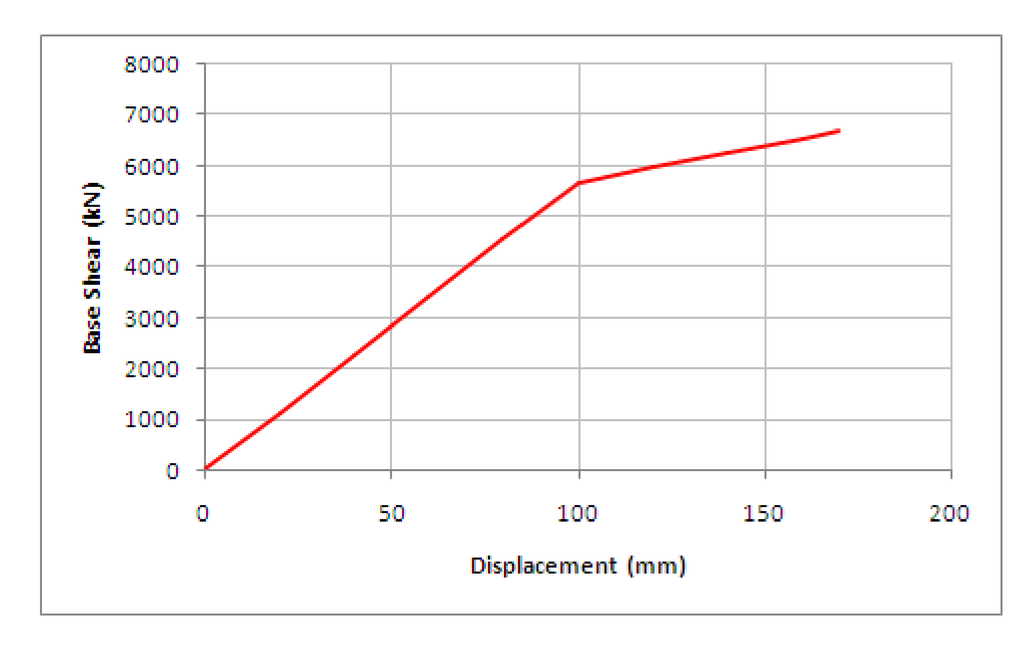


Figure 5-19: Pushover curves for analysis in the longitudinal direction for pier #3 in Alharamain Bridge.

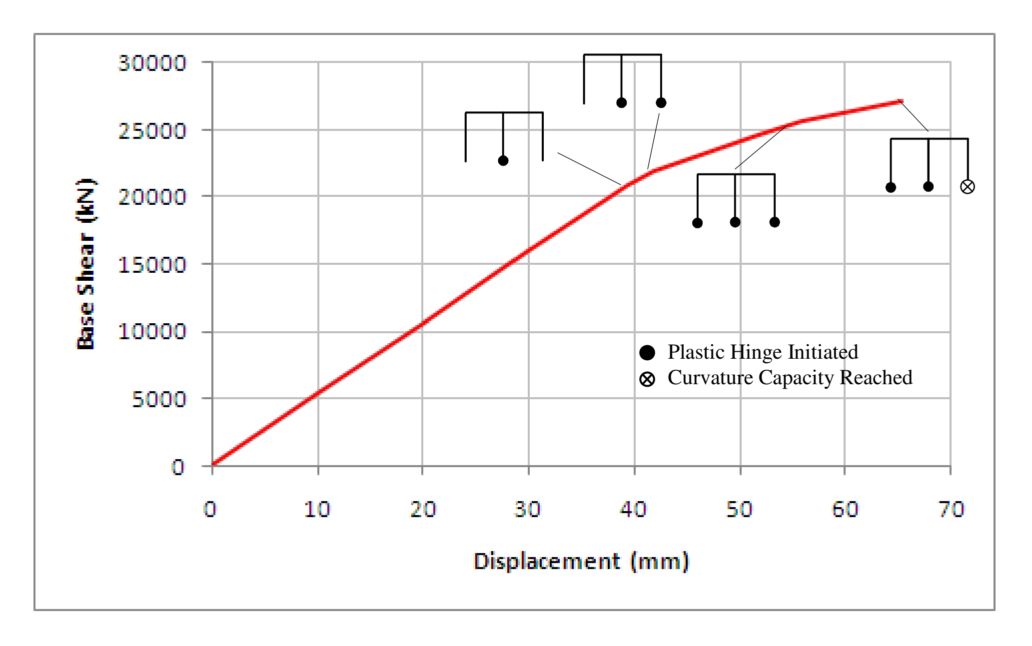


Figure 5-20: Pushover curves for analysis in the transverse direction for pier #5 & 6 in Alharamain Bridge.

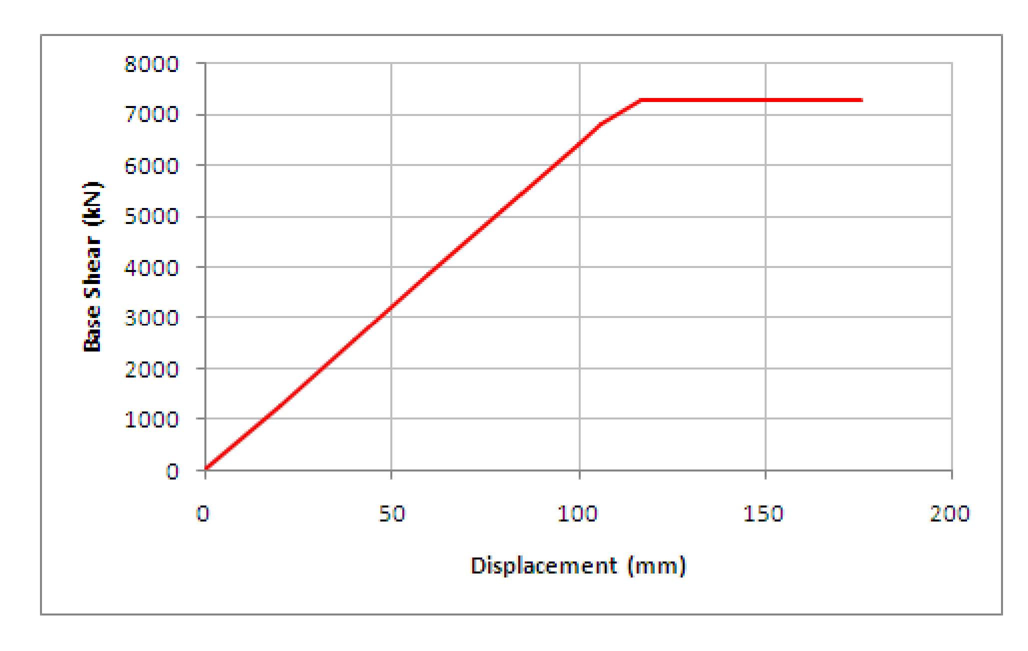


Figure 5-21: Pushover curves for analysis in the longitudinal direction for pier #5 & 6 in Alharamain Bridge.

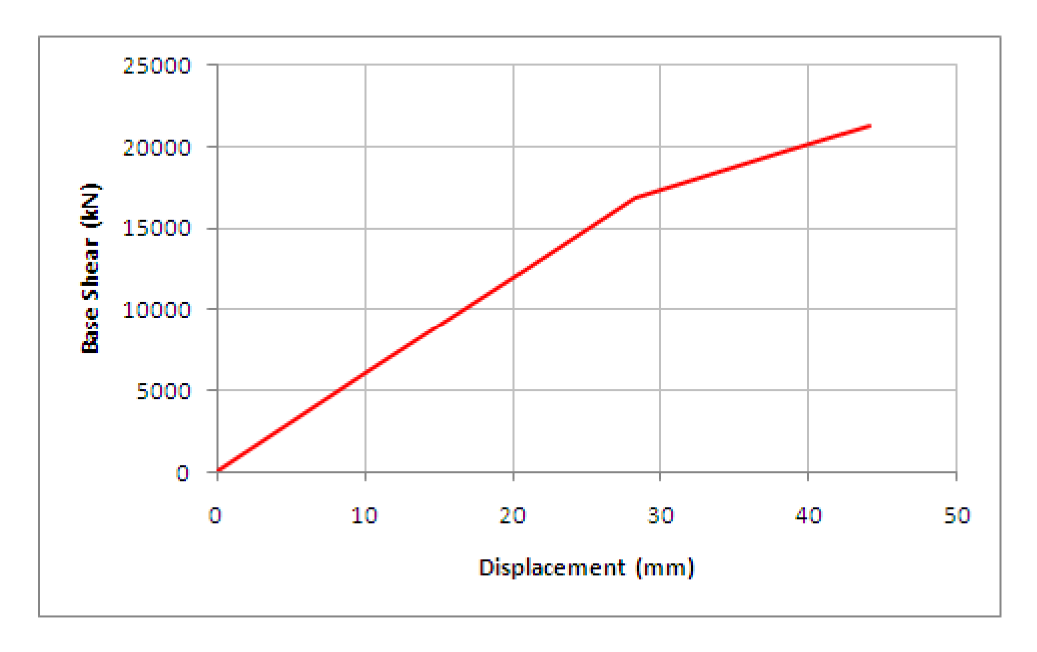


Figure 5-22: Pushover curves for analysis in the transverse direction for pier #8 in Alharamain Bridge.

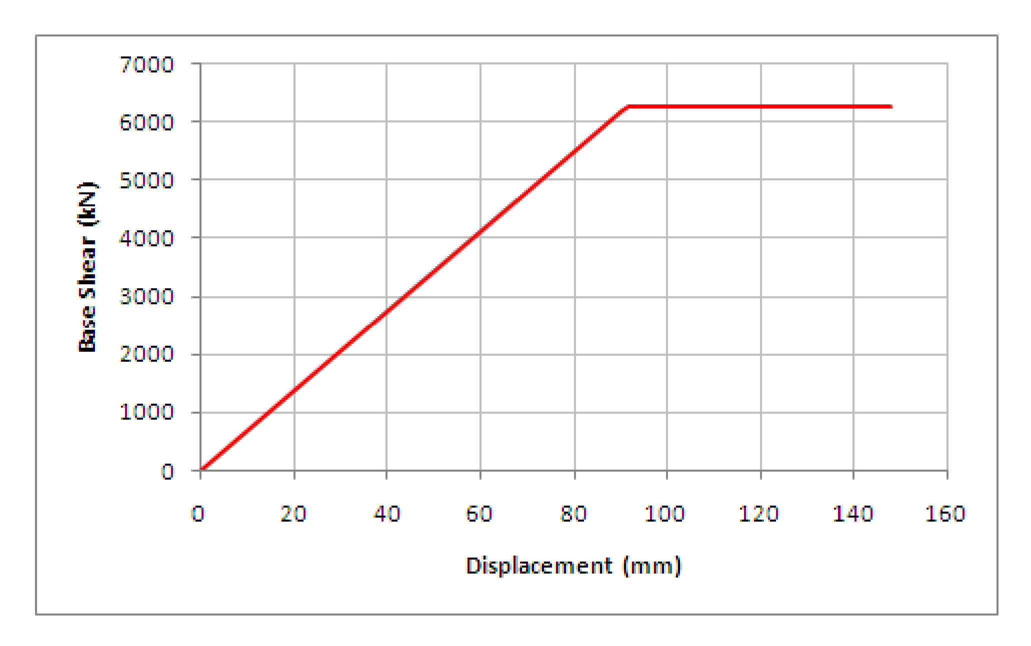


Figure 5-23: Pushover curves for analysis in the longitudinal direction for pier #8 in Alharamain Bridge.

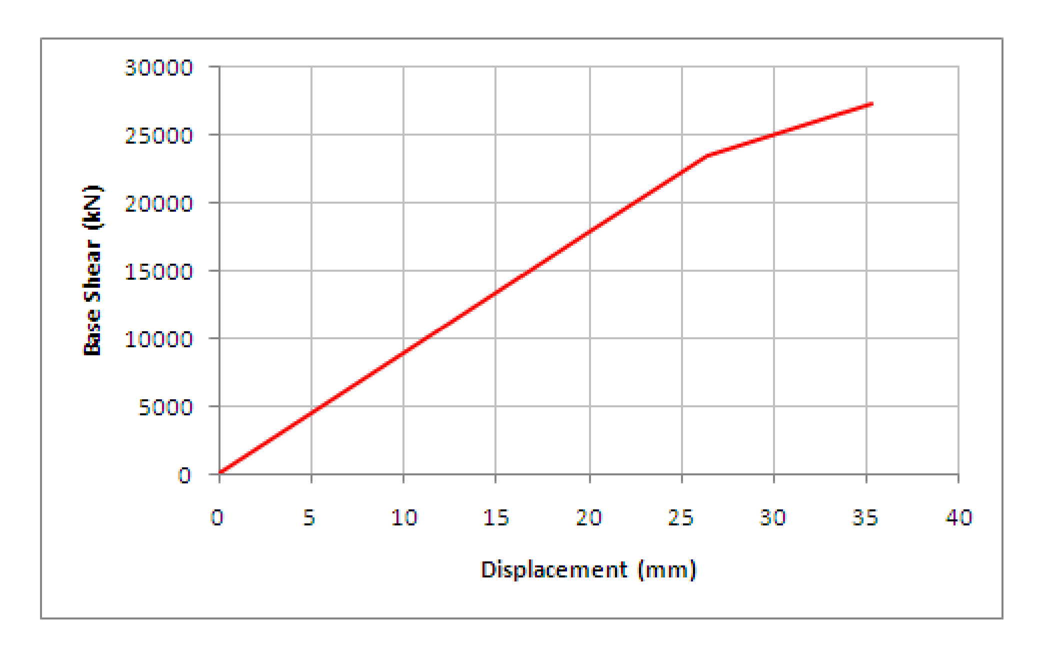


Figure 5-24: Pushover curves for analysis in the transverse direction for pier #9 in Alharamain Bridge.

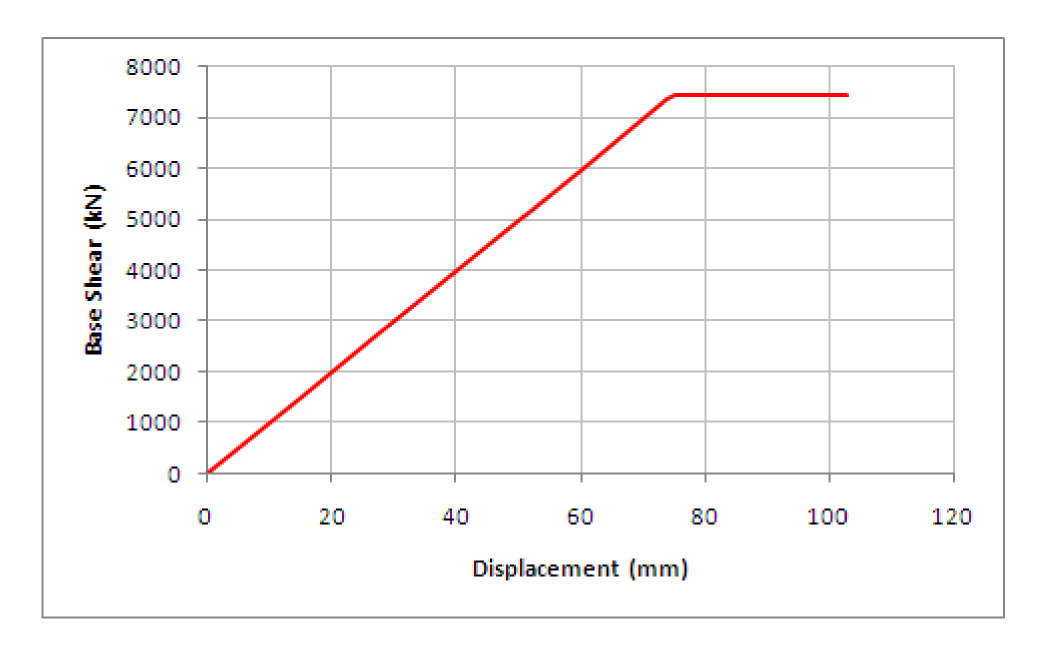


Figure 5-25: Pushover curves for analysis in the longitudinal direction for pier #9 in Alharamain Bridge.

Table 5-25 through Table 5-29 show the displacement C/D ratios for pier #2, pier #4, pier #5 and pier #7. The displacement capacity is obtained from pushover analysis while displacement demand is obtained from elastic response spectra analysis.

Table 5-25: Alharamain Bridge Method D2 – Pier #2.

Non-seismic Displacement Demand:		
Nonseismic displacement demand in global x-axis:	0	mm
Nonseismic displacement demand in global y-axis:	0	mm
Seismic Displacement Demand:		
Compression Model		
($1.0EQ_x + 0.4EQ_y$)		
Seismic displacement demand in global x-axis:	77.94	mm
Seismic displacement demand in global y-axis:	4.6	mm
($0.4EQ_x + 1.0EQ_y$)		
Seismic displacement demand in global x-axis:	31.2	mm
Seismic displacement demand in global y-axis:	10.6	mm
Tension Model		
($1.0EQ_x + 0.4EQ_y$)		
Seismic displacement demand in global x-axis:	68.4	mm
Seismic displacement demand in global y-axis:	4.6	mm
($0.4EQ_x + 1.0EQ_y$)		
Seismic displacement demand in global x-axis:	28.7	mm
Seismic displacement demand in global y-axis:	10.85	mm
Structural Displacement Capacity:		
Displacement Capacity - Transverse Direction:	46.13	mm
Displacement Capacity - Longitudinal Direction:	164.5	mm
C/D Ratios:		
Displacement CD ratio in the transverse direction:	2.111	
Displacement CD ratio in the longitudinal direction:	4.252	

Table 5-26: Alharamain Bridge Method D2 – Pier #3.

Non-seismic Displacement Demand:		
Nonseismic displacement demand in global x-axis:	0	mm
Nonseismic displacement demand in global y-axis:	0	mm
Seismic Displacement Demand:		
Compression Model		
($1.0EQ_x + 0.4EQ_y$)		
Seismic displacement demand in global x-axis:	78	mm
Seismic displacement demand in global y-axis:	8.4	mm
($0.4EQ_x + 1.0EQ_y$)		
Seismic displacement demand in global x-axis:	31.2	mm
Seismic displacement demand in global y-axis:	26.7	mm
Tension Model		
($1.0EQ_x + 0.4EQ_y$)		
Seismic displacement demand in global x-axis:	68.5	mm
Seismic displacement demand in global y-axis:	11.1	mm
($0.4EQ_x + 1.0EQ_y$)		
Seismic displacement demand in global x-axis:	28.7	mm
Seismic displacement demand in global y-axis:	27.85	mm
Structural Displacement Capacity:		
Displacement Capacity - Transverse Direction:	49.52	mm
Displacement Capacity - Longitudinal Direction:	155.46	mm
C/D Ratios:		
Displacement CD ratio in the transverse direction:	1.778	
Displacement CD ratio in the longitudinal direction:	1.993	

Table 5-27: Alharamain Bridge Method D2 – Pier #5 & 6.

Non-seismic Displacement Demand:		
Nonseismic displacement demand in global x-axis:	0	mm
Nonseismic displacement demand in global y-axis:	0	mm
Seismic Displacement Demand:		
Compression Model		
($1.0EQ_x + 0.4EQ_y$)		
Seismic displacement demand in global x-axis:	77.4	mm
Seismic displacement demand in global y-axis:	15	mm
($0.4EQ_x + 1.0EQ_y$)		
Seismic displacement demand in global x-axis:	31	mm
Seismic displacement demand in global y-axis:	36	mm
Tension Model		
($1.0EQ_x + 0.4EQ_y$)		
Seismic displacement demand in global x-axis:	67.9	mm
Seismic displacement demand in global y-axis:	14.6	mm
($0.4EQ_x + 1.0EQ_y$)		
Seismic displacement demand in global x-axis:	28.5	mm
Seismic displacement demand in global y-axis:	35.6	mm
Structural Displacement Capacity:		
Displacement Capacity - Transverse Direction:	65.41	mm
Displacement Capacity - Longitudinal Direction:	183.16	mm
C/D Ratios:		
Displacement CD ratio in the transverse direction:	2.366	
Displacement CD ratio in the longitudinal direction:	1.817	

Table 5-28: Alharamain Bridge Method D2 – Pier #8.

Non-seismic Displacement Demand:		
Nonseismic displacement demand in global x-axis:	0	mm
Nonseismic displacement demand in global y-axis:	0	mm
Seismic Displacement Demand:		
Compression Model		
($1.0EQ_x + 0.4EQ_y$)		
Seismic displacement demand in global x-axis:	65.5	mm
Seismic displacement demand in global y-axis:	14.9	mm
($0.4EQ_x + 1.0EQ_y$)		
Seismic displacement demand in global x-axis:	30.5	mm
Seismic displacement demand in global y-axis:	29	mm
Tension Model		
($1.0EQ_x + 0.4EQ_y$)		
Seismic displacement demand in global x-axis:	66.5	mm
Seismic displacement demand in global y-axis:	14.4	mm
($0.4EQ_x + 1.0EQ_y$)		
Seismic displacement demand in global x-axis:	27.8	mm
Seismic displacement demand in global y-axis:	29.4	mm
Structural Displacement Capacity:		
Displacement Capacity - Transverse Direction:	44.65	mm
Displacement Capacity - Longitudinal Direction:	155.7	mm
C/D Ratios:		
Displacement CD ratio in the transverse direction:	2.312	
Displacement CD ratio in the longitudinal direction:	1.428	

Table 5-29: Alharamain Bridge Method D2 – Pier #9.

Non-seismic Displacement Demand:		
Nonseismic displacement demand in global x-axis:	0	mm
Nonseismic displacement demand in global y-axis:	0	mm
Seismic Displacement Demand:		
Compression Model		
($1.0EQ_x + 0.4EQ_y$)		
Seismic displacement demand in global x-axis:	65	mm
Seismic displacement demand in global y-axis:	9	mm
($0.4EQ_x + 1.0EQ_y$)		
Seismic displacement demand in global x-axis:	30	mm
Seismic displacement demand in global y-axis:	10.3	mm
Tension Model		
($1.0EQ_x + 0.4EQ_y$)		
Seismic displacement demand in global x-axis:	66.4	mm
Seismic displacement demand in global y-axis:	9.1	mm
($0.4EQ_x + 1.0EQ_y$)		
Seismic displacement demand in global x-axis:	28.8	mm
Seismic displacement demand in global y-axis:	10.5	mm
Structural Displacement Capacity:		
Displacement Capacity - Transverse Direction:	36.02	mm
Displacement Capacity - Longitudinal Direction:	109.09	mm
C/D Ratios:		
Displacement CD ratio in the transverse direction:	1.629	
Displacement CD ratio in the longitudinal direction:	2.253	

According to method C of the FHWA-SRM (2005) discusses in Chapter one, pushover analysis should be performed in case C/D ratio for any element is less than one. Accordingly, pushover analysis was conducted for all piers. Table 5-30 shows C/D ratios adapted by applying Method D2.

Table 5-30: Alharamain Bridge C/D-Ratios obtained from Method D2

C/D-Ratios	**Pier2**	**Pier3**	**Pier5&6 (Outer col)**	**Pier5&6 (Center col)**	**Pier8**	**Pier9**
r_{ec} bending moment C/D ratio for column	1.061	1.05	1.130	1.026	1.059	1.150
r_{cv} shear force C/D ratio for column shear capacity	1.061	1.050	1.130	1.026	1.059	2.973
r_{cc} confinement C/D ratio for column transverse reinforcement	3.182	3.150	3.388	3.077	3.176	3.447
r_{ef} bending moment C/D ratio for footing	0.402	0.402	0.280	0.280	0.357	0.322
r_{fr} rotation C/D ratio for footing	0.402	0.402	1.118	1.118	0.357	0.322
Displacement – Method D2						
Longitudinal Direction	2.111	1.993	2.366		2.312	1.629
Transverse Direction	4.252	1.778	1.817		1.428	2.253

The results in the above table show that the bridge footing are not able to with stand the required seismic force due to the poor design of footings which is clear to notice in the drawings. In the next chapter, retrofitting scheme for the deficient footings was proposed.

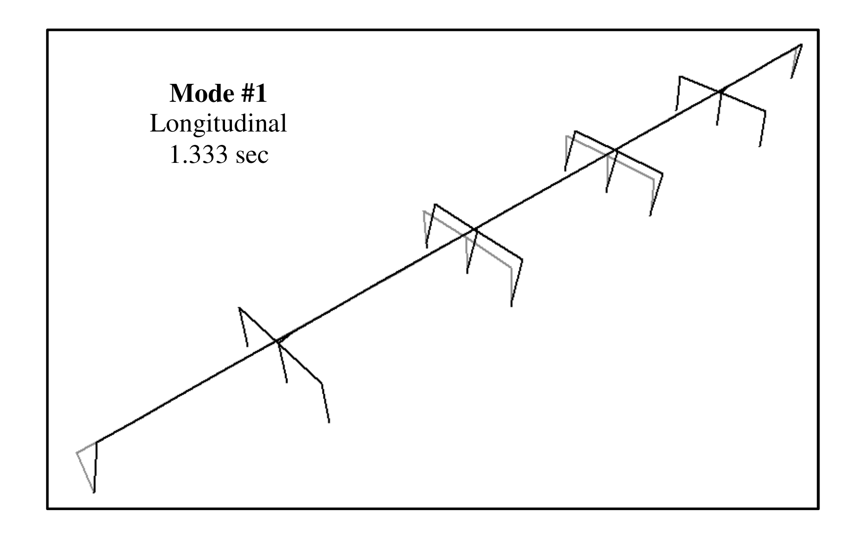
5.3. Almahata Bridge

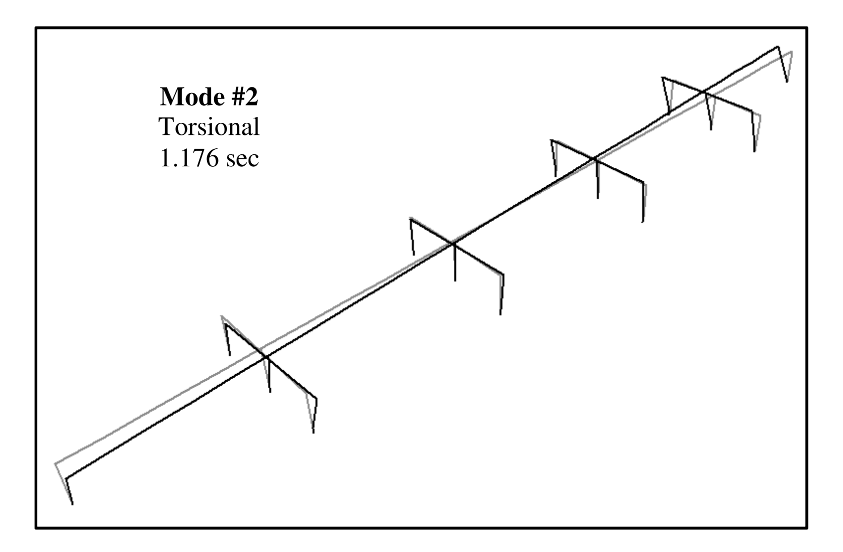
5.3.1. Response Spectrum Analysis

The response spectrum analysis begins with determining the natural frequencies and mode shapes via an eigen value analysis. The longitudinal and transverse natural periods and the associated modal participating mass ratios (i.e., effective modal mass to total mass ratios) are shown for the bridge model in Table 5-31. The longitudinal and the transverse mode shapes for the bridge model are shown in Figure 5-26.

Table 5-31: Almahata Bridge fundamental periods and mass participation ratios

Mode No.	Natural period (sec)	Modal participating mass ratio (%)
1 (Longitudinal Mode)	1.333	0.967
2 (Torsional Mode)	1.176	0.011
3 (Transverse Mode)	0.953	0.966





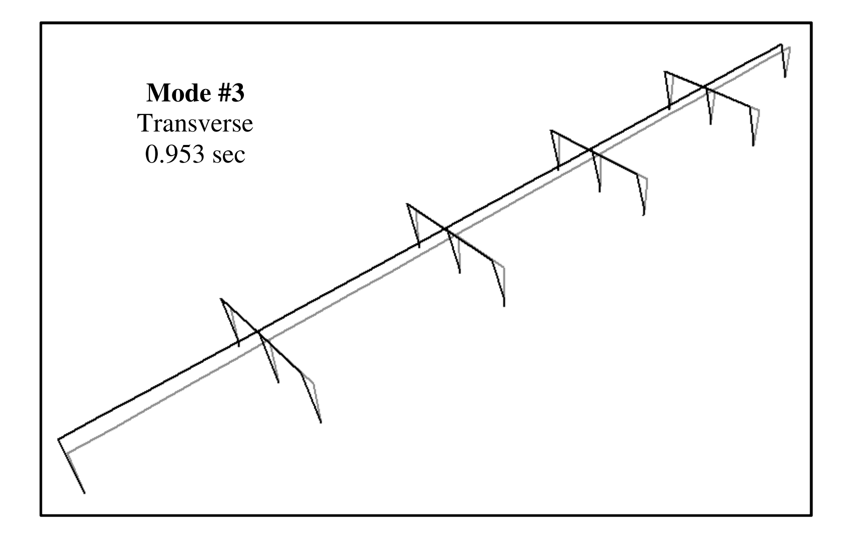


Figure 5-26: Fundamental mode shapes of Almahata Bridge.

The response spectrum analysis determines the bridge response under the effect of the expected seismic forces. The response includes displacements, moment, and shear forces in the longitudinal and transverse directions of the bridge. The 100-40 percent load combination rule as recommended by FHWA-SRM (2005) was used to determine the seismic demand on the bridge. Table 5-32 shows the displacements demand on the bridge as obtained from the elastic response spectrum analysis.

Table 5-32: Almahata Bridge elastic displacement demand.

Pier No.	Δ_x (mm)	Δ_y (mm)
1	148.898	128.172
2	148.804	116.336
3	148.499	105.061
4	148.499	99.828
5	148.804	98.303
6	148.915	100.111

Moment and shear demand on the bottom of the pier columns for the bridge model are shown in Table 5-33. M_{22} indicates moment about the longitudinal axis of the bridge, while M_{33} indicates moment about an axis perpendicular to the longitudinal bridge axis. V_{22} indicates shear force in the direction parallel to the main bridge axis, while V_{33} indicates shear force perpendicular to that axis.

Table 5-33: Almahata Bridge moment and shear force demand.

Combination	**Pier No.**	M_{22} (kN.m)	M_{33} (kN.m)	V_{22} (kN)	V_{33} (kN)
($1.0M_x+0.4M_y$)	2	2927	346	62	518
	3	2456	8750	1491	419
	4	2365	8914	1534	408
	5	2157	297	50	356
($0.4M_x+1.0M_y$)	2	7320	390	70	1296
	3	6142	3692	630	1047
	4	5914	3727	642	1018
	5	5393	261	43	890

Table 5-32 shows that the demand on the columns of pier #2 and pier #5 in the longitudinal direction M_{33} and V_{22}, is very small due to the fact that the bridge is free to slide in the longitudinal direction at these piers.

5.3.2. Method C Seismic Capacity/Demand Ratio

Tables 5-34 through 5-35 show the input and output quantities that were used in calculation of Almahata Bridge C/D ratios. Detailed calculations for the quantities shown in Tables 5-34 through Table 5-35 are shown in Appendix D.

Table 5-34: Almahata Bridge – Pier #2 and Pier #5 C/D ratio calculations

Pier Geometry:		
Clear Height of Column:	5.65	m
Column Length:	5.65	m (For bending about X)
	5.65	m (For bending about Y)
Crossbeam Depth:	1.0	m
Material Properties:		
Specified Compressive Strength of Concrete:	28	MPa
Specified Yield Strength of Reinforcement:	414	MPa
Column Cross-Section:		
Column Cross-sectional Area:	0.785	m^2
Column Dimensions:	1.0	m (Column Diameter)
Longitudinal Reinforcement:		
Number of Long. Bars Reinf.:	26	
Longitudinal Bar Dia.:	32	
Longitudinal Bar Area:	804.25	mm^2
Clear Cover:	40	mm (To transverse rebars)
Clear Spacing:	72	mm
Transverse Reinforcement:		
Transverse Bar Dia.:	12	mm
Spacing of Transverse Reinf.:	300	mm
No of Legs:	2	
No of Legs:	2	
Diameter of transverse hoop or spiral:	0.908	m
Effective Depth of Section:	0.932	m
Area of confined concrete core:	0.648	m^2
Volumetric Ration of Long. Reinforcement:	0.027	

Table 5-34 (Continue): Almahata Bridge – Pier #2 and Pier #5 C/D ratio calculations

Demand Forces:			
Axial Force due to DL:	2100	kN (1.25DL)	
Axial Force due to EQ:	130	kN (100-40Comb.)	
Max. Plastic Force:	2100	kN	
Min. Plastic Force:	1550	kN	
Moment due to DL about X:	0	kN.m	
Moment due to DL about Y:	0	kN.m	
Moment due to EQ about X:	M22: 7320	M33: 390	kN.m
Moment due to EQ about Y:	M22: 2927	M33: 346	kN.m
Nominal Col. Capacity:	3714	(About X, At P_{min_p})	
Nominal Col. Capacity:	3840	(About Y, At P_{DL})	
Overstrength Factor:	1.4		
Plastic Moment Capacity:	5199.6	kN.m (About X)	
Plastic Moment Capacity:	5376	kN.m (About Y)	
Column CD ratio, r_{ec-x}:	0.507	(About X)	
Column CD ratio, r_{ec-y}:	11.098	(About Y)	
Column CD ratio, r_{ec}:	0.507		

Shear-X-Axis:		
Maximum calculated elastic shear force, V_e:	0	kN
The maximum column shear force resulting from plastic hinging, V_u:	941	kN
Initial shear strength, V_i:	1780	kN
Final shear strength, V_f:	833	kN
Case A, r_{cv-x}:	12.79	(Eq. D-16)
Case B, r_{cv-x}:	59.57	(Eq. D-17)
Case C, r_{cv-x}:	63.97	(Eq. D-18)
Controlling Case - X-Direction:	59.57	
Shear-Y-Axis:		
Maximum calculated elastic shear force, V_e:	890	kN
The maximum column shear force resulting from plastic hinging, V_u:	916	kN
Initial shear strength, V_i:	1780	kN
Final shear strength, V_f:	833	kN
Case A, r_{cv-y}:	0.686	(Eq. D-16)
Case B, r_{cv-y}:	3.248	(Eq. D-17)
Case C, r_{cv-y}:	3.43	(Eq. D-18)
Controlling Case - Y-Direction:	3.248	
Transverse Confinement Reinforcement:		
Volumetric ratio of existing transverse reinforcement, ρ_c:	0.001	
Required volumetric ratio of transverse reinforcement, ρ_d:	0.008	
k_1:	0.326	
k_2:	2.28	
μ:	2.27	
C/D ratio for transverse confinement, r_{cc}:	1.565	(Eq. D-20)
Splices in Longitudinal Reinforcement:		
Since splices aren't occur at region of plastic hinge, C/D isn't available in this case, r_{cs}:	N/A	

Table 5-34 (Continue): Almahata Bridge – Pier #2 and Pier #5 C/D ratio calculations

Anchorage of longitudinal reinforcement:		
Anchorage with 90° standard hooks, the effective anchorage length, in mm, is;		
The required effective anchorage length of longitudinal reinforcement, L_{ad}:	480	mm (Eq. D-7a)
K_m:	0.7	
The effective anchorage length of longitudinal reinforcement, L_{ac}:	1285	mm
Detail 5: When the top of the footing contains adequately anchored flexural reinforcement, as for the above detail, and the column bars have been provided with 90° standard hooks, the C/D ratio for anchorage should be taken as 1.0.		
Anchorage length C/D ratio for column longitudinal reinforcement, r_{ca}:	1.0	

Table 5-35: Almahata Bridge – Pier #3 and Pier #4 C/D ratio calculations

Pier Geometry:		
Clear Height of Column:	5.81	m
Column Length:	5.81	m (For bending about X)
	5.81	m (For bending about Y)
Crossbeam Depth:	1.0	m
Material Properties:		
Specified Compressive Strength of Concrete:	28	MPa
Specified Yield Strength of Reinforcement:	414	MPa
Column Cross-Section:		
Column Cross-sectional Area:	0.785	m^2
Column Dimensions:	1.0	m (Column Diameter)
Longitudinal Reinforcement:		
Number of Long. Bars Reinf.:	26	
Longitudinal Bar Dia.:	32	
Longitudinal Bar Area:	804.25	mm^2
Clear Cover:	40	mm (To transverse rebars)
Clear Spacing:	72	mm
Transverse Reinforcement:		
Transverse Bar Dia.:	12	mm
Spacing of Transverse Reinf.:	300	mm
No of Legs:	2	
No of Legs:	2	
Diameter of transverse hoop or spiral:	0.908	m
Effective Depth of Section:	0.932	m
Area of confined concrete core:	0.648	m^2
Volumetric Ration of Long. Reinforcement:	0.027	

Table 5-35 (Continue): Almahata Bridge – Pier #3 and Pier #4 C/D ratio calculations

Demand Forces:			
Axial Force due to DL:	2600	kN (1.25DL)	
Axial Force due to EQ:	115	kN (100-40Comb.)	
Max. Plastic Force:	2100	kN	
Min. Plastic Force:	1550	kN	
Moment due to DL about X:	0	kN.m	
Moment due to DL about Y:	0	kN.m	
Moment due to EQ about X:	M22: 6142	M33: 3692	kN.m
Moment due to EQ about Y:	M22: 8914	M33: 2365	kN.m
Nominal Col. Capacity:	3718	(About X, At P_{min_p})	
Nominal Col. Capacity:	3930	(About Y, At P_{DL})	
Overstrength Factor:	1.4		
Plastic Moment Capacity:	5205	kN.m (About X)	
Plastic Moment Capacity:	5502	kN.m (About Y)	
Column CD ratio, r_{ec-x}:	0.605	(About X)	
Column CD ratio, r_{ec-y}:	0.441	(About Y)	
Column CD ratio, r_{ec}:	0.441		
Shear-X-Axis:			
Maximum calculated elastic shear force, V_e:	1490	kN	
The maximum column shear force resulting from plastic hinging, V_u:	946	kN	
Initial shear strength, V_i:	1779	kN	
Final shear strength, V_f:	831	kN	
Case A, r_{cv-x}:	0.449	(Eq. D-16)	
Case B, r_{cv-x}:	2.082	(Eq. D-17)	
Case C, r_{cv-x}:	2.246	(Eq. D-18)	
Controlling Case - X-Direction:	2.082		
Shear-Y-Axis:			
Maximum calculated elastic shear force, V_e:	1050	kN	
The maximum column shear force resulting from plastic hinging, V_u:	895	kN	
Initial shear strength, V_i:	1779	kN	
Final shear strength, V_f:	831	kN	
Case A, r_{cv-y}:	0.605	(Eq. D-16)	
Case B, r_{cv-y}:	2.904	(Eq. D-17)	
Case C, r_{cv-y}:	3.027	(Eq. D-18)	
Controlling Case - Y-Direction:	2.904		
Transverse Confinement Reinforcement:			
Volumetric ratio of existing transverse reinforcement, ρ_c:	0.001		
Required volumetric ratio of transverse reinforcement, ρ_d:	0.008		
k_1:	0.312		
k_2:	0.7		
μ:	2.27		
C/D ratio for transverse confinement, r_{cc}:	1.019	(Eq. D-20)	
Splices in Longitudinal Reinforcement:			
Since splices aren't occur at region of plastic hinge, C/D isn't available in this case, r_{cs}:	N/A		

Table 5-35 (Continue): Almahata Bridge – Pier #3 and Pier #4 C/D ratio calculations

Anchorage of longitudinal reinforcement:		
Anchorage with 90° standard hooks, the effective anchorage length, in mm, is;		
The required effective anchorage length of longitudinal reinforcement, L_{ad}:	480	mm (Eq. D-7a)
K_m:	0.7	
The effective anchorage length of longitudinal reinforcement, L_{ac}:	1285	mm
Detail 5: When the top of the footing contains adequately anchored flexural reinforcement, as for the above detail, and the column bars have been provided with 90° standard hooks, the C/D ratio for anchorage should be taken as 1.0.		
Anchorage length C/D ratio for column longitudinal reinforcement, r_{ca}:	1.0	

Table 5-36 presents a summary of the C/D ratios for Almahata Bridge according to FHWA-SRM (2005) method C.

Table 5-36: Almahata Bridge C/D-Ratios obtained from Method C

C/D-Ratios	**Pier2**	**Pier3**	**Pier4**	**Pier5**
r_{ec} bending moment C/D ratio for column	0.507	0.441	0.441	0.507
r_{cv} shear force C/D ratio for column shear capacity	2.397	2.044	2.044	2.397
r_{cc} confinement C/D ratio for column transverse reinforcement	1.157	1.001	1.001	1.157
r_{cs} splice length C/D ratio for column longitudinal reinforcement	N/A	N/A	N/A	N/A
r_{ca} anchorage length C/D ratio for column longitudinal reinforcement	1	1	1	1
r_{bd} displacement C/D ratio for bearing seat – Pier1 (Abutment)	1.089			
r_{bd} displacement C/D ratio for bearing seat – Pier6 (Abutment)	1.095			

The Capacity/Demand ratios of the columns for Pier # 2, 3, 4 & 5 were found to correspond to Case III as described in the Method C analysis approach in FHWA-SRM (2005). Under Case III, it is assumed that the column is more likely to yield before the footing. Therefore, this requires an evaluation of columns ductility and their ability to

withstand plastic hinging. Splice length C/D ratios were not reported for all piers because the splices occur outside the plastic hinge region.

5.3.3. Method D2

Method D2 requires a pushover analysis of the bridge piers under consideration. For pushover analysis, nonlinear behavior is assumed to occur within frame elements at concentrated plastic hinges with default or user-defined hinge properties being assigned to each hinge.

Figure 5-27 shows the moment-rotation curve for the columns of pier #5 at their different axial load levels. Curve A present moment-rotation curve at axial force level equal to the load capacity at the maximum confined moment on the section. Curve B presents the moment-rotation curve at axial force level equal to the axial load due to seismic force. Curve C presents the moment-rotation curve at axial load level equal to zero. Figure 5-28 shows the interaction diagrams for columns of pier #5. Detailed calculations of the moment-interaction curves for each pier columns are shown in Appendix C. Table 5-37 and Table 5-38 summarize the coordinates of the moment-interaction curves and the moment-rotation curves for the pier columns of Almahata Bridge.

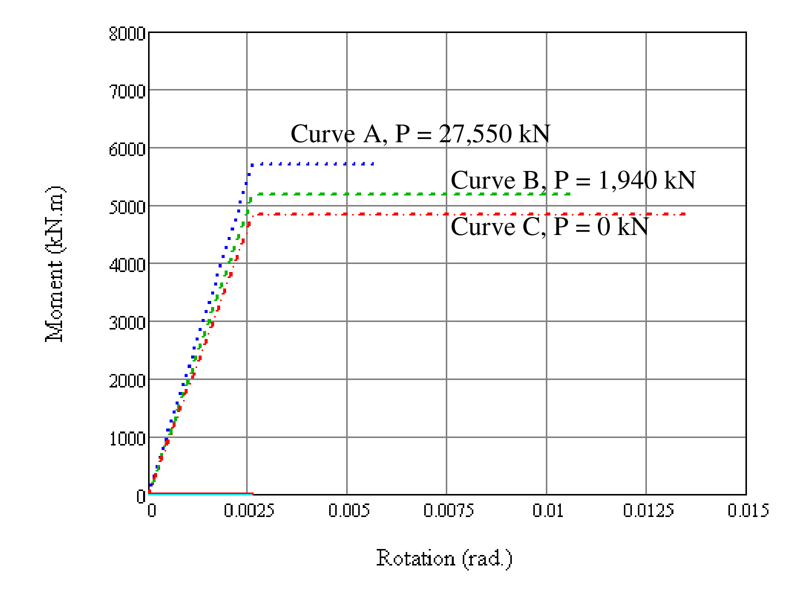


Figure 5-27: Moment-Rotation relationship for columns of Pier #3 in Almahata Bridge.

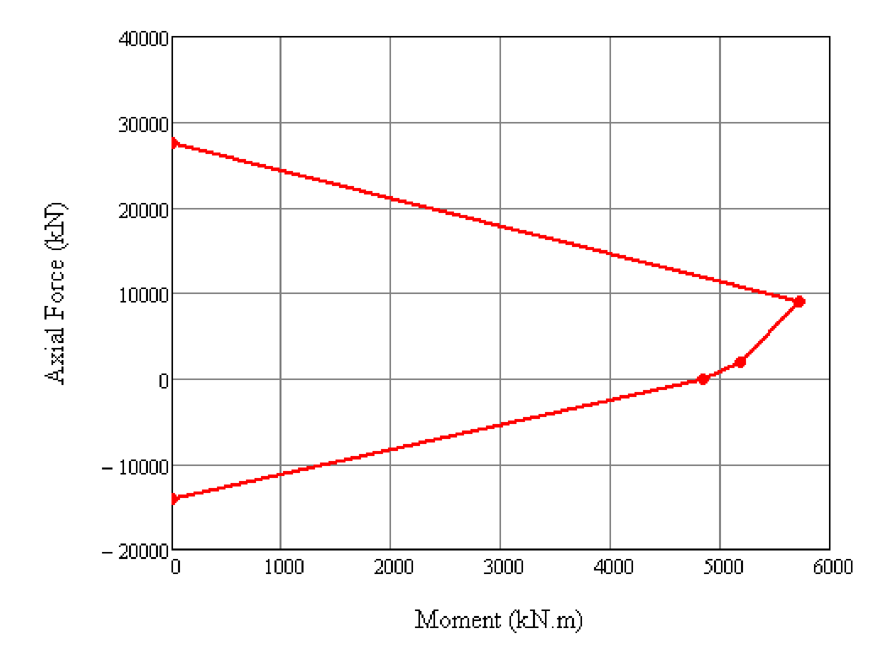


Figure 5-28: Moment-Axial force interaction diagram for columns of Pier #3 in Almahata Bridge.

Table 5-37: Moment-Rotation data-Almahata Bridge

Pier No.	Direction	Curve A				Curve B			
		Point1		Point2		Point1		Point2	
		Rotation (rad.)	Moment (kN.m)	Rotation (rad.)	Moment (kN.m)	Rotation (rad.)	Moment (kN.m)	Rotation (rad.)	Moment (kN.m)
Pier #2	Long	0.002607	5717	0.003125	5717	0.002607	5185	0.008088	5185
	Trans	0.002607	5717	0.003125	5717	0.002607	5185	0.008088	5185
Pier #4 & Pier #5	Long	0.002607	5717	0.003127	5717	0.002607	5176	0.008163	5176
	Trans	0.002607	5717	0.003128	5717	0.002607	5176	0.008163	5176
Pier #7	Long	0.002607	5717	0.003125	5717	0.002607	5185	0.008088	5185
	Trans	0.002607	5717	0.003125	5717	0.002607	5185	0.008088	5185

Pier No.	Direction	Curve C			
		Point1		Point2	
		Rotation (rad.)	Moment (kN.m)	Rotation (rad.)	Moment (kN.m)
Pier #2	Long	0.002607	4842	0.011	4842
	Trans	0.002607	4842	0.011	4842
Pier #4 & Pier #5	Long	0.002607	4842	0.011	4842
	Trans	0.002607	4842	0.011	4842
Pier #7	Long	0.002607	4842	0.011	4842
	Trans	0.002607	4842	0.011	4842

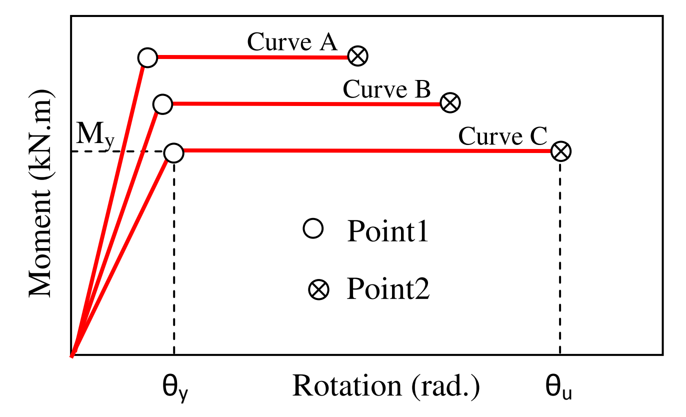


Table 5-38: Moment-Axial force interaction data-Almahata Bridge

Pier No.	Point1		Point2		Point3		Point4		Point5	
	Force (kN)	Moment (kN.m)	Force (kN)	Moment (kN.m)	Force (kN)	Moment (kN.m)	Force (kN)	Moment (kN.m)	Force (kN)	Moment (kN.m)
Pier #2	27550	0	9071	5717	2000	5185	0	4842	-14110	0
Pier #4 &5	27550	0	9071	5717	1940	5176	0	4842	-14110	0
Pier #7	27550	0	9071	5717	2000	5185	0	4842	-14110	0

The pushover curve in the transverse and longitudinal direction obtained from the pushover analysis using SAP2000 is shown in Figure 5-29 through Figure 5-31 for pier #2, pier #3, pier #4 and pier #5 in Almahata Bridge.

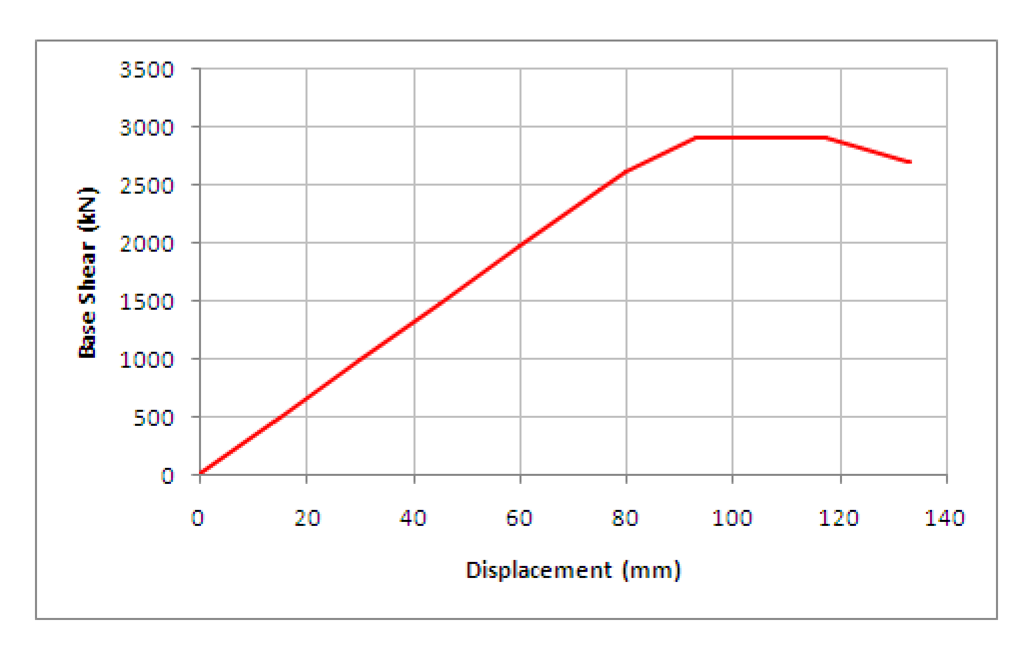


Figure 5-29: Pushover curves for analysis in the transverse direction for pier #2 and 5 in Almahata Bridge.

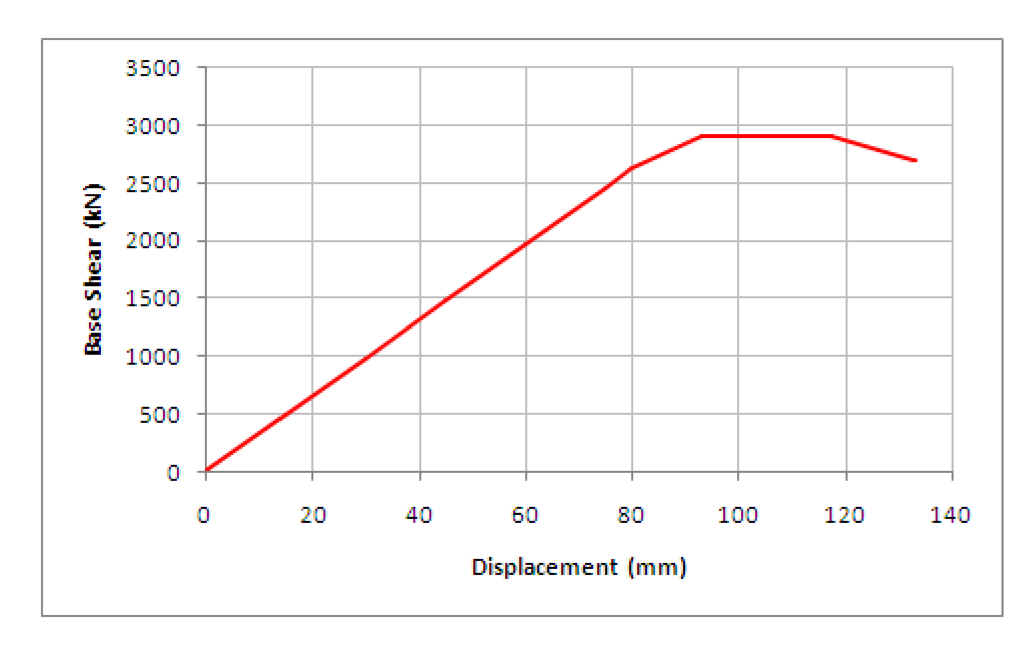


Figure 5-30: Pushover curves for analysis in the transverse direction for pier #3 and 4 in Almahata Bridge.

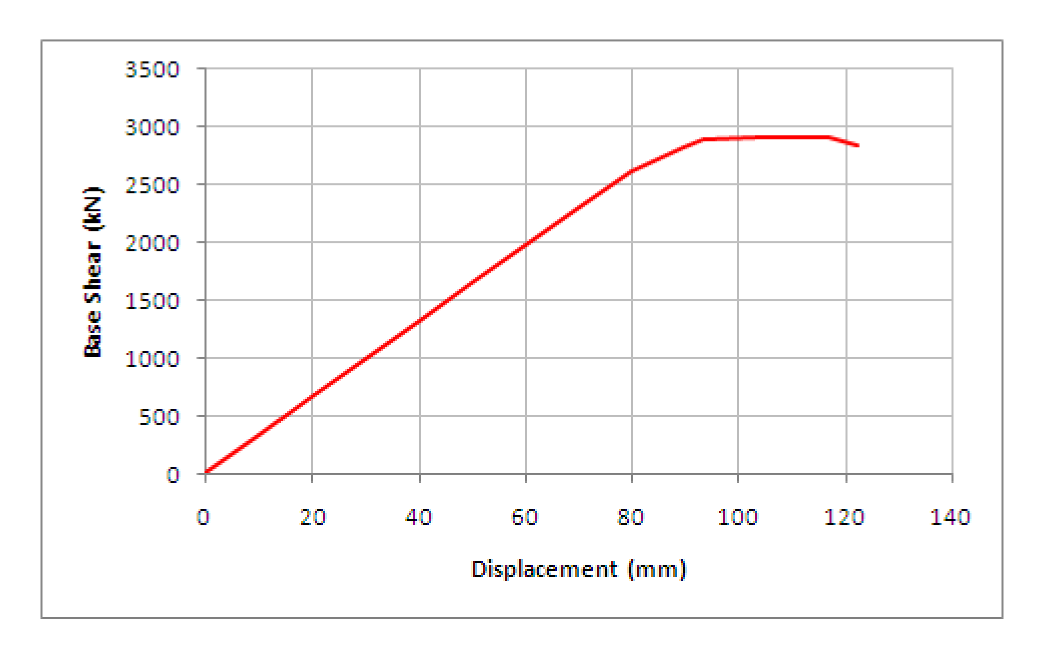


Figure 5-31: Pushover curves for analysis in the longitudinal direction for pier #3 and 4 in Almahata Bridge.

Table 5-39 though Table 5-40 show the displacement C/D ratios for pier #2, pier #4, pier #5 and pier #7. The displacement capacity is obtained from pushover analysis while displacement demand is obtained from elastic response spectra analysis.

Table 5-39: Almahata Bridge Method D2 – Pier #2 & Pier #4.

Non-seismic Displacement Demand:		
Nonseismic displacement demand in global x-axis:	0	mm
Nonseismic displacement demand in global y-axis:	0	mm
Seismic Displacement Demand:		
Compression Model		
(1.0EQ$_x$ + 0.4EQ$_y$)		
Seismic displacement demand in global x-axis:	5.5	mm
Seismic displacement demand in global y-axis:	46.5	mm
(0.4EQ$_x$ + 1.0EQ$_y$)		
Seismic displacement demand in global x-axis:	6.2	mm
Seismic displacement demand in global y-axis:	116.3	mm
Tension Model		
(1.0EQ$_x$ + 0.4EQ$_y$)		
Seismic displacement demand in global x-axis:	5.5	mm
Seismic displacement demand in global y-axis:	46.5	mm
(0.4EQ$_x$ + 1.0EQ$_y$)		
Seismic displacement demand in global x-axis:	6.2	mm
Seismic displacement demand in global y-axis:	116.3	mm
Structural Displacement Capacity:		
Displacement Capacity - Transverse Direction:	133.14	mm
Displacement Capacity - Longitudinal Direction:	122.15	mm
C/D Ratios:		
Displacement CD ratio in the transverse direction:	19.702	
Displacement CD ratio in the longitudinal direction:	1.145	

Table 5-40: Almahata Bridge Method D2 – Pier #3 & Pier #5.

Non-seismic Displacement Demand:		
Nonseismic displacement demand in global x-axis:	0	mm
Nonseismic displacement demand in global y-axis:	0	mm
Seismic Displacement Demand:		
Compression Model		
(1.0EQ$_x$ + 0.4EQ$_y$)		
Seismic displacement demand in global x-axis:	149.8	mm
Seismic displacement demand in global y-axis:	42.1	mm
(0.4EQ$_x$ + 1.0EQ$_y$)		
Seismic displacement demand in global x-axis:	63.2	mm
Seismic displacement demand in global y-axis:	105.2	mm
Tension Model		
(1.0EQ$_x$ + 0.4EQ$_y$)		
Seismic displacement demand in global x-axis:	149.8	mm
Seismic displacement demand in global y-axis:	42.1	mm
(0.4EQ$_x$ + 1.0EQ$_y$)		
Seismic displacement demand in global x-axis:	63.2	mm
Seismic displacement demand in global y-axis:	105.2	mm
Structural Displacement Capacity:		
Displacement Capacity - Transverse Direction:	133.14	mm
Displacement Capacity - Longitudinal Direction:	122.14	mm
C/D Ratios:		
Displacement CD ratio in the transverse direction:	1.266	
Displacement CD ratio in the longitudinal direction:	0.815	

According to method C of the FHWA-SRM (2005) discusses in Chapter one, pushover analysis should be performed in case C/D ratio for any element is less than one. Accordingly, pushover analysis was conducted for all piers. Table 5-41 shows C/D ratios adapted by applying Method D2.

Table 5-41: Almahata Bridge C/D-Ratios obtained from Method D2

C/D-Ratios	**Pier2**	**Pier3**	**Pier4**	**Pier5**
r_{ec} bending moment C/D ratio for column	1.025	1.022	1.022	1.025
r_{cv} shear force C/D ratio for column shear capacity	3.607	3.693	3.693	3.607
r_{cc} confinement C/D ratio for column transverse reinforcement	2.337	2.320	2.320	2.337
Displacement – Method D2				
Longitudinal Direction	19.702	0.815	0.815	19.702
Transverse Direction	1.145	1.266	1.266	1.145

Table 5-41 shows that pier # 3 and pier #4 have not the enough ductility to withstand the demand displacement. Therefore, there is a need for retrofitting scheme for this bridge, as discussed later in Chapter 6.

The longitudinal and transverse natural periods and the associated modal participating mass ratios (i.e., effective modal mass to total mass ratios) are shown for each bridge in Table 5-42.

Table 5-42: Bridges Fundamental periods and mass participation ratios.

Bridge	Model type	Mode No.	Natural period (sec)	Modal participating mass ratio (%)
Alnasha Bridge	**Tension model**	1 (Longitudinal Mode)	0.535	45.3
		2 (Transverse Mode)	0.516	45.5
		3 (Longitudinal Mode)	0.264	22.8
	Compression model	1 (Transverse Mode)	0.516	45.5
		2 (Transverse Mode)	0.256	18.0
		3 (Longitudinal Mode)	0.247	94.0
Alharamain Bridge	**Tension model**	1 (Longitudinal Mode)	0.699	24.5
		2 (Longitudinal Mode)	0.695	25.3
		3 (Transverse Mode)	0.599	24.0
	Compression model	1 (Longitudinal Mode)	0.613	74.8
		2 (Torsional Mode)	0.522	1.7
		3 (Transverse Mode)	0.445	53.2
Almahata Bridge	**Tension model**	1 (Longitudinal Mode)	1.333	0.967
		2 (Torsional Mode)	1.176	0.011
		3 (Transverse Mode)	0.953	0.966

CHAPTER SIX

6. RETROFIT SCHEMES

This chapter discusses the proposed retrofit schemes for the weak elements in each candidate bridge. Based on the results of the evaluation methods, retrofit schemes were proposed to enhance the performance of the weak elements to withstand the expected level of seismic forces.

6.1. Alnasha Bridge

The seismic C/D ratios of the bridge elements based on evaluation method C and evaluation method D2 were greater than one. This means that all the elements that were checked under the requirements of these methods will be able to withstand the expected level of seismic forces. Therefore, no retrofit is required for this bridge.

6.2. Alharamain Bridge

Results of the evaluation methods (Method C and Method D2) showed that some C/D ratios for this bridge were below one. C/D ratio for bearing seat at Abutment #1 and C/D ratios for the footings were found to be less than one, which means that retrofit schemes should be established. The following is a detailed discussion on each weakness.

6.2.1. Bearing seat upgrade at Abutment #1

The C/D ratio of the seat length at Abutment #1 was found to be 0.983 according to method C of the FHWA-SRM (2005). This requires extending the seat by providing a concrete corbel at the top of the abutment underneath the soffit of the

superstructure. Figure 6-1 shows the proposed retrofit scheme for Abutment #1 in Alharamain Bridge.

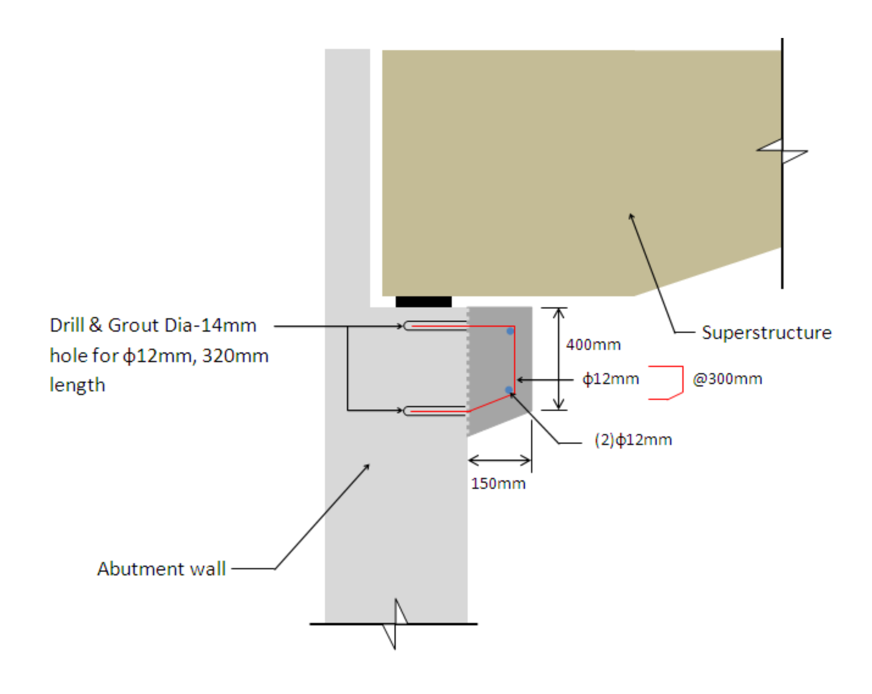


Figure 6-1: Seat extension of Abutment #1 in Alharamain Bridge

Before providing the seat extension, roughening of the existing abutment wall is needed at place where the corbel is being added. Dowel bars need to be drilled and grouted efficiently through the existing abutment wall to ensure enough bond between the existing wall and the new corbel. Increasing the seat length at Abutment #1 by 150 mm will result in an increase in the C/D ratio to 1.196. Based on the average prices of materials in 2011, this retrofit scheme is expected to cost JD 141. Table 6-1 shows material quantities required for this retrofit scheme.

Table 6-1: Materials cost estimate for seat length upgrade in Alharamain Bridge.

Material	Quantity	Unit Price	Cost (JD)
28 MPa Concrete	1.4 m^3	60 JD/m^3	84
G60-Steel Reinforcement	95 kg	600 JD/Ton	57
		Total	141

6.2.2. Bridge Footings

The seismic C/D ratio of the bridge footings were found to be less than one, which means that seismic retrofit of the footings is needed. The as-built drawings of the bridge footings show that the bridge footing at Pier #2, pier #3, pier #6, and pier #7 have a depth equal to 1.75 m, reduces to 0.75 m after a distance of 0.75 m from the face of the column. The footings at pier #4 and pier #7 have a depth equal to 2.5 m and reduces to 0.5 m after a distance of 0.75 m from face of the column. This drop in the footings thickness reduces significantly the capacity of the footing to resist the required seismic force in the longitudinal direction. Figure 6-2 and Figure 6-3 show the proposed retrofit scheme for the existing footings in the bridge. The proposed retrofit scheme includes increasing the thickness of the footing in the depressed zone to a thickness equal to the depth of the footing at the face of the column. This increase in the thickness will enhance the flexural and shear capacity of the footings.

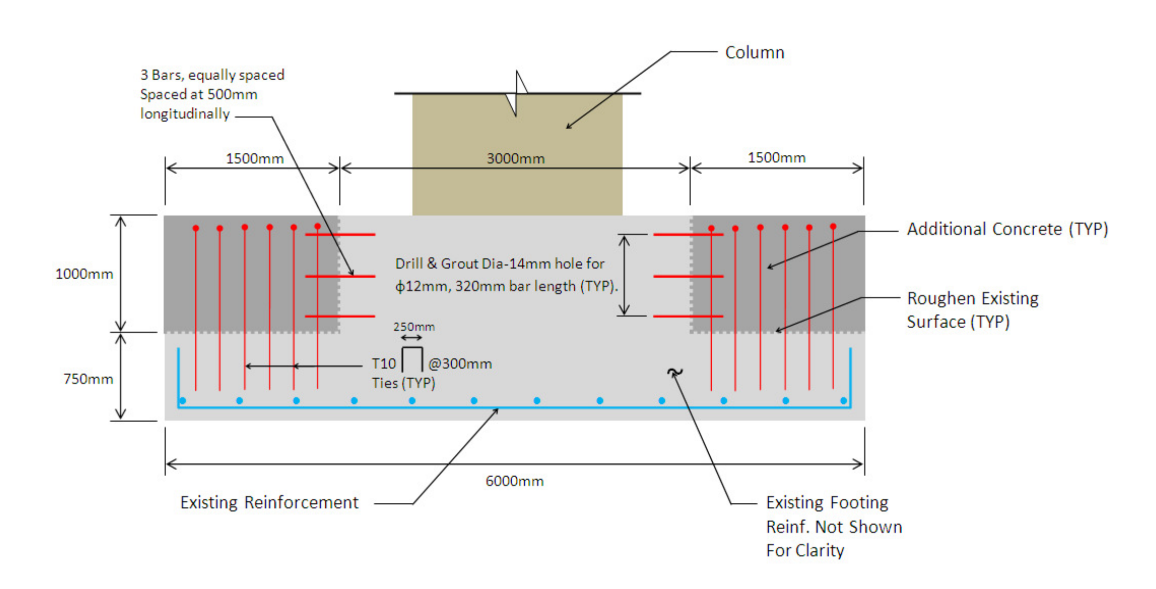


Figure 6-2: Proposed retrofit scheme for the footings in pier #2, pier #3, pier #6, & pier #7.

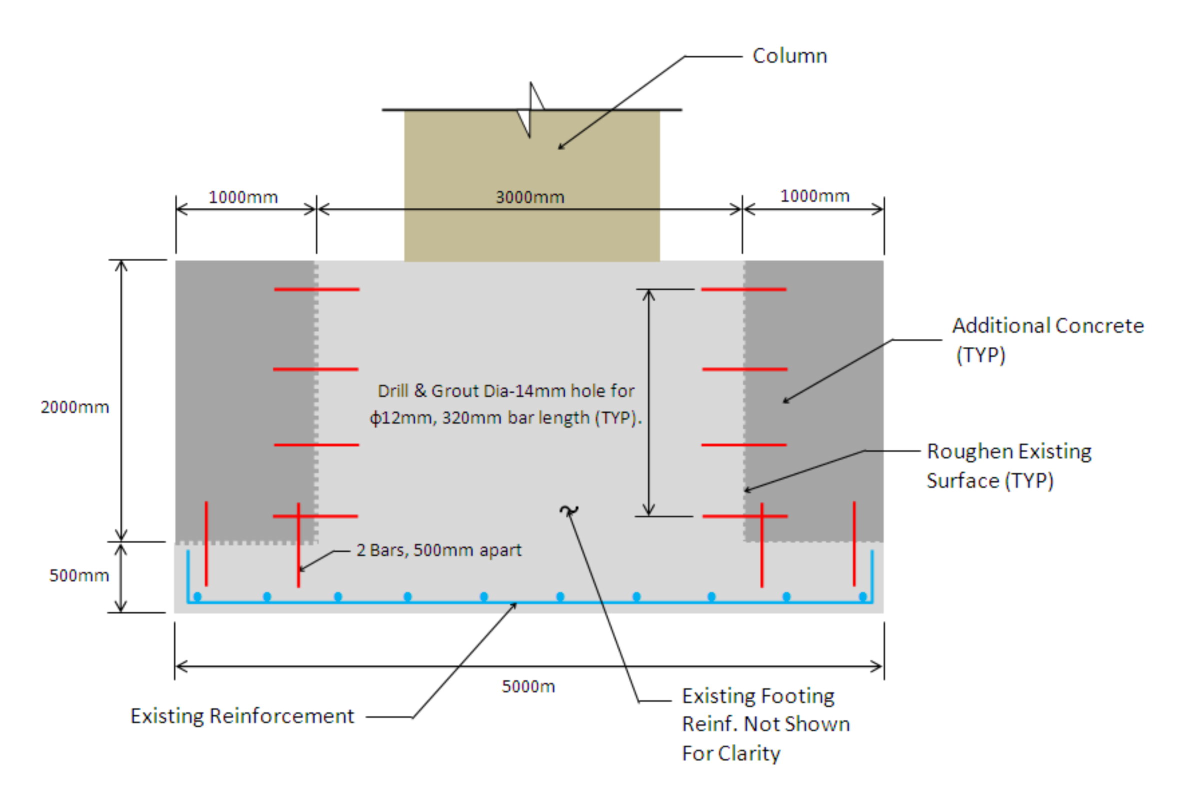


Figure 6-3: Proposed retrofit scheme for the footings in pier #4 & pier #7.

Table 6-2: Materials cost estimate for footings retrofit in Alharamain Bridge.

Material	Quantity	Unit Price	Cost (JD)
28 MPa Concrete	308 m^3	60 JD/m^3	18,480
G60-Steel Reinforcement	1520	600 JD/Ton	912
		Total	19,392

In order to insure that the new concrete and the old concrete will work together, the existing footing surfaces should be roughened and cleaned before casting the new concrete. Also, dowel bars should be introduced between the new and the old concrete by drilling through the existing concrete and fix these dowels by high strength epoxy material. Table 6-2 shows the materials cost estimate for the proposed footing retrofit scheme in Alharamain Bridge. Based on the average prices of materials in 2011, this retrofit scheme is expected to cost JD 19,392. Table 6-2 shows material quantities required for this retrofit scheme.

6.3. Almahata Bridge

The as-built drawings of the bridge showed that the columns have relatively low confinement steel ratios. The columns are reinforced with 12 mm bars spaced at 300 mm. The evaluation methods supported that the columns lack the ductility required to withstand the seismic demand. A typical solution to this weakness is to provide a steel jacket in the vicinity of the plastic hinge zone. However, the general practice is to jacket the whole length of the column as shown in Figure 6-4. The size of the steel jacket is taken as the size of the original column plus 25 mm gap. This gap is usually filled with high strength grout to ensure a full interaction between the old column and the steel jacket. A 50 mm gap is usually introduced between the steel jacket and the face of the footing or the soffit of the superstructure to allow for the plastic hinge rotations that are expected during an earthquake, as shown in Figure 6-4. This gap will also insure that the stiffness of the retrofitted and the old column do not vary significantly and therefore affect the overall behavior of the bridge.

Based on the average prices of materials in 2011, this retrofit scheme is expected to cost JD 7,650. Table 6-3 shows a quantity estimate of the required material for the proposed retrofit scheme.

Table 6-3: Materials cost estimate for piers retrofit in Almahata Bridge.

Material	Quantity	Unit Price	Cost (JD)
Concrete Grout	1.11 m^3	60 JD/m^3	133
G60-Steel Jacket	12.53 Ton	600 JD/Ton	7,517
		Total	7,650

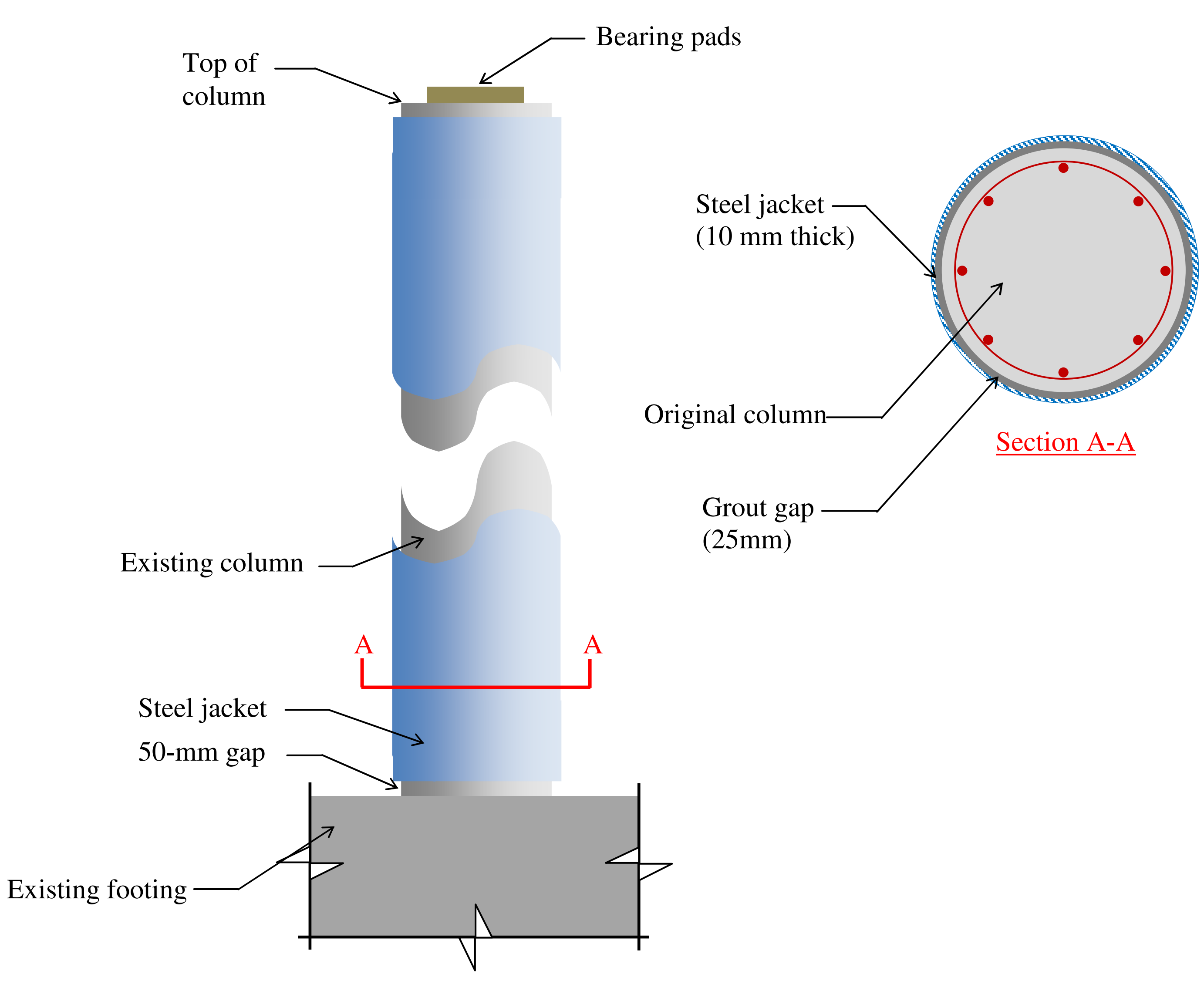


Figure 6-4: Retrofit scheme for Pier #3 and Pier #4 columns in Almahata Bridge.

CHAPTER SEVEN

7. SUMMMARY AND CONCLUSIONS

This study investigated the seismic vulnerability of three vital highway bridges in Jordan according to the FHWA Seismic Retrofitting Manual for Highway Structures (FHWA-SRM, 2005). These bridges are: Alnasha Bridge, Alharamen Intersection Bridge, and Almahata Bridge. Force and displacement demands were established by performing a multimode elastic analysis using the software SAP2000. The structural capacity of the bridge elements were determined based on information shown in the as-built drawings. Capacity/demand (C/D) ratios were used to quantify the likely performance of the candidate bridges during an earthquake. Retrofit schemes that are feasible and effective were proposed to enhance the overall performance of the bridges.

The study showed that all the C/D ratios for the bridge elements in Alnasha Bridge are greater than one. This means that the bridge is expected to withstand the expected earthquake demand without the need for any retrofit.

For Alharamain Bridge, the study showed that the footings and the abutment seat lengths have C/D ratio less than 1. A retrofit scheme that includes increasing the thickness of the footing and increasing the length of the abutment seat was proposed.

The study showed that the columns of pier #3 and pier #4 in Almahata Bridge lack the required ductility to withstand the expected seismic demands. A retrofit scheme that enhance the ductility of the plastic hinges of the weak columns was proposed. The scheme includes installing a steel jacket around the weak columns is expected to cover this vulnerability.

This study includes only three vital highway bridges in Jordan. It is strongly recommended to initiate national program that aims to investigate the seismic vulnerability of all vital bridges in Jordan. Conducting of such program will keep the transportation system to continue functional during and after the occurrence of an earthquake, so that lifelines can continue to provide emergency services and minimize loss of life and economic distress.

REFERENCES

American Association of State Highway and Transportation Officials (2007), **LRFD Bridge Design Specifications**, Washington, DC.

Armouti Nazzal (2008), **Earthquake Engineering: Theory and Implementation**, Second Edition, Illinois, ICC Publication,

Chai, Y.H., Priestley, M.J.N., and Seible, F. (1991), Flexural Retrofit of Circular Reinforced Concrete Bridge Columns by Steel Jackets, **Department of Applied Mechanics and Engineering Sciences**, University of California, San Diego, Report Number SSRP-91/06.

Chen and Lian (2000), **Bridge Engineering Handbook**, New York, CRC Press.

Computers and Structures Inc. (2008), **SAP2000 Structural Analysis Program**, Nonlinear Version 12.0.0, Berkeley, California.

Evan Bentz and Michael Collins (2000), **Response-Reinforced Concrete Sectional Analysis**, Version 1.0.5.

Federal Highway Administration (2005), **Seismic Retrofitting Manual for Highway Bridges**, Department of Transportation, Virginia.

Klinger Y., Avouac J. P., Dorbath L., Abou Karaki N., and Tisnerat N. (2000), Seismic Behavior of the Dead Sea Failt Along Araba Valley, Jordan, **Geophys. J. Int.**, 142, 769-782.

McLean David and Shattarat Nasim (2005), **Seismic Behavior and Retrofit of Bridge Knee Joint Systems**, Washington State University.

Musmar M. A. (2007), A Comparison Between the New and the Old Versions of Jordan Seismic Code, **International Journal of Applied Science, Engineering and Technology**, 42007, 229-232.

Priestley, Seible, and Calvi (1996), **Seismic Design and Retrofit of Bridges**, New York, John Wiley & Sons, Inc.

Rafik Itani and Xin Liao (2003), Effects of Retrofitting Applications on Reinforced Concrete Bridges, **Washington State Transportation Center (TRAC)**, Research Project T 2696, Task 02.

Shattarat Nasim and Assaf Adel (2009), Seismic Behavior and Capacity/Demand Analyses of a Simply-Supported Multi Span Precast Bridge, **International Journal of Applied Science, Engineering and Technology**, 42009, 220-226.

www.ace-mrl.engin.umich.edu.

Yeou-Fong Li, Jenn-Shin Hwang, Shao-Hong Chen, and Yu-Ming Hsieh (2005), A Study of Reinforced Concrete Bridge Columns Retrofitted by Steel Jackets, **Journal of the Chinese Institute of Engineers**, Vol. 28, No. 2, 319-328.

Zvi Ben-Avraham, Michael Lazar, Uri Schattner, and Shmuel Marco (2005), **The Dead Sea Fault and its Effect on Civilization**.

التصرف الزلزالي لعدد من الجسور الحيوية في الأردن

إعداد
عامر الكلوب

المشرف
الدكتور نزال العرموطي

المشرف المشارك
الدكتور نسيم الشطرات

ملخص

الهدف الرئيسي لهذة الرسالة هو دراسة التصرف الزلزالي لثلاث جسور رئيسية في الأردن و تحديد الأجزاء العرضة للضرر في كل جسر بالإضافة إلى إقتراح حلول لتأهيل تلك الأجزاء. تم تحديد القوى و الإزاحات الزلزالية على الجسور بواسطة تحليل طيف التجاوب المرن. إستناداً على توصيات دليل إعادة تأهيل الجسور، و بإستخدام الطريقة "C" تم تحديد قدرة الأجزاء المكونة للجسور. بعد ذلك تم حساب نسبة قدرة المقطع إلى القوة التي يتعرض لها المقطع، وتم حساب ذلك للمقاطع التي يمكن تعرضها للضرر أو الفشل من جراء القوى الزلزالية المتوقعة. تم إجراء تحليل لاخطي لجميع أعمدة الجسور المشمولة في الدراسة إعتماداً على توصيات الطريقة "D2" في دليل إعادة تأهيل الجسور يقوم على دفع أعمدة الجسر في الإتجاة الطولي و العرضي للجسر لحين وصول الجسر لأقصى إزاحة ممكنة.

أظهرت نتائج الدراسة أن جسر النشا قادر على مقاومة القوى الزلزالية المتوقعة دون الحاجة لإجراء أي إصلاح، بينما يعاني جسر الحرمين من عدم قدرة الأساسات على مقاومة القوى الزلزالية المتوقعة، و لمعالجة هذا الضعف تم إقتراح زيادة سماكة الأساسات. كما يعاني جسر الحرمين من قِصر طول مقعد الجسر عند الدعامة رقم 1 حيث تم إقتراح زيادة طول الدعامة و ذلك بإضافة دعامة خرسانية. كما أظهرت النتائج أن أعمدة جسر المحطة غير قادر على إستيعاب الإزاحة الزلزالية المتوقعة من جراء ضعف مطيلية الأعمدة، تم تحسين مطيلية أعمدة الجسر عن طريق إقتراح تركيب غلاف فلاذي على طول الأعمدة رقم 3 و 4.